A study of pupil response components in human vision

Sancho Moro

Dissertation submitted for a Philosophical Doctorate degree at

City University, London

Department of Optometry and Visual Science

July 2004

Table of Contents

List of figures

5

List of tables

Acknowledgements

I must express here my gratitude to my supervisors, professors John Barbur and Larry Weiskrantz, for introducing me to the fascinating field of vision research and their constant encouragement and contagious enthusiasm.

Vision research is, to all intents and purposes, an inter-disciplinary field. It would not have been possible to complete many of the experiments reported here without the help and expertise of colleagues and collaborators. I must thus acknowledge support from many people. First, to all students and subjects that volunteered to participate in the experiments, Larry Weiskrantz for giving me the opportunity to test his blindsight patients, Barbara Wilhem for the collaboration in the studies with Parinaud's syndrome, Byron Lam from the Bascom Palmer Eye Institute in Miami for collecting pupil data in patients with acute optic neuritis and Elizabeth Frost for assisting with the testing of the patients in London.

I would also like to thank many people with whom I have collaborated at City University during different phases of my research. Many people have helped me to make a difficult transition from 'theoretical' physicist to vision scientist. I have profited enormously in this respect from working at a department with a wide variety of research interests. In particular exchanges of ideas with the anatomical and biological group: Dr Gary Baker and Professor Ron Douglas who helped me to navigate through the vast amount of literature concerning the anatomy and physiology of the visual pathways. I also appreciate greatly the opinion and advice from many of my close colleagues: Alistair Harlow, Alison Finlay, Helen Walkey, Catharine Chisholm, Mireia Pacheco and Marisa Rodriguez-Carmona. They provided help in numerous occasions from instructive explanations in general optometry and clinical conditions to common technical problems. This collaborating atmosphere made City University an excellent and friendly workplace.

I also enjoyed the interaction with the students during both Optics and Visual Perception Labs. I now realize that I have learned a lot more from these experiences than what I probably valued at the time. I have to thank David Thomson, Chris Hull and John Barbur for offering me this opportunity.

I grant powers of discretion to the University Librarian to allow this thesis to be copied in whole or in part without further reference to me. This permission covers single copies made for study purposes, subject to normal conditions of acknowledgement.

Abstract

The overall aim of the research described in this thesis was to investigate the basic mechanisms of the pupil of the eye in relation to human vision and brain function. It also evaluates the potential application of new research techniques to clinical studies that involve assessment of the visual function.

Pupil response components were investigated in normal subjects and in patients with damaged visual pathways. A series of experiments were carried out to investigate the pupil response to periodic modulation of several stimulation parameters such as: luminance contrast, stimulus size, spatial and temporal frequency content, and colour.

Much larger responses were found for square-wave as compared to sinusoidal luminance modulation. A model with two populations of neurones (sustained and transient) was developed to explain the non-linear combination of two response components in the light reflex. In contrast to these findings, responses to isoluminant coloured stimuli or sinusoidal gratings whose spatial average luminance is equal to that of the background do not depend of the temporal wave-form of the stimulation. Studies in patients with lesions to specific areas in the brain suggest that these responses are caused by a transient weakening of the steady central sympathetic inhibition to parasympathetic neurones innervating the sphincter muscle as a result of cortical processing of specific stimulus attributes such as colour and spatial structure.

Pupil measurements in patients suffering from demyelinating neurological disorders such as multiple sclerosis and optic neuritis also confirm the existence of distinct pupil response components and reveal selective loss to chromatic and luminance pathways. The results indicate a preferential damage to thinner axons which are thought to predominantly mediate the chromatic responses. These studies suggest that the use of modern pupillometric techniques in neuro-ophthalmology can yield useful information on the extent of the damage and the progression of disease in lesions of the optic nerve.

Thesis outline and summary of research

The general introduction of the visual pathways presented in chapter 1 is followed by a more detailed review of the anatomy and physiology of the neural pathways mediating the pupil response in chapter 2. These two introductory chapters are followed by a detailed description of the methods and techniques (e.g. pupil imaging, psychophysics, photometry, display calibration, etc.) used in all the experiments carried out in this investigation (chapter 3).

The series of experiments described in chapter 4 were carried out to investigate the pupil response to various attributes of the visual stimulus such as: luminance contrast, size, spatial and temporal frequency characteristics and colour. Markedly larger responses were obtained when comparing square-wave with sinusoidal luminance modulation for several contrast levels, stimulus size and across the whole visual field. These results can be explained by a model which takes into account the physiological differences found in the temporal response properties of retinal ganglion cells projecting to the pupillomotor centres in the midbrain (Trejo & Cicerone 1984): sustained neurones, exhibit low contrast gain and fire throughout the duration of the stimulus while transient neurones fire only at stimulus onset, offset or both. Low frequency, sinusoidal luminance modulation is likely to stimulate mainly a 'sustained' mechanism while brisk, square-wave modulation favours a transient mechanism. The much larger pupil responses found for square-wave compared to sinusoidal modulation cannot be accounted for simply as a contribution of higher harmonics present in the square-wave modulation. The unexpected harmonics at even multiples of the stimulation frequency introduced largely by faster constriction than dilation rates invalidate the Fourier frequency analysis of the pupil response. In an alternative model, the larger response to square-wave modulation is explained by the contribution of high frequency harmonics to the neural signal input through temporal summation. The model also explains the better spatial summation found for sinusoidal modulation as a result of smaller receptive field sizes associated to the sustained mechanism. The sustained mechanism has low, almost linear contrast gain and exhibits large spatial summation of light flux changes. This mechanism is therefore appropriate to control the steady state size of the pupil in response to changes in ambient illumination. The transient mechanism exhibits a highly non-linear contrast gain, responding preferentially to rapid luminance contrast changes and is thus more likely to mediate the dynamic pupil light reflex. Both the sustained and transient mechanisms require intact subcortical inputs since they are virtually abolished after pretectal lesions (chapter 6). In addition, PLR deficits in patients with damaged to visual cortical areas (chapter 5) confirm that there is also a cortical contribution to the pupil light reflex pathway.

Pupil responses to visual stimuli that do not involve a light flux change such as isoluminant coloured stimuli or gratings whose spatial average luminance is equal to that of the background (equi-luminant gratings) lack the sustained/transient division of the light response since do not depend on the temporal wave-form of the modulation (i.e. sinusoidal or square-wave). These responses that do not involve light flux changes are thought to be caused by a different mechanism that requires the cortical processing of certain stimulus attributes. Neural activity in the cerebral cortex may cause a transient weakening of the constant central sympathetic inhibition to the parasympathetic neurones resulting in a brief pupillary constriction caused by the increased parasympathetic tone to the sphincter muscle.

Studies in patients with lesions to specific areas in the brain (chapters 5 and 6) explore further the different pupil response components and the role of both subcortical and cortical signals in pupil size regulation. Pupil measurements in patients with damage to pretectal areas in the dorsal midbrain (Parinaud's syndrome) confirm, as has been suggested previously in numerous animal studies, the pretectum as the main neural complex mediating the pupil light reflex. However, the pupil is also influenced by the level of cortical processing as it is revealed by pupillary deficits in patients with damage to cortical visual areas.

The results from these studies suggest that both cortical and subcortical contributions to the pupillomotor response depend strongly on the attributes of the visual stimulus, i.e. luminance contrast, colour, stimulus size and temporal modulation. The cortical involvement in pupil size regulation is also consistent with the longer response latencies found in normal subject to isoluminant colours and gratings.

Finally, chapter 7 considers the potential application of stimulus-specific pupil responses in the assessment of neurological disorders such as optic neuritis (ON) and multiple sclerosis (MS). ON and MS are characterised by remitting and relapsing demyelinative phases of neural axons. Monitoring accurately disease progression in optic neuritis is of great interest given the high risk of developing multiple sclerosis (MS), a more serious neurological disorder. We found that despite significant improvement in visual function (colour vision, visual acuity and fields) important pupillary deficits often remain even after 6 months from the initial attack. Pupil responses to isoluminant coloured stimuli were more affected than the responses to luminance modulation. These results could also reflect differences in the underlying neural pathways: neurones processing luminance contrast signals have generally thicker axons and myelin sheaths than neurones carrying chromatic signals (Reese & Cowey 1988, Kaplan et al 1990) and this could provide them with greater resistance against demyelination. In addition, thick axons are probably less susceptible to a complete blockade of the transmitting neural signals during inflammation or compression of the optic nerve. Recently, direct axon counting in post-mortem examination (Evangelou et al 2001) and studies combining both MRI and visual psychophysics (Caruana et al 2000) in MS patients have also found evidence that supports this hypothesis.

Chapter 1: Anatomy and Physiology of the Visual System

This chapter aims to give a basic description of the anatomy and physiology of the neural visual pathways from the retina to the visual cortex, in the occipital pole of the brain. The next chapter will review in more detail the current knowledge of the subcortical pupillary pathways to the pretectum in the mid-brain and the role of the pupil in visual performance.

Both visual and pupillary fibres leave the retina through the optic nerve, with roughly half of the fibres crossing over at the optic chiasm to join fibres from the contralateral eye to form the optic tract (Fig. 1.4). Visual fibres travel in the optic tract and synapse in the LGN, then continue through the optic radiation to reach the primary visual area or V1 in the occipital cortex (Zeki 1993). Pupillary fibres, however, leave the optic tract before reaching the LGN and run, via the brachium of the superior colliculus, into the Olivary Pretectal Nucleus (OPN), a neural complex in the dorsal mid-brain mediating the pupil light response (see Fig 2.2 in the next chapter for a detailed diagram of this sub-cortical neural pathway and major neural complex in the mid-brain).

1.1 Photo-transduction in the retina

The light entering the eye travels through the ocular media (cornea, aqueous humour, lens and vitreous humour) and is focused onto the photoreceptor layer of the retina where it is absorbed inducing a chain of neurobiological reactions. The light has to travel through almost the entire thickness of the retina before being absorbed by the visual pigment in the photoreceptors (rods and cones) just anterior to the retina pigment epithelium (Fig. 1.1).

Adapted after Hubel (1998) and webvision (http://webvision.med.utah.edu).

GC-Ganglion cell H-Horizontal cell A-Amacrine cell

1. Pigment epithelium	6. Inner nuclear
2. Rod and cone layer	7. Inner plexiform
3. Outer limiting membrane	8. Ganglion cells
4. Outer nuclear	9. Optic nerve fibres
5. Outer plexiform	10. Inner membrane
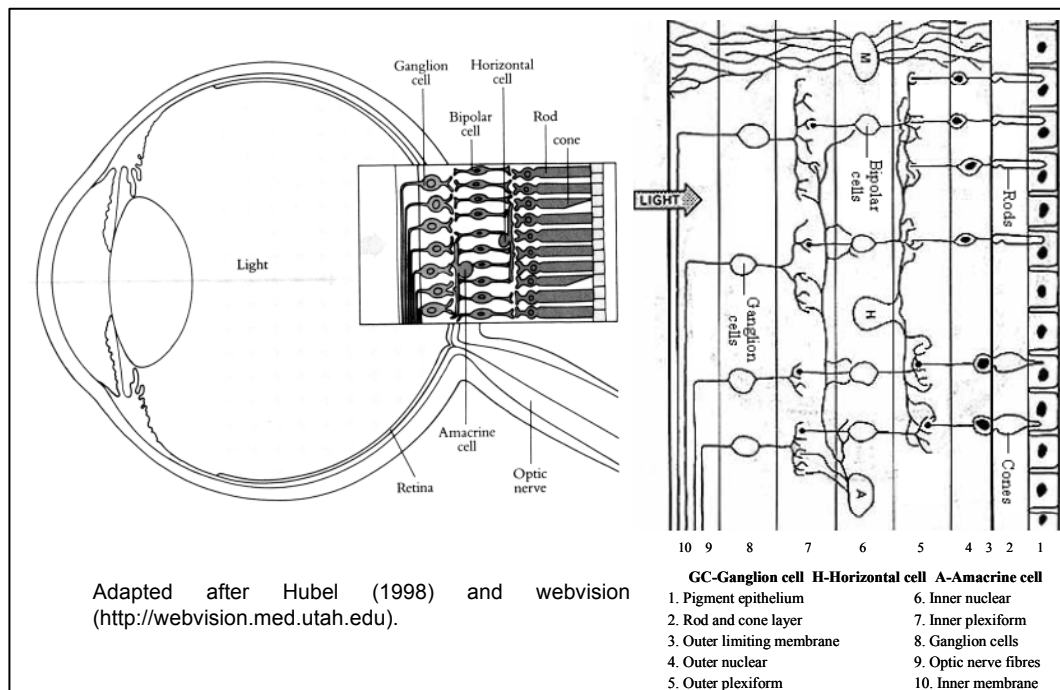
Fig. 1.1 Lateral view of the retina. Light entering the eye must travel through several layers of tissue containing various types of cells (ganglion, amacrine, bipolar and horizontal cells) before reaching rods and cones in the photoreceptor layer at the back of the retina. The retina is traditionally divided into 10 different histological layers (right).

Upon the absorption by rods or cones, the light energy is transduced into electrical nervous impulses that leave the retina via the optic disc to form a bundle of terminal fibres or axons from retinal ganglion cells known as the optic nerve. The optic nerve carries the signals from the retina to visual cortical areas in the occipital lobe of the brain. The detailed neural pathway is intricate but great progress has been made in the last few decades. There are several books worth reading that give an up-to-date detailed description of the current state of knowledge and recent research. See for example the books by Davson (1980), Dowling (1987), Hubel (1988), Rodieck (1998) and Levine (2000). Another good source containing thorough reviews of the visual pathways is the webvision site at the University of Utah (http://webvision.med.utah.edu).

1.2 The retina

The retina is a thin layer of neural sensory tissue that covers the whole of the posterior pole of the eye. It joins to the ciliary body at the ora serrata and is well attached at the optic nerve head and ciliary body. The inner boundary of the retina is in contact with the hyaloid membrane of the vitreous, with the outer surface bounded by the choroid. Near the centre of the retina lies an oval, yellowish area with a central depression known as the macula lutea. This is the location of the fovea centralis, where visual acuity is highest (Davson 1980).

The intrinsic layers and connections of the nerve cells in the retina were first drawn by the spanish anatomist Ramon y Cajal in 1909. Histologically, the retina is a complex ten-layered structure containing a wide variety of cells. The most common and better studied of these cells are: photoreceptors (rods and cones), bipolar cells, ganglion cells, horizontal cells, amacrine cells and Muller cells (see labels on Fig. 1.1).

Spectral sensitivity of rods and cones

The primary sensory neurones in the visual pathway are the photoreceptors, namely the rods and cones, where light is transformed in electrical impulses (phototransduction). Together with their outer segments, end organs, perikarya, axonal processes and synapses, the photoreceptors constitute the rods and cones layer, the external limiting membrane, the outer nuclear layer and the outer plexiform layer, spanning almost half the layers of the retina. However, light has to travel through nearly the entire thickness of the retina to reach the visual pigments, which are located in the outer segments of the photoreceptors (Fig. 1.1).

The visual pigment in the rods is rhodopsin (Rushton 1962), which gives a purplish-red colour to the living retina. When the retina is exposed to light it becomes white and semi-transparent, a phenomenon known as bleaching (Davson 1980). Rhodopsin is sensitive to blue-green light with peak wavelength sensitivity at 498nm (Fig. 1.2). Rods are highly sensitive and very effective in dim conditions at night (scotopic vision). However, with the presence of only one visual pigment, rods are essentially monochromatic.

Cones, on the other hand, contain three cone opsins as their visual pigments: erythrolabe, cholorolabe and cyanolabe. These are maximally sensitive to 567nm, 535nm and 450nm respectively and are frequently referred to as long (L-cones), medium (M-cones) and short wavelength (S-cones) cones (Stockman & Sharpe 2000, Stockman et al 2000, Wyszecki & Stiles 1982). Surprisingly, all the wavelength information in the visible spectrum (390-700 nm) can be encoded only by these three different cones types. There is no need for a vast number of colour-specific photoreceptors for each colour since is the ratio of the three L, M and S cone signals, which ultimately gives rise to colour perception. For example, two monochromatic lights of different wavelengths may appear as different colours, despite both excite the same L and M cones, just because the ratio of the two signals will be different. The broad, overlapping wavelength sensitivity curves of cones (see Fig. 1.2) mean also that two lights with different spectral composition (containing different wavelengths), can elicit identical L, M and S cone signals and thus

cause the same colour sensation (metameric colours). Cones also provide high visual acuity at the fovea under photopic (high luminance) conditions.
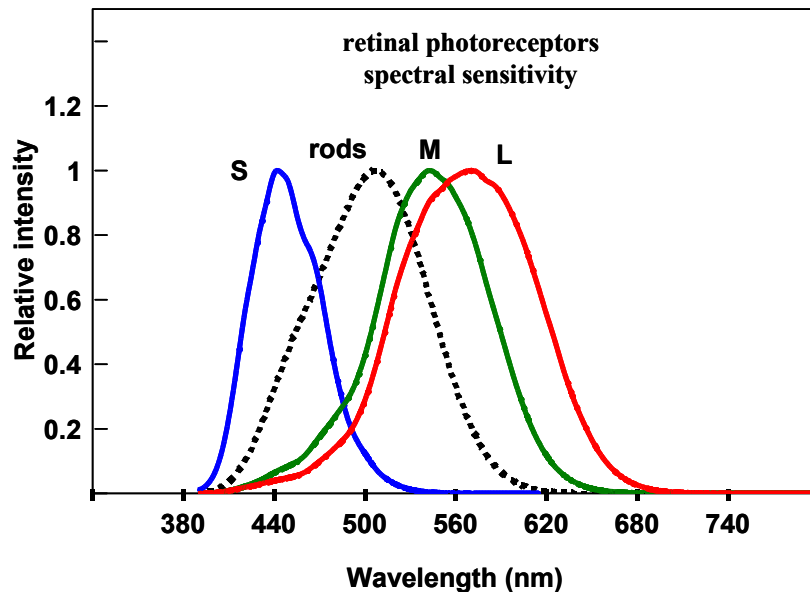
Fig. 1.2. Relative wavelength sensitivities of rods and L, M and S cones. S or 'blue' cones actually absorb maximally in the green-yellow region. So cones are often labeled according to the peak of their wavelength sensitivity (in the graph L, M, S refer to long, middle or short wavelengths respectively). Source: cone data from Stockman et al. (2000) and rod data from Wyszecki & Stiles (1982).

Distribution of rods and cones with retinal eccentricity

Osterberg (1935) estimated that there are about 110 to 125 million rods and 63 to 68 million cones in the human retina. Their distribution is different, with the cones being densest at the foveola, where they achieve a minimum spacing of 2 to 3µm centre to centre, being hexagonally packed (Wassle & Boycott 1991). This accounts for the high acuity at this specialised area of the retina where the bipolar and ganglion cells are displaced away from the foveola centre to reduce scattering of light. Cone density, and thus acuity, falls steeply with increasing eccentricity and is an order of magnitude lower 1mm (10°) away from the foveal centre (Fig. 1.3). The highest rod densities are located along an elliptical ring at the eccentricity of the optic disc (15 to 20°), decreasing 15-25% where the ring crosses the horizontal meridian. Blue cones are sparse and irregularly spaced and are missing in an area of 100µm in diameter near the site of the peak cone density (Gegenfurtner & Sharpe 1999, Curcio et al 1991). These results are consistent with psychophysical reports of foveal tritanopia (Wald 1967).
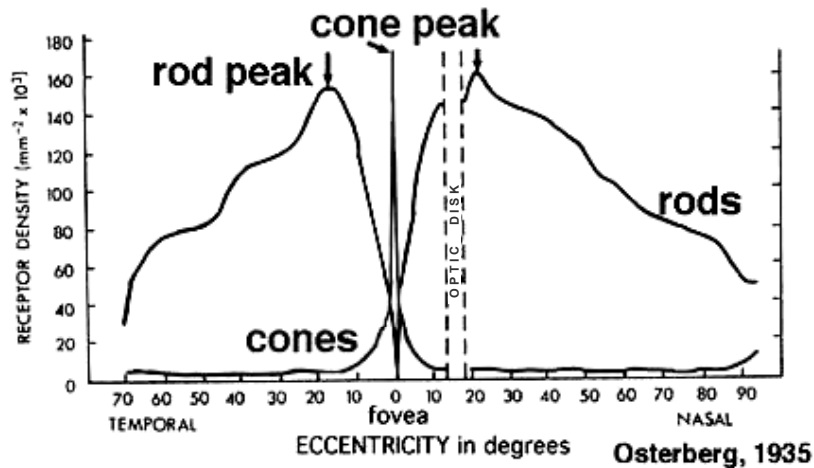
Fig. 1.3. The distribution of rods and cones varies dramatically with retinal eccentricity. Cone density is maximum at the foveola, a rod-free area covering 1 degree of the central visual field, where cone spacing can be as small as 0.5 min of arc (Wandell 1995). Outside the fovea (>5 degrees from the centre of the visual field), cone density and thus acuity falls abruptly. Source: Osterberg 1935.

1.3 Horizontal, amacrine and bipolar retinal cells

Horizontal cells

The electrophysiological response of horizontal cells in response to illumination of the retina are known as S-potentials (after Svaetichin who discovered them in 1953). These responses are sustained or graded as opposed to the brisk and transient action potentials of the ganglion cells. Horizontal cells have relatively large, homogeneous receptive fields, and play a vital role in forming the receptive field surrounds of retinal bipolar and ganglion cells by means of inhibition. The dendrites and axons of these interneurons traverse the outer plexiform layer, forming synaptic contacts with the rod spherules or cone pedicles and bipolar cells, and via gap junctions at the tips of their dendrites with each other (Gray 1995).

Amacrine cells

Amacrine cells were so named by Cajal (1909) because these cells consist only of dendrites and lack axons. Their cell bodies form the inner nuclear layer (layer 6 in Fig. 1.1) together with the nuclei of bipolar and horizontal cells, while the dendrites of these cells contribute to the inner plexiform layer (layer 7 in Fig. 1.1), synapsing with dendrites of ganglion cells. They respond primarily with transient and depolarising potentials. However some amacrines give sustained responses which can be hyperpolarising or depolarising.

Bipolar cells: centre-surround

Bipolars are neurones with one large dendrite. Typically they synapse with a single cone (cone midget bipolars), several cones (cone diffuse bipolars) or several rods (rod bipolars). There are at least nine types of bipolar cells in humans, differing in their connectivity, electrophysiological properties and immunochemical compositions (Wassle & Boycott 1991, see also chapter 8 in Gegenfurtner & Sharpe 1999 for a review). The responses of the bipolar cell, like those of the receptors, are graded potentials. They are classified into two main electrophysiological groups: ON bipolar cells which depolarise when light falls approximately within their dendritic field and hyperpolarise when it falls in the area surrounding the cell centre, and OFF bipolar cells which show the opposite polarisation under the same conditions. (For a recent review of bipolar cells and retinal circuitry see Gengenfurtner & Sharpe 1999).

This spatial centre-surround antagonism in bipolars concentric receptive fields is also found in retinal ganglion cells (see section 1.5 later) and is an important concept in visual processing. Thus, the response of a bipolar cell depends on the distribution of the light in its receptive field and not simply on the total amount of light incident on it. Bipolar cells, therefore, are the first cells in the visual pathway to contribute to contrast discrimination (Levine 2000).

1.4 Retino-geniculate pathway

The optic nerve, optic chiasm and optic tract

Visual signals leave the retina via the ganglion cells axons through the optic disc to form the optic nerve. The optic disc is therefore an insensitive area to light as it contains no photoreceptors. It lies about 3 mm nasal to the macula and its projection into the visual field is known as the blind spot, located about 15 degrees away from the nasal plane and 2-3 degrees below the horizontal meridian (Palmer 1999, Rodieck 1998).
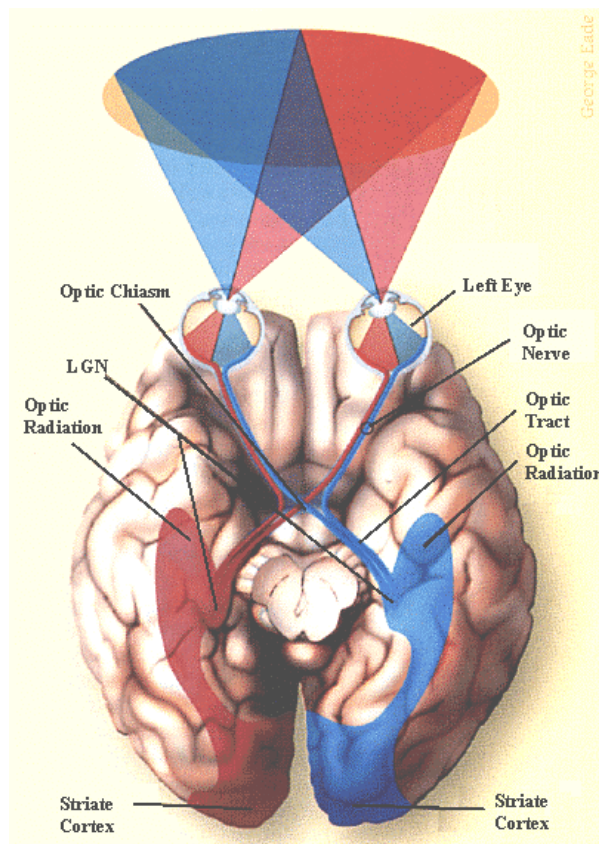
Fig. 1.4. Dorsal view of the visual pathways. Retinal visual signals have their first synapse in the dorsal lateral geniculate nucleus (LGN) of the hypothalamus and then travel, via the optic radiations to cortical visual areas in the occipital lobe. Source: Washington University web page.

The optic nerve extends posteriorly from the back of the ocular globe at the optic nerve head to the optic chiasm in the cranial cavity (Davson 1980). At the optic chiasm, nerve fibres from the nasal side of the eye, where the temporal field of view is projected, decussate or cross over to join the temporal fibres from the other eye mapping the same visual hemi-field (Fig. 1.4). Partial decussation of the nasal retinal fibres was first suspected by Isaac Newton, who emphasized the value of such arrangement for binocular vision and this was indeed later confirmed anatomically by Cajal (1909).

Fibres leaving the optic chiasm form the optic tract, which contains axons of ganglion cells from both eyes mapping the same contralateral visual field. The nervous impulses

then travel via the optic tract to the first synapse in the visual pathway, the lateral geniculate nucleus (LGN) of the thalamus. The axons of the thalamic neurones leave the LGN to form the optic radiations and project through the cerebral white matter towards the primary visual cortex (V1) in the occipital lobe (Hubel 1988, Zeki 1993) . From V1, visual signals travel to other areas in the cortex such as V2, V3, V4 and MT where further analysis of the visual scene takes place. In fact, there are more than 30 areas in the brain involved in visual perception (see for example Fig. 1.1 later in this chapter), including subcortical areas and the parietal and temporal lobes of the brain (Van Essen et al 1992).

1.5 Retinal ganglion cells

The inner nuclear layer (layer 8 in Fig. 1.1) is made up of ganglion cell bodies, and the nerve fibre layer (layer 9) is made up of ganglion cell axons. Fibres of the optic nerves arise from these retinal ganglion cell axons. Each ganglion cell receives inputs from a close-spaced and roughly circular group of photoreceptors that form the receptive field in that cell (Hubel 1988). The number of photoreceptors connecting to each ganglion cell varies enormously with retinal eccentricity from a 1:1 ratio in the fovea to 120:1 in the peripheral visual field (Rodieck 1998). This results in an increase in the receptive field size of ganglion cells and hence a reduction in spatial resolution from fovea to periphery (see later Fig. 1.6).

ON and OFF centre-surround receptive fields

Most of the work on ganglion cells receptive fields was done by Kuffler (1953), who used small spots of light to map the receptive fields of ganglion cells in the cat retina. He observed that ganglion cells receptive field were not uniform but consisted of a small central circular region surrounded by an annulus, a centre-surround configuration (Fig. 1.5). He described one type as "ON-centre" with the central region being excitatory, where an increase in illumination resulted in higher neural firing rates. ON cells were surrounded by an inhibitory surround, where an increase in illumination caused a reduction in the discharge of the central region. Kuffler also found "OFF-centre" cells in which light on the centre inhibited the cell's response and light on the surround increased the firing rate. The discharge pattern of a ganglion cell depends on the summed effects of interacting inhibitory and excitatory pathways (Kuffler 1953). The centre of the receptive field seems to correspond to the spread of the ganglion cell dendritic tree (Amthor et al 1989, Lee 1996, Dacey & Brace 1992) and the surround must reflect lateral interactions carried by amacrine and horizontal cells from neighbouring photoreceptors. Ganglion cells can therefore detect local increments and decrements in light intensity. This sensitivity to contrast changes is the base of a built-in edge-detection mechanism, amplified in cortical cells, which forms the basis for the recognition of shapes and objects in the visual scene.

A surprising characteristic of ganglion cells is that, even when the retina is in total darkness, they are never silent. They always maintain a spontaneous firing activity (Schellart & Spekreijse 1973). Spekreijse and collaborators have proposed that this spontaneous firing would allow a ganglion cell to respond to light with either excitation (ON region) or inhibition (OFF region), since the inhibitory component could be better revealed by a reduction in the averaged spontaneous firing rate.
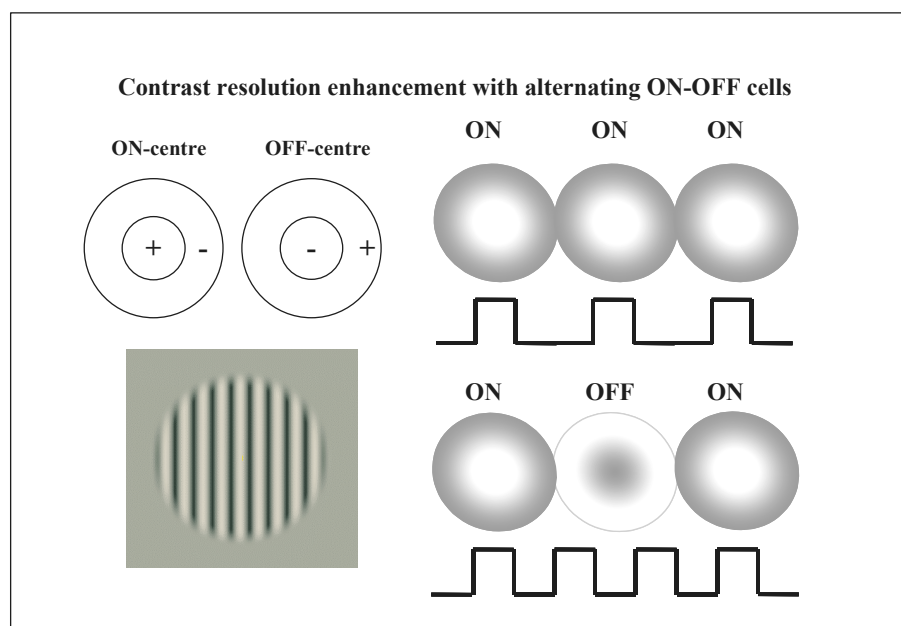
Fig. 1.5. The centre-surround receptive fields of the retinal ganglion cells in the optic nerve are sensitive to local light changes (contrast) and thus constitute the first stage of edge detection which forms the basis for the recognition of objects in the visual scene.

The receptive field of ganglion cells results from the initial photoreceptor and bipolar cell response and the interactions with the horizontal and amacrine cells of the retinal layers. In other words, the receptive field is the area of the retina that is sampled by the ganglion cell. The interactions amongst the cells of the retina produce a roughly circular centre-surround organisation of receptive fields in most retinal ganglion cells. The key feature of this organisation is that the cells respond optimally to differential illumination of the centre and surround of the receptive field. Because of this antagonistic centre-surround organisation, light stimulation of the entire receptive field (both centre and surround) produces a weak response. Therefore, the receptive fields of retinal ganglion cells are organised to respond to differences between illumination of the centre and surround (Kandel et al 2000).

If the retina had only ON but not OFF receptive areas, ganglion cells will act as mere luminance detectors and the signal reaching the brain will be proportional to a luminance-intensity profile of the retinal image. However, the intensity profile of a picture does not contain much information of the objects in the visual scene; it is the local contrast changes or edges which make the basis for object recognition (Fig. 1.5).

Response properties of X, Y and W cells in cat's retina

In the early 1960s, ganglion cells in the cat's retina were considered fairly homogeneous in properties except for their centre-surround receptive field organisation. Nothing was known about the temporal response or functional specificity of these cells in the visual system until Enroth-Cugell & Robson (1966) recorded electrical responses of "ON" and "OFF-centre" ganglion cell fibres to a grating. They proposed a classification with two major classes of ganglion cells, which they called X and Y cells. A third class of ganglion cell was described by Stone & Hoffmann (1972), which were labelled as W cells.

Anatomically, the largest fibres were the Y cells (4μm). X cells were between 2 and 4μm and the smallest fibres, the W cells, were less than 1.5μm in body size. X cells were mostly concentrated in the area centralis, had small receptive fields and were most sensitive to fine gratings. For these reasons, it was suggested that they provided high resolution acuity. Their response depended on the phase of the grating, showed relative slow conduction velocities (15-23 m/s) and a sustained firing rate throughout the stimulus presentation. On the other hand, the larger Y cells showed a transient firing activity

mainly at stimulus onset or offset, respond to all phases of the grating with fast (30-40 m/s) axonal conduction velocity (Enroth-Cugell & Robson 1966, Enroth-Cugell et al 1983).

X cells also produced relatively poor response to rapid moving stimuli, whereas the Y cells responded well to rapid flicker or stimulus motion (ie. high temporal frequencies), suggesting that Y cells may be important for motion discrimination. W cells were described as sluggish (Stone & Hoffman 1972, Sur & Sherman 1982), as they showed extremely slow axonal velocity (2-18 m/s).

Colour was not considered in the stimuli used in these studies with cats, presumably because cats only have a very rudimentary colour vision. Hubel & Wiesel (1960) found that the receptive fields of retinal ganglion cells in the spider monkey, which is probably closer to man than cats, also had concentric receptive fields similar to that of cat ganglion cells. Other investigators (de Monasterio 1978b, Shapley et al 1981) also found a similar functional segregation in the retinal ganglion cells of primates; the P and M cells as the analogous equivalent of X and Y cells in cats.

Sustained (X) and transient (Y) visual mechanisms

The marked different characteristics of X and Y cells forged the idea that the visual pathway can be regarded as a group of parallel channels, each processing a different aspect of the visual input. X and Y cells also differ in their temporal response properties or firing rate activity; X cells have a sustained firing throughout stimulus presentation, whereas Y cells fire transiently at stimulus onset, offset or both (Cleland et al 1971). Thus, transient cells can be ON, OFF or ON-OFF (Barlow 1979, Barlow et al 1964). This differences has also led to a new broad distinction between sustained (slow) and transient (fast) visual mechanisms. The terms sustained and transient have been used in a wide variety of experiments from electrophysiology to psychophysics and sometimes are even used regardless of the neural substrate underlying the two mechanisms (Ikeda & Wright 1972, Kulikowski & Tolhurst 1973, Tolhurst 1975). However, the separation between sustained and transient mechanisms can be ambiguous since the same cell's responses can often been classified as sustained or transient depending on the stimulus frequency, contrast and size (Lennie 1980).

Retinal ganglion cells in primates

Parasol (Pα) and Midget (Pβ) projections to Magno and Parvo layers of the LGN

Primate retinal ganglion cells were later also classified according to cell body size and the shape and extension of their dendritic tree. Based on this morphological categorization, there are more than 20 different retinal ganglion cell types in primates (Rodieck 1998). However, attention has been focused on two of the most numerous cell types; these are the parasol or Pα cells which have large cell bodies and widespread dendritic trees and the midget or Pβ ganglions cells with smaller cell bodies and less extensive dendrites (Fig. 1.6). These two groups were the primate equivalent of X and Y cells in the cat and were labelled as P and M cells by de Monasterio et al. (1976) because of their respective projections to the Parvo and Magno-cellular layers in the LGN. M cells are sensitive to low contrast, responds transiently and have axons which conduct very rapidly (like Y cells in cats). The smaller P cells show a slower sustained firing response, linear contrast gain and spatial summation (like X cells). However, a fundamental difference to the X cells of cats, is that many of the P-cells are wavelength sensitive with colour opponent properties (de Monasterio 1978a, Shapley et al 1981, Kaplan et al 1990). See Table 1-1 for a summary of retinal ganglion cells properties.
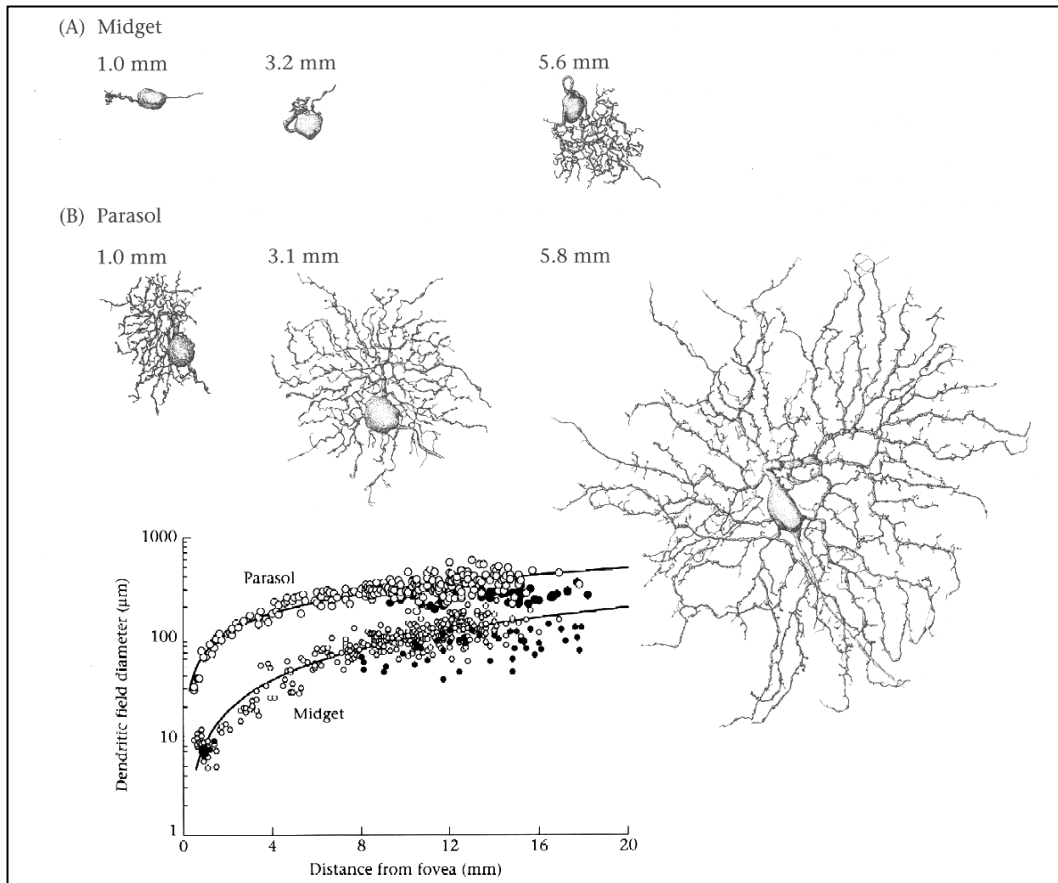
Fig. 1.6. Camera lucida drawings of midget (A) and parasol (B) retinal ganglion cells at three different distances from the fovea. The midget dendritic trees are smaller and denser at any retinal eccentricity than parasol cells, providing a much finer sampling of the retinal image (1 mm equals about 1 degree of visual angle at the fovea). Dendritic trees, and thus receptive fields for both midget and parasol cells, increase significantly with retinal eccentricity (bottom left). Adapted from Wandell (1995) after Watanabe & Rodieck (1989).

Receptive fields of M and P retinal ganglion cells

Each M and P ganglion cell populations include both ON-centre and OFF-centre cells. However, their receptive fields, largely determined by the extension of their dendrites, differ significantly. The dendritic field size increase substantially with retinal eccentricity for both M an P type cells (Fig. 1.6). M cells dendritc field is about 5-10 times larger than that of P cells at any eccentricity. For example, near the fovea, the average receptive field diameter for P cells is about 0.03° while that for M cells is approximately 0.06°. This disparity in the size of receptive fields influence each cell response properties, particularly their sensitivity to fine spatial frequency gratings and spatial summation (the increase of a cell's response with stimulus size). The smaller receptive fields and greater packing density of P cells give this cell class the optimum characteristics for the identification of fine detail (Rodieck & Watanabe 1993, Watanabe & Rodieck 1989).

Ganglion cells properties	Parvocellular (X)	Magnocellular (Y)
Retinal ganglion cell type	Midget	Parasol
temporal response	sustained	transient
axon conduction velocity	slow	fast
contrast sensitivity	poor	good but saturates
field size	small	large
spatial summation	linear	Mx linear, My non-linear
Layers in LGN	3,4,5,6	1,2
Layers in V1	4A, 4Cβ	4Cα
colour selectivity	many cells	none

Table 1-1 Summary of response properties of the Parvo (P) and Magno (M) retinal ganglion cells in primates and their correspondence with the X and Y cells in the cat (Kaplan et al 1990, Rodieck 1998).
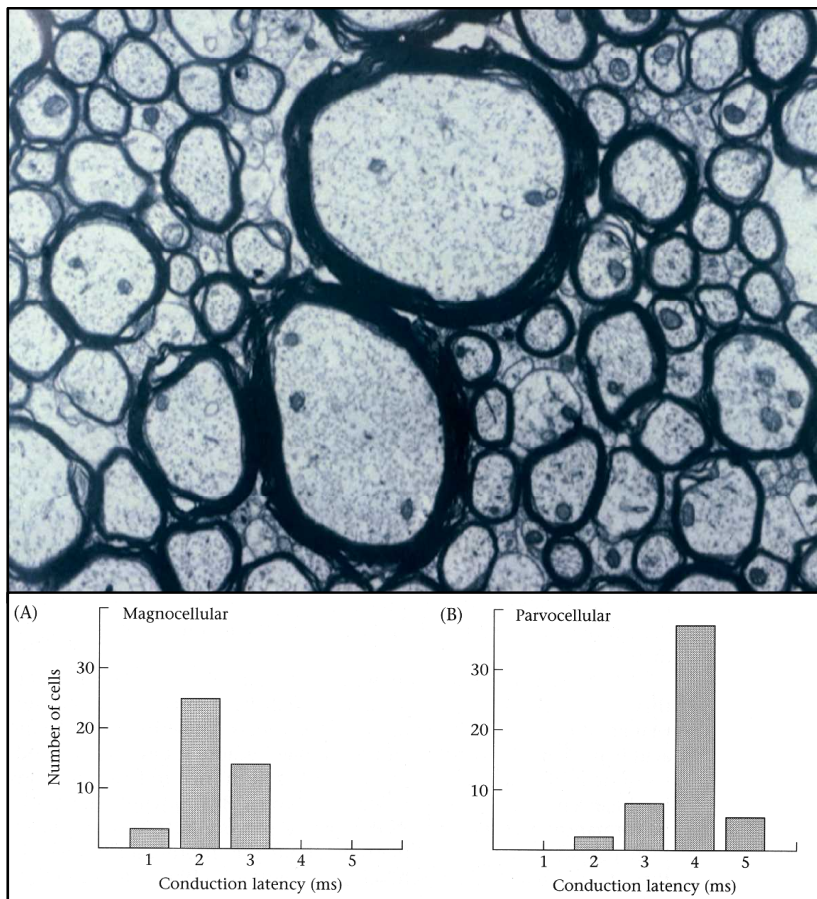
Fig. 1.7. Cross-section of monkey's optic nerve. Thick axons, from M cells, usually have thicker myelin sheaths than P cells. Myelin improves the speed of nerve transmission, resulting in shorter latencies for M cells (bar plots, after Schiller & Malpeli 1978). This morphological differences might also explain the greater resistance of M cells to demyelinating diseases such as optic neuritis (see discussion in chapter 7). Micrograph courtesy of Dr. Gary Baker, City University, London.

Morphological and functional segregation of axons in the optic nerve

There is a general trend for the bigger ganglion cells to have larger diameter axons than smaller cells in the optic nerve. Hence M cells in the retina, typically result in larger diameter axons in the optic nerve than P cells. In addition, the thickness of the myelin sheath (the fatty insulating wrap around axons that enhances nerve impulse speed) is correlated with the diameter of the axon so that larger axons usually have thicker myelin sheaths (Van Crevel & Verhaart 1963, Perry et al 1984, Guillery 1988).

This morphological segregation of axons has important implications in lesions affecting the optic nerve (eg. optic neuritis, tumours or vascular lesions causing compressive damage). It has been suggested, for example, that smaller thin-myelinated axons are more susceptible to damage during demyelinating disorders such as optic neuritis and multiple sclerosis (Evangelou et al 2001, Hess & Plant 1986). Since the two population of cells P and M mediate different aspects of visual function, damage to the optic nerve could affect selectively certain visual tasks making thus possible the use of visual psychophysical tests to give an accurate and correct diagnosis of the disease as well as monitoring the recovery.

Re-ordering of axons in the optic tract

Although axons of different diameter are uniformly distributed across the whole section of the optic nerve, they become partially segregated in the optic tract (Guillery 1988). Small diameter axons are found across the entire optic tract, whereas large diameter axons tend to be found towards the base. This re-arrangement is, in fact, not surprising since larger axons project to the bottom layers of the LGN (magnocellular layers in Fig. 1.8). Thus, axons arising from M-type retinal ganglion cells are partially segregated from the majority of axons of P-type ganglion cells (Reese & Cowey 1988). This seems also to be the case in humans where the morphological and functional segregation of axons have similar implications that in case of damage to the optic nerve; that is, the possibility of selective visual deficits as a result of partial compression or lesions to the optic tract (Reese 1993).
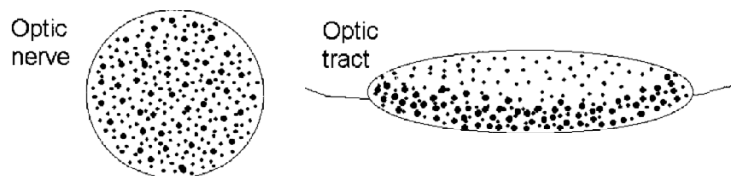
Fig. 1.8. Schematic representation of the distribution of small and large axons in the optic nerve and in the optic tract. Source: (Baker 2000)

Other ganglion cells in primates and terminology

The human retina contains between 1.1 and 1.3 million of ganglion cells but M and P cell types comprise only 10% and 80% respectively, of the total ganglion cell population. The remaining 10% of the cells with a retinal origin have various shapes and size of dendritic fields (eg. bi-stratified, parvicellular giant, etc.) that send axons to other areas in the brain than the lateral geniculate nucleus (Rodieck 1998).

Strictly speaking, the terms M and P should refer only to cells projecting to the LGN while Parasol (Pα) and Midget (Pβ) are more appropriate when describing cells with similar morphology to M and P projecting to other areas of the brain.

1.6   The lateral geniculate nucleus (LGN) of the thalamus

Anatomy and physiology

The lateral geniculate nucleus (LGN) of the thalamus is where retinal ganglion cells axons have their first synapse in the visual pathway. In monkeys, the dorsal and ventral

parts are clearly differentiated; the ventral nucleus consists only of a few dispersed neurones lying rostral to the dorsal (dLGN) nucleus (Polyak 1957). There is no ventral lateral geniculate nucleus in man; its equivalent being referred to as the pre-geniculate nucleus (Gray 1995).

The dome-shaped dorsal nucleus (dLGN) is classically described as a six-layer (laminae) neural complex in which the optic tract fibres terminate in a precise retinotopic pattern (Zeki 1993). These laminae are numbered 1 to 6 from the bottom to the top (Fig. 1.9). Laminae 1 and 2 consist of larger cells and are thus known as the magnocellular (M) layers, while layers 3 to 6, containing smaller cells, are known as the parvocellular (P) layers. Neurones from the ipsilateral eye, mapping the temporal visual field, terminate in layers 2, 3 and 5, whereas nasal field fibres from the contralateral eye terminate in layer 1, 4 and 6 after decussation at the optic chiasm (Kupfer et al 1967).

Fig. 1.9. Cross-section of the right LGN mapping the left visual hemi-field. Retinal inputs from each eye remain segregated to different layers. Layers 1 (right eye) and 2 (left eye) contain large cells and are thus known as the magnocellular layers. Layers 3 to 6 are called parvocellular layers and contain smaller cells. Input to layers 3 and 5 is from the ipsilateral (left) eye, while in 4 and 6 is from the contralateral (right) eye. From Hubel & Wiesel (1977).

Similarities between LGN cells in monkeys and X, Y, Z cells in cats

The parvocellular layers receive predominantly axons similar to cat's X cells (slow conducting and sustained firing throughout stimulus duration). Thus P cells have small receptive fields and are responsive to colour, fine detail and slow-moving objects. The counterpart of Y-cells (fast conducting and transient firing at stimulus onset and offset) are the M cells projecting to the magnocellular layers 1 and 2. M cells are up to ten times more sensitive to luminance contrast and movement than P cells, and have a larger receptive field size and also respond much faster than parvocellular cells (Kaplan et al 1990, Hubel 1988).

The equivalent of cat's W-cells (large receptive fields and slow responses) project mainly to the cell-sparse interlaminar zones separating the layers in the dLGN, known as koniocellular layers (Holdefer & Norton 1995, Dreher & Sefton 1979). Discontinuities in layers 1, 4 and 6 of dLGN were discovered by Kaas et al. (1973) and these were thought to correspond to the photoreceptors-free optic disc (blind spot) in nasal retina.

Retinal topography in LGN

Cells in each layer of the LGN are arranged so that the retinal topography carried by the ganglion cells are maintained. That is, each layer contains a neural retinotopic map whereby neighbouring regions of the retina project to adjacent regions. However, these

topographical maps are not uniform representations of the visual field. Central visual field is particularly well represented. This anisotropic representation arises essentially from the different densities of ganglion cells across the retina. Most ganglion cells are found in the central retina, while in the peripheral retina the cell bodies are much larger and cell density is lower. This disproportion in the amount of neural machinery dedicated to the representation of the central visual field and the periphery in the LGN is also reinforced in the visual cortex areas and is known as cortical magnification (Wandell 1995).

Thus, although the dLGN receives input from both eyes, synaptic connections from each eye are kept separated in ipsilateral and contralateral layers. The reason for this, is combine appropriately signals from each eye for stereoscopic vision, where different combinations reflect different depth planes.

Colour opponency of P cells in the LGN

M cells give similar responses over the whole spectrum and are, in general, not colour sensitive. P cells, however, are wavelength selective. Furthermore, the centre of a P cell receptive field often shows a different spectral sensitivity to that of the surround, and these are known as colour opponent cells.

The first detailed studies of chromatic sensitive P cells were carried out by De Valois (1966) who recorded from P cells in the parvocellular layers of the LGN in the macaque monkey, an animal whose colour vision is very similar to humans. They found that the excitatory response to a particular wavelength illuminating the centre of the receptive field is inhibited by a stimulus of another wavelengths on the surround. For example, a cell might have an excitatory response to red light incident on the centre of its receptive field and an inhibitory response to green light on the surround. These are designated as +R-G (Red ON, Green OFF). The converse of +R-G also exist; that is, cells that are inhibited by red light and excited by green (+G-R). De Valois also found receptive fields with blue-yellow opponency (+B-Y) and their reverse (+Y-B) in the LGN but surprisingly, the +Y-B cell type has never been found when recording directly from retinal ganglion cells instead of the LGN (Malpeli & Schiller 1978, Calkins 1999). Thus, the retina seems to contain only three types of colour opponent cells (+R-G, +G-R and +B-Y). All these chromatic-opponent P cells in the LGN have similar properties to the X cells in the cat, i.e. small cell size and a sustained firing rate (Dreher et al 1976).

Similar results to those of De Valois and collaborators were obtained in the LGN of rhesus monkey by Wiesel & Hubel (1966) who distinguished three types of cells characterised by the chromatic and spatial organisation of their receptive fields:

- Type I cells were the most common. They had concentric receptive fields but centre and surround regions have different spectral sensitivities. For instance, a cell response was boosted by red light incident on the centre and inhibited by green light incident on the surround (Fig. 1.10). The excitatory central region and the inhibitory surround wavelength sensitivity varied from cell to cell. This can be blue, yellow, green or red.

- Type II had spectral but not spatial opponency; that is, cells showed sensitivity to two wavelengths suggesting input from opponent cones but they did not have a differentiated centre-surround receptive field (Fig. 1.10). These were relatively uncommon.

- Type III had a typical centre-surround organised receptive fields to stimuli of the same wavelength, lacking any spectrally opponent organisation.
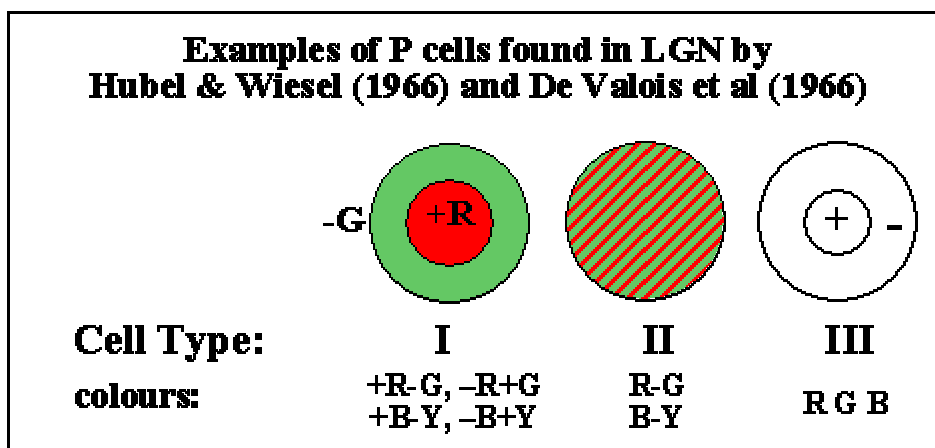
Fig. 1.10 Summary of colour sensitive P-cells found in the parvocellular layers of the LGN. R-red, G-green, B-blue, Y-yellow.

Even more complicated colour opponent cells appear later in the visual pathway, in V1 (Ts'o & Gilbert 1988) and V2 (Kiper et al 1997), probably as a result of interaction between different retinal ganglion cells (Levine 2000).

Colour opponency in the Koniocellular layer in the LGN

Some investigators (Lee et al 1989, Dacey & Lee 1994, Martin et al 2001) have suggested that midget ganglion cells are not the only cells mediating colour vision since recordings from midget cells in the peripheral retina prove that interactions between L and M cones are synergistic rather than antagonistic and therefore it is unlikely that they provide the input to spectrally opponent centre-surround cells found in the LGN. They propose instead that colour-opponent cells in the LGN receive their input from another population of cells whose uniform receptive field receive excitatory inputs from L-cones and inhibitory from M-cones or the converse. These cells have been reported previously in small numbers in the LGN (Type II cells, Wiesel & Hubel 1966) and project to the inter-laminar layers (koniocellular layers) of the LGN. They are also thought to project to the areas of visual cortex where double opponent colour cells are located (Ts'o & Gilbert 1988). This proposition has proven to be difficult to substantiate and needs further research. Another possible interpretation is that the antagonistic organization of midget ganglion cells is lost outside the fovea because peripheral 'midgets' are not truly midget ganglion cells at all; they receive more than one midget bipolar input and multiple cone inputs (Kolb et al 1997, Kolb 1991, Kolb & Dekorver 1991).

Cortical inputs to the LGN

It seems that there is roughly the same number of retinal axons entering the dLGN as neurones leaving it (Wolff 1997). However, only 10-20% of synapses onto geniculate neurones are from retinal input. Nearly 50% arise from descending inputs back from the cortex, and the remainder from local inhibitory and brainstem inputs (Suzuki & Kato 1966). Due to these inter-connections and probably some internal processing, LGN cells responses differ from those of retinal ganglion cells. Hence, the LGN is not simply a relay station in the visual pathway but a dynamic filter passing visual signals to the cortex (Kandel et al 2000). Unfortunately, the precise role of the internal processing, cortical feedback, and thus the function of the dLGN, is still poorly understood (Hubel & Livingstone 1990, Hubel 1988).

1.7 Functional organisation of the brain

The human brain, as opposed to that of other vertebrates, is characterised by its extraordinarily developed and convoluted structure. Higher-order processing of sensory input as well as planning and execution of complex psychomotor tasks takes place in the outer layers of the brain, the cortex. The cortex has numerous convolutions to maximise the area of the superficial layers. It is divisible externally into four areas, or lobes, divided by fissures (sulci) which separate raised regions (gyri). The four areas are: the frontal lobe anterior to the central sulcus, the parietal lobe lying behind this sulcus with its inferior limit defined by the lateral fissure, the temporal lobe as the area below the lateral fissure and the occipital lobe in the posterior part of the skull. The area of the brain associated with vision, the visual cortex, lies in the occipital lobe so retinal ganglion cells axons have to travel a long distance, via the optic radiations, to the posterior part of the head.

1.8 Visual striate cortex (V1)

Basic anatomy and physiology.

The primary visual cortex is probably the best understood of all cortical regions in terms of both anatomy and physiology. It occupies the region within the depth of the calcarine fissure and it is coextensive and most easily identified by the white line or *striae of Gennari*, a line formed partly by fibres from the optic radiation but mainly by intracortical connections and hence its alternative name, the striate cortex (see Fig. 1.4). It is also often referred to as V1 since it is the first stage of cortical visual processing, passing signals to higher cortical visual areas mediating other aspects of visual perception such as colour (V2), form (V4) and motion (V5).

A large number of neurones are dedicated exclusively to the processing of visual information. For instance, the primary visual cortex (4 mm thick) of an average human contains more than 10^{10} neurones in total, covering a surface of about 15 cm^2. Half of this area is dedicated to the detailed representation of the central 10 degrees (2%) of the visual field (Wandell 1995, Hubel 1988). This disproportion between the cortical and the retinal topographical mapping of the visual field is known as *cortical magnification* (Fig. 1.11).
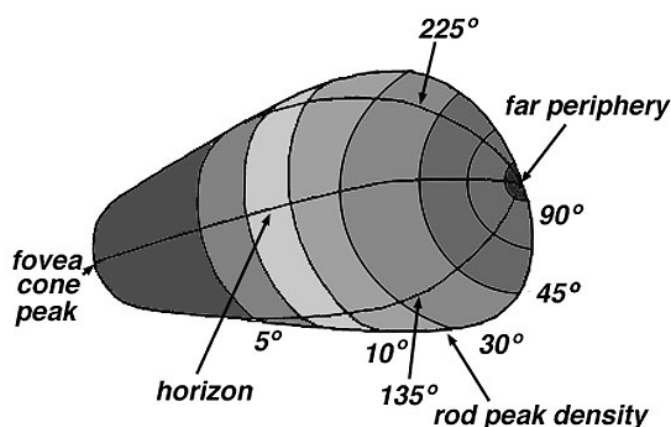
Fig. 1.11 Retinotopic organisation in V1. Like in the LGN, neighbouring cells respond to visual stimuli within adjacent areas of the visual field. The disproportion between the area dedicated to the central visual field in comparison with the periphery begins in the LGN but is exaggerated further in V1 (cortical magnification). Source: Erwin (1999).

Deeper layers and other cortical regions outside the main visual areas, the so-called association areas, are concerned with the integration of information from various cortical

and sub-cortical sources. It has been estimated that there are more than 30 different areas in the primate brain contributing to visual processing (Wandell 1995).

Neural projections to the visual cortex and blood supply

The major input to V1 comes from the magnocellular and parvocellular layers of the LGN whose axons terminate predominantly in layer 4 of V1. Initially, these long axons take a course through a region known as the internal capsule, which is the major route for connections to and from the cerebral cortex. There are two limbs to the internal capsule, the anterior and the posterior limb. The geniculo-cortical axons, which project from the LGN to the primary visual cortex, take a course through the posterior limb of the internal capsule to enter the optic radiations. The internal capsule receives most of its supply of blood through delicate branches of the middle cerebral artery. Cerebral thrombosis most commonly affects this artery or its branches, the lateral striate arteries. If thrombosis or rupture occurs in the branches of the posterior limb of the internal capsule, visual field loss or total blindness follows (Zeki 1993).

Cortical layers in V1

The primary visual cortex has a thickness of about 4 mm in humans and consists of six cellular layers, with an underlying white matter composed of the axons that carry the inputs and outputs to the region. Each cortical layer contains cells varying in size, response properties, and in their input and output connections.

- **Layer 1 - the molecular layer.** This is the most superficial layer and contains few scattered neurons.

- **Layer 2 - the external granular layer.** This contains small neurons that extend their axons only to deeper cortical layers.

- **Layer 3 - the external pyramidal layer**. This contains larger neurons that send axons mainly to other cortical regions, both at near and distant locations.

- **Layer 4 - the internal granular layer.** This consists mainly of stellate (granular) cells. It is sub-divided by the striae of Gennari into layers 4A, 4B and 4C. Layer 4B cells send axons to more superficial cortical layers in V1 as well as to other visual cortical areas. Layer 4C receives the predominant input from the LGN. This layer is further sub-divided in layer $4C\alpha$ and $4C\beta$. Neurones from the parvocellular layers (P cells) of the LGN terminate in 4A and $4C\beta$, whereas magnocellular cells (M cells) terminate in $4C\alpha$ (Hubel & Wiesel 1972). Layer $4C\alpha$ has strong connections with layer 4B, which sends a direct projection to V5 (Lund & Boothe 1975) an area associated with motion perception (Wandell 1995).

- **Layer 5 - the internal pyramidal layer.** This also consists of larger neurons and these cells send axons to the superior colliculus and other structures within the brainstem.

- **Layer 6 - the multiform layer.** As the name suggests, the cells are of various types with most of the axons projecting back to the LGN and other sub-cortical areas.

Therefore, the segregation between M and P cells in the LGN is retained in layer 4C of the primary visual cortex. This segregation is continued beyond the primary visual cortex, to higher visual cortical areas (Fig. 1.12). There are also cells that cannot be classified within the M or P type in the LGN which also project to V1. For example, axons from intralaminar zones (koniocellular layers) terminate in layers 1, 3 and 4A (Hubel & Wiesel 1972).

The primary visual cortex can thus be seen as the first stage in visual processing receiving input from the LGN and sending it to higher visual areas (V2, V3, V4 and V5) for

further processing. However, the visual pathways do not follow strictly a bottom-top or feed-forward architecture; V1 also contains horizontal connections and sends projections back to the LGN and other sub-cortical nuclei (Hubel 1988).
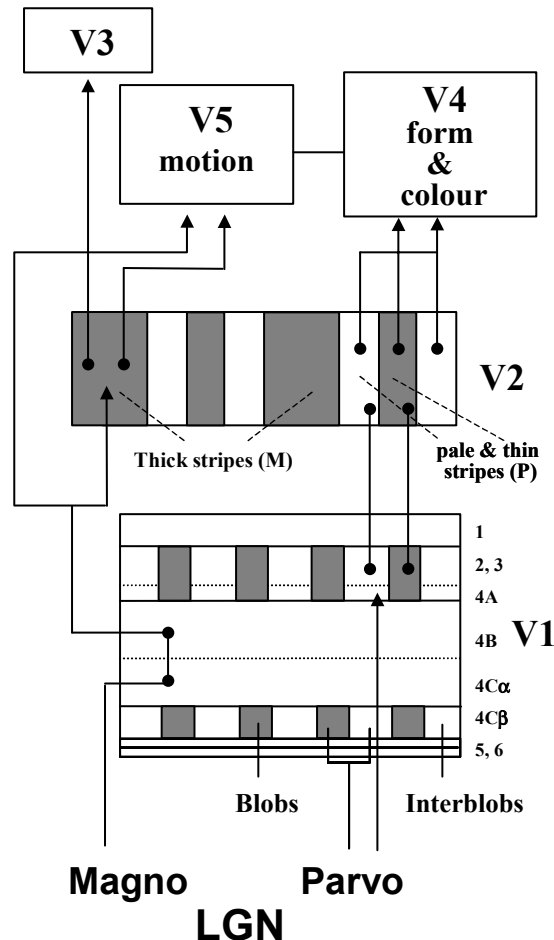
Fig. 1.12 Laminar organisation in V1 and projections to other cortical visual areas. Axons from the magnocellular layers of the LGN provide input to the cells in layer 4Cα in V1. After another synapse in layer 4B, they project to the thick stripes of V2. Parvocellular cells send their axons to anatomically distinct areas in V1: blobs (colour sensitive) and interblobs, which in turn project to the thin and pale (inter-stripes) stripes of V2. V2 distributes these signals for further processing to areas V5 (motion) and V4 (form and colour). Area V3 is still poorly understood. Adapted from Maunsell & Newsome 1987.

Receptive field properties in V1: simple and complex cells

Receptive fields of cells in the LGN, although not completely unmodified, resembled the arrangement of the receptive fields of their inputs, the retinal ganglion cells. That is, they have a concentric centre-surround organisation. In the primary visual cortex, only cells in layer 4C have this receptive field organisation. This is not surprising because layer 4 primarily receives inputs from the LGN. However, in most other parts of the primary visual cortex, the cortical circuitry transforms the concentric centre-surround receptive fields in to non-circular and more complex forms. The degree of this complexity varies, but the main difference is that cortical cells respond optimally when the stimulus is a bar of light or a line segment, as opposed to LGN cells sensitivity to small spots of light.

A number of anatomically different cells have been found in V1. Their electrophysiological properties vary according to the organisation of their receptive fields. Hubel & Wiesel (1959) divided these cells into 'simple' and 'complex' cells. A simple cell has a receptive field that is elongated with distinct ON and OFF regions and of similar width than the receptive fields of the geniculate input (Fig. 1.13). On the other hand, complex cell receptive fields are also elongated but larger. A complex cell receptive field

does not possess easily definable excitatory and inhibitory regions. In addition, their optimal response is often to a stimulus that moves across the receptive field, rather than a specific location within the field. Although it is by no means a strict rule, there appears a tendency for simple cells to be found close to layer 4, while complex cells are found at more distant locations from this input layer, in layers 2, 3, 5 and 6.

Simple cells and orientation selectivity

The shape of simple cells receptive fields was derived from experiments carried by Hubel & Wiesel (1959). They recorded responses from single cells in the V1 of cats in response to visual stimuli and discovered that most of the cells in this area remain silent or fire timidly to small spots of light, but respond vigorously to stimuli such as: long and narrow rectangles of light (slits); line borders between areas of different brightness (edges); and dark rectangular bars against an illuminated background. Thus, effective driving of a cortical cell requires stimuli specific in form, size and position, but above all, a precise orientation. Each cell has an optimum angle of orientation which evokes a maximum response only when the stimulus is oriented at a particular angle. If the stimulus is tilted or oriented orthogonally, the cell responds weakly.

The width of the excitatory region in simple cells is approximately the diameter of a LGN receptive field centre. This prompted Hubel & Wiesel (1977) to propose that the elongated receptive fields of simple cells arise from a convergent input of several geniculate cells (Fig. 1.13). This hypothesis was also supported by the observation that simple cells are grouped together in the cortical layer 4, where many of the LGN axons terminate.
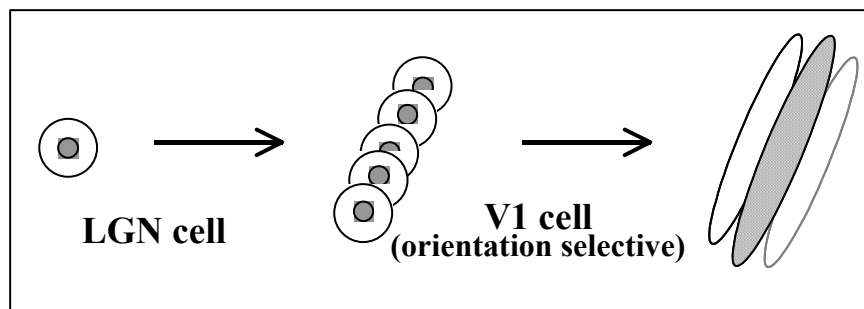
Fig. 1.13 The receptive field of simpl e and complex cells in V1 is determined by the input they receive from a number of LGN cells. Simple cells respond vigorously to a bar of light with the correct size, orientation and position within its receptive field. Complex cells are less restrictive regarding stimulus position; their response is not phase dependent (ie. does not depend on the phase of the stimulating grating).

Complex cells

Complex cells are found mainly in layers 2, 3 and 5 and were so named as their response to light could not be predicted from arrangements of excitatory and inhibitory regions. These are, essentially, more sophisticated cells, although they also exhibit orientation selectivity similar to simple cells (Hubel & Wiesel 1962). Slits, edges and dark bars, stimuli which activate simple cells, are also effective for complex cells. However, for complex cells, a stimulus is effective regardless of its position within its receptive field provided that it has the right orientation. Another difference is that inhibition of the surround of complex cells is also less effective than in simple cells. More importantly, complex cells are responsive to movement and show motion selectivity to particular directions. They respond only when the stimulus moves in one direction and not when it moves in an orthogonal direction. Complex cells have also larger receptive fields than single cells and thus may arise from projections of a number of simple cortical cells, all having the same receptive field arrangement and orientation.

The increasing complexity of both single and complex cells receptive fields may be the result of a convergent hierarchy from simpler receptive fields. For example, a simple cell

receptive field might be produced by a number of ON centre-surround inputs from simple cells, being aligned along an axis that determines the cell's orientation selectivity.

End-stopping (hyper-complex cells)

Even more complicated cells were discovered. These were initially labelled as 'hypercomplex' cells by Hubel & Wiesel (1965). They also responded to lines of specific orientation, but of limited length and thus their receptive field is characterised by the presence of an end-zone inhibition (end-stopping). However, hypercomplex cells are no longer considered a distinct cell class but either as simple or complex cells whose receptive fields are limited in length (Dreher 1972).

Columnar organisation in V1

Cells with similar functional or anatomical properties are often arranged vertically from the surface of the cortex to the white matter. These cortical columns can be defined on the basis of anatomical features (e.g. cells with similar morphology), functional features (e.g. columns of cortical cells all responding to the same stimulus orientation) or both. For instance, many types of columns have been proposed including ocular dominance, orientation, spatial frequency, and colour columns.

Generally, all the cells within a column respond to stimuli presented in one particular part of the visual field and cells in adjacent regions respond to stimuli within adjacent parts of the visual field. Hence, the retinal mapping of the visual field is relatively maintained in the visual cortex but, like in the LGN, the map metric is not uniform because of cortical magnification (more cortical area is dedicated to the detailed representation of the central region of the visual field than to the periphery, see Fig. 1.11).

Orientation and ocular dominance columns.

Cells down through the cortical layers (with the exception of the input layer 4) have an optimal response to stimuli with the same axis of orientation regardless of whether they are simple or complex. These are called orientation columns. Orientation columns are arranged in an ordered manner across the visual cortex and cells in adjacent columns of about 0.4 mm width have orientation preferences that differ only slightly (about 10°). There is a continuing progression of slightly different orientation preferences changing in the same clockwise or anti-clockwise direction in further distant columns (Fig. 1.14).

Another feature of cells in a column is ocular dominance. Visual signals from the two eyes remain segregated in the LGN and in the fourth layer of V1. This segregation can be observed by measuring the electrophysiological responses of the units in layer 4C. As the recording electrode is moved within layer 4C, there is an abrupt shift as to which eye drives the unit. Signals from these bands converge on individual neurones in the superficial layers of the cortex, thereby forming columns dominated by one eye or the other in an alternating fashion. These so-called 'ocular dominance columns' are wider (0.5 mm) than orientation columns (Fig. 1.14). The degree of ocular dominance may range from complete monocular preference to merely preference of one eye over the other.

Both retinotopic and columnar organisation provide the architecture for analysing individual components of the visual scene, according to a number of key features. Only one of these features, orientation specificity, has been covered so far. The subject will now be expanded to examine how other features, including detection of movement and colour, appear to be specialised in different cortical areas.
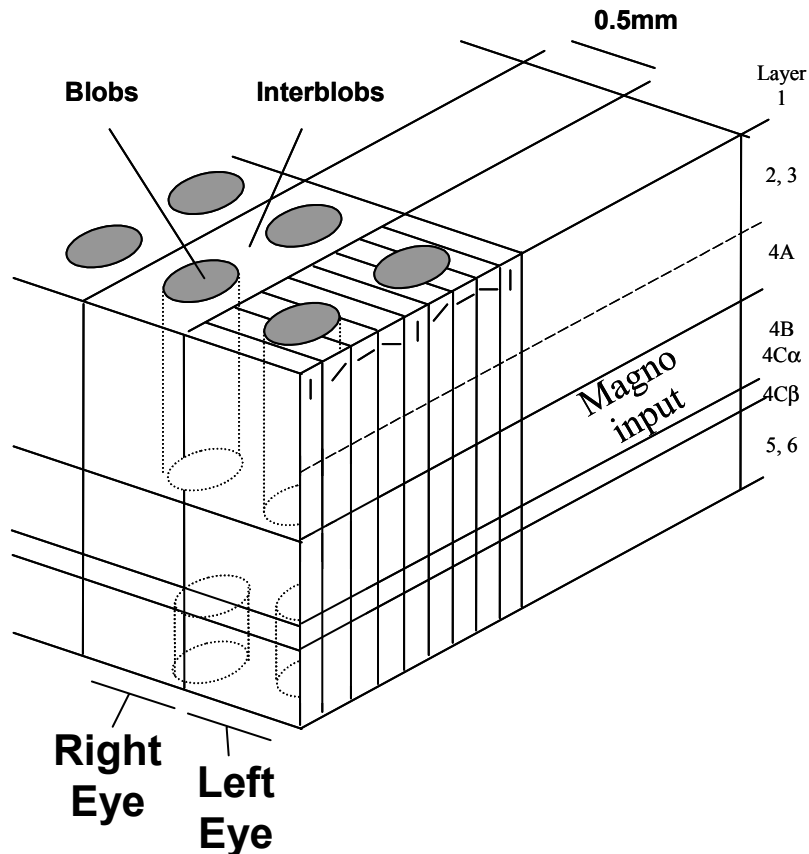
Fig. 1.14 Structural organisation of orientation and ocular dominance columns in V1. Cells inside the blobs do not have a preferred orientation but depend on stimulus colour. Redrawn after Zeki (1993).

Functional segregation in V1: blobs and inter-blobs

By the early 1960s, V1 was already known to have a complex structure in which cells processing similar features of the visual scene were arrange along the same line through all the cortical layers. Hubel & Wiesel (1977) coined the term 'hypercolumns' to refer to pairs of ocular dominance columns, one for each eye, containing all possible orientations of receptive fields.

Further evidence for functional segregation in V1 came in 1978 when Margaret Wong-Riley (1979) discovered that staining slices of V1 with cytochrome oxidase (CO), an enzyme used as cell activity indicator, reveals a striking array of CO-stained and non-stained regions. She observed that layer 4C of the cat's V1 stained darkly, 4B stained lightly, and 4A revealed dark stained patches which extended in a columnar fashion through layers 1 and 3 and are also found marginally in layers 5 and 6. These CO rich patches or columns are commonly known as 'blobs' and the non-stained regions as 'inter-blobs' (Fig. 1.14). The blob-interblob regions are located in the middle of each ocular dominace column and they were also found in V1 of both monkey and man (Horton & Hedley-Whyte 1984).

This discovery prompted Livingstone & Hubel (1984) to investigate if cells in the 'blobs' were functionally different from cells in the surrounding 'inter-blobs'. They were surprised to find that the response of cells in 'blobs' depended on stimulus wavelength but not on stimulus orientation whereas 'interblob' cells were mainly orientation selective and somewhat independent of stimulus colour. These findings suggest that there is indeed a segregation of function within V1 between form and colour (Zeki 1993).

1.9 Extra-striate areas V2, V3, V4 and V5

Basic anatomy and physiology

Studies in primates have shown that extra-striate areas surrounding the primary visual cortex (V1) also receive signals originated in the LGN either directly or through V1 itself (Lennie 1998). These cortical visual areas have been labelled as V2, V3, V3A (all within area 18, in the former classification by Brodmann 1909), V4 and V5 to designate zones that are different in terms of their function and anatomy (Van Essen et al 1992, Zeki 1993, Levine 2000). Although the anatomical and physiological organisation of visual cortical areas in primates are becoming better understood (Fig. 1.15), the precise functional relationships among these areas is still an active subject of current research.
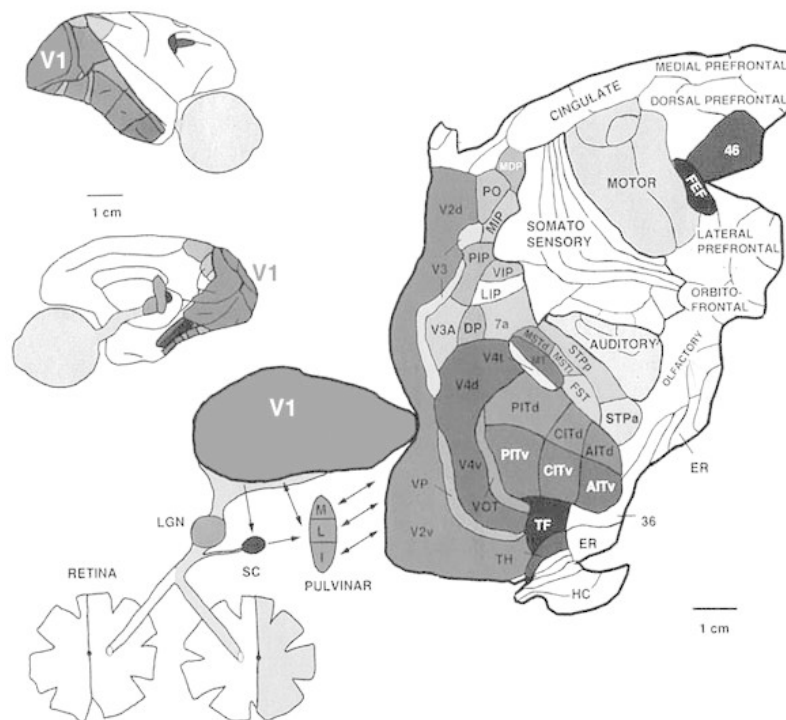
Fig. 1.15 Unfolded map of visually responsive areas (shaded in gray) in the brain of the macaque monkey (Van Essen et al 1992).

V2. Binocular integration

V2 occupies most of area 18 and lies immediately adjacent to V1. It receives a major input from V1 and like V1, is also organised retinotopically. Injection of CO marker in V2 reveals, as in V1, a heterogeneous staining pattern, although the arrangement is not one of blob-interblob variation but instead forms a pattern of thick, thin and pale stripes (Livingstone & Hubel 1982).

The thin stripes of V2 receive input from blobs in V1, where half of the cells display wavelength sensitivity and then project to V4; an area that is concerned with colour perception. V4 also receives input from orientation selective cells in the 'pale stripes' (or inter-stripes) areas in V2 (Fig. 1.12).

The thick stripes of V2 receive their input from orientation-selective cells in layer 4B. Electrophysiological recordings have shown that cells in these thick stripes are orientation and direction selective (Shipp & Zeki 1985). In other words, receptive fields of these cells appear to be of the complex variety found in area V1. Many cells in V2 also exhibit 'end-stopping' (like V1 cells), responding only to visual stimuli of a particular length as well as orientation. 'End-stopping' is also a common feature of cells in area V3 which receives input from the thick stripes in V2. Hence, properties of neurones in V2 and V3 make them

very specific in terms of form and texture extraction from the visual scene. The thick stripes of V2 also send a projection to V3 and V5, an area in which 'texture' information is needed to extract motion (see for example David Regan's book for more on motion from texture)

In addition, V2 does not show any sign of the monocular dominance columns that are such a distinctive feature of V1 (Ts'o et al 1986). In contrast, there are some cells that prefer binocular stimulation in the thick stripes of V2 (DeYoe & Van Essen 1985, Shipp & Zeki 1985, Hubel & Livingstone 1987, Gegenfurtner et al 1996). As a result of this mixture in the physiological properties of neurones in V2, one can extract some indication of what V2 might do: V2 might be related to the localization of similarities in image structure that are used to support binocular single vision and at least short-range perceptual grouping along any dimension of stimulus variation (Lennie 1998).

V3. Form and texture

V3 is still one of the most enigmatic of the occipital areas because its cells generally lack distinctive visual characteristics; they respond to a wide variety of stimuli. Recordings from area V3 showed that the majority of the cells were responsive to lines of specific orientation and direction (Zeki 1978b, Felleman & Van Essen 1987). Colour-selective cells are relatively frequent (Burkhalter et al 1986) and the population of neurones that are both colour-selective and direction-selective seems to be distinctive (Gegenfurtner et al 1997). In addition, many neurones appear to be sensitive to binocular disparity, and thus provide the information necessary for stereoscopic depth analysis.

V3 receives input from the M pathway via the thick stripes of V2 but its intermediate position suggest that these signals reach V4 and V5 later than do signals from V2. These observations, coupled with the fact that V3 apparently provides only a small fraction of the input to V4 and V5 suggests that its role might be to provide a spatially coarse, and perhaps relatively slow, modulation of information transmission in the principal pathways connecting V1 and V2 to the parietal and temporal lobes (Lennie 1998). A better appreciation of the role of V3 might have to await studies that explore the effects of lesions restricted to this area.

V4. Colour

V4 cells, unlike most cells in area V3, are primarily colour selective and involved in the analysis of chromatic information in the visual scene. V4 receives some direct input from V1 and mainly from the thin stripes and pale stripes of V2, but not the thick stripes (Shipp & Zeki 1995). Zeki (1973) discovered that cells in V4 were sensitive to chromatic contrast; with the cell's response depending also on the colour of light falling on the surrounding region. This led to suggest that V4 cells contribute to colour constancy; a remarkable ability of the visual system to preserve colour appearance under changing illumination (Zeki 1978a). This hypothesis has been indeed confirmed by experiments demonstrating that lesions in area V4 result in a substantial and long-standing defect in colour discrimination and thus a breakdown of colour constancy but have little effect on wavelength discrimination (Wild et al 1985). This suggests that V4 collects information from large parts of the visual field to generate colour sensation (Zeki 1993).

V4 also contains numerous cells with complex spatial and orientation tuning, suggesting that the area is also important for form and spatial vision. This has been confirmed in further studies in which lesions in V4 followed a significant detriment in form and shape discrimination (Heywood & Cowey 1987). This is not surprising given the fact that orientation cells derived from the P pathway reach V4 via V2. V4 also sends a conspicuous projection to the inferior temporal cortex and receives a feedback projection (Steele et al 1991).

V5 (MT). Motion

Area V5 is also known as MT since it is located in the middle temporal lobe. V5 receives a direct and highly convergent input from V1 but also from V2, V3 and V4 and cells in this area show direction-selectivity, responding to movement of the stimulus in a preferred direction, and exhibit evidence of tuning for speed of movement. Impediment of visual

motion perception in patients with damage to area V5 and brain scans showing an increase of activity in this area while subjects look at moving objects suggest strongly that V5 is a region specialised for motion perception (Zeki & Ffytche 1998, Barbur et al 1993, Vaina & Cowey 2001, Zihl et al 1983).

Functional specialisation outside V1. Evidence from brain imaging and lesion studies

Evidence for functional segregation in the brain comes from experiments studying the impairment of particular functions in patients who have suffered a lesion in specific areas of their brains. Probably the first and most notorious case was described by Broca (1878). He described a patient who survived a severe injury affecting the whole of the frontal lobe and had lost his ability for any language communication. Broca then concluded that the frontal lobe was the area of the brain processing speech.

In relation to visual function, Pearlman et al. described a patient with a posterior cerebral lesion, presumably in area V4, whose colour vision was severely impaired but yet preserved intact his ability to read and perceive depth and motion (Pearlman et al 1979). Later, Zihl and collaborators (1983) found a patient with a bilateral symmetrical pre-striate lesion in V5 demonstrated by a CT (Computer Tomography) scan who was unable to detect motion (akinetopsia) but was perfectly able to read, see form, colour and depth.

Brain Imaging: fMRI, PET and MEG

Confirmation of functional categorization in cortical visual areas comes from brain imaging techniques such as fMRI (functional Magnetic Resonance Imaging) and PET (Positron Emission Tomography). Both rely on the localization of regions with an increase in cerebral blood flow while the brain undertakes a particular task providing thus an indirect measure of brain activity (Kandel et al 2000). fMRI provides better spatial resolution (2-3 mm) than PET but both techniques have serious limitations in terms of temporal resolution. fMRI signal monitors oxygen demand and this may indeed be correlated to brain activity, but would almost certainly be the result of an averaged time-window of a few seconds (Belliveau 1991, Logothetis & et al. 2001).

MEG (Magneto-encephalography) is a new technique that might provide the much needed temporal resolution for certain studies. It has attracted much research lately but still needs further development and is not yet as widely used as fMRI. MEG estimates brain activity by detecting very small variations in the magnetic field generated by tiny electrical currents in the cortex (Dale et al 2000). These magnetic fields are at least 10^4 times smaller that earth's own magnetic field and its detection require a shielded room and extremely sensitive sensors (SQUIDs or Superconducting Quantum-Interference Devices). This pose an extraordinary technical challenge since any superconducting device works only at extremely low temperatures. However, these technical difficulties have been successfully overcome and it is now possible to measure the brain magnetic fields from 40 or more locations in the skull simultaneously.

The spatial resolution of MEG is significantly poorer than fMRI and thus the only reliable method to monitor local rapid changes in brain activity still requires the use of electrodes to record the electrical impulses of either individual neurones (single-cell recordings) or a collection of cells. Simultaneous recordings for extended periods of time of more than 50-100 neurones (multi-cell recordings) are now possible with the introduction of arrays of micro-electrodes whose tips are flexible enough to avoid cell damage.

1.10 Non geniculo-striate pathways

The output from each retina contains about one million ganglion cell nerve fibres bundled together in the optic nerve. The main target of these neurones is the dorsal part of the LGN of the thalamus but a small proportion leave the optic tract via the superior brachium

to the pulvinar, the superior colliculus, the pretectum, the accesory optic system and the suprachiasmatic nucleus. These small nuclei mediate a number of different functions from eye movements to pupil reflexes (Rodieck 1998).

Superior colliculus (SC) and saccadic eye movements

Almost 10% of the total ganglion cell population leave the optic tract before reaching the LGN to terminate in the superficial layers of the superior colliculus. Each of these paired nuclei, located either side of the midline on the anterior roof of the mid-brain, receive fibres predominantly from the contralateral visual hemifield although recent recordings from neurons in the SC of the cat identified neurons responding bilaterally that may be involved in the analysis of stereopsis and the planning of vergence eye movements during changes in gaze fixation (Mimeault et al 2004).

Traditionally, seven layers are recognised in the superior colliculi; the superficial layers (1-3) and the deeper layers (4-7) (Rodieck & Watanabe 1993, Rodieck 1998, Baker 2000). However, unlike the LGN, in which inputs from each eye are segregated in different layers, fibres from both eyes terminate in the same layer of the superior colliculus. The activity of deep collicular neurones is correlated with the onset of saccadic eye movements, which is indicative of an involvement of the deeper collicular layers in visuomotor function. The superficial layers of the superior colliculi also receive major inputs from other areas of the brain related to visual function. For example, there are inputs that arise from a number of visual cortical areas where information relayed through the LGN has undergone higher level processing. Such inputs also have a retinotopic organisation although the representation of central visual field does not appear to be as magnified as it is in the lateral geniculate nucleus (Oyster 1999, Zeki 1993).

The output of the superficial layers includes the lateral geniculate nucleus, the pulvinar complex as well as the pretectal nuclei. As the pulvinar complex has onward projections to the visual cortex, this route may represent an additional pathway for visual information processing in parallel with the direct retino-geniculo-cortical pathway which may play a role in blindsight, a residual visual capacity without conscious visual perception in patients with damaged geniculo-striate pathways (Weiskrantz 1997, Cowey & Stoerig 1991, Sahraie et al 1997b). See experiments in chapter 5 in patients with blindsight and other brain lesions.

Pretectum

The pretectal complex is a collection of small cell groups with relatively indistinct borders that are located immediately anterior to the superior colliculus in the mid-brain.

The pretectum is generally described as group of five major sub-nuclei:

- Nucleus of the Optic Tract (NOT).

- Olivary Pretectal Nucleus (OPN).

- posterior, medial and anterior pretectal nuclei.

The nucleus of the optic tract and the pretectal olivary nucleus receive dense bilateral inputs from retinal ganglion cell axons, whereas the ganglion cell inputs to the other nuclei appear to be sparse and predominantly from the contralateral retina. The dendritic extents of retinal ganglion cells, which send axons to the pretectal region, are among the largest found in the ganglion cell population (Rodieck & Watanabe 1993, Rodieck 1998, Young & Lund 1998, Kourouyan & Horton 1997, Perry & Cowey 1984). As a consequence of these large dendritic trees, cells mediating the pupil response summate retinal signals over large areas of the visual field and thus the size of the pupil is largely determined by the ambient level of illumination (see chapter 4 for more on the spatial summation of the pupil response).

Olivary Pretectal Nuclei (OPN) and the Pupil Light Reflex (PLR)

Each pretectal olivary nucleus (OPN) receives a direct retinal input mapping the contralateral visual hemi-field. Electrical stimulation of cells in these nuclei triggers a pupillary constriction (Trejo & Cicerone 1984) and a large number of studies have demonstrated indeed that cells in the OPN mediate the pupillary light reflex (Sillito & Zbrozyna 1970, Trejo & Cicerone 1984, Clarke & Ikeda 1985, Gamlin & Clarke 1995, Young & Lund 1998). Cells within the olivary pretectal nuclei (OPN) send axons that terminate bilaterally in the Edinger-Westphal (EW) nuclei within the oculomotor nuclear complex. Parasympathetic fibres leave the EW synapse in the ciliary ganglion and form the short ciliary nerves that innervate the sphincter muscle of the iris. See the next chapter for a detailed description of the anatomy and physiology of the pupillo-motor pathways.

Nucleus of the Optic Tract (NOT) and eye fixation

The activity of cells of the nucleus of the optic tract appears to be related to the direction of stimulus movement, particularly movements from the periphery to the centre of the visual field. Also, electrical stimulation of the nucleus results in horizontal eye movements and this nucleus has therefore been implicated as having a role in both fixation and the optokinetic nystagmus (Oyster 1999).

Accessory optic system

Eye rotation to stabilise retinal image during head movements

The accessory optic system arises from a small bundle of axons that leave the main route of the optic tract, prior to its entry into the superior colliculus. The pathway courses to three small nuclei: the dorsal, medial and lateral terminal nuclei. The vast majority, if not all, of the retinal input to these accessory nuclei arises from ganglion cells in the contralateral eye.

The receptive fields of these ganglion cells are directionally selective responding to movement in a preferred direction but giving no response to movement in the opposite direction. The different ganglion cell populations that project to the individual accessory optic nuclei have different direction preferences. Each of these directions corresponds to one of the three axes of motion that activates the semicircular canals, and the vestibular sensory apparatus. Such activation occurs as a result of head movements. Such head movements would be accompanied by a change in the position of the retinal image if the eyes were fixed in position. In order that retinal image position is stabilised during movements of the head, compensatory eye movements are made at the same velocity and in the opposite direction to the head movement. However, the angular velocity of the compensatory eye movements may not quite counteract the head movement, resulting in a 'slippage' of the retinal image. Through their connections with vestibular nuclei and the inferior olive, the accessory optic nuclei correct for these minor errors in the compensatory eye movements and stabilise the retinal image (Oyster 1999, Rodieck 1998).

Suprachiasmatic nucleus.

Light detection and regulation of circadian rhythm

The suprachiasmatic nuclei are small hypothalamic cell groups situated on either side of the third ventricle and, as the name suggests, immediately dorsal to the optic chiasm. Each nucleus receives bilateral projections from retinal ganglion cells via the retino-hypothalamic tract. The axons comprising this input appear to be collateral branches of axons that course into the optic tract. The nucleus functions as part of a biological clock that generates the body's circadian rhythm and influences diurnal cycles that include eating, drinking, sleep and hormonal release. The precise identity of the ganglion cell type or types, which give rise to the input, are not yet known. However, the cells of the suprachiasmatic nucleus are most active during the light phase of the day-night cycle, and it seems likely that the ganglion cell input conveys information relating to the light intensity itself rather than differences in light intensity (Rodieck 1998, Loving et al 1996).

1.11 Models for visual perception

Hierarchical organisation and parallel processing

The discovery of simple and complex cells by Hubel and Wiesel led them to propose a hierarchical model for the processing of visual signals in which higher visual areas receive direct excitatory input from V1 and each stage analyse successively different aspects of the visual information (Hubel & Wiesel 1959, Hubel & Wiesel 1961). However further research has shown that this model is somewhat insufficient and it has also been demonstrated that other visual cortical areas apart from V1 receive separate inputs from the LGN.

Evidence for functional segregation

In the past twenty years, research in areas as diverse as anatomy, physiology, psychophysics and more recently imaging studies, have strengthen the idea that different visual attributes are process in parallel rather than sequentially. As has been described before, routing of information from retina to cortex is divided in two main neural channels: the parvocellular (colour-sensitive) and the magnocellular (luminance) pathways. This segregation occurs in the first stages of visual processing, at the level of the optic nerve.

It is clear that these two separate neural channels operate in parallel. On one side, colour-sensitive P cells (parvocellular), with small and spectrally-opponent cells mediating colour vision and fine detail (high spatial frequencies). On the other, the large achromatic M cells (magnocellular) with higher contrast sensitivity and faster response encode luminance contrast information (Livingstone & Hubel 1987). The M and P pathways have been used as a recurrent example of parallel processing in the visual system. This parallel processing also take places in higher visual areas where different aspects of the visual scene (eg. texture, motion and depth) are processed.

The M and P visual pathways also resemble the original functional classification of X (slow) and Y (fast) cells in cats (Enroth-Cugell & Robson 1966). The X Y equivalent in primates are the P and M cells that project respectively to the parvo and magnocellular layers of the LGN (Kaplan et al 1990).

Further support for the hypothesis of parallel processing comes from experiments in monkeys using injections of ibotenic acid to destroy selectively P cells or M cells at precise locations of the LGN (Merigan & Maunsell 1993). Destruction of P cells led to a severe deficit in colour discrimination, shape perception, texture and pattern perception. When M cells were destroyed in a separate study, motion perception was greatly impaired (Schiller et al 1990). Contrast sensitivity is also selectively affected at low (M lesion) and high (P lesion) spatial frequencies. These results are consistent with the receptive field classification obtained from electrophysiological recordings; M cells have large centre-surround receptive fields and respond fast, an ideal configuration for the detection of spatial variations in luminance and moving stimuli while P cells have small, spectral-opponent receptive fields to analyse chromatic contrast and fine detail.

Parvocellular (P) pathway

The three types of cones connect via bipolar cells to the midget or P-type ganglion cells. After their first synapse in the parvocellular layers of the LGN, they reach layer $4C\beta$ in V1, which send projections to both the blobs (colour) and interblobs (texture) of layers 2 and 3 in V1 .

These parvocellular connections to the blob and interblob zones are often regarded as representing two functionally different sub-pathways. This is because cells within the blob and interblob regions exhibit very different physiological properties and connections. Cells within the blobs are wavelength-sensitive but do not possess orientation tuning. Interblob cells have orientation specificity but are not responsive to chromatic stimuli. Furthermore, this division in the P pathway continues in V2 with axons from cells in the blobs projecting to the thin stripes and interblob cells to the pale stripes of V2. V2 also receives a M-

pathway projection from layer 4B in V1 but is confined to the thick stripes in V2, and thus kept separated from the thin and pale stripes of the P-pathway.

Zeki (1993) has proposed three main stages of colour processing in the cortex. The first, performed in V1 and possibly V2, is the detection of different wavelengths and their intensity. The second deals with colour constancy operations and is probably located in V4. The final stage seems to be located in the inferior temporal and frontal cortex and has to do with the perception of coloured objects or extracting form from colour (Zeki & Marini 1998).

Magnocellular (M) pathway

Magnocellular (M) cells from the LGN project to orientation and direction selective cells in layer 4Cα of V1 (Hubel & Wiesel 1972). These cells do not respond unless the visual stimuli sweeps the cell's receptive field along its preferred direction, acting thus as basic motion detectors. Indeed, cells in layer 4Cα project via layer 4B to V5 (Lund & Boothe 1975), an area where signals from direction selective cells are used to extract motion information. For this reason, the magnocellular pathway is also often referred to as the motion pathway.

Colour and Luminance channels.

The neural mechanisms for colour processing depends on the trichromatic sampling of the visual image by three classes of cone photoreceptor maximally sensitive to long (L), middle (M), or short (S) wavelengths. The manner in which the various cone signals are combined gives rise to three perceptual dimensions of normal human vision: 1) a red-green axis, 2) a blue-yellow axis, and 3) an achromatic or luminance axis (Derrington et al 1984).

The two chromatic axes are defined by antagonistic, or opponent, colour pairs. It is now generally accepted that at an early stage in the red-green opponent pathway, signals from L and M cones are opposed, and in the blue-yellow pathway signals from S cones oppose a combined signal from L and M cones. P cells in the central retina receive antagonistic input from a single cone type (L or M) to both centre and surround and thus show clear spectral opponency providing the neural substrate for the red-green colour axis. Another type of midget ganglion cells (small bistratified) are thought to provide the neural basis for the blue-yellow channel (Dacey & Packer 2003).

Luminance signals are dominated by rods at low luminance levels and by cones at photopic luminance levels. Both M and P cells receive input from rods, but they differ substantially in their responses to cone signals. M cells responses are larger when L and M cone contrasts have the same sign (L+M) whereas P cells combine opposing centre-surround signals (L-M or M-L) in the central retina but are similar to M cells in the periphery (Lee 1996, Dacey & Packer 2003).

Rod and Cone inputs to the M and P pathways

M cells are known to respond mainly to luminance contrast. Their signals are dominated by rod input at low luminance and by synergistic (L+M) cone signals at photopic luminance levels (S cone signals contribution to luminance is much smaller, compared to L and M cones as can be seen from the CIE luminous efficiency function plotted in Fig. 3.1. For this reason, luminance signals are often referred to as L+M under photopic conditions, when rods are fully saturated and their contribution is therefore minimal).

Magnocellular neurons thus respond to different wavelengths but they do not show spectral opponency like the P cells. Although a minority of M cells have been shown to receive antagonistic cone input (M-L) to the surround (Reid & Shapley 2002), there is common agreement that the M pathway does not provide a very efficient mechanism to encode colour signals .

P cells in the central retina show red-green spectral opponency. Both the receptive field centre and surround receive antagonistic input from a single cone type (L and M cones). However, in the peripheral retina, P cells dendritic trees enlarge greatly and

receive convergent input from a number of midget bipolar cells. Thus peripheral midget cells show additive input from L and M cones to both receptive field centre and surround, thus weakening spectral opponency. As a result P-cells in the periphery of the visual field show similar spectral sensitivity to M cells and the psychophysical luminance channel (Dacey & Packer 2003, Diller et al 2004).

P cells also receive rod input, but rod contribution is only important at lower luminances. P cells also respond to luminance contrast, but their contrast gain is much smaller than that of M cells (see Fig. 4.1). The difference in contrast gain between P and M cells remains even in the mesopic and scotopic luminance range (Purpura et al 1988). Shapley and collaborators (1990) have suggested that the greater contrast gain of M cells may be a direct result of M cells large receptive fields, with M cells being more efficient in collecting luminous flux (quanta per second).

Interaction between the M and P parallel pathways

Though separate pathways exist for motion, colour and form, these are unlikely to be completely independent (Maunsell & Newsome 1987). Motion direction-selective cells have been found in the P pathway by Zeki (1978c) and connections have been discovered between V5 and V4 in the macaque monkey (Rockland & Pandya 1979). Moreover, there are multiple inter-connections between areas receiving input from either magno or parvo regions. For example, connections between the thin (P) and the thick stripes (M) of V2, projections from V4 (P) back to the thick stripes (M) and also direct connections between MT, V4 and V3.

These anatomical results are consistent with the ability of human observers to perceive coloured targets moving in a background which has the same brightness (isoluminance) as the targets (Lu et al 1999). An experiment related to this is described in chapter 7, where a colour discrimination tasks was used to assess colour vision loss in patients with diagnosed optic neuritis.

Absolute silencing of the luminance (M) pathway or, in other words, complete isolation of pure chromatic signals is impossible to achieve given the large variations in luminous sensitivity that occur with retinal eccentricity and across different observers. However, dynamic luminance-contrast noise can be added to the background to ensure that observers cannot make use of luminance signals (M pathway) to detect motion (Barbur et al 1994a). Extraction of motion signals from isoluminant colours must, therefore, involve the neural pathway connecting V4 with V5 mentioned above.

Chapter 2: The Role of the Pupil in Human Vision

2.1 The iris and the pupil

The iris is an opaque sheet of tissue with a circular hole or aperture, known as the pupil of the eye, that regulates the amount of light entering the eye in order to maximise visual performance. In young adults, pupil diameter can range from about 2 to 8 mm. These variations in pupil size help to keep the level of retinal illumination at the optimal operating range of retinal photoreceptors in a wide range of luminance conditions from rod mediated night vision (scotopic) to bright sunlight (photopic).

The pupil also has great influence on the quality of the retinal image. A small pupil optimises visual performance by increasing the depth of focus and minimising the effects of aberrations (Oyster 1999, Campbell & Gregory 1960). The size of the pupil is thus determined by the balance between the minimum level of retinal illumination needed by photoreceptors and image quality.

2.2 Effects on retinal image quality

The iris acts as an aperture stop for the optical system of the eye and therefore influences the quality of the retinal image. Increasing pupil size reduces the image quality due to the effect of aberrations whereas reducing pupil size degrades the image quality by increasing the effects of diffraction. Diffraction is less significant than aberration in the normal range of pupil size and therefore the smallest pupil size permitted for a given ambient illumination level is generally the best solution. The optimum pupil diameter for maximum visual acuity is normally between 2 and 3 mm.

The size of the pupil will also affect the depth of focus of the image formed on the retina; the range in image space within which focus or image sharpness is acceptable. The smaller the pupil, the larger the depth of focus. Experimental studies in the human eye have shown the following relationship between depth of focus (E, in dioptres) to pupil diameter (d, in mm) (Campbell & Gregory 1960).

$$E = \pm [(0.75/d) + 0.08] \qquad \text{Eq. 2-1}$$

2.3 Factors affecting pupil size

The pupil is in constant motion and numerous factors affect its size. We will review briefly the most significant here. For a thorough review of these and other aspects relating to the pupil, see the excellent and extensive book by Loewenfeld (1993).

Level of ambient illumination

Both retinal photoreceptors, rods and cones, contribute to the pupil response (Alpern & Campbell 1962). The diameter of the pupil can vary between 2 mm at high illumination (photopic conditions <0.01 cd/m^2) and 8 mm in darkness (scotopic conditions >10 cd/m^2). The rate of diameter change with ambient luminance generally follows a non-linear function (see Fig. 2.1).

(Moon & Spencer 1944) proposed an equation relating pupil diameter in mm (P_d) to background luminance (L) in cd/m^2 that modelled well the data by Reeves (1920):

$$P_d = 4.90\text{-}3.00 \tanh [0.400 (\text{Log } L+10)] \qquad \text{Eq. 2-2}$$

A similar equation was proposed by DeGroot (1952):

$$\text{Log } P_d = 0.8558 - 0.000401(\text{Log } L + 8.1)^3 \qquad \text{Eq. 2-3}$$

where L is luminance in mL (1 mL= 3.18 cd/m^2).
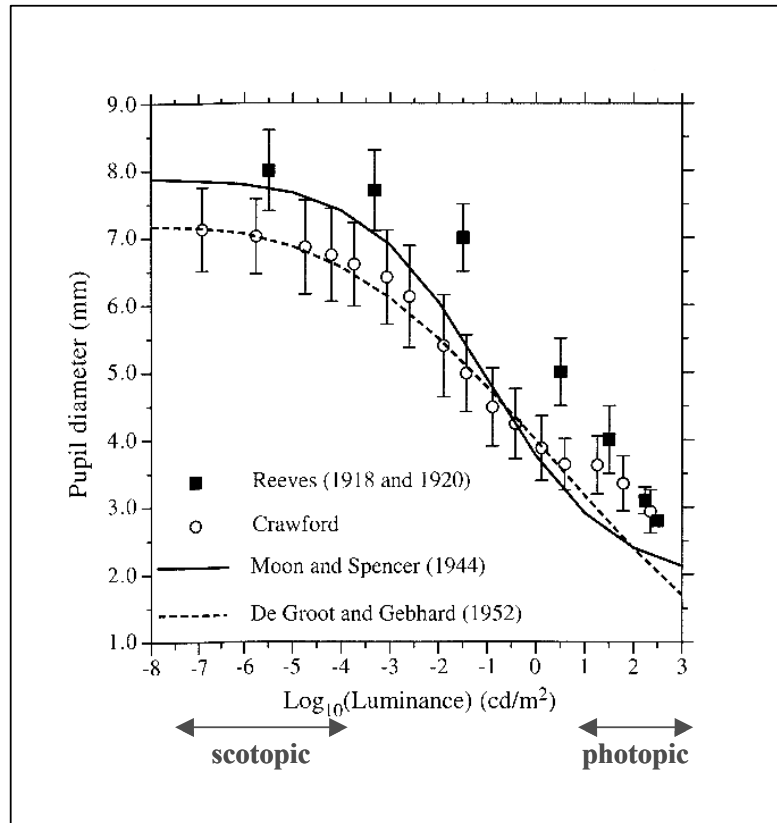
Fig. 2.1. The level of ambient illumination determines the steady-state size of the pupil which is defined as the averaged pupil diameter for a fixed background luminance. From (Atchison & Smith 2000).

The pupil also exhibit a similar Stiles-Crawford effect to that measured in vision (Atchison et al 2000), that is the luminous efficiency of light has been shown to be greater when entering the centre than when entering the edge of the pupil. This effect arises as a consequence of the optical properties of the cone receptor cells (Stiles & Crawford 1933).

Light flux change

The pupil needs to adjust constantly the retinal illumination to optimise contrast visual acuity. In humans, the pupil can follow periodic changes in luminance as fast as 3Hz (eg. three bright flashes every second). The rapid pupil response is important because changes in ambient illumination can occur suddenly. For example, when walking from shade into bright sunlight, the pupil needs to react quickly to reduce the total light flux entering the retina and to avoid over saturation of the retinal photoreceptors (a phenomenon also known as bleaching). The amount of light entering the eye through the pupil will be proportional to its area. Therefore, a change in pupil size from 8 to 2 mm will reduced the light flux by a factor of 16, helping the photoreceptors to adapt to the new light level.

The pupil response to transient changes in illumination is often referred to as the dynamic pupil response or the pupil light reflex (PLR) whereas the stabilised pupil diameter for a fixed level of illumination (averaging out normal fluctuations over time) is known as the steady-state size of the pupil. The pupil light reflex is mediated by dorsal

areas in the mid-brain, more precisely by a small neural complex, the olivary pretectal nuclei (OPN).

Accommodative changes and the near reflex

The pupil also decreases in size when changing fixation from far to near objects. This is known as the pupil near response or near reflex. Its role is to increase the depth of field for near objects by reducing the size of the pupil that would otherwise appear blurred. The change in pupil size is almost linear for changes in accommodation between 1 to 3 dioptres at a rate of approximately 0.3 mm per dioptre (Alpern et al 1961, Oyster 1999). For example the tolerance in focus with a 5 mm pupil is ±0.23 D and ±0.38 D for a 2.5 mm pupil (Oyster 1999).

In order to minimise pupil oscillations caused by changes in accommodation throughout the experiments presented in this thesis, subjects were asked to look at a fixation point on the computer display used for the presentation of visual stimuli. For a typical subject, these fluctuations never exceed 0.04 mm at a viewing distance of 70 cm (see for example pupil traces for a blank stimulus in Fig. 4.5).

Pupil oscillations (hippus)

The pupil is changing in size even when fixating at distant objects. This spontaneous and rhythmic fluctuation under constant lighting conditions are generally small and are known as hippus (Yoss et al 1970). Hippus is normal in healthy subjects and becomes larger as ambient illumination increases. Moreover, its absence can be indicative of damage to the innervation of the iris or to the iris itself (Oyster 1999).

Sleepiness and fatigue

The level of awakeness also affects the pupil which oscillates during drowsiness and sleep (Wilhelm et al 1998, Yoss et al 1970) and its size is reduced during anaesthesia.

Psychological factors

There are a number of psychological influences on pupil size. For example, the level of alertness is mediated by the reticular activating system which regulates the pupil size and the gain of the light reflex via a supranuclear inhibitory sympathetic tone on the parasympathetic nuclei in the mid-brain. Emotions also influence the limbic system on the hypothalamus. Pleasant, arousal mental images cause the pupil to dilate. This dilation has probably a cortical origin causing an increase in the sympathetic tone to the dilator via the hypothalamus. The same mechanism mediates dilation during pain or fear (Passatore et al 1977). Other factors such as attention, alertness and the amount of mental workload seems also to affect the pupil size and its sensitivity (Van Orden et al 2001, Wilhelm et al 1996b, Wilhelm et al 1996a).

Circadian rhythms and pupil size

Circadian rhythms are thought to have marked influence on several biological functions. The steady state size of the pupil and therefore its sensitivity, depends also on the time of the day. This effect, although small, is significant. However, it has been shown that although the baseline size of the pupil varies during the day, the times of the peaks in pupil diameter occur randomly throughout a 24 hour period (Loving et al 1996, Wilhelm et al 2001).

Age

It has been reported that the mean steady state size of the pupil diminishes with age. There is also a reduction of the light reflex although this is not uniform for all light intensities. It decreases at about 0.04 mm/year at low light intensities and 0.015 mm/year at high light intensities (Hasegawa & Ishikawa 1989).

2.4 Innervation of the iris sphincter and dilator muscles

The pupil size is constantly regulated by two antagonistic muscles which are under autonomic control.

- The sphincter muscle, which is a smooth muscle innervated by parasympathetic fibres from the 3rd cranial nerve that synapse in the ciliary ganglion and reach the iris via the short ciliary nerves (Fig. 2.2). The sphincter is an annular band of smooth muscle, 0.8 mm broad in man, encircling the pupillary border, which on contraction draws out the iris and constricts the pupil (Davson 1980).

- The dilator muscle, which is more primitive and consists of myo-epithelial cells that extend radially from the sphincter into the ciliary body. The dilator is controlled by the cervical sympathetic innervation, the fibres synapse in the superior cervical ganglion; post-ganglionic fibres enter the eye in the sort and long ciliary nerves.

This is the traditional description of the iris innervation although it is possible that both sympathetic and parasympathetic fibres reach each muscle (Loewenfeld 1993). This dual innervation is also common in many other organs in humans (Martini 1998).

2.5 The neural pathways of the pupil light reflex (PLR)

The afferent pupillary pathway

The afferent pathway of the pupil light reflex starts in the retina with both receptors, rods and cones, contributing to the light reflex. Ganglion cell fibres leave the retina through the optic nerve and, after crossing over in the optic chiasm, pupillary fibres leave the optic tract before reaching the LGN and run, via the brachium of the superior colliculus, into the Olivary Pretectal Nucleus (OPN), a group of cells at the junction of the diencephalon and the tectum of the mid-brain where they have their first synapse (See Fig. 2.2 for a detailed diagram of this sub-cortical neural pathway).

The fibres from the nasal retina cross over at the level of the optic chiasm to the contralateral OPN, whereas temporal fibres project to the ipsilateral OPN. Kupfer (1967) found that this hemidecussation is not perfectly symmetric in humans; there are slightly more crossed than uncrossed fibres and the ratio is approximately of 53% to 47%. Interestingly, a much clearer asymmetry is found in human albinos. This asymmetry, however, seems to have little effect on the pupil. Constriction differences after stimulating nasal versus temporal retina are rarely larger than 0.04mm and these small differences, in any case, are not significant for clinical applications of pupil perimetry (see chapter 4).

Thus, each OPN receives input from both eyes mapping the contralateral visual field. Generally, anomalies in pupil constriction when stimulating one or both eyes will provide indication of the localization of the lesion in the pupillary pathways; any damage to the neural fibres along the afferent pathway in the optic nerve will result in one pupil constricting more than the other or a Relative Afferent Pupil Defect (RAPD) (Kardon & Thompson 1998). Whereas, if the lesion occurs in the optic tract, between the optic chiasm and the OPN, it will result in constriction asymmetries between nasal and temporal visual field stimulation in both eyes.

Retinal ganglion cells projecting to the pretectum in the midbrain

Several studies have identified the olivary pretectal nuclei (OPN) in the dorsal midbrain as the major neural complex mediating pupillomotor responses to light (Perry & Cowey 1984, Trejo & Cicerone 1984, Young & Lund 1998, Pong & Fuchs 2000, Gamlin & Clarke 1995). These studies often refer to neurons in the OPN as light detectors that is, cells that increase their firing rates following a light increment, causing the pupil to constrict. Retrograde labeling after injection of HRP (horseradish peroxidase) in the OPN shows that ganglion cells projecting to the pretectum have large dendritic fields (Trejo & Cicerone 1984, Perry & Cowey 1984) suggesting that OPN neurons receive input from

signals that are pooled across large areas in the retina. These anatomical findings are also consistent with the large receptive fields measured during electrical recordings from neurons in the OPN both in the rat (Clarke & Ikeda 1985, Trejo & Cicerone 1984) and the monkey (Clarke et al 2003). Clarke et al. found that the receptive field size in the OPN can vary greatly, from 2-3 degrees centrally to 10-20 degrees in the periphery. They also found that, in the monkey, 40% of the neurons responded to central stimulation in both visual hemi-fields, 30% to contralateral stimulation and the remaining 30% to ipsilateral stimulation.

There are also recent reports of a subset of intrinsically-photosensitive retinal ganglion cells that project to the OPN (Lucas et al 2003, Gamlin et al 2004). The phototransduction system(s) utilized by these cells are not still well known but melanopsin and cryptochromes have been proposed as candidate photopigments for this system. In any case work on melanopsin driven cells suggests that these cells need high light levels to generate significant responses (Lucas et al 2003). These retinal illuminance levels are well above those associated with vision in the low photopic range and thus the contribution such cells may make to pupil responses under the experimental conditions reported in this thesis is likely to be minimal.

In summary, cells in the pretectum seem to have much larger receptive field size than those mediating vision (Trejo & Cicerone 1984, Clarke et al 2003). They also appear to lack chromatic sensitivity (Perry & Cowey 1984, Schiller & Malpeli 1977). These results suggest that pupil fibres do not share the same retinal projections as visual fibres (i.e. pupil fibres are not just a ramification of visual fibres but receive an independent retinal projection). However, pupil fibres still show some similarities with visual fibres. For example, both sustained and transient neurons have been found in the pretectum (Trejo & Cicerone 1984, Pong & Fuchs 2000), in analogy with the sustained and transient nature found in visual fibres projecting to the parvocellular and magnocellular layers of the LGN. The study of Trejo et al. found that transient pupillary neurons have larger receptive fields than those showing a sustained response suggesting that they may belong to a morphologically different cell population with larger dendritic fields.

Parasympathetic pupillary pathway
After Alexandridis (1985)
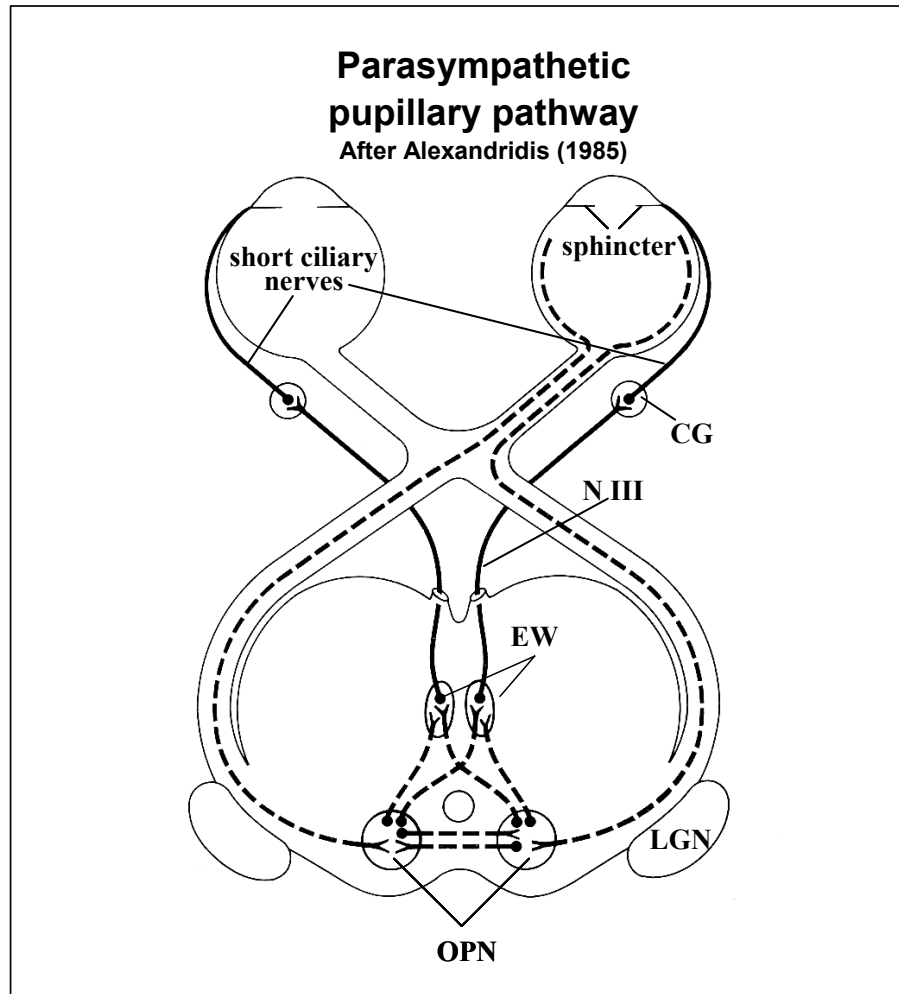
Fig. 2.2 Parasympathetic pathway of the pupil response. After light is shone on either eye, afferent fibres (dotted lines) from the retina carry the luminance signals to the olivary pretectal nuclei (OPN) and then to the Edinger-Westphal (EW) nuclei in the dorsal mid-brain. Efferent parasympathetic fibres leaving the EW send the pupilloconstrictors signals to the iris sphincter muscle after synapsing in the ciliary ganglion. CG, ciliary ganglion; N III, the third intra-cranial nerve; LGN, lateral geniculate nucleus. Adapted from Alexandridis 1995.

The efferent pupillary pathway

Fibres leaving the OPN project to the Edinger-Westphal nuclei (EW), a small neural complex in the mid-brain, with a large proportion crossing over again so that each EW receives inputs from both nasal and temporal visual fields, each in turn originated from both eyes (See Fig. 2.2). This second crossing allows both pupils to constrict even when one eye is not exposed to light changes. In monocular viewing, the response of the covered eye is referred to as the indirect or consensual pupil response. Any damage along the efferent pupillary pathway (eg. from the EW to the sphincter via the ciliary ganglion) will therefore result in constriction differences between the direct and consensual response under monocular stimulation. We monitored the consensual response to test the possibility of an efferent pupil defect in the experiments described in the following chapters.

A number of studies (Smith & Smith 1980, Cox & Drewes 1984, Smith 1992, Gamlin & Reiner 1991) suggest that this second decussation of fibres from OPN to EW is asymmetric with more crossed than uncrossed fibres. However, there are no significant differences between consensual and direct constriction amplitudes in humans suggesting that this asymmetry is not relevant for any clinical study. Other species (e.g. cats) show a clear asymmetry and this is easily detectable when comparing consensual and direct pupil responses (Loewenfeld 1993).

Parasympathetic innervation of the sphincter muscle

The parasympathetic innervation to the sphincter consists of a two-neurone chain synapsing in the ciliary ganglion. Axons of the pre-ganglionic neurones leave the Edinger-Westphal (EW) nucleus and join with motor fibres from the ipsilateral oculomotor nuclei to form the fascicle of the third cranial nerve. The parasympathetic fibres accompany the oculomotor nerve throughout its intracranial course, lying superficially where they are susceptible to compressive injury. Within the orbit, the axons leave the inferior division of the oculomotor nerve and travel with the nerve to the inferior oblique muscle before synapsing in the ciliary ganglion (Kerr & Hollowell 1964). The cell bodies of the post-ganglionic neurones lie within the ciliary ganglion. Their axons emerge with other autonomic and somato-sensory fibres to form the short ciliary nerves. These pass forward through the suprachoroidal space to reach the iris sphincter muscle (See Fig. 2.2).

Sillito et al. (1970) studied the parasympathetic input to the sphincter muscle by recording the electrical activity of single neurones from the EW nucleus in cats whose cervical sympathetic was sectioned to avoid any influence from the sympathetic system on the dilator muscle. He found that maximal constriction of the pupil occurred for a firing rate of about 8Hz but the frequency range was from 0 to 28Hz. This means that there is temporal integration of the pupillomotor signals at the level of the sphincter muscle since the pupil cut-off frequency is about 4-6 Hz in mammals.

Sympathetic innervation of the dilator muscle

The sympathetic innervation to the iris dilator muscle is classically described as a three-neurone chain with synapses in the spinal cord and the superior cervical ganglion near the angle of the mandible (See Fig. 2.3).

The pupillary sympathetic pathway derives from area A1/A5 in the brainstem, extend to the hypothalamus where the first-order (central) neurones leave the ipsilateral posterior hypothalamus and descend uncrossed through the lateral part of the brainstem to terminate in the ciliospinal centre of Budge-Waller (level C8-T2). The second-order sympathetic neurones leave the spinal cord with the ventral spinal roots and ascend, without any synapse, passing around the sub-clavian artery close to the apex of the lung to terminate in the superior cervical ganglion at the level of the angle of the mandible. From here, the third-order (post-ganglionic) neurones travel on the surface of the internal carotid artery into the intracranial space. Within the cavernous sinus, they leave the artery to join the ophthalmic division of the trigeminal nerve before entering the orbit with the nasociliary nerve and passing forward to the iris dilator muscle in the long ciliary nerves. For a more detailed description of the pupillary pathways see Loewenfeld 1993, Alexandridis 1985 or Bremner 2001.

Sympathetic
pupillary pathway
Source: Thompson HS (1992). Adler's Physiology of the Eye
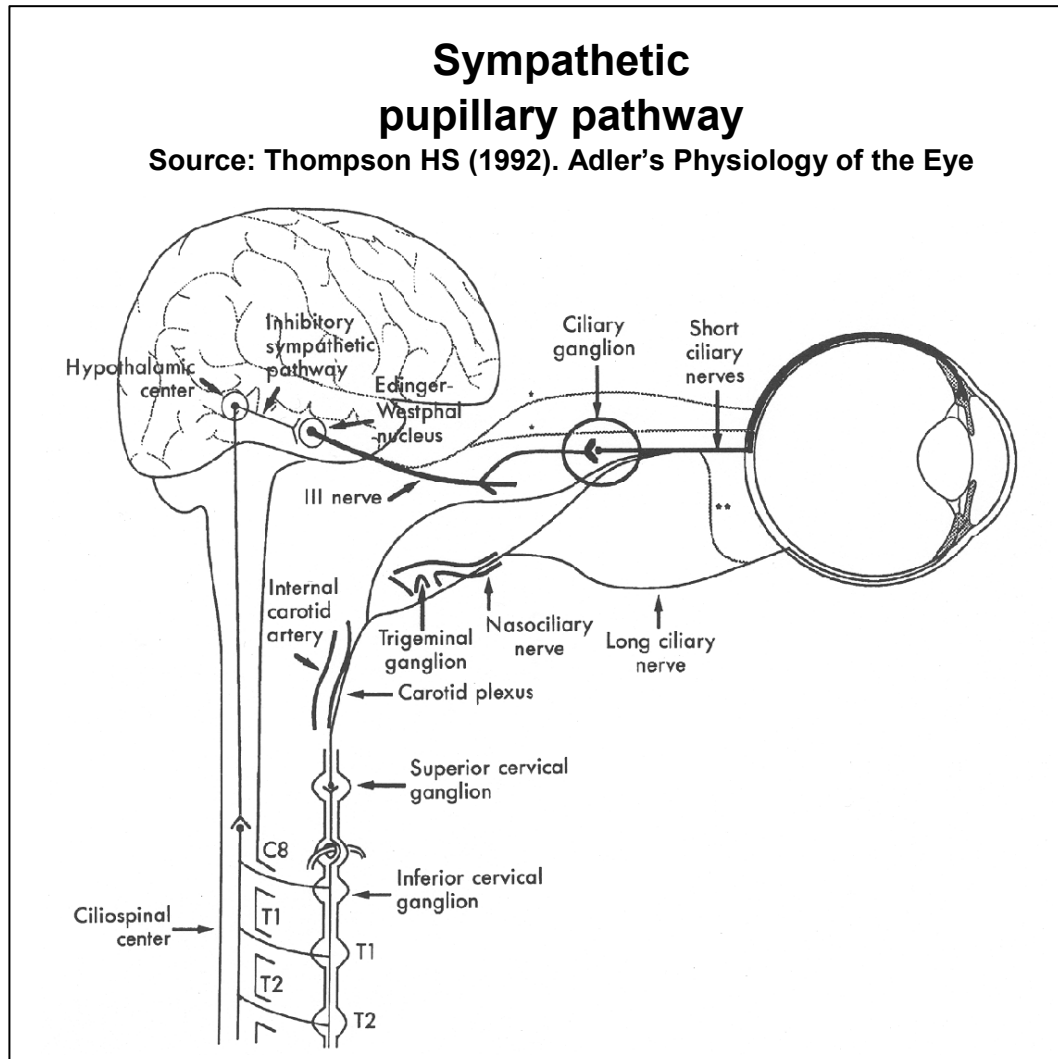
Fig. 2.3 Sympathetic innervation to the pupil dilator muscle. Cortical influences on pupil size are thought to reach the iris via cortico-thalamic connections.

Sympathetic and parasympathetic interaction

The role of the sympathetic innervation to the pupil is clear; sectioning of the sympathetic nerve in the neck interrupts the sympathetic outflow to the dilator and causes the pupil to constrict (miosis). Passatore et al. (1977) have also shown that the discharge rate of the cat's sympathetic nerve fibres increase with the onset and maintenance of darkness and also when applying painful stimuli to the skin and cornea. It seems therefore that dilation caused by increased sympathetic activity triggered by either a reduction in the mean light level or during fear or painful experiences are mediated by the same sympathetic neurones. Dilation during mental workload, arousal or alertness can also be attributed to a rise in the general sympathetic tone.

Sympathetic central inhibition on the parasympathetic efferent pupillary pathway

Even nowadays, the precise role of sympathetic activation and inhibition on the pupil and the detailed underlying neural pathway is not as well understood as the parasympathetic pupillary pathway (Parkinson 1988). Sillito et al. (1970) found that electrical stimulation of the hypothalamus in sympathectomised cats produced pupil dilation and even a block of the light reflex suggesting that these effects were mediated by inhibition of spontaneous parasympathetic activity in the EW. Since this supranuclear inhibition of the light reflex does not involve the known sympathetic pupil pathways, where does that inhibition come

from?. Well, these results may challenge the traditional view of the EW (Davson 1980, Burde & Williams 1989) as a pair of nuclei receiving purely an excitatory parasympathetic input (Loewy & Saper 1978). Furthermore, since the hypothalamus is involved in the regulation of sympathetic activity (see Fig. 2.3), this could suggest a yet unknown input from the sympathetic system causing inhibition of parasympathetic fibres either at the level of the EW (Cassady 1996) or the ciliary ganglion. This would result in a dual innervation of the iris sphincter muscle, something which is not uncommon in other muscles and organs in the human body, many of which receive both sympathetic (excitatory) and parasympathetic (inhibitory) innervation.

Other inputs to the EW and OPN from supranuclear structures

Other studies have described several other inhibitions and influences on the parasympathetic tone to the pupil such as projections from different areas in the cortex and the diencephalon to the EW (Forrest & Snow 1968, Hartmann-von Monakov et al 1979). The OPN itself does not seem to connect directly to the thalamus but it receives projections from the visual cortex (Benevento et al 1977).

2.6 Sympathetic and parasympathetic neuro-transmitters

Parasympathetic neuro-effector junctions are small and have narrow synaptic clefts. Most of the acetylcholine released is inactivated within the synapse by the enzyme acetylcholinesterase. As a result, the effect of parasympathetic stimulation is short-lived in comparison to sympathetic activation. The action of sympathetic neuro-transmitters is principally terminated by an active re-uptake process (Martini 1998). These differences in the effective duration of neuro-transmitters release between the parasympathetic and sympathetic systems is likely to contribute to the faster constriction (parasympathetic mediated) that dilation (sympathetic) rates measured in the pupil response (see Fig. 2.4).

2.7 Asymmetry in constriction and dilation rates

Pupil constriction generally takes a fraction of a second whereas full pupil dilation following a decrease in ambient illumination may take up to a minute (Reeves 1920, Crawford 1936). This asymmetry in constriction and dilation rates are also manifest in dynamic pupil responses to brief bright flashes or periodic modulation of luminance (Fig. 2.4).
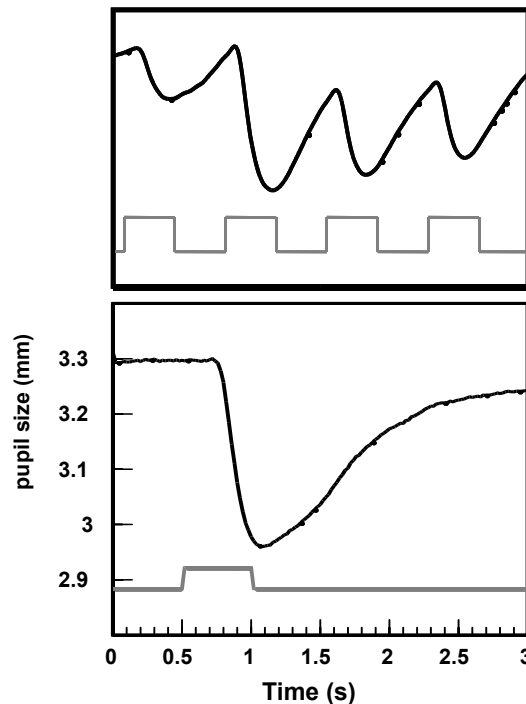
Fig. 2.4. Pupil responses to a bright flash (bottom) and brisk square-wave periodic luminance modulation (top). Constriction is generally much faster than dilation. This asymmetry expose the different nature of the sphincter and dilator muscles but may also reflect fundamental differences in the neuro-transmitter re-uptake mechanisms of the underlying parasympathetic (constriction) and sympathetic (dilation) pupillary pathways (Martini 1998).

2.8 Drugs affecting pupil size

Autonomic drugs affect the pupil by altering either the sympathetic innervation of the dilator or the parasympathetic innervation of the sphincter.

Adrenergic and Cholinergic Agents

Because the size of the pupil is regulated by the balance between sympathetic flow to the dilator and parasympathetic tone sphincter, pharmacological agents affecting the pupil are often divided between those causing dilation and constriction. Drugs causing dilation will either stimulate sympathetic tone to the dilator (adrenergics) or block the parasympathetic flow to the sphincter (anti-cholinergics) whereas drugs causing constriction will decrease the sympathetic tone (anti-adrenergics) or activate parasympathetic flow (cholinergics). The terms 'adrenergic' and 'cholinergic' refer to the general action of pharmacological agents on the central nervous system, not only on the pupil. Adrenergic is used for those drugs producing a similar effect to the liberation of norepinephrine or noradrenaline (stimulation of the sympathetic system) whereas cholinergic refers to the liberation of acetylcholine (stimulation of the post-synaptic parasympathetic neurones). There are also substances that bind to the neuro-receptors blocking in this way the sympathetic (anti-adrenergics) or parasympathetic (anti-cholinergics) receptors.

Drugs affecting pupil size		
PUPIL DILATION	**ADRENERGIC** sympathetic stimulation	Epinephrine Phenylephrine Cocaine*
	ANTI-CHOLINERGIC parasympathetic block	Tropicamide Cyclopentolate Homatropine Atropine
PUPIL CONSTRICTION	**CHOLINERGIC** parasympathetic stimulation	Pilocarpine Carbachol
	ANTI-ADRENERGIC sympathetic block	Guanethidine Thymoxamine

* Cocaine is an indirect adrenergic enhancing the effect of adrenaline, also called epinephrine, by blocking its re-uptake mechanism.

Table 2-1. Summary of the most common drugs affecting pupil size causing either dilation or constriction. Adrenergics mimic the effect of epinephrime and norephrine stimulating the sympathetic post-ganglionic receptors. Cholinergics (or anti-cholinergics) liberate (or block) acetylcholine affecting the parasympathetic input to the iris sphincter muscle. A more detailed list is given elsewhere (Alexandridis 1985, Thompson 1992, Oyster 1999).

2.9 Disorders of the pupil

Pupil size differences between eyes (anisocoria)

The most common pupil abnormality to be noticed by a patient is anisocoria (unequal pupil sizes). 10-20% of the population have pupils which are not the same size as each other. This anisocoria is physiological and it is caused by 'normal' differences in the balance of parasympathetic and sympathetic drive to the two pupils. The main features of physiological anisocoria are: that it lessens when measured in bright light, it varies over time and the reactions of the pupil to a bright light or an accommodative target are brisk and normal (Loewenfeld 1977). These features should be contrasted with pathological anisocoria caused by parasympathetic or sympathetic block. If the larger pupil is abnormal, then the difference in pupil size will be exaggerated in bright light implying

parasympathetic block. Conversely, if the smaller pupil is abnormal, then the difference in pupil size will be more apparent under dimmer conditions; this implies sympathetic block (Bremner 2001, Loewenfeld 1993, Loewenfeld 1977).

Unreactive pupils: pre-ganglionic parasympathetic block

Damage to the pre-ganglionic neurones leaving the EW nuclei (Fig. 2.1) is generally characterised by large, unreactive pupils and absence of accommodation. This pupil disorder is associated with oculomotor nerve palsy and can be accompanied by pain which has great clinical significance since, in many of these patients, the cause is a structural lesion such as an intracranial aneurysm or tumour that requires urgent medical attention.

Dilated or tonic pupil: post-ganglionic parasympathetic block

The tonic or dilated pupil is most commonly found in Adie's syndrome, a benign idiopathic condition which typically affects young women in their third to fifth decades. It is unilateral in 80-90% of cases and may present with sudden blurring of vision, photophobia and anisocoria. This condition can be diagnosed by demonstrating reduced reflexes (especially knee or ankle), excluding other atypical causes such as: autonomic neuropathies, herpes zoster, or orbital injuries and surgery (Bremner 2001, Kardon & Thompson 1998).

The shape of the pupil often appears oval. Accommodation recovers quickly but the pupillary abnormalities persist although pupil size can fluctuate; in some cases, the tonic pupil can even be smaller than in the fellow eye. The tonic pupil can also exhibit light-near dissociation (Thompson 1992), that is, reduced pupil response to light but normal constriction when eyes change focus to a near target.

Horner's syndrome: sympathetic block

Damage to the sympathetic supply to the iris produces a characteristic clinical condition known as Horner's syndrome although it was first described by (Ogle 1858). The pupil of the affected eye is smaller and the anisocoria increases in dim light conditions. Redilatation following constriction to a light or accommodative target is also slower than normal. Patients with Horner's syndrome may also show secondary effects such as anisocoria or ptosis (Thompson 1992, Bremner 2001).

Relative Afferent Pupil Defects (RAPD)

The normal pupil constricts briskly to a light stimulus or an accommodative target, and redilates at a slightly slower rate to the averaged steady-state size according to the level of ambient illumination.

Lesions to the efferent pupillary pathways (sympathetic or parasympathetic) can be easily identified by abnormal pupil size or associated anisocoria during a fixed level of illumination. It also results in different constriction amplitudes between the direct (stimulated) and consensual (non-stimulated) eye in response to flash stimuli. In contrast, damage to the afferent pupillary pathways generally result in pupils with normal size and shape but which do not react normally to light and near stimuli.

Examining the pupil light reflex is arguably the most useful test in a patient with unexplained visual loss. Clinically, this is assessed with the swinging light test (Levatin 1959), where a flashlight is alternated between the two eyes and the pupil reactions compared. This test is best performed in dim light conditions using an intense stimulus (such as the beam from an ophthalmoscope) allowing enough time for the pupils to equilibrate with the bright light (1-2 seconds) but not so long that the retinal pigment is bleached (>3 seconds). Any difference in constriction amplitude between the two eyes will be a sign of a relative afferent pupil defect (RAPD). The RAPD can also be quantified using neutral density filters or infra-red video pupillography.

As a general rule, the presence of a severe RAPD implies retinal or optic nerve disease. Lesions in the optic radiation (after the optic chiasm) can also result in a RAPD but is generally smaller and more difficult to detect than in case of damage to the optic

nerve (Hamann et al 1979). The extent of the RAPD broadly correlates with the degree of loss of visual field rather than visual acuity (Kardon et al 1993). An individual may have a normal Snellen visual acuity of 6/6 and yet show a marked RAPD because of extensive peripheral visual field loss.

Mid-brain lesions. Parinaud´s syndrome

Lesions to the pupillomotor nuclei in the dorsal mid-brain, unlike afferent defects, typically result in a bilateral symmetrical pupil defect (no sign of RAPD) without affecting visual function.

The two most common disorders are Parinaud's syndrome and Argyll-Robertson pupils. Argyll-Robertson pupils are extremely rare nowadays; they were common when untreated syphilis was widespread (Loewenfeld 1969). In this condition, the pupil response is characterised by light-near dissociation: the pupil response to light is reduced but the pupil still constricts normally when changing focus from a distant to a near target. Pupils are also generally small, often of irregular shape, dilating poorly in darkness suggesting interruption of both the afferent light pathway and the sympathetic fibres innervating the iris dilator muscle. Parinaud's syndrome generally occurs after pineal tumours causing damage to the dorsal side of the OPN in the mid-brain but preserving the fibres mediating focus accommodation changes in the ventral part. It is therefore also characterised by light-near dissociation but usually more severe than in Argyll-Robertson pupils; the pupil response to light is absent (or extremely reduced). It also presents other secondary signs: vertical gaze deficit, lid retraction on attempted upgaze and skew deviation.

In chapter 6, two subjects with Parinaud's syndrome show normal pupil responses to isoluminant gratings and coloured targets (Wilhelm et al 2002). These stimulus-specific responses are significantly reduced in patients with damaged cortical visual areas (Barbur & Prescott 2002). The results in Parinaud's syndrome suggest that cortical processing required for the perception of colour and form may influence, via cortico-thalamic projections, the central sympathetic tone to the iris dilator muscle by-passing the damaged area in the dorsal mid-brain. Therefore, cortical processing could cause a transitory weakening of the sympathetic input to the dilator resulting in pupil constriction in the same way as psychological factors acting on the same pathway can affect pupil size; eg. dilation in response to alertness or an auditory stimuli (Bala & Takahashi 2000).

2.10 Summary

The pupil regulates the light flux entering the eye facilitating the adaptation of retinal photoreceptors to a new light level. It also optimises visual function by increasing the depth of focus and minimising the effects of aberrations.

The anatomy of parasympathetic and specially the sympathetic neural pathways mediating the pupillary response in man is not yet fully understood. The traditional view is that the sub-cortical parasympathetic pathway acts on the iris sphincter muscle independently of the sympathetic pathway innervating the dilator. However, it seems that the pupillary pathways are more complicated than initially thought, with the pupil receiving both sub-cortical and cortical input. There is also strong evidence suggesting that the sympathetic and parasympathetic systems may interact before reaching the iris. Unlike parasympathetic fibres, sympathetic neurones do not synapse in the ciliary ganglion (Lowenstein & Loewenfeld 1969). However there must be some interaction between the two systems since dilation after section of the sympathetic cervical ganglion following stimulation of the hypothalamus suggest a sympathetic inhibition on the parasympathetic system (Sillito & Zbrozyna 1970). It has even been suggested a sympathetic input to the sphincter and there is also evidence of a dual innervation to the dilator (Jackson 1986).

Summarising, we can number four possible mechanisms that can produce changes in pupil size. These are:

1. <u>Increase in parasympathetic flow (constriction):</u> light increments (detected by OPN neurones) cause an increase of the parasympathetic flow from the EW to the sphincter. Evidence for this comes from constrictions elicited by electrical stimulation of EW parasympathetic fibres in sympathectomized cats (Sillito & Zbrozyna 1970), where the constriction is not simply caused by a transitory reduction of sympathetic tone to the dilator.

2. <u>Reduction of sympathetic flow (constriction):</u> this is what causes a small pupil size during anesthesia and acute fatigue or sleepiness. Transitory reductions in the sympathetic tone are responsible for spontaneous pupillary fluctuations (hippus) and pupillary fatigue waves (Wilhelm et al 1998).

3. <u>Sympathetic input to dilator (dilation):</u> in the awaken state is what prevents the pupil to become small due to the spontaneous activity of parasympathetic constrictor neurones. Stimulation of cortical areas using transcranial magnetic stimulation (TMS) in humans (Niehaus et al 2001) or emotional excitement can also cause pupil dilation. This suggest that this mechanism is influenced by activity in cortical areas as well as in the hypothalamus (eg. during the alert or 'fear' response).

4. <u>Reduction in parasympathetic flow (dilation):</u> causing relaxation of the sphincter. This reduction in the parasympathetic tone is presumably the result of not yet fully understood sympathetic inhibition on the EW or ciliary ganglion from supranuclear structures or cortical areas (Sillito & Zbrozyna 1970, Cassady 1996, Niehaus et al 2001). This dilation is small and sub-maximal when the sympathetic flow is blocked (with drugs) or the sympathetic nerve is sectioned (Lowenstein & Loewenfeld 1969).

Chapter 3: Methods

3.1 Introduction

All the visual stimuli used in the experiments described in the following chapters were generated in an standard cathode ray tube (CRT) computer display. In order to understand better the physical characteristics of the visual stimuli used, some basic technical concepts about computer graphics, photometry and colorimetry will be discussed here. It will be followed by a detailed description of the experimental methods used during pupil and psychophysical recordings.

3.2 Basic Photometry and Colorimetry

An image in a computer display is made up of small independent dots or pixels, each of which, has a brightness value. Brightness is defined as the attribute of a visual sensation according to which an area appears to emit more or less light. This definition of brightness is obviously subjective and inappropriate to quantify image data, so a standardised brightness metric based on an ideal human observer, luminance, is often used instead. Grayscale images can be determined solely by their luminance values whereas colour images are fully described by tristimulus values (see overview of the CIE colour space later in this section). Both luminance and tristimulus values, usually follow a nonlinear transfer function that mimics the brightness perception of human vision (Wandell 1995).

Radiant Intensity and Radiance as a measure of light intensity

Radiant intensity refers to the power (light flux) of radiation in a particular, specified direction per unit of time. That is, the rate at which energy is radiated, per unit solid angle. Radiant intensity is measured in Watts per stereoradian (W/sr).

Radiance is defined as radiant intensity per unit area. It is expressed in Watts per stereoradian per meter squared (W/sr/m^2).

Luminous efficiency functions of the human eye

In physics, radiant intensity and radiance are measured across a wide range of wavelengths, from gamma-rays (<10^{-11} m) to radio waves (>10^{-1} m). Vision scientists are, however, only interested in wavelengths falling on the visible band (370-730 nm). Sensitivity of the human retina changes for each wavelength contributing to the overall brightness sensation and a new magnitude is introduced to take this into account. The weighting factor for each wavelength is given by the luminous efficiency function (Fig. 3.1) of an ideal human observer standardized by the international commission on illumination, the CIE (Commission Internationale de l'Eclairage).

Luminance is the most important quantity relating to human vision since it is related to perceived brightness. Luminance is defined as the luminous intensity radiated per unit area of the source (Table 3-1), or in other words, the radiance weighted by the spectral sensitivity of the human retina. An object of uniform luminance looks equally bright from any direction despite that the effective area of the object changes with the cosine of the angle of viewing. Luminance is generally expressed in units of candelas per meter squared (cd/m^2).

The luminous efficiency functions have been measured by the CIE for both scotopic (less than 0.001 cd/m^2) and photopic (luminance levels higher than 10 cd/m^2) conditions using initially a 2° target and then extended to 10° target (CIE 1986). The photopic efficiency function peaks at about 555 nm while the scotopic peaks at about 505 nm (Fig. 3.1). Therefore luminance is proportional to the energy radiated by the light source but depends on the spectral power distribution (SPD) of the light emitted.

Radiometric Units		Photometric Units	
Radiant Energy	Joules (J)	Photometric Energy	(lm s)
Radiant Flux	Watts or J/s	Luminous Flux	Lumens (lm)
Radiant Intensity	W/sr	Luminous Intensity	Candelas (cd) lm/sr
Radiance	W/sr/m2	Luminance	cd/m^2

Table 3-1. Summary of physical or radiometric units commonly used in light measurements and their correspondent photometric units which are defined according to the sensitivity of the human eye to different wavelengths. A radiant flux of light of one Watt at a wavelength of 555 nm is equivalent to a luminous flux of 683 lumens. Intensity is defined as the flux emitted per solid angle or stereoradian (sr), in a specific direction.
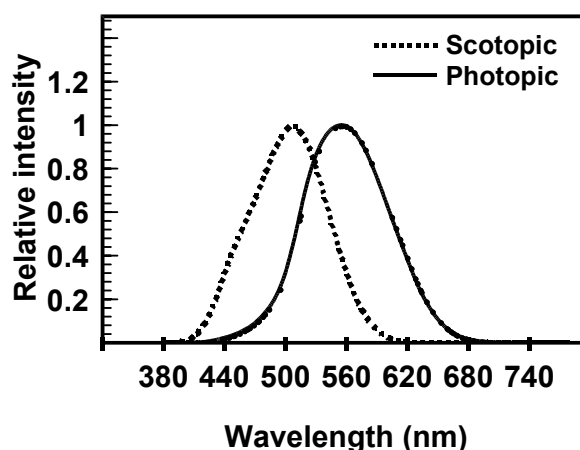
Fig. 3.1 Luminous efficiency functions for both low (scotopic) and high (photopic) luminance conditions of a standard human observed as defined by the CIE. (Data from Wyszecki & Stiles, 1982).

Luminance can be computed as a properly-weighted sum of red, green, and blue primary lights or tristimulus components. Luminance signals in photopic vision are generated mainly from L and M cones signals, with a minor contribution from S cones. Scotopic vision is mainly rod-mediated, resulting in a significant loss of sensitivity to red wavelengths. This is the reason for the shift in the peak towards blue wavelengths in the scotopic efficiency function, known also as the Purkinje shift. The Purkinje shift also explains why pale colours tend to look gray-blueish in the dark.

In vision research, computation of luminance is generally based on the CIE luminous efficiency functions. Individual variations are often assumed to approximate that of an ideal or CIE standard observer. However, this approximation is not valid for visual stimuli presented at more than 10° away from the fovea or large targets exceeding the central 10° of the visual field. The obvious reason for this is the substantial change in photoreceptor density with retinal eccentricity (Fig. 1.3). Luminance, as it is defined by the CIE, will thus vary slightly across the visual field. However its perceptual equivalent, brightness, seems to vary very little with retinal eccentricity. This is consistent with our

everyday experience: objects do not look darker in the periphery in spite of a decrease in photoreceptor density.

Colorimetry: The CIE colour space

Colorimetry is an extensive topic, only a brief description of the CIE colour space and its relation to human vision will be given here. For an accessible but thorough introduction to colour vision see for example the textbook of Kaiser & Boynton (1996). However the key reference in colour science is the book by Wyszecki & Stiles (1982) which contains virtually any table and mathematical formula relating to colour measurements and its applications to human vision.

In general, any coloured object is fully described by its luminance, hue and saturation. Luminance is the perceived brightness standardised by the CIE. The hue determines the appearance of the colour in relation to the visible spectrum. If the light reflected by the object contains a mixture of wavelengths, then the perceived colour will be determined by the peak of the SPD (spectral power distribution). If the dominant wavelength of the SPD shifts, the hue of the associated colour will also change. Finally, saturation indicates how colourful or vivid a colour is in proportion to its brightness. Saturation runs from neutral gray or white (depending on luminance) to complete saturation (monochromatic light). Achromatic lights (with gray or white appearance depending on luminance) are usually defined by a roughly flat SPD, containing the same power at any wavelength. Roughly speaking, the more an SPD is concentrated at one wavelength, the more saturated will be the associated colour and the greater its distance from the achromatic point in the CIE colour diagram Fig. 3.2. Any colour can be desaturated by adding light that contains power at all wavelengths.
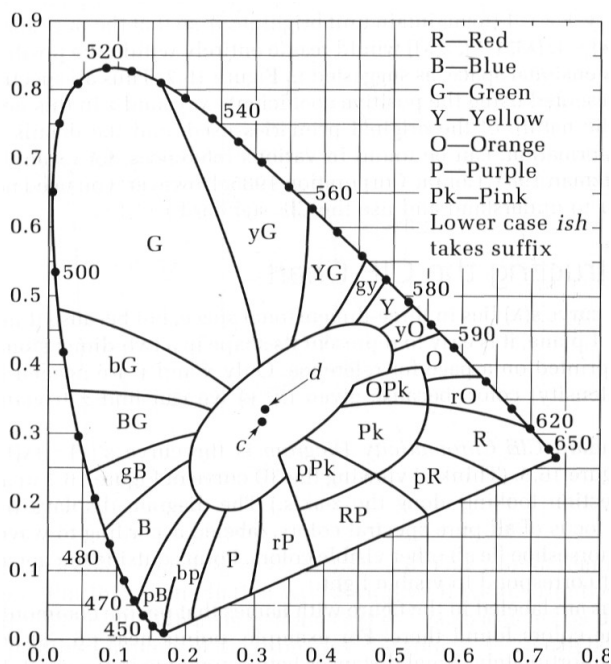
Fig. 3.2 CIE x-y chromaticity diagram. Pure saturated colours containing only one wavelength (monochromatic lights) lie on the edge of the spectral locus (numbers indicate wavelength in nm). For a good coloured reproduction of this diagram see for example Kaiser (1996) or the website of the Colour Group of Great Britain at www.city.ac.uk/colourgroup.

CIE XYZ colour space

Any colour specification system needs to be able to reproduce any given colour with particular values of luminance, hue and saturation. The colour hue is numerically

described by three functions (colour matching functions) which are obtained experimentally by matching the colour of a test light to a mixture of three chosen colours, or primaries, which typically appear as red, green and blue (Wandell 1995).

In a colour-matching experiment the observer sees a circular field composed of two halves. One hemi-field contains an arbitrary test light, the other contains a light mixture of the three chosen primaries. The observer adjusts the intensity of the primary lights so that the two sides of the bipartite field appear identical. Although the two sides can match perceptually, they can be very different physically. Since the light on the primary side of the bipartite field is the weighted sum of the primary lights, and the light on the test side of the bipartite field can be any light at all, the two sides of the field are not generally close to being physical matches. Pairs of lights that are visual matches, but not physical matches, are called metamers (Kaiser & Boynton 1996).

The CIE adopted one particular set of colour matching functions ($\bar{x}\,\bar{y}\,\bar{z}$) as an international standard for human colour vision. These functions determine a transformation for any test light $t(\lambda)$ with a specific spectral power distribution (SPD) into a triplet or tristimulus values (XYZ). The CIE tristimulus values XYZ describe any colour as a luminance component Y, and two additional components X and Z as follows:

$$X = \sum_{\lambda} \bar{x}(\lambda) \cdot t(\lambda) d\lambda \qquad\qquad \text{Eq. 3-1}$$

$$Y = \sum_{\lambda} \bar{y}(\lambda) \cdot t(\lambda) d\lambda \qquad\qquad \text{Eq. 3-2}$$

$$Z = \sum_{\lambda} \bar{z}(\lambda) \cdot t(\lambda) d\lambda \qquad\qquad \text{Eq. 3-3}$$

Thus, the XYZ tristimulus values are proportional to the physical energy contained at each wavelength $t(\lambda)$ but also contain information of the spectral composition by means of a basis of colour-matching functions.

Is also quite common to describe colour in the absence of luminance Y, specially when using colours that have the same luminance (isoluminant stimuli), by means of chromaticity coordinates (x, y):

$$x = \frac{X}{X+Y+Z} \qquad\qquad y = \frac{Y}{X+Y+Z} \qquad\qquad \text{Eq. 3-4}$$

Solving Eq. 3-4 recovers X and Z from (x,y) chromaticities and luminance (Y):

$$X = \frac{x}{y}Y \qquad Z = \frac{1-x-y}{y}Y \qquad\qquad \text{Eq. 3-5}$$

The (x,y) chromaticity coordinates define a colour diagram in which pure saturated colours (monochromatic lights) lie on the edge of the spectral locus shown on Fig. 3.2. Any colour can, therefore, be specified by its chromaticity and luminance, in the form of an xyY triplet. This is the colour specification used throughout this thesis. When presenting coloured isoluminant stimuli, the luminance (Y) of both target and background is fixed and an equivalent representation in polar coordinates is used: the colour hue is given as an angle measured anticlockwise from the horizontal axis (Fig. 3.2) whereas colour saturation is numerically expressed as a chromatic distance (CD) from the chosen background. The background used throughout all the experiments, is the achromatic white reference (x,y= 0.305, 0.323) used by MacAdam (1942). Chromatic distance (CD) can therefore be computed from x-y coordinates as an adimensional quantity:

$$CD = \sqrt{x^2 + y^2} \qquad\qquad \text{Eq. 3-6}$$

3.3 Computer displays: luminance and colour calibration

Most computers have 8 or 10 bits graphics cards to control the voltage of each gun to the three phosphors (red, green and blue) of a typical computer display. The number of bits determines the range of gun levels, 0-255 (2^8 = 256) for an 8-bit card and 0-1023 (2^{10} = 1024) for a 10-bit card. The RGB triplet is sent to the video card's lookup table. During each video frame the video card retrieves each pixel, one by one, from its video memory and passes it to the lookup table.

The resulting triplet is fed to three digital to analogue converters (DACs) that each produce a voltage linearly related to its number. For example in an 8-bit card, 0 produces zero volts and 255 produces one volt. Each voltage controls a separate gun and all have similar nonlinear luminance-voltage relationships, differing by scaling.

Approximations and assumptions

Visual stimuli with particular values of luminance and chromaticity need to be generated on a computer display. To achieve this, one needs to express the required luminance and chromaticity coordinates as RGB triplets containing the gun level values to each of the 3 phosphors for each pixel. In doing this, we assume that the power spectral distribution satisfy superposition. Generally, we can make two assumptions:

1. As we increase the gun level of each phosphor the power spectral distribution retains the same shape. This is valid for almost any available monitors.

2. The total monitor output is the weighted sum of the three spectral power distributions (SPD) of the individual phosphors (Brainard & Pelli 2002). This is called additivity.

The loss of additivity in the SONY monitor used in all the experiments described here was too small to have any influence in the measurements carried in the experiments described in this thesis.

Monitors with an inadequate video bandwidth, DC restoration, or high-voltage regulation can also result in a lack of pixel independence. Denis Pelli (1997) and David Brainard (2002) have both written excellent reviews about calibration procedures and limitations of computer displays in vision research. Calibration routines are included in their Psychophysical Toolbox developed for MATLAB (www.psychtoolbox.org).

Display calibration

The visual stimuli presented in all the experiments described in the remaining chapters were displayed on a 21" SONY Trinitron monitor (refresh rate 85 Hz, resolution 1024x768 pixels) driven by a 10-bit graphics adapter. Luminance-voltage curves were measured at each voltage-gun level for each phosphor (for a 10-bit graphic card this gives 2^{10} = 1024 levels). To check for luminance additivity a fourth curve was measured for the three phosphors simultaneously at each gun-voltage level Fig. 3.3. The lost of additivity in the SONY display used was only 0.6 cd/m^2 at an average operating luminance level of 24 cd/m^2 representing a relative error of less than 2.7% but this never exceeded 6% even at very low luminance levels (e.g. 3 cd/m^2).

In addition to measurements of luminance output, the spectral radiance of each phosphor of the computer display was measured using a Gamma Scientific telespectroradiometer (Model 2030-31). These measurements provide the display calibration data needed to generate any combination of luminance and chromaticity coordinates desired, following standard colorimetric transformations (for details see equations 3-1 to 3-5).

Luminance output of the SONY 500PS monitor

The total luminance of the white light emitted by the combined signal of the three phosphors is a non-linear function of the applied voltage signal. In a conventional CRT monitor this function follows a power-law response to voltage (Fig. 3.3). The numerical value of the exponent of this power function is known as gamma and can oscillate between 2.2 and 2.5 depending on the monitor (Brainard & Pelli 2002).

$$L_{(R+G+B)} = \alpha V^{\gamma} + \beta$$

$$\gamma = 2.2$$
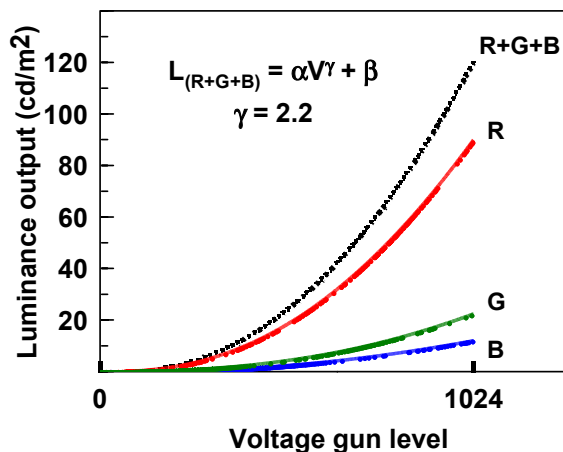
Fig. 3.3 The luminance output of the three phosphors of the SONY 500PS monitor are non-linear functions of the applied voltage signal. The total luminance of the white light emitted by the combined signal of the three phosphors follows a power-law response to voltage whose exponent, known as gamma, has a typical value of 2.2. Data obtained using a LMT luminance meter (model 1003, www.lmt-berlin.de).

Output of red, green and blue phosphors

The visual system allows us to distinguish millions of different colours by comparing the signals of only three different receptors in the retina (L, M, and S cones). We do not need hundreds of different photoreceptors, each sensitive to a specific wavelength, because cones have a very broad wavelength sensitivity function and their signal output is independent of wavelength provided that the power at each wavelength is weighted according to their sensitivity. Still two monochromatic lights of different wavelength will generally not appear as the same colour because the relative ratio of signals from L, M and S cones will be different (Fig. 3.4).

A coloured object typically reflects light containing several different wavelengths. The amount of each wavelength defines the spectral power distribution (SPD) of the light radiated by the object. Each of these wavelengths is absorbed in one or more of the three cone types (L, M and S) in the retina. The ratio of these three cone signal outputs is what ultimately causes the sensation of a particular colour. Thus, since cone sensitivity functions cover a broad range of different wavelengths, it is possible to have two coloured objects that are perceived as identical but have different SPD (known also as metameric colours).

The relative output intensity of each phosphor type (red, green and blue) measured for the display used in all experiments is plotted in Fig. 3.4 together with the spectral sensitivity of the cones in the human retina. The shape of the relative spectral power distribution (SPD) of the phosphors is roughly the same at any luminance, only the absolute values change. The SPD of the red phosphor is very narrow and this could lead to think that the display of different red tonalities is very limited. However, as it has been discussed above, what gives rise to colour perception in the human eye is the relative ratio of the three cones signals and not the light intensity absorbed at a particular wavelength. Thus, any coloured surface (yielding a particular set of cone signals) can be reproduced in a computer display by just adjusting the intensity of the phosphors to elicit the same cone signals despite the light emitted by the display being physically different from the light reflected by the surface.

An example will illustrate better how any colour can be rendered from the narrow SPD of a phosphor in a standard computer display. Let's consider the light reflected from a red surface. This light will contain, for example, wavelengths between 640-660 nm that are impossible to reproduce in the computer display (Fig. 3.4). However the same L cone signal, and thus the same colour sensation, can be elicited by light at 630 nm (1st peak in Fig. 3.4) emitted by the phosphor if the radiance intensity is adjusted according to the L-cone sensitivity. The light emitted by the red phosphor is physically different from the one emitted by the object but has the same colour appearance, that is, they are metameric lights.

The broad range of cone sensitivity means also that many different colours can be generated in a computer display or optical system adjusting only three lights (or primaries) of different wavelengths.
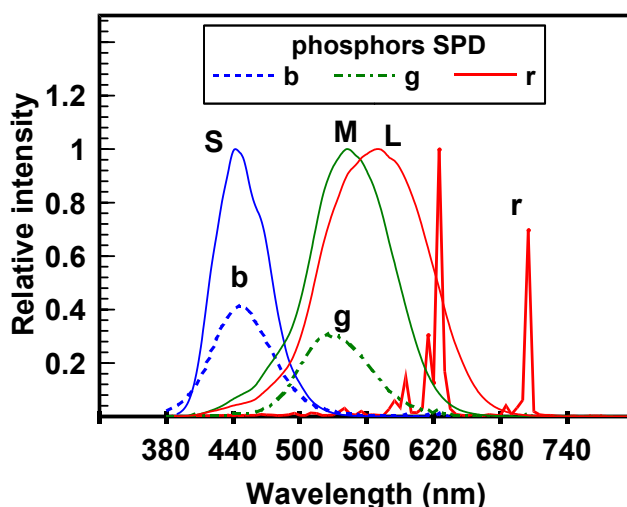
Fig. 3.4. Relative output intensity of each phosphor (rgb) of the display used in the experiments. The shape of the relative spectral power distribution (SPD) is roughly the same at any voltage gun-level, only the absolute radiance values change. The SPD of the red phosphor is very narrow but this does not limit the number of colours that a computer display can reproduce since cones have a broad wavelength sensitivity. Light at 630 nm (first major peak of red phosphor) can generate the same L-cone signal output than light at 660 nm. It is the relative value of the L, M and S cones signal not the physical wavelength falling on them what generates the sensation of a particular colour. Cone sensitivity curves from Stockman & Sharpe (2000).

3.4 Experimental set-up during psychophysics and pupillometry

Subjects looked to the calibrated computer display at a viewing distance that varied between 0.5 and 0.7 meters except for contrast sensitivity measurements when it was increased to 3 meters in order to be able to display gratings of high spatial frequency. The computer display subtended a visual angle of 23° by 18° at 70 cm and 31° by 24° at 50 cm.

All the experiments were carried out in a dark room painted matt-black. An external response box linked to the computer was used to initiate the presentation of visual stimuli or to record responses during psychophysical experiments. A head and chin rest were used to prevent any head movements and help fixation during recordings. Pupil traces were inspected visually and data was discarded from further analysis if observers had too many consecutive blinks or showed excessive eye movements.

3.5 Pupil measurements: the P_SCAN system

The P_SCAN system (see schematic diagram in Fig. 3.5), designed by John Barbur and collaborators (1987) at the Applied Vision Research Centre in City University, London (http://www.city.ac.uk/avrc), was used for both presentation of visual stimuli and simultaneous recording of pupil size.

The illumination of each iris for pupil imaging was achieved by means of infrared Light Emitting Diodes (LEDs) producing 5 ms light pulses of an average peak wavelength of 860 nm. The light from the LEDs is reflected by the iris and then collected into 2 infra-red sensitive cameras by means of a partially silvered mirror that allowed a clear view of the visual stimuli presented on the computer display. During monocular viewing, an infra-red transmitting filter covered the fellow eye allowing simultaneous recording of both the stimulated (direct response) and the non-stimulated eye (consensual response).

The P_SCAN measures pupil size at a sampling rate of 50 Hz (every 20 ms) by fitting the best circle to the pupil diameter. Pupil size is extracted in real-time from the pupil image by an edge-detection algorithm which isolates the dark pupil from the coloured iris (white dots in Fig. 3.5). This algorithm uses an adjustable threshold that is set before the recordings and works well even in subjects with a dark iris and low contrast pupil images. The imaging of the pupil edges can be severely corrupted if the Purkinje reflection of the infra-red light falls on the pupil-iris margin. The location and orientation of the LEDs was adjusted so that the peak of the reflection always fell outside the pupil.

Measurement of pupil constriction amplitudes

Recorded pupil data is saved to the computer hard disk after each stimulus presentation and once the experiment is finished, pupil traces are averaged and analysed with custom designed software. Further statistical analysis and graphic plots were carried out using software available commercially (Visual Basic Macros for Excel, MATLAB and standard graphic software packages).

Two different stimulation techniques were used for pupillometric recordings: presentation of a single flash of variable duration or cyclic periodic modulation of stimulus attributes (ie. luminance, colour, spatial frequency) during 10 seconds at different temporal frequencies (varying the number of cycles per second).

The extraction of pupil constriction amplitudes depends on the type of stimulation chosen:

- For single flash stimuli, the pupil constriction amplitude is extracted from the averaged trace as the difference between the mean pupil size just before stimulus onset (a minimum of 15 points corresponding to a time interval of 280 ms is normally used to estimate this) and the point of maximum constriction.

In case of a cyclic periodic modulation, both amplitude and time delay of the pupil response are computed from the amplitude and phase-shift of the 1st (or fundamental) harmonic in the Fourier analysis of the averaged trace (see Fig. 3.5).
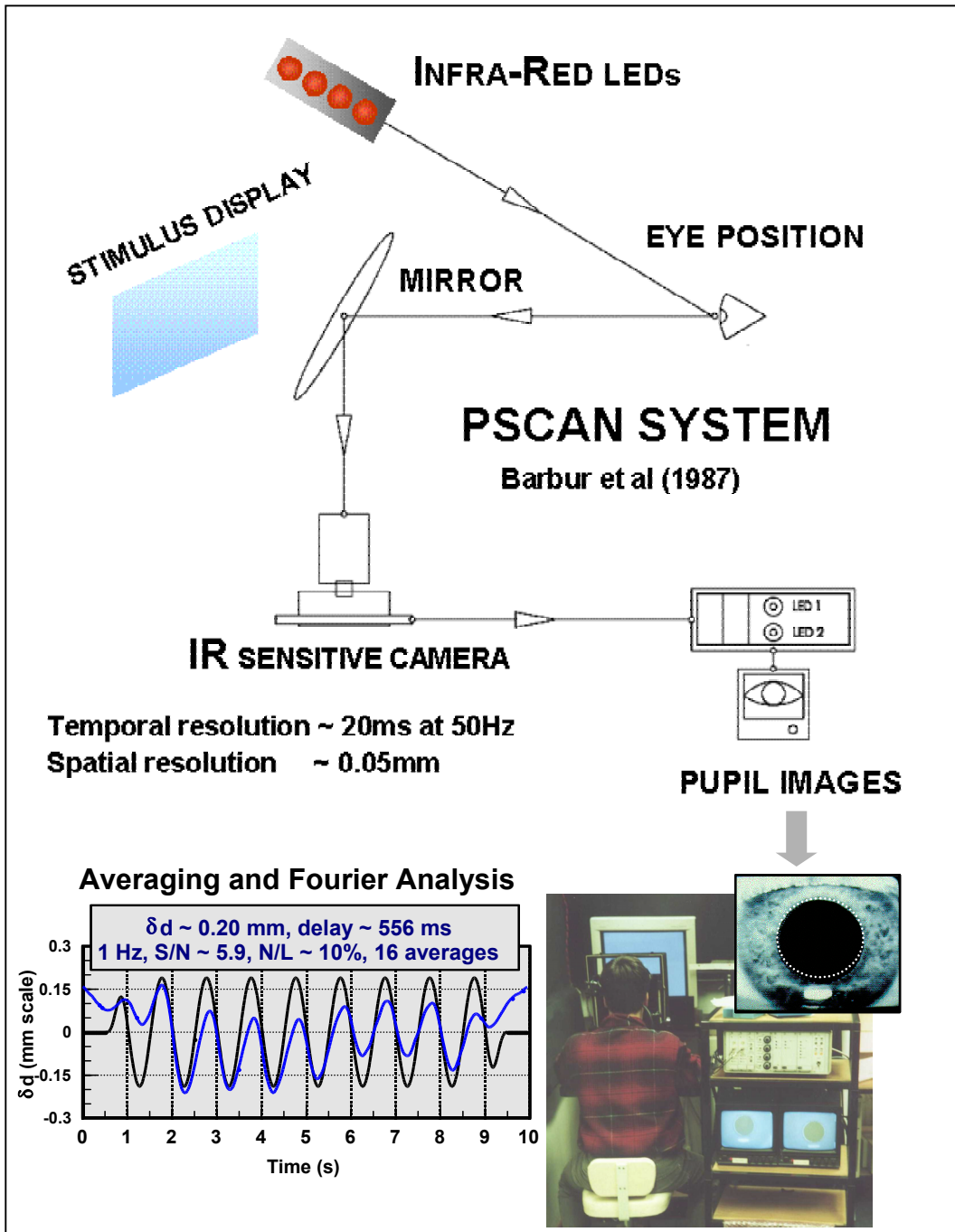
Fig. 3.5. Schematic diagram of the P_SCAN system (Barbur & Thomson 1987) used for pupil measurements. The eyes can be stimulated in conjunction or separately. An infra-red transmitting filter can block the view of one eye but still allowing the pupil imaging of both the direct (stimulated eye) and the consensual (non-stimulated eye) pupil response. Pupil response traces (blue line, bottom left graph) to luminance modulation (black line) of the computer display are extracted by fitting the best circle to the data points on the pupil-iris margin (picture inset).

Measurement of the time delay of the pupil response (latency)

The latency of the pupil response is usually defined as the time delay between stimulus onset and the beginning of the constriction. The computation of the pupil latency is not as straight forward as it seems at first sight. The precise starting point of constriction is difficult to establish by visual inspection of the response trace. This imprecision is unavoidable regardless of the sampling rate used to obtain pupil data.
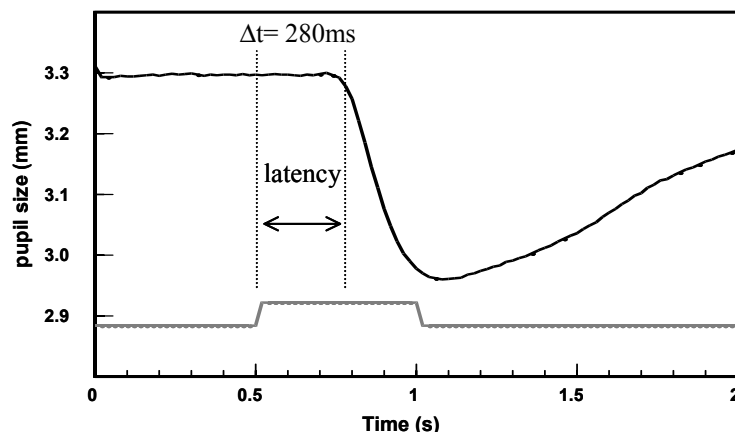
Fig. 3.6. The precise point of the start of the pupil constriction is difficult to establish because of continuous fluctuations in pupil size. Even if sample rates much higher than 50 Hz were used, the precision at which latencies can be extracted would not be much better because 20 ms is approximately the typical value of the standard deviation when measuring pupil latencies in humans. The constriction amplitude is computed as the difference in the average pupil size before stimulus presentation and the maximum constriction.

A sampling rate of 50 Hz means that there is information about pupil size only every 20 ms. However, if the sampling rate is synchronised with the stimulus presentation onset, 20 ms is enough because the standard deviation of the typical human response is more than 20 ms (Freedman et al 1997). Therefore, increasing the sampling rate in pupil measurements above 50 Hz will contribute little to the precision with which latencies can be measured. It could help to identify better the starting point of constriction but, because of the continuous fluctuations in pupil size, this is also probably limited to a resolution of 10-20 ms. The conclusion from this analysis is that latencies can be computed from data extracted at a sampling rate of 50 Hz (every 20 ms) with a reasonable accuracy provided that a minimum of 20-30 traces are averaged.

Difference between pupil latencies to a single flash and periodic modulation

Pupil response latencies are computed from the phase-shift needed in the first Fourier harmonic to match the stimulus modulation. Therefore the time delay measured using periodic modulation is from stimulus onset to the peak of constriction not from onset to start of constriction as in the pupil response to a single flash. As a result time delays are in the order of 450-550 ms much longer than the 250-350 ms response to a single flash. The advantage of the periodic response is that requires fewer traces in the averaging (12-16 is generally sufficient) to obtain a good signal to noise ratio.

3.6 Periodic modulation and Fourier signal analysis

Computation of pupil amplitude and latency

A minimum of 16 traces were averaged for each eye and both the pupil amplitude and the time delay of the response were computed from the fundamental harmonic of the Discrete Fourier Transform (DFT) of the averaged trace following standard numerical

computation techniques (Press et al., 1992). Typical parameters of interest in a pupillogram are the amplitude of the constriction in mm and the time delay of the response in ms. The signal to noise ratio measures the signal strength and the non-linearity indicates the contribution from harmonics other than the fundamental in the DFT analysis of the response.
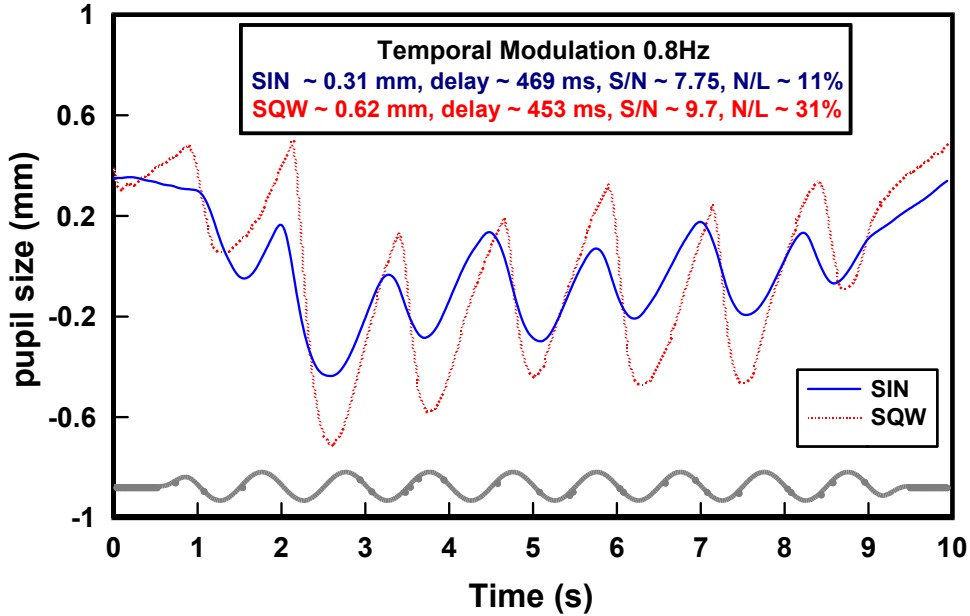
Fig. 3.7. Example of an averaged pupil response to sinusoidal (solid line) and square-wave (dotted line) luminance modulation. The amplitude (mm) and time delay (ms) of the pupil response are computed from the fundamental harmonic of the Fourier expansion of the response trace. The fundamental harmonic has the same frequency as the stimulus modulation (bottom trace in grey shown only for sinusoidal luminance modulation). SIN-sinusoidal; SQW-square-wave.

Fundamentals of Fourier signal analysis

Fourier analysis is a way to express any periodic signal with period T (frequency $f = 1/T$) as a summation of a series of sinusoidal functions with increasing frequency, with each frequency (harmonic) being a multiple of the fundamental frequency or 1st harmonic.

For example, a temporal modulation of luminance following a square wave $y(t)$ with period $T = 1/f_0$, mean amplitude L_{mean} (also known as dc level) and peak to peak amplitude equal to L_{max} can be mathematically expressed as follows:

$$y(t) = \begin{cases} (L_{max} + L_{mean}) & \text{if } [2n\pi < t < (2n+1)\pi] \\ (-L_{max} + L_{mean}) & \text{if } [(2n+1)\pi < t < (2n+2)\pi] \end{cases} \qquad \text{Eq.3-7}$$

where n= 0,1... is the cycle index

This function can also be expressed as a Fourier series $Y(t)$, that is, an approximation by a summation of sinusoids of increasing frequency:

$$Y(t) = L_{mean} + \frac{2L_{max}}{\pi}\left[Sin\, 2\pi f_0 \cdot t + \frac{Sin\, 2\pi (3f_0)\cdot t}{3} + \frac{Sin\, 2\pi (5f_0)\cdot t}{5} + ...\right] \text{Eq.3-8}$$

In the equation above f_0 is known as the fundamental frequency or harmonic. The terms containing higher frequencies have less significance as their amplitude is reduced;

the 3rd harmonic has a factor of 1/3; the 5th 1/5 and so on. Thus, the advantage of the Fourier analysis is that, in general, it is sufficient to take only a few terms in the series to get a good approximation to the original function (or data) regardless of the complication of the original mathematical expression.

Fourier analysis has obvious applications to signal processing and pupil data manipulation. For example, the pupil size oscillates in response to either sinusoidal or square-wave luminance modulation at the same frequency as the stimulus in a range between 0.5-2 Hz. The pupil response trace data, in both cases, fits well a sinusoidal function with the same frequency as the stimulus modulation, that is, a Fourier series of only one term.

Noise originated by the recording system can be filtered out easily because its frequency will be much higher than that of the stimulus. In the same way, spontaneous pupil fluctuations will not distort the computation of pupil constriction amplitudes, first because they will be averaged out during trace averaging and secondly because their contribution to the Fourier series will be at a different frequency from that of the stimulus.

Non-Linearity in the pupil response due to constriction and dilation asymmetries

Interestingly, the pupil response to a square-wave luminance modulation also contains terms with a significant amplitude for even multiples of the stimulus frequency (2 and 4 Hz for a stimulus frequency of 1 Hz). These even harmonics are not present in the mathematical Fourier expansion of a square-wave in (Eq. 3.8) and arise as a result of not having a perfectly symmetric sinusoid (Fig. 3.8). In fact this asymmetry is well known characteristic of the pupil response and is a consequence of faster constriction than dilation rates due to physiological differences between the sphincter and dilator iris muscles. These 'even' harmonics are also present, with smaller amplitude, in the response to sinusoidal modulation.

Despite these non-linearities, the constriction amplitude can be extracted accurately from the fundamental harmonic discarding higher harmonics. Higher harmonics affect mainly the shape of the approximated function but not its amplitude. Latencies, on the other hand, are slightly overestimated as a result of not having a perfectly symmetric sinusoid (maximum constriction occurs before the peak of the first harmonic). However, this shift is approximately constant for the small range of amplitudes (0.1 to 0.5mm) considered here and does not introduce significant errors in the analysis of latencies.

The time-delay is computed as the time-shift needed in the Fourier approximation of the pupil trace to match that of the stimulus modulation. It is, therefore, a time delay from stimulus onset to maximum constriction. There is thus, a contribution from the reaction of the pupil to the stimulus, which is typically in the same range as the latency for a single flash (i.e. 200-300 ms depending on stimulus strength), and the additional time delay to maximum constriction (almost 250 ms for 1 Hz modulation).
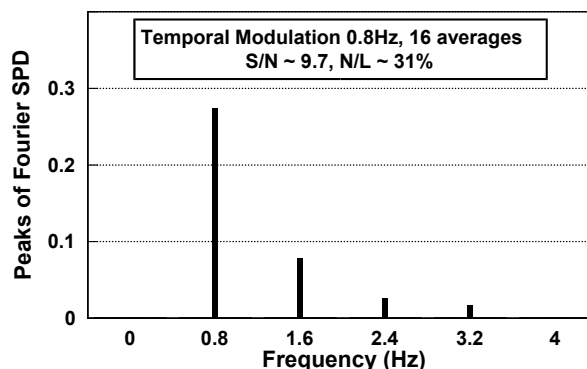
Fig. 3.8. Fourier spectrum from the square-wave data in Fig. 3.7. Asymmetry in constriction and dilation rates introduces unexpected harmonics at even multiples (1.6 and 3.2 Hz) of the fundamental frequency not present in the Fourier expansion of a square-wave. The non-

linearities introduced by these harmonics only affect the shape of the pupil trace and do not introduce significant errors in the computation of amplitudes and latencies from the fundamental frequency.

3.7 Use of isoluminant stimuli

Besides the classical pupil light reflex, the pupil is also known to respond to colour, texture (gratings) and motion, even in the absence of a total light flux change (Barbur 2002). Measurement of these non-light responses requires a careful luminance calibration of the visual stimuli chosen to avoid triggering the light reflex: both background and target (colour or gratings) need to have the same averaged luminance (isoluminant stimuli).

For gratings defined by a sinusoidal change in luminance contrast, i.e. containing dark and bright bars, the averaged spatial luminance can be easily adjusted to be equal or even lower than the background. However, the calibration of coloured stimuli is more problematic. In order to isolate the pupil colour response (PCR) from the pupil light reflex (PLR), two main approaches can be used:

1. D-isoluminant stimuli, for which the colour of the stimulus and the achromatic background have to be chosen carefully to be doubly isoluminant (d-isoluminant) i.e. to be perceptively of equal luminance both under scotopic (low luminance) and photopic (high luminance) conditions (Young & Teller 1991). This imposes an additional constraint in the photopic isoluminant plane of Fig. 3.2, and as a result, there are only two solutions (two colours) for which both isoluminant conditions can be satisfied. Geometrically, the solution can be interpreted as the line that results from the intersection of two planes: the photopic and scotopic isoluminant planes.

2. Spatio-temporal luminance contrast noise (Barbur et al 1994c). Photopically isoluminant stimuli are widely used in many areas of vision research since there is a lot of evidence that chromatic and achromatic signals follow different neural pathways. Therefore, there is much interest in isolating pure chromatic signals from luminance signals. However, the human photopic efficiency function has been derived according to the CIE standard observer and some individual differences do exist. To avoid re-calibration of the isoluminant point for each observer, dynamic spatio-temporal luminance noise is often added to visual stimuli in order to mask any possible residual luminance signals. This technique has been described previously (Gamlin et al 1998).

3.8 Doubly isoluminant coloured stimuli

Isoluminant colour stimuli have the same luminance (computed using the CIE photopic luminous efficiency function) as the background in which they are presented (Wyszecki & Stiles 1982). Isoluminant stimuli are widely used in vision research to study visual signals that are not defined by luminance (motion, texture and colour) because these signals are supposed to be mediated by anatomically different neural pathways. For example, evidence from electrophysiological recordings (Shapley 1990) suggest that isoluminant coloured targets stimulate mainly parvocellular neurones whilst luminance contrast signals are carried mainly by magnocellular neurones (see table 1-1 summarising magno and parvo cells properties in chapter 1). Although this is a general, oversimplified approximation (parvo cells carry also luminance signals and magno cells do not lack totally chromatic sensitivity), it is widely used in many models of vision research.

Because photoreceptor density varies significantly with retinal eccentricity and existing variation from the ideal CIE observer among individuals, the complete silencing of the luminance channel is virtually impossible. However, if isoluminant targets are restricted to the ten central degrees of the visual field (CIE luminous functions are available for 2 and

10 degrees), luminance signals will be reduced enough to satisfy the working assumptions in many experimental conditions.

These assumptions are certainly valid in the case of pupil responses; although a target of low luminance contrast (eg. 5%) is conspicuously visible, is not strong enough to elicit a significant pupil constriction (0.02 mm) compared to the response to a fully saturated coloured stimulus (typically 0.20 mm).

However, pupil recordings are often carried out in mesopic rather than photopic luminance conditions. Using isoluminant stimuli can introduce significant rod contrast signals. In order to minimise the contribution from rods when measuring the pupil response to colour, stimuli that are doubly isoluminant (d-isoluminant) for both photopic and scotopic conditions stimuli need to be used (Young & Teller 1991). Considering the isoluminant colour plane of Fig. 3.2, this means that d-isoluminant stimuli must belong to the intersection formed by the photopic and scotopic isoluminance planes resulting in a subset of colour hues along a line in the isoluminant plane. Thus, once the chromaticity of the background is fixed, d-isoluminant colours can be modulated in saturation along only two directions in the x-y chromaticity space. For the achromatic background (x= 0.305, y=0.323) used here, these two colours appear as magenta and green.
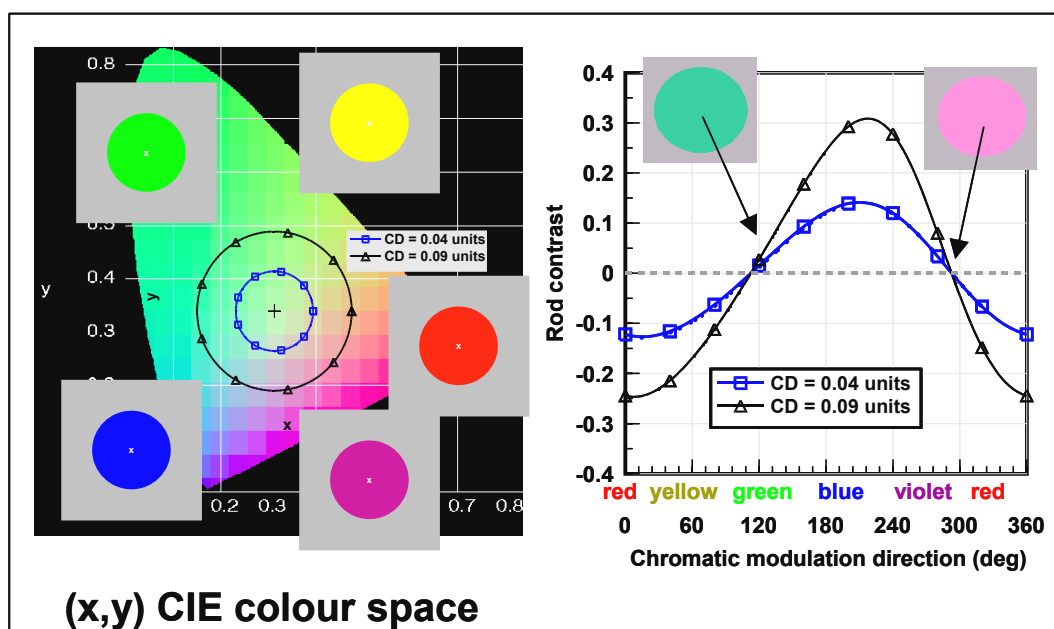
Fig. 3.9. Among all the colours in the CIE photopic isoluminant plane (left), only two colours (right) remain also isoluminant with the background under scotopic conditions. Doubly isoluminant (d-isoluminant) stimuli ensure a minimal contribution from rod signals to the pupil response. This is important because luminance levels during pupil recordings are often substantially lower than in the ideal photopic conditions. (Graph courtesy of John Barbur).

3.9 Visual psychophysics

This section describes the methods used during the psychophysical experiments (i.e. measurements of both achromatic and chromatic contrast sensitivity) described in chapters numbers 5 to 7.

Constrast Sensitivity (CS) measurements

Contrast sensitivity (CS) gives a better estimation of visual performance than standard letter charts. CS is defined as the inverse of the minimum contrast (threshold) needed to detect sinusoidal gratings of different spatial frequencies (cycles per degree of visual angle) presented in a uniform background. The contrast sensitivity function typically peaks at about 5 cycles per degree (see Fig. 7.6 in chapter 7), and falls steeply at higher

frequencies (finer gratings). For a review on the effects of grating size, location and background luminance on CS see for example David Regan's book (Regan 1999b).

A standard adaptive staircase procedure (Levine 2000) was used to measured the minimum contrast needed to detect gratings of different spatial frequencies embedded in a uniform background of 24 cd/m^2.

The higher luminance resolution of 10-bit over 8-bit cards is essential for accurate measurements of contrast sensitivity. Depending on the spatial frequency, humans can detect changes in luminance contrast as low as 0.3% giving CS values higher than 300. This implies that, for a grating with a space-averaged luminance of 24 cd/m^2, the difference in luminance between the bright and dark bars of a grating needs to be as small as 0.07 cd/m^2. Such small increments in luminance cannot be achieved using a 8-bit graphics card since the minimum increment from one gun level to the next is about 0.5 cd/m^2 at 24 cd/m^2 and even at 12 cd/m^2 never smaller than 0.3 cd/m^2 (from Fig. 3.3).

Colour vision test

Colour vision was assessed using a computer-based psychophysical test developed at the City University, London by John Barbur and collaborators. The test is available online at http://www.city.ac.uk/avrc.

In each presentation, a coloured target is presented foveally, moving in 4 possible diagonal directions. The task of the observer is to identify in which direction the target has moved. This 4-alternative forced choice procedure (4AFC) is repeated, following an adaptive staircase, increasing or decreasing the colour saturation of the target according to the responses given by the observer. If the observer detects the target the stimulus intensity in the next presentation will decrease, and viceversa. After each reversal, the step size in the staircase is reduced. The test finished after 9 reversals. The first 3 reversals are ignored and only the last 6 reversals are averaged to compute the chromatic threshold, defined as the minimum colour saturation needed to distinguish a coloured target embedded in the achromatic white background. Chromatic distance (CD) is thus computed for each direction as the distance in the x-y colour space from the achromatic background of coordinates (0.305, 0.323) using Eq. 3.6. This background is known also as MacAdam white, since it has the same chromaticities coordinates used in MacAdam's original experiments (MacAdam 1942). This achromatic background appears perceptually as an uniform grey and is used to avoid adaptation to a particular colour and mask possible after-effects following each stimulus presentation.

For an example of colour threshold measurements in patients suffering a demyelinating disease see Fig. 7.4 in chapter 7. To test colour vision, it is generally sufficient to measure CD thresholds for 18 different directions (colour hues) in the CIE xy-1931 colour space. In the experiments reported in this thesis, the coloured moving targets were isoluminant with the achromatic background (luminance = 12 cd/m^2) and were presented embedded in a square array of 14 X 14 checks subtending 4° at the fovea from a viewing distance of 70 cm (see Fig. 5.1 in chapter 5 for a picture of the stimuli used). The colour patch moved diagonally at a speed of about 3.5° per second (stimulus duration of 1.6 s).

In order to mask residual luminance signals arising from individual deviations from the CIE ideal observer, and to avoid re-calibration of the isoluminant point, a dynamic luminance random noise was added to the background; the luminance of each check changes randomly in time every 2 refresh frames (ie. every 23.4 ms for a refresh rate of 85 Hz) but the space averaged luminance of the whole stimulus field remains constant and equal to that of the surrounding background. A more detailed description of luminance masking techniques for the measurement of chromatic sensitivity has been reported previously by Barbur et al. (Birch et al 1992, Barbur et al 1994c)

Chapter 4: Pupil responses to different visual stimulus attributes

A number of experiments were carried out to investigate pupil responses to sinusoidal and square wave modulation of different stimulus attributes such as amplitude of light flux change (contrast), location in the visual field, chromatic saturation and spatial frequency. The aim of these studies was to investigate the spatio-temporal properties of the mechanisms that drive the pupil response. The results suggest that at least two mechanisms mediate the pupil light reflex: a transient mechanism favoured by square-wave luminance modulation and a sustained mechanism that predominates during slow or gradual changes in luminance such as low frequency sinusoidal modulation. On the other hand, responses to chromatic contrast or sinusoidal gratings whose spatial average luminance is equal to that of the background (equi-luminant gratings) do not depend on the temporal wave-form of stimulation.

4.1 Pupil Light Reflex (PLR) response measurements

Contrast gain of the pupil: sinusoidal and square-wave luminance modulation

The first experiment was designed to investigate the relationship between the amplitude of pupil constriction and the luminance contrast of the visual stimulus (i.e. the contrast gain of the pupil response). The stimulus employed in this experiment was a disc of 9º diameter whose luminance changed over time following either a sinusoid or a square-wave for a period of 10 seconds at 0.8 Hz (i.e. 8 full cycles). The disc was presented foveally in an achromatic uniform background of 12 cd/m^2 and CIE (x,y) coordinates of (0.305, 0.323) which corresponds to the achromatic white background used by MacAdam in his original experiments (MacAdam 1942).

The percentage of contrast modulation determines the change in luminance above and below an averaged level of 48 cd/m^2. For example, a maximum contrast modulation of 100%, means than the maximum and minimum luminance values of the stimulus were at 96 and 0 cd/m^2, respectively. The average level of 48 cd/m^2 was chosen to maximise the contrast amplitude since the maximum stable luminance level that can be achieved on the CRT computer display used in these experiments was about 100 cd/m^2.

Pupil traces were measured in response to eight different levels of contrast modulation (from 5% to 100%), randomly interleaved for each stimulus presentation. A minimum of 16 traces were averaged for each contrast level and the averaged trace was used to extract the pupil constriction amplitude (see chapter 3 for more details about measurement procedures). The mean data obtained from 6 subjects (Fig. 4.1) show that, although the light flux change is the same for both types of modulation, the response is much larger to square-wave modulation than the response elicited with sinusoidal modulation for each of the different contrast levels tested.
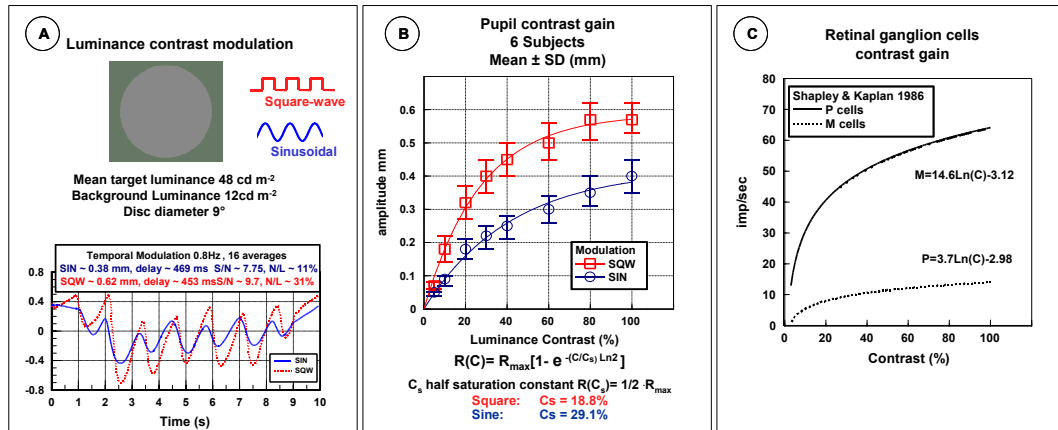
Fig. 4.1. (A) Example of pupil response traces from one subject to sinusoidal (solid line) and square-wave (dotted line) luminance modulation at 100% contrast. The stimulus consisted of a disc subtending a visual angle of 9° at the fovea. Its luminance was modulated at 0.8 Hz for a period of 10 seconds. (B) Constriction amplitudes as a function of contrast for 6 subjects. The responses to square-wave modulation are much larger and saturate more rapidly with stimulus contrast. The non-linear curve fitting was obtained using the Levenberg–Marquardt algorithm (Press et al 1992). This disparity in the pupil contrast gain is likely to reflect the differences in temporal response characteristics between sustained (P cells) and transient (M cells) and their contribution to the pupil response (panel C). SIN-sinusoidal; SQW-square-wave.

Pupil frequency response

The frequency response of the pupillary system was investigated to determine whether one single linear mechanism (or neural substrate) could account for the larger responses found when using square-wave, instead of sinusoidal modulation. The results for two observers in Fig. 4.2 show that the square-wave response is much larger for several stimulation frequencies. Moreover, even when the contribution of higher harmonics are added to the sinusoidal responses at 0.6, 0.8 and 1 Hz, the Fourier sum with the corresponding weighting factors (see equation 3-8 in chapter 3) is smaller than the measured response to the square-wave. This implies that the pupil is a non-linear[1] system in which rapid contrast changes boost the response. From Fig. 4.2, is also clear that the pupil response is markedly low-pass: pupil oscillations are very small for any stimulation frequencies above 2-3 Hz. This low-pass filtering is caused by the particularly slow dynamics of the human iris muscle. In other vertebrates, e.g. in birds, the pupil can follow oscillations as fast as 20 Hz (Loewenfeld 1993).

---

[1] Another source of non-linearity comes from the asymmetry in pupil constriction and dilation rates which introduces unexpected harmonics at even multiples of the stimulation frequency. However, this non-linearity affects mainly the shape of the response wave-form and not its amplitude (see discussion in chapter 3, section 3.6 and Fig. 3.8).
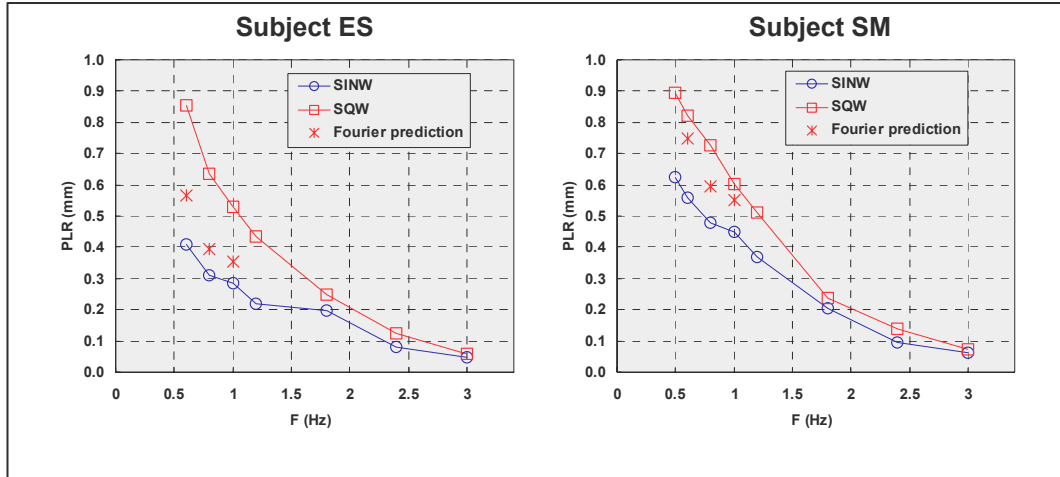
Fig. 4.2. (A) The larger constriction amplitudes elicited by square-wave luminance modulation, cannot be accounted for by adding the contribution of higher harmonics present in the square-wave input. Fourier analysis suggest that the pupil is a non-linear system: the contribution from high frequencies cause a larger response amplitude than expected from a linear system. The Fourier prediction was computed assuming a non-linear contrast dependence of the sinusoidal response obtained from the curve fitting of Fig 4.1B. SIN-sinusoidal; SQW-square-wave.

Fourier analysis and non-linearities in the pupil system

Several researchers have studied the pupil frequency response and proposed detailed models to include the various non-linearities of the pupil system (Clynes 1962, Troelstra 1968, Semmlow et al 1975, Milton & Longtin 1990, Myers et al 1993, Stark 1984, Bressloff et al 1996). I present here a simple model to account for the results shown in Fig 4.2.

In system analysis, a system with a response function $R[i_1]$ to input i_1 is said to be linear if it has the following properties:

1-	Homogeneity	$R[\alpha i] = \alpha R[i]$	where α is a scalar	Eq.4-1
2-	Additivity	$R[i_1 + i_2] = R[i_1] + R[i_2]$		Eq.4-2

Thus, if the pupil were to behave as a linear system, the pupil response (R) for a square-wave of amplitude A and frequency f_0 could be predicted by a Fourier expansion as follows:

$$R[A\ Sqw\ (2\pi f_0 t)] = 2/\pi \{ R[A\ Sin(2\pi f_0 t)] + 1/3\ R[A\ Sin(3\ 2\pi f_0 t)] + ... \} \qquad \text{Eq.4-3}$$

That is, the response to a square-wave will be the weighted sum (by $2/\pi$) of the responses to sinusoids of increasing frequency (knows as harmonics). Each sinusoid has a frequency that is an odd multiple of the original frequency contained in the square-wave. The terms containing higher frequencies have less significance as their amplitude is reduced; the 3rd harmonic has a factor of 1/3; the 5th 1/5 and so on. Since the pupil do not follow oscillations to frequencies higher than 5-6 Hz (these high frequencies produce a sustained pupil constriction known as the pupil response to flicker) is usually enough to take 2 or 3 terms in the Fourier sum. For example, the linear Fourier prediction for a square-wave of 1Hz could be computed from the weighted sum (multiplied by $2/\pi$) of the responses to sinusoidal stimulation with the same amplitude and frequencies of 1, 3 and 5 Hz but each attenuated with their corresponding factor (1, 1/3, 1/5).

However, it is clear from Fig 4.1 that the pupil contrast gain is non-linear even for a sinusoidal input. So the data in Fig 4.1 could be used to compute the expected Fourier amplitude from sinusoidal responses to increasing frequencies without assuming that the pupil has a linear contrast gain (ie. assuming Eq. 4-2 holds but not Eq. 4-1). As we can see from Fig 4.2 the Fourier prediction underestimates the actual response. Therefore, the non-linearity in contrast gain alone cannot account for the much larger amplitude

measured for square-wave modulation and other non-linear mechanism(s) must influence the pupil amplitude at low frequencies. Two obvious non-linear mechanisms that have been neglected so far are:

- <u>the non-linearity of pupil size with luminance</u> (with a steady background as shown in Fig 2.1): this non-linearity reveals the effect of retinal adaptation on the pupil size and is likely to contribute to the well known asymmetries in the pupil constriction and dilation rates. Retinal adaptation may play an important role at very low frequencies (< 0.5 Hz) and when large changes in luminance are involved (several log units). The effect of retinal adaptation is likely to decrease rapidly for frequencies above 0.5 Hz since the adaptation of retinal photoreceptors is generally slow. The pupil responses reported here were measured in response to luminance modulation of a maximum of 2 log units (a peak to peak amplitude from 1 to 100 cd/m^2) and the change in pupil diameter for such a small range can be considered almost linear (see Fig 2.1).

- <u>non-linear summation of higher harmonics:</u> contribution from high frequencies may cause larger pupil responses at low frequencies for square-wave modulation. We cannot measure directly responses to these high frequencies because these fast varying signals, although they are present in the firing of neurons of the EW (Sillito & Zbrozyna 1970), are transformed into slow muscle constriction signals with low-frequency characteristics. However, as the study of Sillito et al. suggest, these high frequency signals in the EW probably modulate the constriction amplitude of the sphincter muscle. Additional support for this idea comes from studies that have shown that the pupil responds to sinusoidal flicker with a sustained pupil constriction of increasing amplitude for frequencies up to 8 Hz. For frequencies above 8-10 Hz, the pupil amplitude of the sustained constriction decreases (Troelstra 1968, see also page 182 of Lowenfeld's book referring to the original work of Webster and Heller 1968). The low-pass frequency response is also consistent with studies showing a maximal pupil response after electrical stimulation of the EW for frequencies of 8 Hz or higher (Sillito & Zbrozyna 1970). It has also been shown that the neural firing rate of OPN neurons can follow high frequency oscillations (up to 20Hz) in response to sinusoidal light modulation (Clarke & Ikeda 1985). It seems therefore, that despite the iris cannot follow frequencies above 3-4 Hz, these high frequencies may have an influence on the pupil response amplitude at low frequencies. Based on these results, we can expect that the contribution from high frequencies rapidly decrease for frequencies above 8 Hz. Is then easy to see why stimulation at frequencies above 2 Hz are less effective in eliciting large constriction amplitudes (Fig 4.2). For example, a square-wave of 1Hz, has contribution from harmonics at odd multiples of the fundamental frequency i.e. 1, 3, 5, 7, 9 Hz. For a square-wave of 2 Hz, the contribution comes from harmonics at much higher frequencies (2, 6, 10, 14... Hz). It is easy to see that for frequencies of 3 Hz or above the contribution comes from harmonics (3, 9, 15 Hz) with frequencies that are too high to be efficient in driving the pupil.

4.2 Pupil responses to isoluminant stimuli

The pupil is also known to respond to isoluminant colours or spatial patterns (e.g. equi-luminant gratings) even in the absence of a net light flux change (Barbur 1995). These responses are essentially different from the pupil light reflex (PLR) since different neural pathways may be involved. Numerous electrophysiological and psychophysical recordings (Shapley 1990; Wandell 1995) suggest a segregation between luminance and isoluminant chromatic signals early in the visual pathways (see also chapter 1 for a detailed description of magnocellular and parvocellular visual pathways). The question of

interest in this study was thus to determine whether the pupil colour response (PCR) and the pupil grating response (PGR) show similar characteristics as the PLR.

4.3 Pupil Colour Response (PCR) measurements

In order to isolate the PCR from the classical pupil light reflex (PLR), the colour of the stimulus and the achromatic background need to be doubly isoluminant (d-isoluminant) i.e. to be of equal luminance for both rods and cones (Young & Teller 1991, see also chapter 3). The stimulus used here consisted of a reddish coloured disc subtending 7° and centered foveally on a uniform achromatic background with CIE (x,y) coordinates (0.305, 0.323) corresponding to MacAdam's white (MacAdam 1942). The chromatic contrast of the disc was modulated using square-wave or sinusoidal waveforms at 0.8 Hz for a period of 10 seconds. The maximum chromatic saturation allowed by the phosphors of the display for the red disc was 0.16 units, measured as the distance from the background chromaticity in the x-y CIE chromaticity diagram (Wyszecki & Stiles 1982).
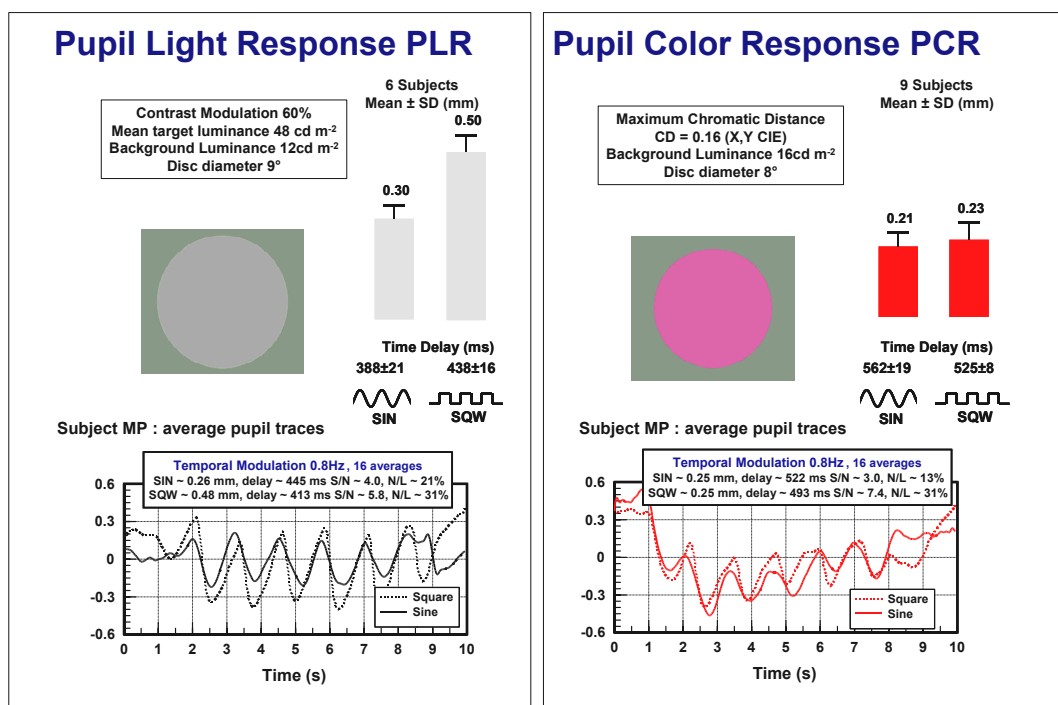
Fig. 4.3 Pupil responses to isoluminant chromatic modulation (right panel) do not depend on the temporal waveform of the stimulus. Unlike luminance modulation (left panel), the high frequency components in a square-wave do not cause a larger constriction when the visual stimuli is isoluminant. This is consistent with the traditional view that describe isoluminant neurones as low-pass temporal filters. Pupil amplitudes and time delays for each subject were computed from the fundamental harmonic of the Discrete Fourier Transform (DFT) from the averaged trace (plotted only for subject MP) of a minimum of 16 responses. Bars show the mean amplitude from a group of subjects.

Results both for the PCR (Fig. 4.3) and the PGR (Fig. 4.4) show that, unlike the PLR, there are no significant differences between sinusoidal and square-wave modulation. This suggest that the enlarged pupil light response to square-wave modulation is a unique characteristic of the achromatic luminance pathway which has little or no effect on the isoluminant pathway. This finding is also consistent with numerous electrophysiological studies that describe the isoluminant pathway mainly as slow or sustained (parvocellular), whereas the luminance pathway receives contributions from both sustained and transient (Schiller et al 1990, Kaplan et al 1990, Shapley 1990).

4.4 Pupil Grating Response (PGR) measurements

Pupil cyclic oscillations were also measured in response to gratings whose luminance changed sinusoidally along the horizontal direction, resulting in alternating dark and bright bars but with a total space-averaged luminance equal to that of the background (see Fig. 4.4). In addition, the difference in contrast between bright and dark bars of the grating was modulated in time following a sinusoid or a square-wave at the same stimulus frequency as in the studies of the PLR and PCR.

The main interest of comparing sinusoidal and square-wave modulation was to determine any possible differences between the two responses since is it is widely accepted that, in achromatic vision, transient neurones (magno cells) respond mainly to low spatial frequencies and high temporal frequencies whereas sustained neurones (parvo cells) have higher sensitivity to high spatial frequencies and low-pass temporal characteristics (Schiller & Malpeli 1977, Reese & Cowey 1988). According to this, the optimal stimulus for the transient pathway would be a coarse, square-wave grating while the sustained pathway would prefer a fine sinusoidal grating.

Surprisingly, the results for the PGR did not show any significant different between the sinusoidal and square-wave modulation (Fig. 4.4). In the PCR, the absence of response enhancement in the square-wave modulation was more or less expected since the isoluminant colour pathway lacks neurones responding to high frequencies (transient cells) but the PGR is thought to stimulate both sustained and transient cells in the achromatic luminance pathway. Thus, these 'non-light' pupillary responses do not reflect the division found in the pupil light response into sustained and transient subcortical mechanisms. A possible explanation for this is that, unlike the PLR, responses to colour and grating stimuli may involve further stages in visual processing (eg. cortical processing of texture and colour) that smooth out any fast varying signals. Cortical influences on pupil size have been previously suggested by several researchers (Benevento et al 1977) and indication of a longer, cortical pathway mediating non-light pupil responses comes from the increased pupil latencies measured to isoluminant stimuli (at least 80 ms longer than for the PLR, see Fig. 4.3). Consistent with this idea is also the fact that such responses survive the destruction of subcortical pupillomotor centres in the pretectum (Barbur 2002, Wilhelm et al 2002)

However, it is interesting to note that the dependence of the PGR constriction amplitude with spatial frequency might still reflect differences in the receptive field size of neurones in the optic nerve that remains even after cortical mediation (see also experiments on spatial summation further later in this chapter). Although measurements of PGR to high spatial frequencies were not carried out due to restrictions in recording time and a minimum viewing distance needed to avoid changes in lens accommodation (and thus excessive pupil fluctuations), it is expected that the sensitivity of the pupil drops again at high spatial frequencies in a similar fashion as the visual sensitivity does (see for example Fig 7.6 in chapter 7).

Another interesting observation is that, at low spatial frequencies (eg. 0.5 cycles/deg), the response is in the same order (0.1 mm) as the response to a disc of low contrast (see Fig. 4.4). Both responses can be explained as a result of the normal cortical activity following the presentation of a stimulus in the visual field and a subsequent transient disruption of the sympathetic tone to the iris dilator muscle via cortico-thalamic connections (Wilhelm et al 2002).
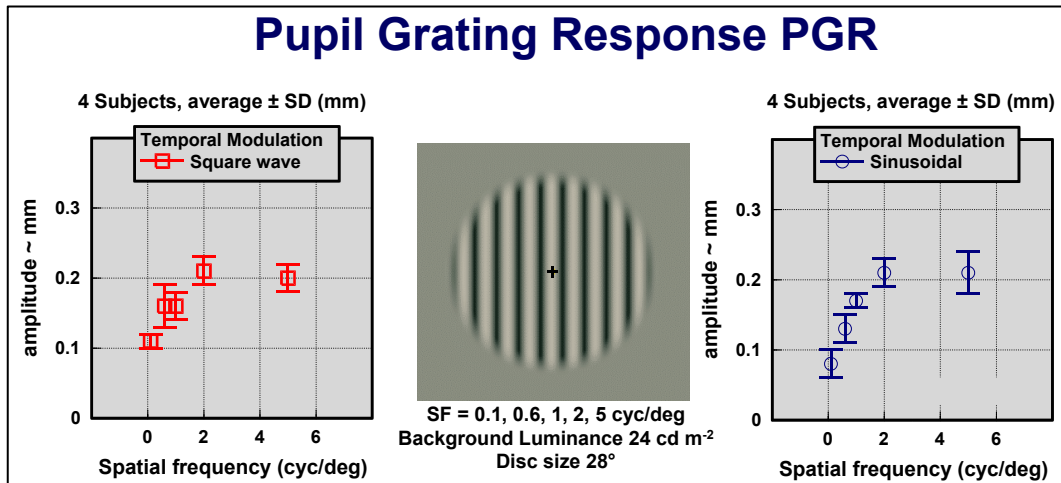
Fig. 4.4 Square-wave temporal modulation (left) of isoluminant gratings did not result in larger constrictions in comparison to sinusoidal modulation (right). This result is similar to that found in the PCR (Fig. 4.3) and reinforces the idea that high temporal frequencies enhance the pupil response only when luminance changes are involved but not when isoluminant stimuli are used.

Contribution of accommodative changes to the PGR

Since pupil size can constrict vigorously when the eye changes fixation from far to near (Alpern et al 1961), there is the possibility that the PGR reflects partly the constriction elicited when subjects are asked to fixate their view on the computer display at the beginning of each trial. To address this issue directly, responses to a blank stimulus (see Fig. 4.5) were measured and averaged to determine the significance of accommodative changes on pupil size at the same viewing distance used throughout all experiments (70 cm).
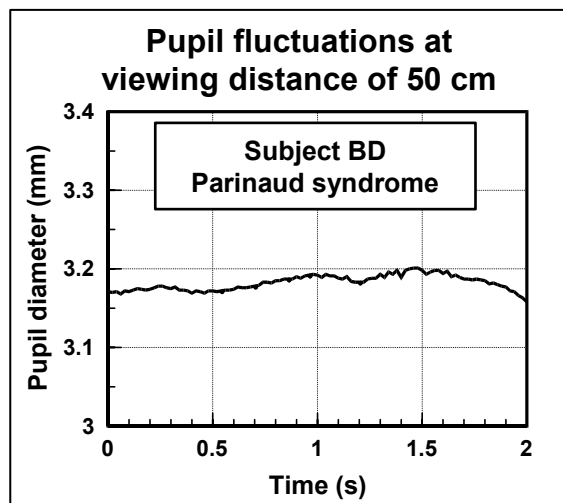
Fig. 4.5 Oscillations in pupil size when a subject was asked to fixate to a blank stimulus at the same viewing distance used throughout all experiments (70 cm) were much smaller (<0.04 mm) than those elicited by the grating patterns. Further proof that the PGR is a 'true' response and not cause by accommodation changes comes from the increase of the PGR amplitude with spatial frequency found in Fig. 4.4 which cannot arise simply from changes of accommodation.

4.5 Pupil Perimetry

A newly developed, pupil perimetry program using the P_SCAN system was used to investigate the correlation between pupil perimetry and standard visual field perimetry (evaluated with the Humphrey's visual field analyzer). This program was aimed to gather further evidence towards establishing whether pupillomotor fibres are affected in the same way as visual fibres in cases of lesions to the early visual pathways, namely optic nerve damage caused by tumours, vascular lesions or demyelination (see also chapter 7). The possible stimuli consisted of 24 rectangular sectors presented individually or in groups to test a particular region in the visual field. These sectors were arranged in 3 concentric rings with maximum outer diameters of 9°, 15° and 21° of visual angle (see Fig. 4.6 for a geometrical view of stimuli used).
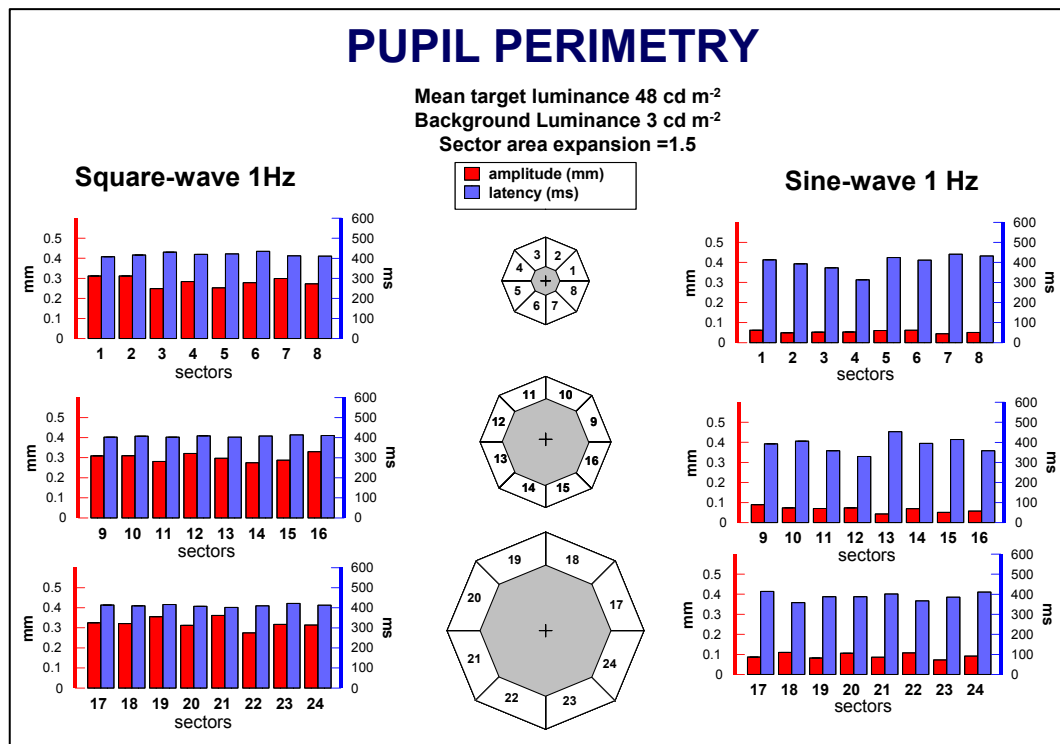
Fig. 4.6. A Pupil Perimetry test was developed to investigate the variation of pupil sensitivity across the visual field. Amplitudes and latencies were extracted at each location for sinusoidal (right) and square-wave (left) luminance modulation at 1 Hz (mean luminance 48 cd/m^2, 100% modulation). The sector area increased by a factor of 1.5 at each eccentricity to achieve approximately the same pupil response across the visual field. The pupillomotor system has therefore a different magnification factor than the visual system in which much more significance is given to the central 5° than the periphery. This factor should be taken into account when comparing pupil with visual field perimetry maps.

Preliminary experiments were carried out to establish the optimum parameters for the test, i.e. frequency of modulation, luminance and stimulus size. The choice of sector size is particularly critical: in order to compare pupil responses in patients with a localised visual field loss is essential to use stimuli that elicit the same pupil response when presented at different locations. To achieve this, the area of sectors from the inner ring to the next outer ring increased by a factor of 1.5. This also allowed to obtain pupil traces of similar signal to noise ratio over the central 21° of the visual field as can be seen in Fig. 4.6. The pupillomotor system has therefore, a different magnification factor than the visual system in which much more significance is given to the central 5° (cortical magnification) than the rest of the peripheral visual field (Wandell 1995). This difference should be taken into account when comparing pupil with visual field perimetry maps. The main disadvantage of pupil perimetry is that, in general, the spatial resolution is lower than with visual field perimetry. Small visual field defects may not be easily detectable

with pupil perimetry because rather large stimuli are often needed to elicit a measurable response. However, pupil perimetry can still add useful information in certain clinical studies since it provides an objective evaluation of optic nerve damage. Moreover, some lesions seem to affect pupil responses despite a recovery of visual function (see also chapter 7 for an example of remaining pupil deficits after recovery of visual acuity in optic neuritis).

There are not many studies correlating visual and pupil perimetry. Results in patients with lesions in different locations along the visual pathway have found a relatively good correlation (Barbur et al 2000, Kardon et al 1993) but still discrepancies between visual and pupillary function are likely to occur because of substantial differences in the respective topographical mappings. One way of correcting for this differences would be to use pupil stimuli that yield comparable pupil responses across the whole visual field.

Sinusoidal and square-wave responses

Given the conspicuous differences in amplitudes between sinusoidal and square-wave luminance modulation found for one subject across the entire visual field in Fig. 4.6, more data were obtained from 8 subjects to test the significance of this difference. In this case, each stimulus consisted of 2 sectors instead of 1 to obtain sufficiently large responses even for those subjects with small and less reactive pupils, and testing time was also shortened considerably by collecting data at only one eccentricity instead of three. The results, shown in Fig. 4.7, confirmed that constriction amplitudes elicited by square-wave modulation were significantly larger than for sinusoidal modulation ($p<0.01$ unpaired t-test). However, latencies times varied little and were roughly the same (460-470 ms) for the two conditions.

Subjects fixated at a central point in the computer display with their left eye covered so as to stimulate only their right eye. Thus, sectors 9+10 and 15+16 in the graph fell on the nasal retina while the sectors 11+12 13+14 stimulated the temporal retina. It follows from the amplitude data in Fig. 4.7 that the nasal retina seems slightly more sensitive than the temporal retina. However, these differences failed significance ($p>0.05$ t-test) both during sinusoidal and square-wave modulation. In fact, the order of magnitude (0.03-0.04 mm) of naso-temporal differences is well within the variability expected among individuals (the smallest standard deviation measured here was 0.07 mm). Other authors (Smith & Smith 1980, Kardon et al 1991) have also obtained similar asymmetries when stimulating different quadrants in the visual field, but these never reached significance. There is even some anatomical evidence of small differences in the strength of these naso-temporal retinal projections (Kupfer et al 1967) in the optic nerve, but it seems that the effect in the amplitude of the pupil response is very small. Only very precise measurements of pupil size changes will reveal these differences and the interest will be thus limited to research in the field. The naso-temporal asymmetry, however, may be of some importance in clinical studies using pupil perimetry to compare nasal and temporal sensitivity within a particular individual since pupil response variability within the same subject is then much smaller.
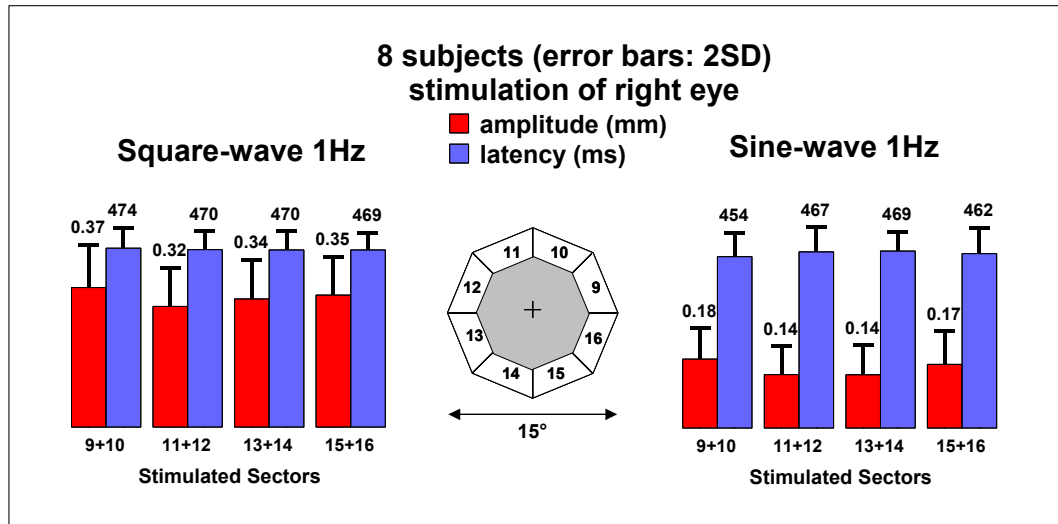
Fig. 4.7. Significantly larger amplitudes (p<0.01) were elicited using square-wave (left) compared to sinusoidal (right) luminance modulation while latencies were roughly the same. The small differences found after stimulating the nasal retina (sectors 9+10 and 15+16) compared to the temporal retina (11+12 and 13+14) failed to reach statistical significance (p>0.05).

Direct and consensual responses

In normal subjects with intact efferent pupillary pathways there is, a priori, no difference between the direct and consensual pupil response because there are roughly the same number of neurones projecting to the ipsilateral and contralateral Edinger-Westphal (EW) nuclei from the Olivary pretectal nuclei (OPN). See Fig 2.2 in chapter 2 for a schematic view of the pupillary pathways.

Michael Rosenberg (personal communication, ARVO 1999) has proposed the possibility of being more crossed than uncrossed fibres projecting to the EW nucleus from the OPN in man. He studied patients with visual field hemianopias (in which one half of the visual field is blind) and measured pupil responses after nasal or temporal stimulation. He found that, during nasal stimulation (when retinal fibres project to the contralateral OPN), the direct pupil response is greater than the consensual. Interestingly, this is exactly the same result we obtained with the P_SCAN system, which allows the recording of the consensual (non-stimulated) eye by means of a visually opaque, infra-red transmitting filter. After nasal stimulation (locations highlighted in Fig. 4.8 following temporal visual field stimulation) the direct pupil response tends to be stronger than the consensual.
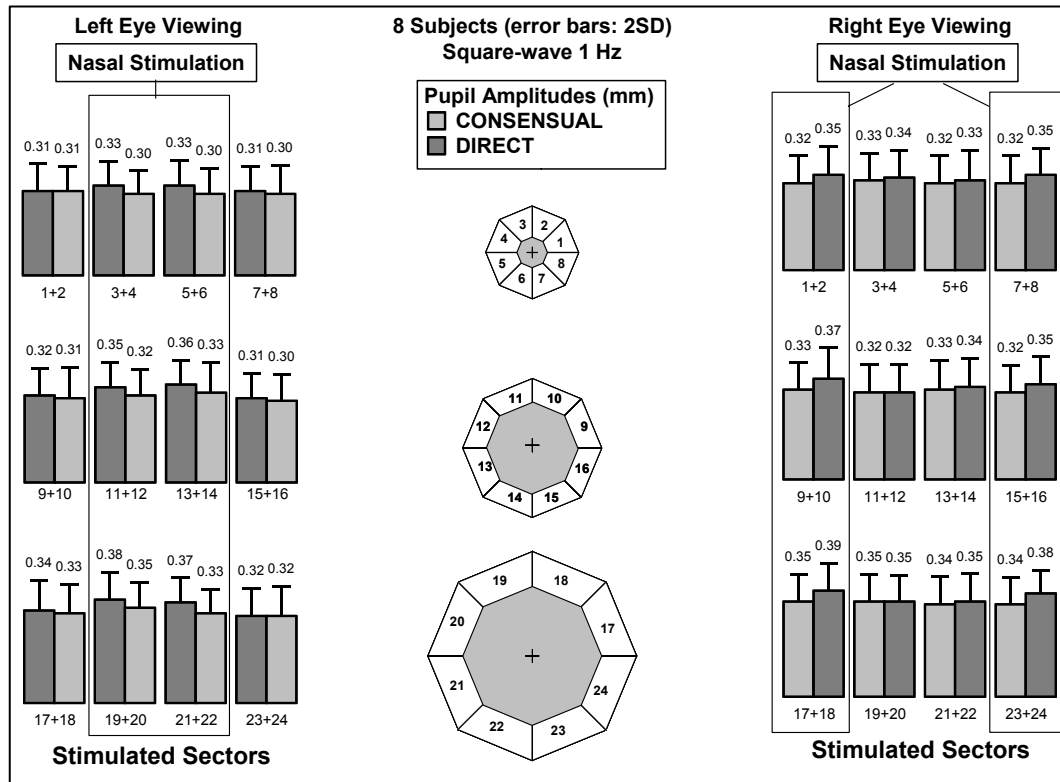
Fig. 4.8. After nasal stimulation (temporal visual field stimulation), when retinal fibres project to the contralateral OPN, the pupil direct response is always larger than the consensual (non-stimulated eye). This result suggests that there could be more crossed than uncrossed fibres projecting from the OPN to EW in man. Data were obtained from 8 subjects after stimulating either the left (left graph) or the right eye (right graph) in monocular viewing.

4.6 Spatial summation in the PLR

In order to investigate the spatial summation properties after square and sinusoidal luminance modulation, we compared at the same three eccentricities used before, responses to stimuli composed of 2 sectors with the mean response obtained when stimulating each of the 2 sectors individually. An index was then computed to indicate spatial summation (Fig. 4.9). If the index equals to one, this means perfect summation (doubling the stimulus area doubles the response amplitude). An index of zero means the complete absence of spatial summation. An index greater than one (over-summation) can also occur since neural signals elicited by small stimuli might not reach a pupillomotor threshold to trigger a significant response and doubling stimulus size may enhance the integration of the neural signal input to the pupil luminance detectors in the olivary pretectal nuclei (OPN).
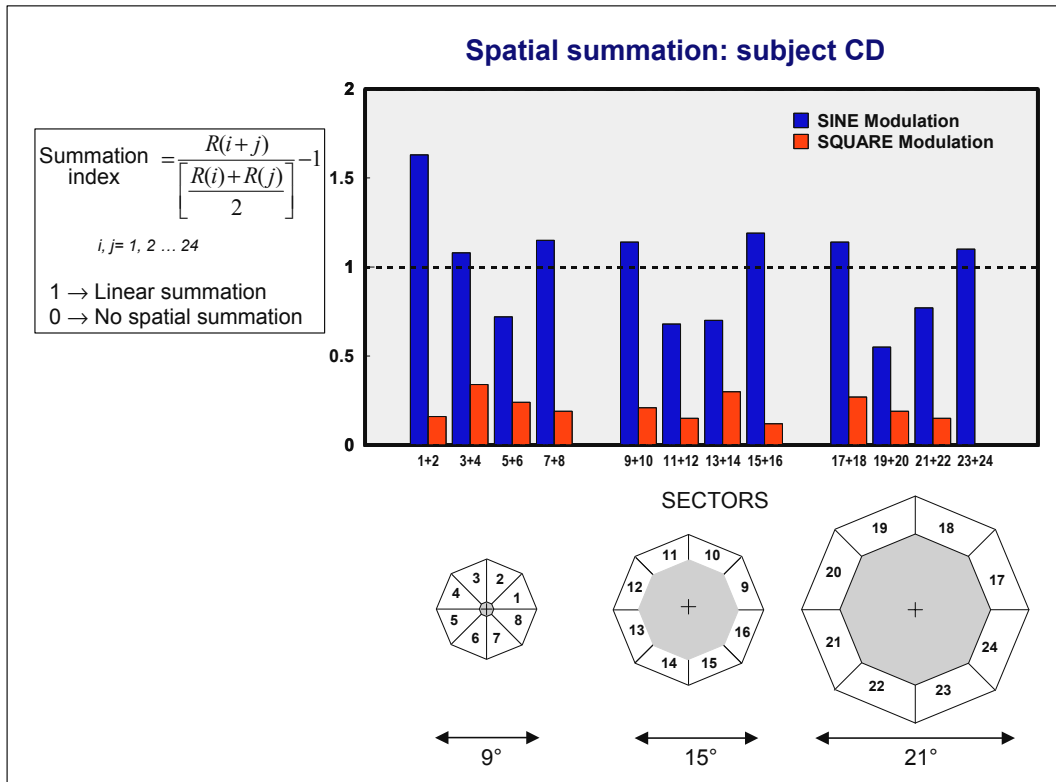
Fig. 4.9 Marked spatial summation differences occur across the entire visual field when comparing sinusoidal to square-wave luminance modulation. Much better spatial summation (almost linear) was found for sinusoidal stimulation.
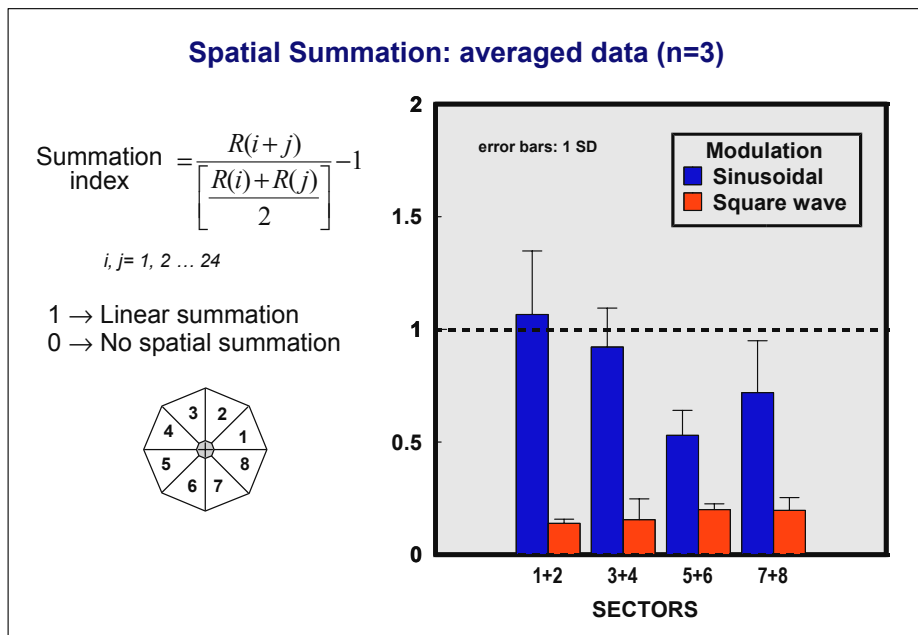
Fig. 4.10 Data obtained for another 3 subjects confirms the results of Fig. 4.9 but also show large inter-subject variability.

Interestingly, spatial summation for square wave stimuli was found to be significantly poorer than that for sine wave stimuli across the entire visual field (Fig. 4.9) and similar results were also obtained for another 3 subjects (Fig. 4.10). Small differences seem also to arise in the spatial summation after nasal and temporal stimulation. However, it is important to point out that any conclusions drawn from these results are limited by two facts: first, large inter-subject variability yields large errors and second, the high relative

error propagation introduced in the mathematical computation of the summation index (specially when the index is small). In any case, it is clear that despite the large inter-subject variability, the data suggest that stimulus spatial summation for square-wave and sinusoidal luminance modulation can be markedly different.

Effect of stimulus size

The analysis of the spatial summation results obtained from pupil perimetry encourage further experiments to study the relationship between stimulus size and the pupil constriction amplitude. In this experiment, the stimulus consisted of a disc presented foveally in a achromatic uniform background of luminance 3 cd/m^2. The diameter of the disc varied from a visual angle of 2° to 18° which is the maximum size that can be displayed in a 21" computer screen at a viewing distance of 70 cm. The averaged results for 3 subjects are shown in Fig. 4.11. The data confirm the previous results presented in figures 4.9 and 4.10 for a much wider range of stimulus sizes. Sinusoidal modulation show approximately linear spatial summation across all sizes tested , whereas square-wave responses exhibit limited summation and saturate quickly with stimulus area.
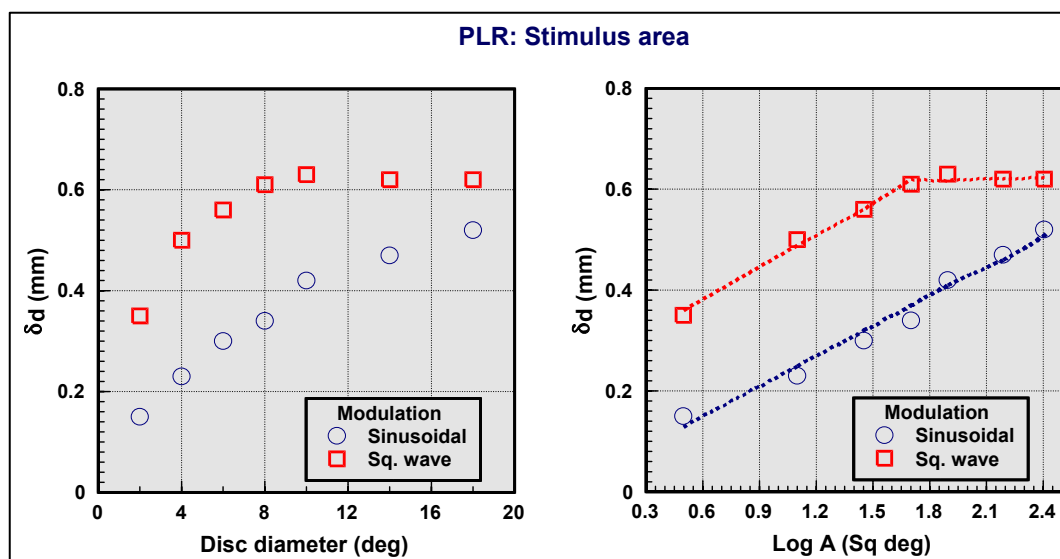
Fig. 4.11. (Left graph) Responses to sinusoidal modulation shows good spatial summation for a wide range of stimulus sizes (2 to 18 degrees) while the square-wave response saturates quickly. The data points were re-plotted (right graph) on a Log scale of stimulus area (square degrees) to illustrate the fact that pupil responses increases with the Log of the total light flux entering the eye. Average data from 3 subjects.

A simple model for spatial summation

The data from Figures 4.9 to 4.11 provide evidence for the hypothesis that sinusoidal and square-wave responses may involve different neural pathways. A simple model containing two populations of neurones, each with different effective 'receptive field' sizes, could account for the differences found in spatial summation between square-wave and sinusoidal modulation. This model, schematically illustrated in Fig. 4.12, is also consistent with electrophysiological recordings that report significant differences in dendritic field size of sustained and transient pretectal neurones[2] involved in the pupil light reflex (Trejo & Cicerone 1984, Pong & Fuchs 2000).

For instance, if one assumes that the spatial sensitivity of the receptive field of pupillary neurones follows a gaussian function, the spatial summation of stimulus area will depend strongly on the receptive field size.

---

[2] A similar size segregation is also known to occur amongst retinal ganglion cells that project to the geniculo-striate visual pathways. See Fig. 1.6 in chapter 1.

Trejo et al. reported that pretectal transient neurones in the rat have very large receptive fields covering several degrees of the visual field, whereas sustained neurones were much smaller and were more densely packed. Thus, the signal from low-contrast sustained cells would increase linearly with stimulus size since it would be roughly proportional to the number of neurones that fall within the stimulus area. This would explain the linear spatial summation found for sinusoidal modulation for a wide range of stimulus areas in Fig. 4.11. On the other hand, transient neurones will only show partial summation for stimulus areas that are small compared to their receptive fields. The summation of the signal will be less than linear and will also saturate quickly because enlarging the stimulus area will only add a small contribution to the total signal since most of the light will fall either far from the centre of the receptive field or on the edge of nearby neurones where sensitivity is low.

This model is also consistent with the idea that transient cells have higher contrast gain than sustained cells (i.e higher gaussian peak values, not shown to scale in Fig. 4.11).
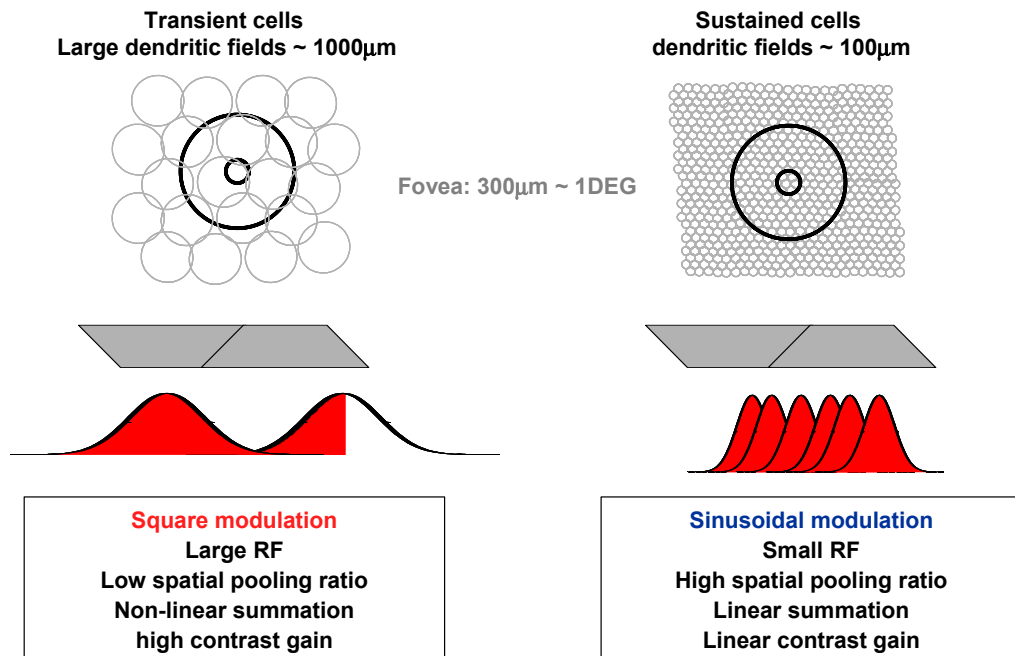
Fig. 4.12 A model of spatial summation of neural signal input to the pupil. The disparity in spatial summation properties could originate from differences in the 'effective' receptive field size (modelled here as gaussian functions) of sustained and transient cells found in the pretectal pupillomotor neurones (Trejo & Cicerone 1984, Pong & Fuchs 2000). Transient neurones (left) exhibit saturation of spatial summation because enlarging the stimulus area beyond the receptive field will only add a small contribution to the total signal. Sustained neurones (right) are much smaller and more densely packed. Thus, the signal from low-contrast sustained cells would increase linearly with stimulus size since it would be roughly proportional to the number of neurones that fall within the stimulus area. The two concentric circles represent the minimum and maximum disc sizes in the experiment of Fig. 4.11. and the grey shaded sectors the doubling of stimulus size in the experiment of Fig. 4.9.

4.7 Discussion

Square-wave modulation of luminance showed distinct spatio-temporal characteristics from those observed with sinusoidal modulation. These differences might reflect the nature of two separate mechanisms (or neural substrates) mediating the pupil light response. Although these two mechanisms are likely to operate simultaneously to control

pupil size, the waveform of the luminance modulation seems to affect significantly the relative contribution of each of these two mechanisms.

Non-linear model of the pupil light reflex (PLR)

The rapid changes in the square-wave modulation can be attributed to high-frequency components in the Fourier expansion of a square-wave in sinusoids (see equation 3-8 in chapter 3). Thus, the larger response to a square-wave modulation could be explained by means of a pupil model system in which high frequencies enhance the response, but whose final output, through temporal integration of the neural signal input, is mainly in the low frequency range. In other words, the pupil is not simply a low-pass filter; rapid changes in luminance (high frequencies) boost the constriction amplitude.

Such a pupil output could arise either from one non-linear neural substrate with a complex frequency response curve (tuned to both low and high frequencies) or as a result of two interacting mechanisms with different frequency response characteristics.

Mechanisms in the pupil light response: working hypothesis

Hypothesis 1. There is one single linear mechanism mediating the pupil response.

If the pupil acted as a linear filter, then the square-wave response could be predicted by the Fourier sum of the responses to sinusoidal modulation. But, as we can see in Fig. 4.2 showing results from two subjects, the Fourier prediction of the square-wave response underestimates the actual response. This means that the pupil system is non-linear, that is, the response is enhanced when high temporal frequencies are present as is the case of rapid contrast changes in a square-wave modulation,.

Hypothesis 2. There are two mechanisms whose combination is non-linear.

The response could be mediated by two mechanisms, each with a response curve tuned to different frequency ranges: a sustained mechanism which responds to slow changes in contrast modulation (favoured by the sinusoidal modulation) and a transient mechanism whose contribution in the high frequency range can explain the larger pupil constrictions to the square-wave modulation. The frequency response curve of each of these mechanism would be something similar to the one illustrated in Fig. 4.13. None of these mechanisms alone can explain the boost of the response obtained with a square-wave and the final low-pass pupil output obtain in Fig. 4.2. The non-linearity could be explained by a transient mechanism operating at high frequencies which enhances the typically low gain of a low-pass sustained mechanism. Both mechanisms operate simultaneously and thus are difficult to isolate but stimulus parameters can influence the relative contribution of each mechanism.

Hypothesis 3. There is one mechanism but is non-linear.

There is still the possibility of having one system whose response increases with the brisk changes of stimulus contrast. Although the final output of such system should be low-pass, the frequency response should receive significant contributions from high frequencies to explain the larger responses to square-wave modulation. Thus the frequency response would be similar to the combined output of the two mechanisms shown in Fig. 4.13. The contribution from high frequencies could then explain the larger constrictions of the response to square-wave modulation at low frequencies (0.5-1 Hz). However, differences in spatial summation between sinusoidal and square-wave modulation can only be explained by differences in the effective receptive fields of the neurones mediating each response and this implies the existence of two morphologically distinct pathways.

Sustained and transient mechanisms in the PLR

The data from the pupil frequency response, contrast gain and spatial summation in this chapter, suggest that the most plausible hypothesis is that containing two mechanisms. The idea of sustained and transient components in the pupil light response was first proposed by Young et al. (1993) using a statistical principal components analysis. Their

proposal was based mainly on the statistical analysis of responses to single flashes since the contributions from each component were inseparable. In this study a different approach was used. Stimulus parameters (contrast, size and frequency) were manipulated to influence the relative contribution of each mechanism and thus investigate directly the effect on the pupil response.

The hypothesis of two distinct neural pathways underlying the differences found in response to slow (sine) and fast (square-wave) luminance modulation is favoured by a well known segregation of neurones in the optic nerve. Visual fibres in the optic nerve (Shapley 1990) have been traditionally divided into two main categories: that is the M and P retinal ganglion cells projecting respectively to the magno and parvo layers of the LGN. M cells were also classified as transient (or phasic) neurones because they showed activity mainly at stimulus onset and offset and thus respond to rapid variations in luminance (high frequencies). On the other hand, P cells proved to be sustained (or tonic) neurones since they exhibit a continuous firing activity throughout stimulus presentation and their response reflects the mean light level averaged over time. In addition, for any given retinal eccentricity, P cells have much smaller receptive fields than M cells and, as a result, exhibit better spatial summation properties.

A similar division into sustained and transient cells has been found in the pupillomotor cells of rats (Trejo & Cicerone 1984, Pong & Fuchs 2000). In addition, there were significant differences in the respective receptive field sizes (a range of 12-124 degrees for transient cells compared 16-60 for sustained cells) which could also cause different spatial summation properties. We can thus reason that the response differences due to the wave-form of modulation reported here could arise from these two distinct populations of cells in the pretectum, with each cell class mediating different aspects of the pupil luminance response. Transient neurones (the pupillary equivalent to M-cells) would be favoured by the rapid contrast changes in the square-wave modulation while slow changing sinusoidal modulation would favour sustained cells (the pupillary equivalent to P-cells). Indeed the data presented here suggest a striking parallelism between the pupil light response characteristics and the properties of the sustained and transient visual pathways. For example, the marked differences in contrast gain shown in Fig. 4.1 resemble that of the M and P retinal ganglion cells. The sinusoidal response shows an almost linear increase with stimulus contrast (similar to sustained cells). On the other hand, the contrast gain for square modulation is highly non-linear, it increases quickly at low contrast levels but saturates at high contrast (like transient cells). There are also other elements that adds support to this correspondence. For instance, the better spatial summation found for sinusoidal modulation could also be explained as a result of smaller receptive field sizes associated to the sustained mechanism and the larger responses during square-wave modulation by the higher contrast gain in the transient pathway as a consequence of the contribution of high frequency harmonics present in a square-wave.

There is, however, some important evidence against a full association of pupillary components with sustained and transient visual fibres that should be considered here. Firstly, there is a lot of controversy related to whether pupillary fibres can be classified in the same way as visual fibres. The division between sustained and transient visual cells (X, Y cells) derived from electrical recordings in the cat's visual fibres. It was first found that cells differed in their spatial linearities to sinusoidal gratings (Enroth-Cugell & Robson 1966) and also in their temporal properties. These studies were later extended to monkeys (de Monasterio et al 1976) which found similar properties to the cat's cells for P (sustained) and M (transient) cells. The functional classification followed closely a morphological categorisation: sustained neurones have small cell bodies (midget type) whereas transient neurones were large (parasol type). But the division between sustained and transient is far to be a clear cut. There are many other morphologically distinct classes of cells (Rodieck 1998) and some unclassified cells behave like transient or sustained depending on various stimulus parameters such as: adaptation, stimulus size, frequency, and contrast. Another anatomical study in the macaque (Perry & Cowey 1984) did not find any morphological equivalent of sustained neurones (P-like cells) projecting to the pupillomotor centres in the mid-brain. However, these studies rely on the use of a retro-labelling substance (HRP, Horseradish peroxidase) and may not be conclusive

since HRP preferentially marks cells with larger axons and smaller cells may not have picked up the tracer.

Temporal integration of the neural signal input to the pupil

Direct evidence for a significant contribution of high frequencies to the pupil constriction amplitude (non-linear summation of higher harmonics) comes from electrical recordings of cells mediating the pupillomotor response in rats (Clarke & Ikeda 1985, Pong & Fuchs 2000). The response of cells in the Olivary Pretectal Nuclei (OPN) to sinusoidally modulated light showed increasing firing activity for stimulation frequencies of up to 20 Hz whereas the amplitude of the constriction decreases with frequency in a similar way as shown in Fig. 4.2, except that in rats, the cut-off frequency is higher (8-10 Hz instead of 2-3 Hz in humans). These results also suggest that the neural signal input to the sphincter muscle undergoes temporal integration after leaving the pretectal pupillomotor complex. In addition, it can also explain why high frequencies present in the square-wave modulation enhance the pupil constriction amplitude by increasing the firing activity of cells in the OPN.

Support for the extrapolation of the results obtained in rats to humans comes from pupil measurements to luminance flicker (Troelstra 1968): a flickering light of 20 to 30 Hz causes the pupil to remain constricted (pupillary capture) whereas lower stimulation frequencies or presentation of a single flash allow the pupil to re-dilate (pupillary escape).

These results suggest that, although the pupil cannot follow rapid oscillations, the neural signal input to the sphincter muscle undergoes temporal integration with high firing frequencies contributing to the pupil constriction amplitude. In other words, the pupil is not simply a low-pass filter; rapid changes in luminance (high frequencies) boost the constriction amplitude.

Input: Luminance modulation

$$sQW = \frac{2A}{\pi}\left[Sin\,2\pi f_0 t + \frac{Sin\,2\pi(3f_0)t}{3} + \frac{Sin\,2\pi(5f_0)t}{5} + ... \right]$$

Pupil Transfer Function H(jw)

Sustained

Transient

Response

Frequency

Output: Pupil size

$$A \cdot Sin\,2\pi f_0 t$$
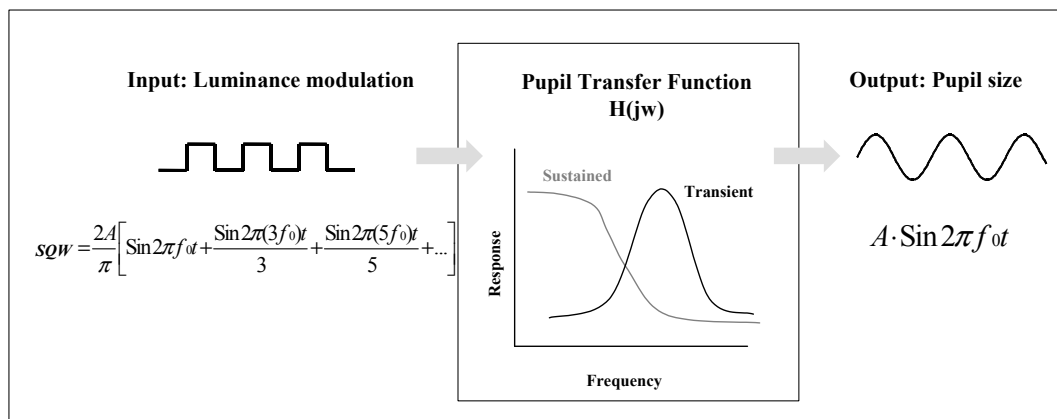
Fig. 4.13 Hypothetical frequency tuning curves for sustained and transient mechanisms in the pupil response. Transient neurones detect rapid variations in luminance (high frequencies) whereas sustained neurones respond to the mean light level averaged over time. The final pupil output is mainly low-pass (Fig. 4.2) due to temporal integration of the neural input signal. But the pupil does not behave simply as a low-pass filter: high firing frequencies of transient neurones contribute to constriction amplitude at low frequencies. Electrical stimulation in the EW suggest that the peak of the transient mechanism may occur around 6-8 Hz (Sillito & Zbrozyna 1970).

But where in the pupillary pathways does the temporal integration of the fast varying neural signals occur?. Significant temporal summation of the pupillomotor signal is likely to occur at the level of the iris sphincter muscle. Experimental support for this comes from electrical stimulation of neurones innervating the sphincter in cats. Neurones in the cervical ganglion show a maximal response for stimulation frequencies above 8 Hz (Sillito & Zbrozyna 1970). Such frequencies are too fast to be followed by the pupil. As can be seen from Fig. 4.2, the pupil output is markedly low-pass. This suggests that the fast oscillatory neural signal to the sphincter undergoes significant temporal integration.

The most likely explanation for the slow characteristics of the pupil is that, for obvious mechanical and energetic reasons, muscle fibres in the sphincter do not contract at very high rates. Instead, the sphincter adjusts pupil constriction amplitude and rate according to the incoming neural signal (ie. the actual firing rate and its modulation over time). It is indeed plausible to think that sphincter muscle would not be able to cope with the energy demand in response to high frequency neural activity if each of these neural impulses would result in a constriction signal to the sphincter. Thus the neural signal must undergo some kind of temporal integration or summation. That is, only when a sufficient number of spikes occur in a given period of time, the muscle fibres constrict. This model will result in a pupil system that responds well to sudden changes in luminance contrast because these rapid changes elicit high firing rates (Sillito & Zbrozyna 1970), but at the same time, results in a sluggish system that cannot follow rapid oscillations in luminance.

Low-pass temporal filtering and cortical mediation in the PCR and the PGR

Recent studies in man (Barbur 1995, Barbur 2002) have confirmed that the pupil also responds to changes of chromatic saturation and isoluminant gratings even when there is a reduction in the mean light level during the presentation of the stimulus. These responses seem to be essentially different from the classic pupil light reflex (PLR). Studies in patients with damaged cortical areas showing a much reduced response (Weiskrantz et al 1999) and increased response latencies in normal subjects (Wolf et al 1999) suggest that these responses involve a top-down modulation from cortical to pupillomotor areas in the mid-brain (Barbur 2002). This idea is also consistent with anatomical observations claiming that cells projecting to the subcortical pupillomotor centres lack any chromatic sensitivity (Schiller & Malpeli 1977). Our results show that neither the PCR (Fig. 4.3) nor the PGR (Fig. 4.4) depend on the temporal modulation chosen, suggesting that the isoluminant pupillary pathways are mainly cortical and lack a fast or transient component. It is possible that the involvement of further stages in the overall processing results in the loss of fast varying signals (low-pass temporal filtering), causing the final signal output to be averaged over time. These observations are also consistent with the traditional view of the isoluminant fibres as sustained in nature.

4.8 Summary

The classical view of the pupil is that it responds to light flux changes acting as an aperture mechanism regulating the amount of light entering the eye. Numerous animal studies suggest that the neural complex mediating this response is located in the pretectal area of the mid-brain (Sillito & Zbrozyna 1970, Pong & Fuchs 2000). However, direct evidence of substantial contribution from cortical signals to the traditionally 'sub-cortical' pupil light reflex pathway comes from studies in blindsight patients with unilateral damage to primary visual cortical areas (Barbur et al 1999, see also chapter 5).

The data presented in this chapter suggest that two different mechanisms mediate the pupil light reflex response: a sustained mechanism with an almost linear contrast gain which integrates the input signal over large areas of the visual field and is therefore appropriate to control the steady state size of the pupil in response to gradual changes in ambient illumination, and a transient mechanism which is highly sensitive to sudden changes in luminance contrast and is responsible for the dynamic pupil light reflex. On the other hand, pupil responses to isoluminant colour modulation or gratings, that are thought to involve cortical processing (Wilhelm et al 2002), do not seem to depend on the temporal characteristics of the stimulation.

In summary, the square-wave modulation differs from the sinusoidal modulation in the following aspects (see Table 4-1 below):

Contrast gain: is significantly higher for square-wave modulation. It also saturates quickly and is highly non-linear in comparison to sinusoidal modulation. Low contrast, square-wave stimuli elicit a substantial pupil response while much higher contrast is needed

when using sinusoidal modulation. A similar segregation in contrast gain has also been found in retinal ganglion cells projecting to the LGN. Transient (M-cells) show a much higher contrast gain than sustained (P-cells) , they also show saturation at high contrast like the square-wave response in Fig. 4.1.

Frequency response: the square-wave response showed similar low-pass characteristics as the sinusoidal, however, the higher frequency harmonics present in the square-wave modulation enhance the response amplitude in comparison to sinusoidal responses, particularly at low frequencies (0.5-1 Hz).

Spatial summation: square-wave responses showed less spatial summation than sinusoidal responses across the whole visual field (Fig. 4.9). Although for the same stimulus size the square-wave responses are generally larger, these difference decrease rapidly for stimulus sizes larger than 10 degrees (Fig. 4.11).

Luminance modulation	SIN	SQW
Contrast gain	linear	non-linear, fast saturation
Frequency response	low pass	low pass
Spatial summation	good, linear	partial, non-linear

Table 4-1. Summary of pupil response properties to sinusoidal (SIN) and square-wave (SQW) modulation.

Non-linear mechanisms in the pupil system

To conclude, we can point out several non-linear mechanisms that may be present in the pupil response, with their relative contribution depending strongly on stimulus parameters

- retinal adaptation and the Log dependence of the pupil diameter with luminance (see Fig 2.1).

- uni-directional selectivity of the pupil system (Clynes 1962). This idea is also consistent with reports of transient cells in the OPN that fire more strongly at stimulus onset than offset (Trejo & Cicerone 1984).

- non-linear response to contrast as shown in Fig 4.1

- temporal integration of high frequency components (non-linear summation of higher harmonics) as described in Fig 4.13 and text.

- non-linear feedback caused by the variable light flux entering the pupil as a result of dynamic changes in pupil diameter (Stark 1984).

Several researchers have proposed models that include various of these non-linearities of the pupil system. See for example the work of Clynes 1962, Troelstra 1968, Semmlow et al 1975, Milton & Longtin 1990, Myers et al 1993, Stark 1984, Bressloff et al 1996.

Chapter 5: Effect of cortical lesions on the pupil response

1.1 Introduction: 'blindsight'

Blindsight is a striking phenomenon in which cortically blind patients show astonishing residual visual abilities even though they consistently deny being aware of any perceptual experience. Patients exhibiting blindsight are able to 'guess' the correct visual target when presented with two or more alternatives in a forced-choice experiment (Weiskrantz 1986). Blindsight patients are often surprised about their good performance (typically well above chance level with scores of 90% or more) after repeated presentations of what they regard just a 'guess'. Numerous studies have reported that blindsight patients have the ability to detect light, discriminate orientation of gratings and direction of movement in their 'blind' fields (Weiskrantz 1997, Azzopardi & Cowey 2001, Morland et al 1999, Barbur et al 1993).

Blindsight research has received strong criticism almost since it was first reported. Detractors (Wessinger et al 1997) have argued that blindsight might be the result of small intact areas or incomplete lesions in V1. It has also been argued that scattered light falling on the unaffected visual hemi-field could provide a signal strong enough to detect visual targets. However careful experiments have addressed each of these issues and there is now enough evidence proving that blindsight cannot be attributable to any of these artefacts (Weiskrantz 1997). For instance, experiments in monkeys with complete removal of V1 by means of surgery have also demonstrated similar visual capacities as human blindsight patients (Stoerig & Cowey 1997), a proof that blindsight is not a result of an 'incomplete' lesion. Monkeys, like blindsight patients, can detect and locate visual stimuli in a forced-choice experiment but perform at chance in a yes-no experiment (Cowey & Stoerig 1997). Scattered light cannot explain either the high accuracy of blindsight patients locating targets in their 'blind' hemi-fields. Otherwise they could also use the small amount of scattered light to locate the same targets when they are presented in the blind-spot but they fail to do so (Weiskrantz 1986).

Conscious versus unconscious visual perception

Residual visual capacities in cortically blind patients, with and without conscious perceptual awareness, has been demonstrated in numerous studies (Barbur et al 1994b, Weiskrantz et al 1995, Weiskrantz 1997, Azzopardi & Cowey 1998). This residual visual capacity is usually explained in terms of undamaged non-geniculate pathways. At least about 100,000 retinal fibres leave the optic nerve bypassing the major known visual pathway (from retina to V1 via the LGN) to reach non-striate cortical areas. Some of the neural pathways that have been postulated to mediate blindsight include: projections from the retina to the extrastriate cortex via the superior colliculus or the pulvinar, and intralaminar neurones in the LGN surviving the removal of V1.

It is widely accepted that we are aware only of a small fraction of all the visual information available to our brain. Through attention our brain selects the relevant information, based on factors such as: stimulus saliency (pre-attentive selection), location

(spatial attention) and object relevance (object-based attention). For instance, we are not aware of our natural blind spot because our visual system 'fills in' the gap according to the surrounding information. More surprisingly, patients with cortical scotomas (blind areas) also experience a similar 'fill in' effect (Stoerig & Cowey 1997).

Studies on patients with localised brain lesions have attracted much attention precisely because they provide an interesting approach, not only to investigate where in the brain different visual attributes might be analysed, but also the role of the affected areas on the subject's conscious visual experience. Some cortically blind patients have even reported awareness for rapidly moving or transient stimuli, but seem to be unaware of stimuli changing more gradually. For example, there are reports that GY is aware of motion (Barbur et al 1993) but DB claims that he is not (see also results reported here in Fig. 5.1). Awareness for certain stimuli does not fall within the formal definition of blindsight (residual vision without awareness) but has important consequences because implies that conscious visual perception is perfectly possible without V1. Some researchers have even suggested that V1 might not even be necessary at all for conscious visual perception (Crick & Koch 1995).

How precisely awareness arise from brain activity is one of the greatest challenges that neuroscience research have to tackle in the coming decades. As early as 1915, John Hughlings Jackson put forward the idea that consciousness does not arise from activity in a particular area in the brain but rather emerges from association cortices in different locations (Jackson 1915). This hypothesis has been elaborated further by Zeki (2001).

5.1 Patients' medical histories

The two subjects of this study are blind in half of their visual field (i.e. homonymous hemianopia) as a result of damage to the contra-lateral primary visual cortex (V1). Both patients (GY and DB) that had shown previous evidence of blindsight under a wide variety of conditions (Morland et al 1999, Weiskrantz 1986). Pupillometry and psychophysical tests were carried with the consent of each subject. All experiments were approved by the City University Research and Ethical Committee.

Patient GY

Patient GY had a car accident when he was 8 years old, which resulted in loss of vision in the right hemi-field (right homonymous hemianopia). MRI scans in GY (Goebel et al 2001) show unilateral damage in the posterior left hemisphere and measurements of visual-field sensitivity reveal the corresponding loss of vision in his right hemi-field, except for a small central region of macular sparing (3.5°).

Patient DB

DB suffered from persistent and severe migraine headaches from the age of 14 caused by a mass of enlarged blood vessels in the right visual cortex. During the attacks, he reported a flashing light and visual disturbances in his left visual field. Later, when DB was in his twenties he also reported a persistent scotoma (blind area). At the age of 33, he underwent surgery to remove the malformed blood vessels. The operation successfully relieved his symptoms but rendered most of his left visual field blind since the malformation covered cortical visual areas in his right hemi-sphere. For a detailed account of the first report of blindsight and DB's case history see Weiskrantz's book 'Blindsight: a case study and its implications' (Weiskrantz 1986).

5.2 Methods

All pupil measurements were recorded using the pupil scan system (P_SCAN) as described in chapter 3. A minimum of 16 pupil traces were averaged for each location and luminance. When using coloured stimuli, at least 32 traces were included since the signal-to-noise ratio of the pupil colour response is generally poorer than the pupil light response. Pupil perimetry mapping of both the blind and sighted hemi-field follow up the

pilot experiments in normal subjects presented in chapter 4. The chromatic discrimination of moving targets was tested using the same technique as the colour vision test already described in chapter 3.

5.3 Experiments and results

Detection of chromatic moving targets in blindsight

One of the most surprising aspects of blindsight, is that some patients have the ability to select the correct choice when they only can make use of chromatic signals, despite the subjects consistently deny that they can see or discriminate any 'colours'. There are even reports (Stoerig & Cowey 1989) of qualitatively normal spectral sensitivity functions in blindsight patients, and also of a clear Purkinje shift with dark adaptation. These results suggest that both rod and cone signals contribute to blindsight and that some colour opponency processing remains. Another strong evidence for a colour opponency mechanism in blindsight comes from measurements of the pupil response to coloured isoluminant stimuli; blindsight patients not only show a clear pupil response to green isoluminant stimuli but also to the complementary red after-image (Barbur et al 1999; see also Fig. 5.5 later in this chapter).

Patient DB volunteered to participate in a new computer-based colour vision test. The test, developed by John Barbur and collaborators at City University, consists in the detection of moving coloured targets embedded in a dynamic luminance noise to ensure that observers cannot used luminance signals to detect the coloured test pattern (for a detailed description of the test see chapter 3). Some previous studies had reported residual processing of chromatic signals in blindsight (Stoerig & Cowey 1992) but this is the first investigation of colour discrimination in blindsight patients using dynamic luminance noise. This technique ensures that subjects make only use of pure chromatic signals and has been successfully tested in normal and colour deficient observers (Barbur et al 1994a).

Results in Fig. 5.1 show that patient DB performance is clearly better than chance when asked about the direction of motion of a target moving in four possible directions within his blind hemi-field. These series of randomized presentations is a very common procedure in experimental psychology known as 4AFC or 4-alternative forced choice. Both background and test patterns consisted of checks that varied randomly in luminance every 2 frames of a computer display running at a refresh rate of 85Hz. The background noise ensures that observers cannot used luminance signals to detect the coloured test pattern (see more on methods in chapter 3). DB's performance was at similar or worse levels when targets had the same chromaticity than the background and only differed in luminance (target luminance contrasts between 50 and 300% higher than the averaged luminance of the background). Thus, the high levels of performance with isoluminant coloured targets suggest that there is genuine chromatic processing in blindsight.

Motion detection in BlindSight

4-AFC procedure

500 ms

MOTION

425 ms

750 ms

NOISE

NOISE

Time (ms)

12º

Stimulus parameters
Luminance contrast noise 35% (42Hz, refresh rate 85Hz)
Background 16 cd/m2 CIE (x,y) = (0.305, 0.323)

Detection of achromatic moving targets	correct / total	Performance %
target contrast +300%	27/34	79%
target contrast +100%	30/34	88%
target contrast +50%	29/32	91%

Detection of coloured isoluminant moving targets	correct / total	Performance %
green (CIE CD = 0.12)	28/32	88%
green (CIE CD = 0.60)	30/32	94%
red (CIE CD = 0.17)	32/32	100%
red (CIE CD = 0.75)	30/32	94%

Fig. 5.1. Patient DB is a striking case of 'blindsight' or residual vision without awareness. DB suffered a lesion in V1 that rendered his left visual field blind. DB was clearly better than chance when asked about the direction of motion of a target moving in four possible directions within his blind hemi-field. The moving targets were patterns that differed from the background either in luminance or in colour (only the two colours used, red and green, are shown here). Performance did not decrease even when isoluminant coloured targets were used despite DB's was unable to discriminate or name any colours. For a detailed account of the first report of blindsight and DB's case history see Weiskrantz's book 'Blindsight: a case study and its implications' (Weiskrantz 1986). For a demonstration of the City University motion-based colour vision test visit http://www.city.ac.uk/avrc/colourtest.html.

Pupil responses without V1

Pupillometry provides a quantitative method of testing blindsight. Although the classical description of the pupil reflex pathways is entirely subcortical, blindsight patients with sustained lesions to cortical area V1 but intact subcortical pupillomotor pathways show a much reduced pupil response. See results from figures 6.2, 6.3 and 6.4 confirming reports published previously (Barbur et al 1999).

Pupil perimetry

A modified version of the pupil perimetry test, already described in chapter 4, was used to investigate the stimuli parameters (i.e. background luminance, contrast, size and temporal modulation) that affects most the pupil response in subjects lacking a direct geniculo-cortical projection. Pupil constriction amplitudes and latencies were measured in response to cyclic luminance modulation of sectors in the computer display restricted either to the blind or sighted visual hemi-field of GY and DB. Subjects had to maintain

fixation by looking at a small cross presented in a computer display (viewing distance of 70 cm). The location of stimuli excluded the central 5 degrees of visual field since this area is often spared during cortical lesions (macular sparing).
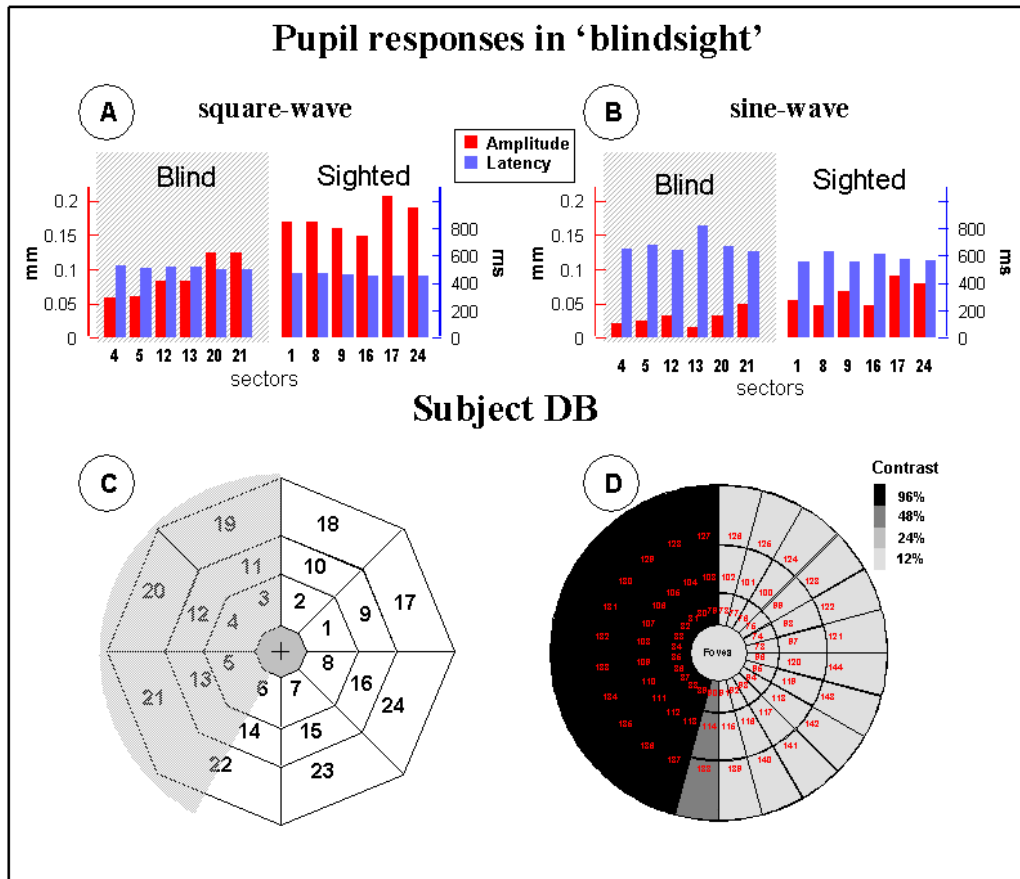
Fig. 5.2. Pupil light responses in the blind region (shaded plots) of patient DB show reduced amplitudes and longer reaction times when compared to the sighted hemi-field for both sinusoidal (A) and square-wave (B) luminance modulation of the stimulus. The data confirms earlier reports that cortical lesions affect the pupil response despite pupillomotor pathways have been traditionally considered to be entirely sub-cortical (Barbur et al 1997). (C) The stimulus consisted of a single trapezoid (numbered sectors) at a particular location in the visual field that changed in luminance periodically at 1Hz either following a square wave (A) or a sinusoid (B). Sectors were arranged concentrically at three different eccentricities (6.5°, 10.5° and 15°) at a viewing distance of 50 cm. The area of each sector increased with a factor of 1.5 from the centre so as to achieve comparable pupil responses across the whole field. Graph (D) shows the results of a contrast perimetry test that measured DB's ability to detect a flash of a given contrast presented in a uniform background of 24 cd/m^2. The test confirmed the extension of the blind region (shown in black) obtained with standard visual field perimetry.

Fig. 5.2 shows significantly smaller pupil responses in the blind hemi-field of patient DB. Like the normal population, DB show larger constriction amplitudes in response to square-wave compared to sinusoidal modulation, however the relative pupil attenuation in the blind hemifield (40-60% of the sighted response) is very similar for both types of modulation. Since square-wave modulation causes overall larger pupil reactions, it was used in Fig. 5.3 to study the effect of stimulus contrast in patient GY. As expected, amplitudes increased with stimulus contrast (contrast was defined as the percentage of modulation above and below a mean luminance level of 36 cd/m^2).
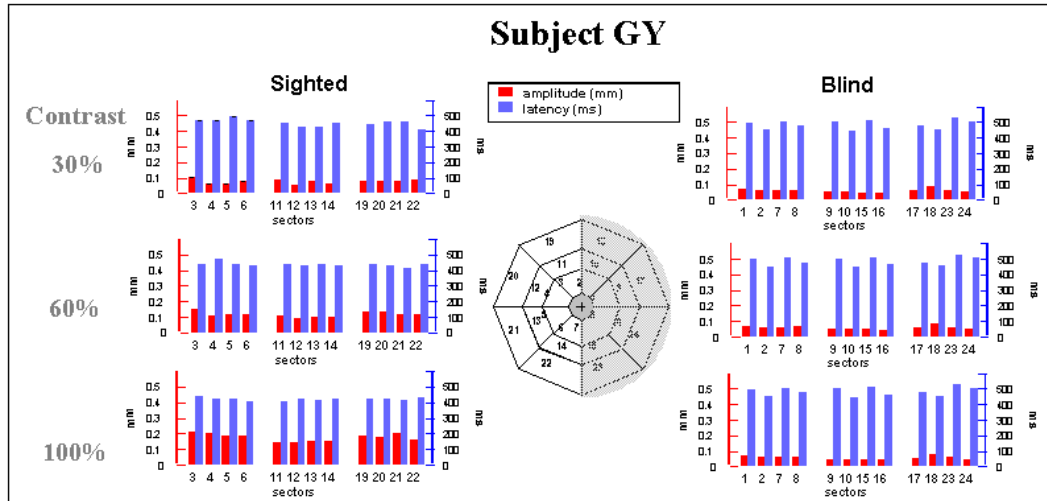
Fig. 5.3. Pupil light responses in another patient exhibiting blindsight (GY, right homonymious hemianopia). The difference in constriction amplitude between the blind and sighted regions of the patient's visual field increase with the luminance contrast of the stimulus. Three contrast levels were used with 30, 60 and 100% modulation above and below a mean luminance level of 36 cd/m^2. The temporal modulation in luminance contrast of the stimulus followed a square wave at a frequency of 1Hz to favour the differences between the blind (shaded area) and sighted hemi-fields.

Spatial summation of stimulus size

Differences between the two hemi-fields also increase with stimulus size as shown in Fig. 5.4, suggesting that spatial summation is significant in the cortical component of the pupil response.
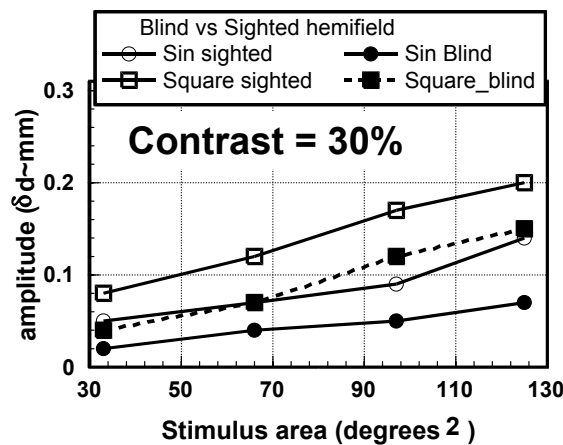
Fig. 5.4. Differences in constriction amplitudes between the blind and sighted regions at 30% luminance contrast vary little with stimulus size (patient GY). Since the sub-cortical pupillomotor complex is intact in GY, both the sighted and blind hemi-fields show substantial spatial summation.

In summary, these results obtained with pupil perimetry show a reduction of pupil constriction amplitudes and longer latencies in absence of a direct geniculo-striate projection. In order to reveal significant difference between the blind and sighted hemi-fields, stimuli must have sufficient contrast (Fig. 5.3) and size (Fig. 5.4). That is, there is a trade-off between the maximum luminance of the display used and the extension of the lesion to be mapped with pupil perimetry. It seems also that the speed of temporal luminance modulation (square compared to sinusoidal) affects, as in normal subjects, the absolute value of the pupil constriction but does not influence the relative differences between the blind and sighted hemi-fields.

Pupil colour response and after-images

Pupil traces were measured in response to sinusoidal modulation of chromatic saturation at a frequency of 0.8 Hz. Each presentation consisted of eight cycles (during 10 seconds) of modulation, from the achromatic background (MacAdam's white) to the maximum colour saturation that could be achieved with the display used (0.15 units for red and 0.09 for green in a SONY triniton 500PS). Pupil constriction amplitude and latency were computed from the discrete Fourier transform of each averaged trace as described before (chapter 3).

Both subjects reported the perception of strong coloured afterimages at each stimulus offset when stimuli were presented to their normal visual fields as most observers do. The averaged response traces in Fig. 5.5 show that the pupil responds well to chromatic modulation in the long-wavelength range (red) of the spectrum, both in the sighted and the blind hemi-fields (graphs A & B).
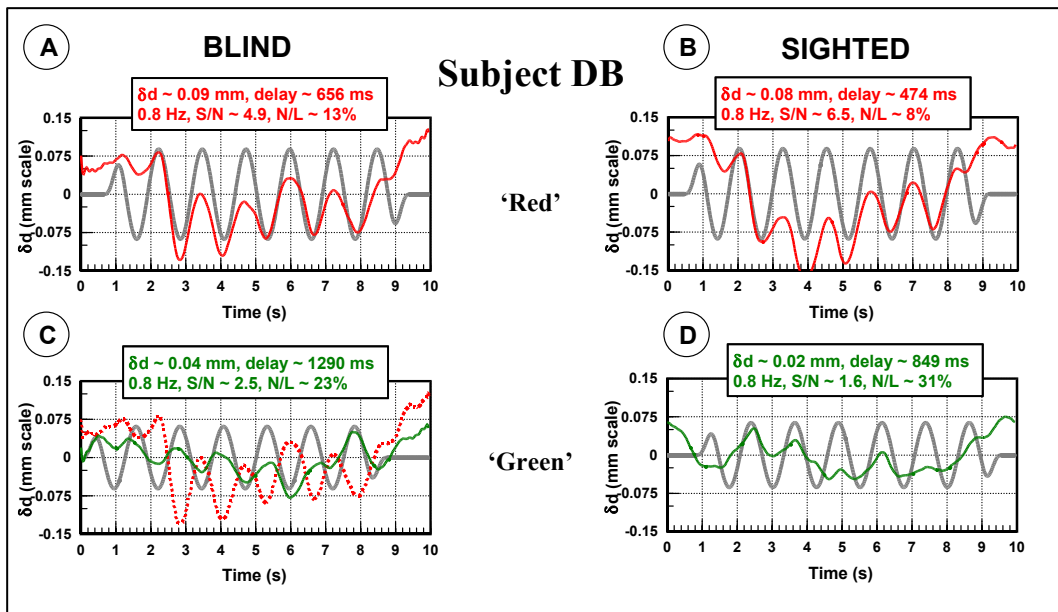
Fig. 5.5. Pupil colour responses to a stimulus disc that was restricted either to the blind (left) or the sighted (right) visual hemi-fields of patient DB. The stimulus consisted of a coloured disc subtending 21° in diameter and presented in a uniform background of luminance 12 cd/m². The colour of the disc changed as the chromatic distance (CD) from MacAdam's white (x=0.305 y=0.323) was modulated sinusoidally (thick grey line) during 8 cycles at 0.8Hz along two directions in the xy-CIE chromatic diagram. These two directions corresponded perceptually to red (A&B, top panel) and green (C&D, bottom panel) and they are the only two possible solutions imposed by the d-isoluminant constraint for the background chosen (see chapter 3). In the blind hemi-field, the 'green' response (C) is dominated by the red afterimage and the time delay (1290 ms) is precisely half-cycle (625 ms) longer than the delay measured for the red response (656 ms, dotted line in C re-plotted from A). The response to green in the sighted hemi-field (D), is paradoxically smaller since the combination of the green component and the corresponding red afterimage cancel out, as it is suggested in C (see text). Similar results have been published in subject GY (Barbur et al 1999).

On the other hand, pupil responses to the green stimulus were much smaller (C & D). In the blind hemi-field, the response is dominated by the red afterimage. The dotted red trace in graph C shows the response to 'red' modulation taken from A. Comparison of the two traces confirms the half-cycle delay between red and green responses as predicted by a model proposed by Barbur et al. (1999) of colour afterimages following signal adaptation of retinal receptors. In the sighted hemi-field (D), a red afterimage to the green offset cause a doubling in the frequency of the response as reflected by the high non-linearity ratio (NL 31% in D). The response in the sighted hemi-field is therefore a combination of the green component and the corresponding red afterimage. These two components cancel out (as shown in C since the green response in that case is essentially the red afterimage), producing paradoxically a smaller response to green

modulation in the sighted than in the blind hemi-field because the blind response is dominated by a strong red afterimage.

In principle, a similar effect of green afterimages would be expected to appear during red modulation (A & B). However, this effect is negligible since the spectral sensitivity of the pupil is biased towards the long-wavelength range (red) of the spectrum and the response to middle wavelengths (green), arising either from a real colour or an after-image, is reduced substantially.

5.4 Summary and discussion

The data presented in this chapter demonstrates that pupil light responses to periodic stimulation are significantly reduced in patients with damaged to primary cortical visual area (V1). It also confirms previous results obtained with a single flash stimulus (Weiskrantz et al 1998, Weiskrantz et al 1999). These findings suggest, against the commonly held view, that the neural pathways mediating the pupil light reflex are not entirely subcortical.

In addition, pupil responses to isoluminant colour modulation are reduced significantly but not abolished completely in patients with damage to the primary visual cortex. A possible mechanism mediating such responses would be the processing of stimulus attributes in extrastriate visual areas that survive the destruction of V1. It is well established that signals of retinal origin can reach extrastriate areas via subcortical projections to the SC and the pulvinar (Cowey & Stoerig 1991). Barbur and Weiskrantz (1999) have proposed that such stimulus-specific pupil responses may arise as a result of transient weakening of the constant sympathetic outflow to the dilator muscle (sympathetic inhibition of the parasympathetic EW nucleus). This temporary reduction in the sympathetic outflow could result from sudden changes in neural activity in extrastriate visual areas when a stimulus is presented. Thus, pupil responses elicited by isoluminant colour modulation are likely to be originated in extra-striate cortical visual areas and then propagate 'downstream' to the sub-cortical pupillomotor centres. The longer constriction latencies measured in normal subjects to isoluminant colours, as much as 80 ms longer in comparison to the pupil light reflex (see Fig. 4.3) provide additional support for this hypothesis.

In summary, pupil responses in 'blindsight' can be measured provided that the stimulus has sufficient contrast or size but still are much reduced in comparison with normal subjects (Barbur et al 1994b, Weiskrantz et al 1999).

Chapter 6: Effect of pretectal lesions on the pupil response[*]

Evidence from electrophysiological experiments (Sillito & Zbrozyna 1970) and studies in patients with post-geniculate lesions (Alexandridis 1985, Barbur et al 1999) have demonstrated a 'top-down' influence from cortical areas to the pupillomotor centres in the dorsal mid-brain. Neurones in these pupillomotor centres, namely the olivary pretectal nuclei in the mid-brain, respond mainly to luminance changes (Trejo & Cicerone 1984, Young & Lund 1998). They also seem to have very limited colour sensitivity (Perry & Cowey 1984) and large dendritic fields, which indicates a restricted capacity to encode spatial frequency information. Thus, pupil responses elicited by stimulus attributes such as colour or spatial frequency are likely to originate in other visual areas of the brain where signals then propagate 'downstream' to the sub-cortical pupil centres.

However, little is known about the site of integration of these cortical signals into the subcortical pupillomotor pathway that mediates the pupil light reflex. In this chapter, we present a novel study of pupil responses in two subjects with damage to the pretectal areas in the dorsal mid-brain (Parinaud's syndrome) to various stimulus attributes such as light flux, isoluminant gratings and colour. The results show that the light reflex response is practically abolished, as expected from a damaged pretectum. But interestingly, the lesion has little effect on pupil grating or colour responses, suggesting that the cortical signals mediating these 'non-light responses' interact with the pupillomotor at the level of the Edinger-Westphal nuclei (EW) and do not rely on the normal functioning of pretectal nuclei (OPN) involved in the light reflex response.

6.1 Introduction: Parinaud's syndrome

Parinaud's syndrome (also known as pretectal, Sylvian aqueduct or Koerber-Salus-Elschnig syndrome) is caused by lesions to the pretectal area in the dorsal mid-brain resulting in large and unreactive pupils. Typically, the damage is bilateral and, either the pupil light reflex is absent, or an extremely bright light is needed to trigger even a small reaction if damage is not complete. However, both pupils still constrict normally when subjects change eye fixation from a distant to a near target (pupil near reflex). This light-near dissociation is also a characteristic of other pupil disorders (see chapter 2) and reflects the anatomical segregation of pupillary and accommodative fibres in the pretectum, at the level of the Edinger-Westphal (EW) nuclei. Most cases of Parinaud's syndrome are caused by pineal tumours or enlargement of the third ventricle. This generally causes damage to the pupillomotor fibres in the dorsal mid-brain but preserves the neural fibres mediating accommodation which follow a more ventral route. Other typical clinical signs in Parinaud's syndrome include vertical gaze deficit, convergence-retraction nystagmus, Collier's sign (lid retraction on attempted upgaze) and skew deviation (Bremmer 2001).

6.2 Patients' medical histories

The two patients (J.M. and B.D) with Parinaud's syndrome included in this study, were both male and aged 26 and 33 years. Damage to the pretectum was confirmed by MRI

---

[*] Note: Part of the results reported in this chapter have been published in the journal Brain: Wilhelm, B. J., Wilhelm, H., Moro, S., & Barbur, J. L. 2002, "Pupil response components: studies in patients with Parinaud's syndrome", Brain, vol. 125, no. Pt 10, pp. 2296-2307.

imaging as a result of a compressive tumour in the region of the pineal gland. In addition, six normal subjects volunteer to act as controls (mean age ± standard deviation of 28± 8 years).

All the experimental procedures were approved by the City University Research and Ethical Committee and each subject gave his or her formal consent to participate in this investigation. MRI scans and ophthalmological tests were part of the routine follow-up examinations.

Patient JM

J.M.'s visual problems started with double vision in 1981 followed by unsuccessful strabismus surgery in 1983. Further tests in 1984 revealed raised intracranial pressure with a primary diagnosis of an extended intracranial mass in the region of the pineal gland (for pictures of MRI scans see Wilhelm 2002). Further surgery and removal of tissue in 1986 resulted in post-operative left lower quadrantanopia (5° to 20°). Two further surgeries were carried out in 1987 and 1989 to deal with local recurrence, with complete removal of the tumour (including the capsule) in 1989. Since then, annual follow-up examinations have not revealed significant changes in symptoms, although the small visual field defect has improved slightly.

The ophthalmological test in J.M. revealed that the anterior eye segments and fundi were normal in both eyes. The patient had high contrast visual acuity in the right eye (6/5) and slightly worse than normal in the left eye (6/7.5). A more detailed measurement of contrast sensitivity using sinusoidal gratings of different spatial frequencies (Fig. 6.5) confirmed that his vision was near to normal levels. There was also a slight anisocoria (the left pupil was slightly larger) but in general both pupil responses were similar. We excluded the left eye responses in some of the pupil trace graphs for clarity. Motility examination revealed a vertical gaze palsy, divergent strabismus and convergence retraction nystagmus when attempting to look upwards.

Patient BD

B.D. suffered an accidental damage to the head causing traumatic palsy during childhood (1979), with slight residual symptoms (facial nerve paresis). He also suffered from a sudden cerebral ischaemia in 1989 with temporary paralysis that affected his right side, but recovered completely. In 1992 his symptoms started with severe headaches. Diagnostics for a cerebral tumour started the same year and he had a stereotactic biopsy with ventriculo-atrial shunting to alleviate high intracranial pressure. Histological examination of the removed tissue revealed a dysgerminoma of the pretectum and a secondary smaller tumour rostral of the left anterior horn of the lateral ventricle. After two chemotherapy cycles he received radiotherapy. Since then he has undergone regular follow-ups, including ophthalmological, neurological examinations and neuro-imaging, without evidence of recurrence.

The eye test also shown normal anterior eye segments and fundi in both eyes, with high-contrast visual acuity of 6/6 in the right eye and 6/7.5 in the left eye. Contrast sensitivity measurements also showed near to normal vision (Fig. 6.5). D.B. also exhibited a small anisocoria (left pupil larger), vertical gaze palsy and convergence retraction nystagmus when attempting to look upwards.

6.3 Methods

All pupil measurements were recorded using the pupil scan system (P_SCAN) already described in chapter 3, which includes a head and chin rest to adjust the position of the subject's head to minimize involuntary movements. Several response traces were averaged for each stimulus. After averaging, further analysis of the pupil response trace was carried out to extract the amplitude and latency of each response.

Both patients were examined following standard ophthalmological tests. In addition, visual performance was assessed more precisely by means of achromatic and chromatic

contrast sensitivity measurements (Fig. 6.5). Six randomly chosen healthy volunteers with normal pupil responses, who also took part in some of the experiments described in chapter 3, acted as a control group to test the statistical significance of the results obtained in the two patients with Parinaud's syndrome.

Pupil perimetry

The first experiment consisted in measuring the pupil light response to a 250 ms flash presented at 5 different locations in the visual field. The purpose of this test was to test the extension and uniformity of the lesion affecting the olivary pretectal nuclei in each patient.

Each subject viewed a uniform background field of luminance of 24 cd/m^2 luminance, and CIE chromaticity x = 0.305, y = 0.323, subtended a visual angle of 30° horizontally and 24° vertically which provided a steady-state light adaptation of the retina. A cross was always presented in the centre of the visual display and provided the fixation mark. The test stimulus was a disc of 10° diameter and was presented either in the central foveal region or in each of the four quadrants (see inset in the centre of Fig. 6.1 for size and spatial arrangement of test stimuli). The flash luminance was 72 cd/m^2 (i.e. a contrast increment of 2). The stimulus position was interleaved randomly and 24 measurements were averaged for each location.

Pupil contrast gain

In order to assess the extent to which damage in the pretectum affected the amplitude of the pupil constriction, responses were measured to a flash of 500 ms whose luminance was gradually increased to 50, 100, 200 and 300% respect to that of the background which remained at 24 cd/m^2 as in the previous experiment.

Pupil colour response

In this experiment the stimulus was a colour-defined disc of 10° diameter and was buried in a large circular field of dynamic luminance contrast (LC) noise (see stimulus picture in Fig. 6.3). The dynamic LC noise ensures that residual luminance contrast signals arising from individual variations of the isoluminant point are effectively masked (Barbur et al 1994a). Since previous studies have shown that pupil responses to red colours are generally larger (Barbur et al 1992, Barbur et al 1994a), a red coloured target was selected for this study to obtain a good signal to noise ratio in the response.

Pupil grating response

Pupil responses to gratings with a space-averaged luminance equal to that of the uniform background were also measured in exactly the same condition as with the coloured stimuli. The sinusoidal grating subtended 10° of diameter and had 95% contrast. Three different spatial frequencies that yield a good response in normal subjects were employed.

To avoid pupil size fluctuations produced by fixation changes (pupil near response) a fixation cross was maintained in the centre of the field. We also ensured that the pupil grating response was genuinely triggered by the visual pattern and not fluctuations in the subject's fixation by measuring responses to a blank stimulus (see Fig. 4.5 in chapter 4) at the same viewing distance of 70 cm. These oscillations in pupil size due to accommodative changes add up to other spontaneous fluctuations and proved to be of a much smaller magnitude than those triggered by the presentation of the visual pattern. Moreover, the effect of small fluctuations can be safely neglected after averaging several response traces since they these fluctuations are not correlated with the stimulus onset.

Contrast sensitivity

Chromatic and achromatic contrast sensitivity were measured using standard visual tests implemented on the P_SCAN system (see methods on chapter 3). Subjects viewed the screen binocularly for both tests and the stimulus was presented for 0.25 s in the centre

of the screen. A staircase procedure with variable step sizes was used to estimate the stimulus contrast the subject needed to detect the gratings bars on 50% of presentations. The uniform background field was of 12 cd/m^2 luminance, with CIE (Commission Internationale de l'Eclairage) chromaticity coordinates x = 0.305, y = 0.323.

As in the pupil recordings to coloured targets, the viewing distance was 70 cm and the chromatic test patterns were also embedded in a dynamic luminance contrast noise to isolate chromatic signals (Barbur et al 1994a). The viewing distance for achromatic contrast sensitivity measurements was increased to 3 meters in order to display gratings of high spatial frequencies.

6.4 Experiments and results

Pupil perimetry

Pupil perimetry showed that there were not significant differences with retinal eccentricity suggesting that, in both patients, the lesion extends over a substantial portion of the patient's visual field. The results for both patients J.M. and B.D. are shown in Fig. 6.1 together with responses obtained from a group of six age-matched healthy volunteers. Stimulation of the foveal region in normal subjects yields the largest pupil constriction with smaller response amplitudes in each of the four quadrants. In contrast to the normal subject group, the response amplitudes in J.M. and B.D. were very small, with no dependence on stimulus location (see bar graphs in Fig. 6.1 giving response amplitudes at each location). Pupil response latencies in both J.M. and B.D. were long and difficult to estimate accurately because of the small response amplitude. The mean response trace for the normal group yields a latency of 0.23 s.
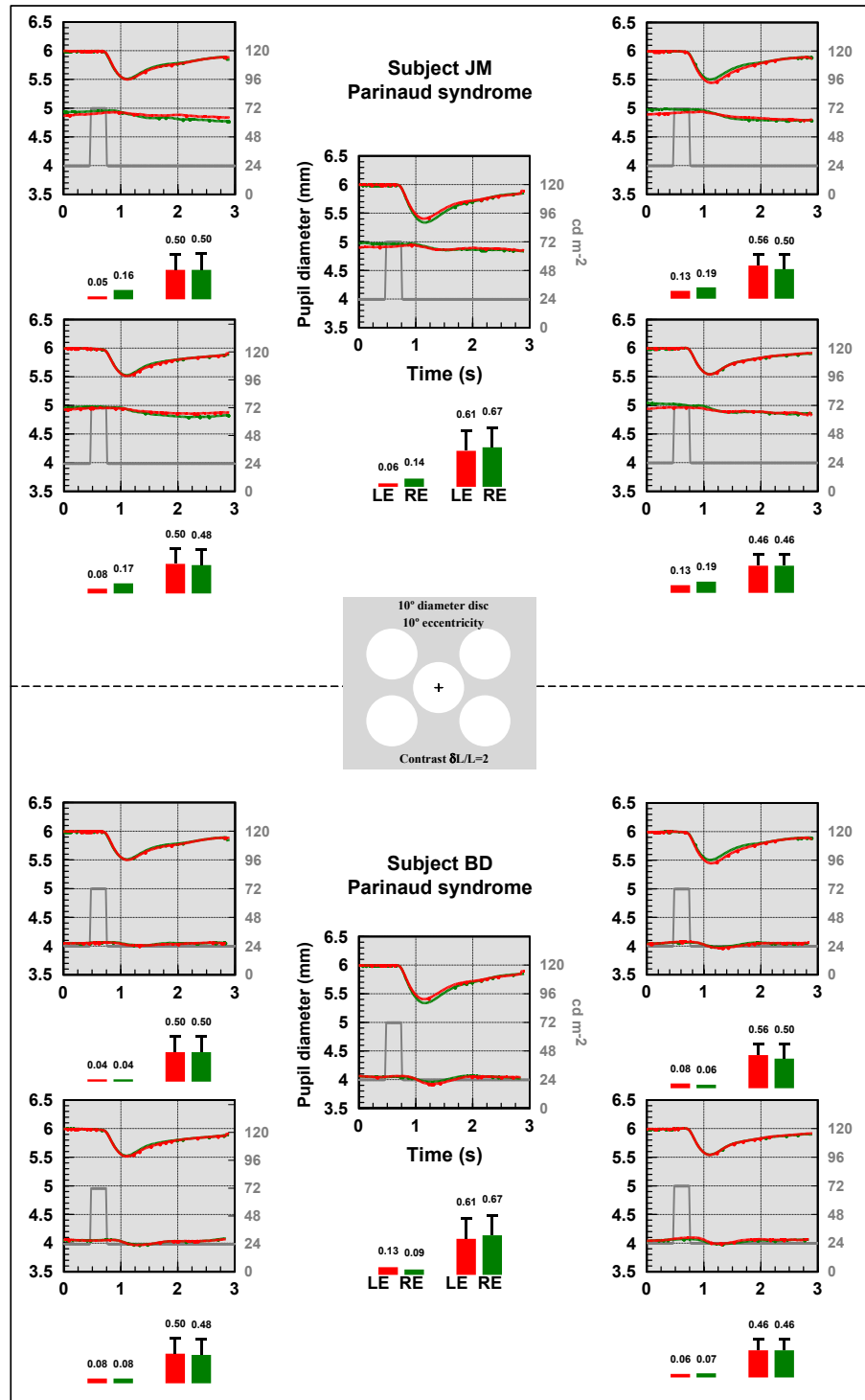
Fig. 6.1 Pupil light reflex responses to a flash of light presented at five different retinal locations (see inset in the centre). Data for J.M. is shown in the upper panel and similar results for B.D. in the lower panel. The spatial arrangement of the graphs reflects the position of each stimulus in the visual field with the central graph representing the foveal region. The display was viewed binocularly and the pupil response was measured simultaneously in each eye (RE-right eye, LE-left eye). The stimulus trace (shown in dark grey) shows both the duration and the luminance of the test flash. Mean data for six normal subjects measured under identical stimulus conditions are also shown in each graph (upper traces) for comparison. The bar graphs show the right and left eye response amplitudes for each patient and the mean response amplitudes for the normal subject group (n=6).

Pupil contrast gain

The duration of the test flash was increased to 500 ms and a number of measurements were averaged in response to increasingly bright stimuli. The results, presented in Fig. 6.2, show small pupil responses even for the highest brightness that could be achieved in the CRT display used (flash luminance of 96 cd/m^2). Increasing the luminance contrast of the stimulus had little effect on the measured response amplitudes as opposed to the steep contrast gain generally observed in young normal subjects.
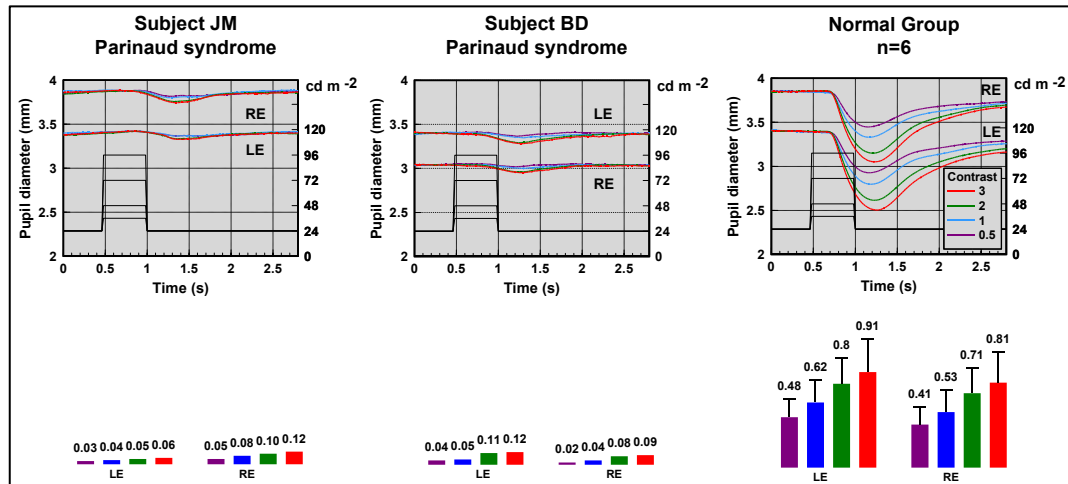
Fig. 6.2 Pupil constriction amplitudes remain small in two patients with Parinaud's syndrome despite the increasing luminance contrast of the flash stimulus elicit very large responses in the normal control group. The bar graphs show response amplitudes for increasing contrast amplitudes. The flash lasted for 500 ms and its luminance was gradually increased to 50, 100, 200 and 300% respect to that of the background which remained at 24 cd/m^2. RE-Right Eye; LE-Left Eye.

Pupil colour response

Pupil responses to chromatic stimuli are normally associated with processing of chromatic signals in extra-striate visual areas, since such responses can be abolished selectively in patients with cerebral achromatopsia (Barbur et al 1994a). It was therefore of great interest to investigate whether pupil colour responses (PCR) could still be elicited in the absence of a functioning pretectum that abolishes the classical pupil light reflex (PLR). The results in Fig. 6.3 show that isoluminant coloured stimuli can trigger substantial PCRs in both patients. A study of six normal subjects for stimulus conditions identical to those employed in this study was carried out to assess the expected level of inter-subject variability. The PCR response amplitudes (J.M.: d = 0.14; B.D.: d = 0.18) are slightly smaller than the mean amplitude for the normal group (d = 0.31, SD = 0.14, n = 6). However, given the large inter-subject variability within the normal group and the fact that we were able to test only two patients, there is not sufficient statistical power to claim that these differences are statistically significant.
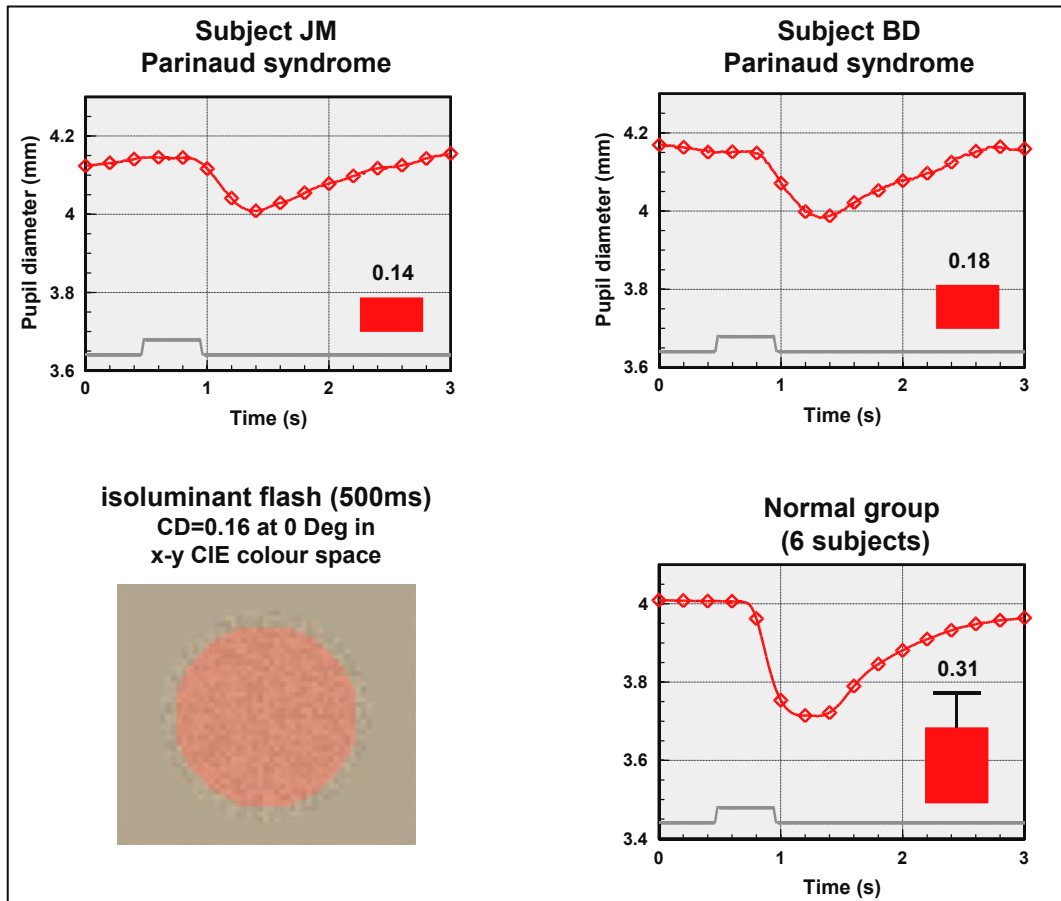
Fig. 6.3 Pupil colour responses measured under stimulus conditions that isolate the use of chromatic signals. In addition to the two patients, six normal subjects were also investigated using identical stimulus conditions. Upper left: J.M.'s response trace averaged from 16 measurements. Upper right: similar results for B.D. Lower right: the normal subject data showing considerable inter-subject variability (d = 0.31, SD = 0.14, n = 6). The results supports the hypothesis that pupil colour responses do not require a functioning pretectum but arise instead as a result of cortical proccesing.

Pupil grating response

Pupil grating responses were measured in both patients for three different spatial frequencies that elicit significant response amplitudes in normal subjects. Both PCRs and pupil grating responses (PGRs) show considerable inter-subject variation in amplitude and latency (Wolf et al 1999). The results for J.M. and B.D., and the mean data for the normal subject group are shown in Fig. 6.4 for each spatial frequency tested. The averaged data for the normal subject group for the 3.5 cycles/degree grating yields a mean PCR amplitude of 0.41 ± 0.13 mm. The corresponding response amplitudes for the two patients were: 0.25 mm for J.M. and 0.28 mm for B.D. Pupil responses to gratings and chromatic stimuli are usually of smaller amplitude and have increased latency by comparison with light reflex responses (Barbur 1995). The PGR response amplitudes in both J.M. and B.D. were smaller than the mean amplitudes measured in the normal subject group. Again, we cannot test statistical significance reliably because of the large inter-subject variability in the normal group.
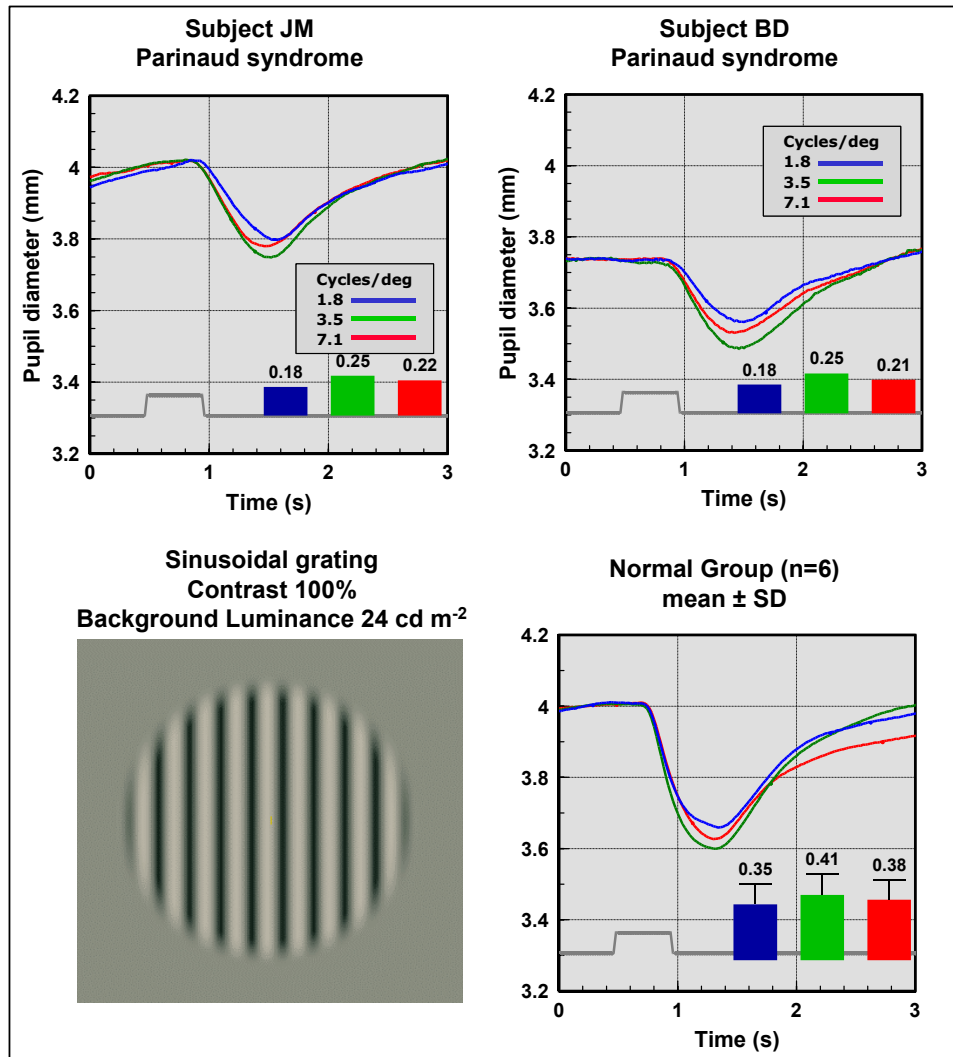
Fig. 6.4 Pupil responses to sinusoidal gratings whose space-averaged luminance was equal to that of the uniform background field. The grating stimulus subtended a visual angle of 10° and was viewed binocularly from a distance of 70 cm. Six normal subjects were also investigated using identical stimulus conditions. Upper left: J.M.'s responses to different spatial frequencies. Upper right: similar results for B.D. Lower right: the normal subject data show considerable inter-subject variability (e.g. for a spatial frequency of 3.5 c/°; d = 0.41, SD = 0.13, n = 6).

Contrast sensitivity tests

The results of contrasts sensitivity tests are shown in Fig. 6.5. As expected, the results show that both J.M. and B.D. have normal achromatic (Fig. 6.5A) and chromatic (Fig. 6.5B) sensitivity. The slight reduction of achromatic sensitivity in the high spatial frequency range for both patients is probably caused by rapid eye movements and nystagmus. The major and minor axes and the orientation of the chromatic threshold ellipse (Fig. 6.5B) are similar to those measured in normal trichromats.
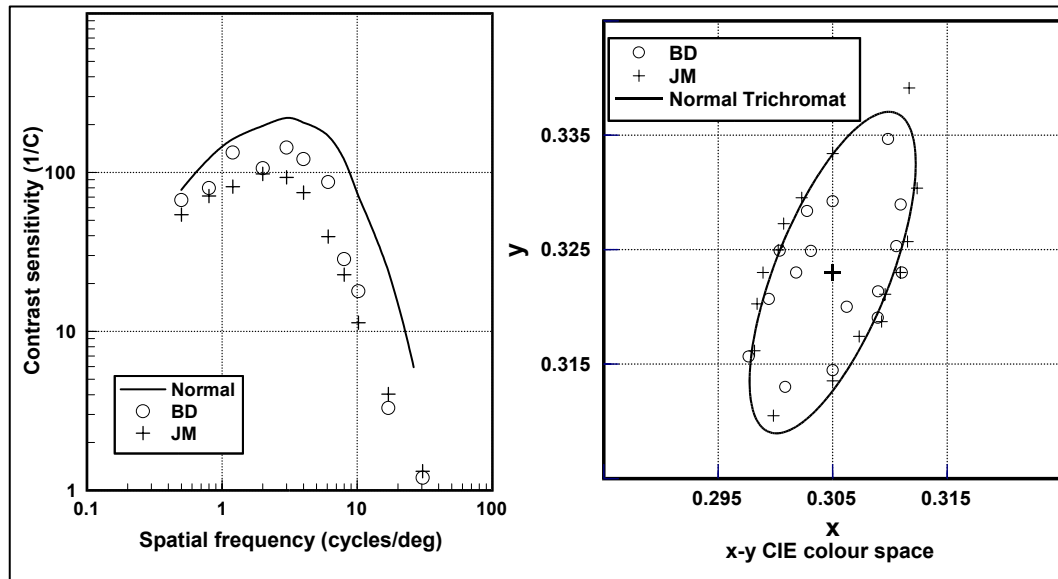
Fig. 6.5 Contrast sensitivity (left) and chromatic threshold measurements (right) in both J.M. and B.D show near to normal vision.

6.5 Summary

In general, results show that damage to the olivary pretectal nucleus abolish the pupil light reflex (Fig. 6.1 & Fig. 6.2) but has little effect on pupil grating or pupil colour responses (Fig. 6.3 & Fig. 6.4). The light reflex response, on the other hand, is virtually abolished, with only a small residual component that is similar to the pupil grating response and may not require an afferent projection to the mid-brain. These findings suggest that the site of integration of cortical signals in relation to pupil colour and grating responses and the generation of sleepiness-induced oscillations of the pupil do not rely on the normal functioning of pretectal nuclei that are involved in the light reflex response.

6.6 Discussion

Previous studies have shown that the pupil responds to stimulus attributes such as colour or spatial patterns (gratings), even when the stimulus conditions eliminate artefacts that can trigger a pupil light reflex response (Barbur et al 1992, chapters 3&4). In general, such pupil responses are absent or significantly reduced when the stimulus is presented in the blind hemi-field of cortically blind patients (Barbur 1995, chapter 5).

The findings reported here in two patients with serious damage to the pretectal areas of the mid-brain, show that the pupil still responds to visual stimuli other than light flux increments (isoluminant colours and gratings). These non-light responses remain even when there is not direct input from the OPN to the parasympathetic EW nuclei that innervates the pupil sphincter muscle.

Although the amplitude in the PCR (Fig. 6.3) and the PGR (Fig. 6.4) in both patients was close to the mean of the control group. The small reduction in patients compared to controls could be easily account by the fact that, even if we could achieve perfect isoluminance, the pretectum is still likely to contribute marginally to the PCR and the PGR in healthy subjects (the isoluminant stimuli used here is indeed an approximation and thus some small residual luminance signals from the pretectum do contribute to larger PCR & PGR in the normal group).

A possible explanation for these non-light pupil responses is that perturbation of neural activity in extrastriate areas of the cortex, as a result of processing certain stimulus attributes, causes transient weakening of the constant central sympathetic inhibition to

EW parasympathetic neurones innervating the sphincter muscle (Barbur et al 1992, Sahraie et al 1997a). This temporary reduction of the central sympathetic tone would then result in an outbalanced parasympathetic outflow to the sphincter muscle causing a pupil constriction (Barbur 1995).

The presence of pupil sleepiness waves in J.M. and B.D. under sleep deprivation conditions confirm that, in spite of extensive damage to pretectal nuclei, the sympathetic inhibition of the parasympathetic pupillary system is functioning normally (Wilhelm et al 2002). The sleepiness-related pupillary oscillations observed in both patients are regarded as the effect of intermittent fluctuations in central sympathetic inhibition at the level of the EW nucleus (Lowenstein & Loewenfeld 1969, Lowenstein & Loewenfeld 1969, Wilhelm et al 2001).

Another explanation for this residual response could involve changes in sympathetic input to the dilator muscle of the iris, caused by a large increment in light flux level on the retina. The pathways involved in the control of sympathetic innervation of the dilator muscle in response to a change in ambient illumination may rely, at least in part, on a direct cortical input. The longer latencies that characterize these residual pupil light reflex responses support this view.

Although the PCR and PGR in patients suffering from Parinaud's syndrome do not differ much from the normal population (significance cannot be tested reliably since there were only 6 subjects in the normal group and only 2 Parinaud's patients variance was large across subjects and group).

Chapter 7: Clinical applications of the pupil response

7.1 Optic neuritis (ON) and Multiple Sclerosis (MS)

Optic neuritis (ON) is a demyelinating disease of the optic nerve. It typically results in a loss of vision and is usually accompanied by ocular pain. The severity of visual loss ranges from a slight visual defect to a complete loss of light perception.

The annual incidence of optic neuritis ranges from 1.4 to 6.4 new cases per 100,000 population. The initial attack is usually unilateral in 70% of the patients and bilateral in 30%. The acute phase of the attack generally lasts for a few days and recovery occurs after 2 weeks with the majority of improvement after 4 weeks (Cornblath 1995). Most of the patients recover the visual acuity almost completely but in the long term there can be a residual loss in vision and quite frequently, as shown here, a pupil sensitivity loss even when the visual function is normal. Despite the spontaneous recovery after the first few weeks, an accurate assessment of the evolution of the disease is important due to the high risk of developing more complicated neurological diseases such as Multiple Sclerosis (MS). Indeed, ON symptoms are often seen as a first warning sign of MS and the percentage of ON cases that subsequently develop MS can be as high as 50% (Brodsky et al 1997). A number of studies also show that the risk of developing MS after optic neuritis increase over time (Druschky et al 1999). This together with the fact that recurrence is quite common, explains the great interest in the development of quick and reliable tests that can reveal possible damage even when the visual function seems to be normal.

The term optic neuritis is generally reserved for a specific type of optic neuropathy of which the most significant characteristic is the loss of myelin, the fatty insulating wrapping of the neural fibres. Diagnosis can be sometimes difficult to establish and each patient needs a thorough examination. The optic disc can appear swollen (papillitis) or normal (retrobulbar optic neuritis) depending where in the optic nerve the inflammation occurs. A number of clinical signs permit to distinguish it from other optic neuropathies caused by vascular lesions or tumours such as Anterior Ischemic Optic Neuritis (AION) or compressive optic neuritis.

Despite that the loss of visual function can be quite similar in ON and AION, there are usually specific clinical signs that differentiate them. Among these we can include: the presence of pain (particularly during eye movements), the absence of optic disc oedema, which is commonly found in AION (Rizzo & Lessell 1991, Swartz et al 1995) and a different age range (typically 20-40 years in ON and 60 or over in AION). A summary of the different features of AION and ON is given in Table 7-1. For a more detailed description of the diagnosis of optic neuritis and other lesions of the optic nerve see the review by Heron (1986) and the studies comparing AION and ON of Kardon (1992, 1993). The visual loss in ON can progress over a week after which the symptoms usually remit. Progression over a longer period of time would alert the clinician of other possible aetiology than demyelination and a brain scan might then be advisable.

The Optic Neuritis Treatment Trial (ONTT) (Beck 1991), one of the most complete clinical trials to date, monitored 448 patients with optic neuritis between 1988 and 1991 and has provided some basic recommendations for clinical diagnosis and treatment. The use of magnetic resonance imaging (MRI) is only recommended when the patient's course is atypical or the clinical signs rule out demyelination suggesting the possibility of a compressive lesion or tumor. Indeed, MRI does not seem to be very cost-effective as a basis for initiating treatment, specially taking into account that the limited resolution (1-2

mm) of current scanners (De Groot et al 2001) can detect signs of demyelination only in the most severe cases (Ormerod et al 1987).

Clinical signs in ON and AION		
	Optic Neuritis	**Anterior Ischemic Optic Neuritis**
Age range	18-40	>60
Pain	Often present 60-90% of cases	Rarely present
Visual acuity loss	Any range	Any range
Field Defect	Any type, mostly central	Any type, often altitudinal (inferior more common than superior)
Optic Disk	Maybe disc edema	Always disc edema
Improvement (% of cases)	65%. Recovery of visual acuity after 2-8 weeks from attack	16%. Recovery of visual acuity is rare

Table 7-1. A number of clinical signs allow the clinician to differentiate between optic neuritis (ON) and Anterior Ischemic Optic Neurits (AION). Source: Rizzo & Lessell 1991.

Despite numerous clinical trials, the most appropriate treatment remains a subject of debate (Beck 1998). Treatment with cortico-steroids (e.g. intravenous methylprednisolone or oral prednisone) is thought to improve recovery rates if taken during the first weeks after the attack but these drugs have not been proven to be useful reducing subsequent attack frequency (Sellebjerg et al 1999) or to have any effect on the final recovered visual acuity. On the basis of the ONTT, general systematic treatment with cortico-steroids is not longer advised. However, it should be pointed out that recent clinical trials with cortico-steroids in patients with MS showed a significant improvement compared to a placebo but they were not conclusive about which, oral or intravenous, administration is the most appropriate (Polman et al 2001). Perhaps, the most promising approach to treat ON and MS comes from experiments using modern gene therapy techniques in mice (Guy et al 1999) and studies using cell implantation treatments (Mitome et al 2001). These techniques have been proven successful in reducing or protecting against demyelination and might open a new path for an effective treatment of ON and MS in the future.

7.2   Methods and subject groups

All patients included in this study were diagnosed unilateral optic neuritis, although in a few cases, the asymptomatic fellow eye could also have been involved at some stage. We excluded patients whose clinical diagnosis was indicative of a pathology other than optic neuritis. We include two patients with confirmed MS and others with suggestive

symptoms of MS. Since the two diseases are intimately related we did not expect a priori, a different pattern of results in the two groups. This was later confirmed in the analysis of the responses.

We tested visual function using a wide range of techniques: infra-red video pupillometry, visual field perimetry, contrast sensitivity and a new dynamic colour vision test developed at City University (MCVTEST). This combination of both supra-threshold and sub-threshold techniques allowed an exhaustive study of the possible effects caused by the optic nerve lesion. This is specially interesting in cases where the aetiology is not clear and can help to diminish any margin of error in diagnosis.

Subjects were divided into three different groups according to the time since onset.

Group 1. Short-term follow-up: 8 patients during the acute phase of the attack, then followed up after a period of 4 to 12 weeks while the recovery was still not complete.

Group 2: Long-term follow-up: 15 patients with a previous history of optic neuritis and tested after a long-term period of recovery (mean 25 weeks) when most cases had recovered visual acuity to almost near-normal levels and some still had a residual visual field loss.

Group 3: Normal group: 16 normal subjects in an age range of 20-35 years that matched approximately that of the 2 patients groups, with a Snellen visual acuity of 6/6 (LogMAR = 0) or better and normal visual function.

Pupil responses to light (PLR) and colour (PCR)

Besides the pupil light response, the pupil is also known to respond to colour even in the absence of a total light flux change (Barbur 2002). In order to isolate the pupil colour response (PCR) from the classical pupil light reflex (PLR), the colour of the disc and the achromatic background were carefully chosen to be doubly isoluminant (d-isoluminant) i.e. to be perceptively of equal luminance for both rods and cones (Young & Teller 1991). Isoluminant stimuli are widely used in many areas of vision research since there is a lot of electrophysiological evidence that achromatic and chromatic signals are carried by substantially different neurones. This functional segregation occurs very early in the visual pathways, at the level of the optic nerve before reaching the Lateral Geniculate Nucleus (Kaplan et al 1990). There is therefore much interest to apply this recent knowledge of the anatomy and physiology of the visual pathways to the development of new tests for non-invasive assessment of visual anomalies.

The classical assessment of pupillary function in clinical practice is the swinging light test. In this test, the pupil is illuminated with a small lamp for 2-3 seconds alternating between the eyes to evaluate for any deficit or asymmetry in constriction amplitude. This simple technique, firstly used in the 1960s by Paul Levatin (1959), is a fast and reliable method for detecting mild to severe pupillary defects.

However, during certain clinical conditions, neuro-ophthalmologists often need to quantify more precisely the pupillary deficit or Relative Afferent Pupil Defect (RAPD), i.e. the differences in pupil size between the two eyes. This is done by alternating a light between the two eyes using a series of neutral density filters with increasing opacity placed in front of the unaffected eye of the patient until the pupil constriction matches that of the affected eye. A neutral density filters transmits only a fraction of the light incident on them but, unlike a coloured filter, the light attenuation in a neutral filter is the same for any wavelength or colours across the visible spectrum. Transmission rates are usually given in Log units as Optical Density (OD). 1 Log unit means that only 10% of the light is transmitted, 2 Log units a 1% and so on.

$$OD = -LogT \Rightarrow Transmission = 1/10^{OD} \qquad (6.1)$$

The RAPD is measured accordingly in Log units as the light attenuation needed to match the pupil sizes in the two eyes. A RAPD of 0.3 Log units or more is usually

considered as a sign of clear pupillary dysfunction (Kardon 1995). For a good review of clinical conditions causing a RAPD see for example Thompson (1992).

In this study, we measured directly with high precision (0.01mm) pupil constriction asymmetries between the affected and the unaffected eye. We get in this case a more accurate version of the RAPD test with the advantage that we stimulate each eye with the same light intensity. This is very convenient when comparing results in a patient tested during the acute phase of a disease and re-tested after a few days or weeks to assess recovery. This gives a direct measurement under the same luminance conditions while the classical RAPD measurement is more susceptible to variations specially in severe cases of pupillary dysfunction. Another disadvantage of the RAPD measurements is that neutral density filters are generally available only in 0.3 Log units steps and this precision is not sufficient to assess pupil recovery in most cases.

Pupil measurements

The P_SCAN system (Barbur & Thomson 1987), previously described in chapter 3, was used to record the pupil diameter by fitting the best circle to the pupil at a rate of 50 Hz. Patients looked to a calibrated computer display at a distance of 70 cm. All the measurements were done in monocular viewing. An infra-red transmitting filter covered the fellow eye allowing the simultaneous recording of both the stimulated (direct response) and the non-stimulated eye (consensual response).

Pupil stimuli

Two different stimuli were used: either an achromatic (luminance modulation) or a red-coloured (chromatic modulation) disc, each subtending 7° of visual angle at a distance of 70cm and centered foveally in an uniform achromatic background with CIE coordinates (x,y)= (0.305, 0.323) corresponding to MacAdam's white (MacAdam 1942). Since the pupil colour response is favoured by highly photopic luminance conditions, the luminance of the background was set to 16 cd/m^2 in order to trigger a substantial response to colour, while a lower background of 8 cd/m^2 was used to favour the PLR. This difference in luminance of the background only changes slightly the mean pupil size and has little effect on the dynamic pupil response.

Both the luminance and chromatic saturation of the disc were modulated sinusoidally at 1Hz during 10 seconds, this frequency was chosen from preliminary studies so as to achieve a large pupil constriction without compromising the signal to noise ratio of the response. The mean luminance of the achromatic disc was 32 cd/m^2 reaching a maximum value of 64 cd/m^2. The maximum chromatic saturation allowed by the phosphors of the display for the red disc was 0.16 units of distance[1] in the CIE (x,y) chromaticity diagram (Wyszecki & Stiles 1982).

A minimum of 16 traces were averaged for each eye and both the pupil amplitude and the time delay of the response were computed from the fundamental harmonic of the Discrete Fourier Transform (DFT) of the averaged trace following standard numerical computation techniques (Press et al 1992). Typical parameters of interest in a pupillogram are the amplitude of the constriction in mm and the time delay in the response in ms. Additional parameters allow to check for the reliability of the response such as the signal to noise ratio and the non-linearity, which indicates the contribution from other harmonics than the fundamental in the DFT analysis of the response. See for an example of a pupil response trace from a typical case of ON.

---

[1] Chromatic distance is defined as CD = $[(x-x_0)^2 + (y-y_0)^2]^{1/2}$. In this case, $(x_0, y_0) = (0.305, 0.323)$ refers to the achromatic background. The CD changes in different colour spaces since generally, the transformations in coordinates (eg. from x,y to u',v') do not preserve the metric or even the angles (non-conformal transformation).
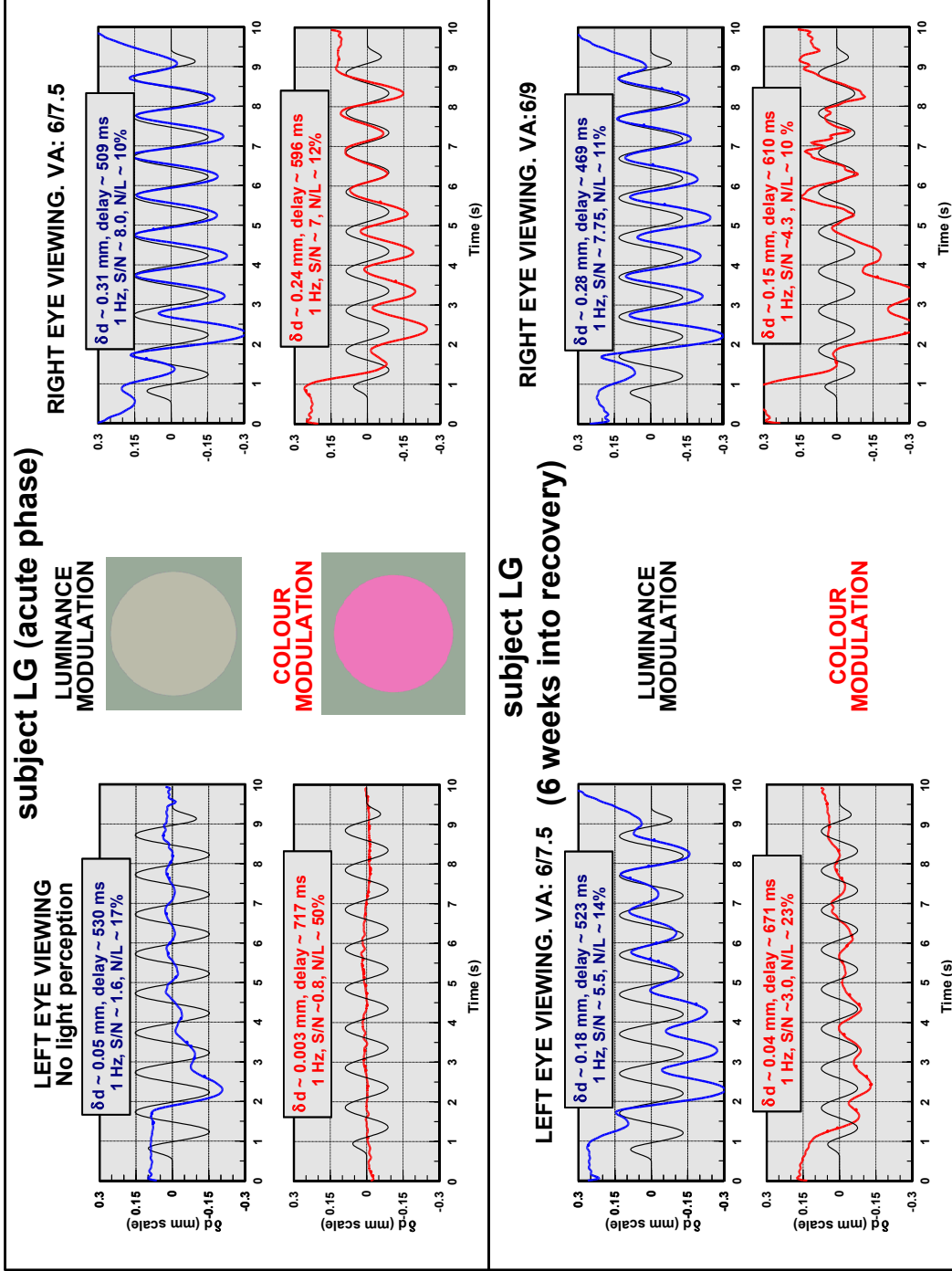
Fig. 7.1 Graph shows pupil respnses (blue, red) of a subject during the acute phase of optic neuritis when stimulating the affected eye (left) and the unaffected eye (right) separately for both achromatic and chromatic modulation. Each pupillogram is the average of a minimum of sixteen traces. The amplitude (mm) and latency (ms) of the response were computed from the fundamental harmonic of the fourier series of the averaged trace.

Visual acuity and Humphrey visual fields

Visual acuity was measured for all subjects using a LogMAR (Log of the Minimum Angle Resolution) letter chart (Bailey & Lovie 1976) at a viewing distance of 6 meters. Unlike the Snellen letter chart, the LogMAR chart has the same number of letters in each row and these are also scaled linearly in size. It is therefore more convenient than the Snellen chart to investigate correlations between visual acuity loss and visual field or pupil perimetry loss. However, since Snellen notation is used widely in clinical studies, a conversion from LogMAR to Snellen values is given in the graphs. Visual acuity is considered normal when a subject can resolve 1 minute of arc (MAR=1', LogMAR=0), which is equivalent to a Snellen visual acuity of 6/6 (20/20 is more common in the US where feet are used instead of meters).

Visual fields were tested using the Humphrey Field Analyzer program 30-2 which measures luminance detection thresholds across 30° of the visual field with a 2° target separation. The algorithm used by the machine automatically estimates the reliability of the test, evaluating the number of fixation losses and false positives in the response. The severity of visual field defects are estimated in terms of the mean threshold deviation, which is the center-weighted difference between the visual threshold in comparison to a population of age-matched normal subjects (Haley 1987). The difference in the mean deviation (dB) between the affected and unaffected eyes was compared with the pupil response and visual acuity to explore possible correlations between visual function loss and pupillary deficit.

Although some studies claim that in optic neuritis the visual field loss is greater in the central region than in the far peripheral visual field (Keltner et al 1999), other studies have challenged this idea and showed that almost any kind of visual field loss can be found in ON. Asymmetries in the visual field thresholds have therefore limited value as a diagnostic tool to differentiate ON from other optic nerve lesions (Fang et al 1999).

At the level of the optic nerve, the fibres are topographically well organized; the top half of the optic nerve fibres map the visual field below the horizontal meridian whilst the fibres in the bottom half map the upper visual field (Zeki 1993). Since the central visual field is represented by a much higher density of retinal fibres than the periphery, a central loss is probably more common in lesions affecting the entire optic nerve. This will have also implications in the damage caused by compressive lesions to the optic nerve. A tumor causing a compression of the superior section of the optic nerve would produce an inferior visual field defect and viceversa. Therefore, an asymmetric visual field threshold could indicate the possibility of a compressive lesion while a central visual loss would be more likely to be caused by a condition affecting the whole of the optic nerve.

At the end of the optic nerve, fibres from the nasal retinae cross over in the optic chiasm to form the optic tract, where fibres from both eyes map the contralateral visual field. A unilateral damage to the optic tract will result then in a marked asymmetric visual field defect of similar intensity in both eyes as opposed to the inter-ocular difference typical of unilateral lesions in the optic nerve.

Psychophysics: contrast sensitivity and colour vision test

Patients in the long-term recovery group (Group 2) performed additional psychophysical tests for the assessment of achromatic and chromatic sensitivity loss. The aim of these tests was to detect any residual visual loss in patients who had recovered their visual acuity almost completely and to find out how well achromatic and chromatic sensitivity correlated with pupillary deficits.

Achromatic contrast sensitivity was measured using a adaptive staircase procedure (Levine 2000). The target was presented in a uniform background of luminance 24 cd/m^2. It consisted of a sinusoidal grating embedded in a disc (4° diameter at 2m) and attenuated with a gaussian envelope. The gaussian envelope minimizes the facilitation of detection caused by abrupt changes in contrast at the grating edge. The contrast of the grating (the luminance difference between dark and bright bars as a percentage of background luminance) varied according to an adaptive staircase procedure which estimated the minimum contrast threshold needed for detection.

Chromatic sensitivity was measured using a computer-based psychophysical test (MCVTEST). The computer program was developed at City University (see chapter 3).

Chromatic thresholds were measured in 18 different directions (colours) in the CIE xy-1931 colour space (Wyszecki & Stiles 1982). The threshold is defined as the minimum colour saturation needed to distinguish a coloured target from the achromatic background. In each presentation, a coloured target is presented foveally, moving in 4 possible diagonal directions. The task of the observer is to identify in which direction the target has moved. This 4-alternative forced choice procedure (4AFC) is repeated for each colour until the observer is not able to detect any chromatic signals. The program uses an adaptive staircase procedure, increasing or decreasing the colour saturation of the target according to the responses given by the observer. After each reversal the step size is reduced. For each patient the test finished after 9 reversals. Only the last 6 reversals are averaged and considered to compute the chromatic threshold as the distance in the x-y space from an achromatic background of coordinates (x= 0.305, y= 0.323) corresponding to the white reference used by MacAdam (1942). The first 3 reversals were ignored since the step size of the staircase is large and they would be a poor estimation of the threshold.

The colour patterns were chosen to be of equal luminance as the background (isoluminant stimuli for photopic conditions) in order to isolate luminance from chromatic signals in the visual pathways. Both the affected and the unaffected eyes were measured separately in monocular viewing.

7.3 Data analysis and results: Group 1

Pupil responses during the acute phase

Pupil responses during the acute phase of the disease and after short-term follow-up are summarised in Table 7-2 for a group of 8 patients with diagnosed unilateral optic neuritis. The mean and the standard deviation are given for the two conditions measured; the response to an achromatic light modulated sinusoidally in intensity, producing variations in the light flux entering the retina, and the pupil response to pure colour saturation modulation without a change in the mean light flux level.

In addition to the expected reduction of constriction amplitudes, pupil response latencies were also substantially affected during the acute phase of the disease, yielding to delays as large as 60 ms for the PLR and 150 ms for the PCR in comparison to the normal group.

The analysis of the pupil responses did not show any difference between the stimulated eye (direct response) and the non-stimulated (consensual response). This was expected a priori, since a lesion to the optic nerve in optic neuritis affects only the afferent pathway of the pupil response (Alexandridis 1985), and confirmed that the efferent pathways were intact. Therefore all subsequent analysis was carried out considering only the direct pupil response.

During the acute phase of ON, it was found that the Pupil Light Reflex (PLR) was significantly smaller than in the control group, but perhaps the most interesting fact is that the Pupil Colour Response (PCR) amplitude was absent in all but two patients. This is clearly illustrated in the pupillogram for a patient LG in . Similar results were obtained in the majority of the patients with different degrees of pupillary loss. But there was a common trend: while the coloured stimulus is strong enough to elicit a clear signal in the unaffected eye, the pupil of the affected eye is unable to follow the change in colour saturation. For example, in subject LG (), the pupil responds well to a luminance modulation although it is significantly reduced in the affected eye. Similar results were obtained for the other patients. A different degree of PLR loss was found but all patients showed a systematic deficiency in the PCR yielding an average PCR of only 0.02 mm.

PLR	AMPLITUDE (mm)		LATENCY (ms)	
	AFFECTED EYE	UNAFFECTED EYE	AFFECTED EYE	UNAFFECTED EYE
ACUTE (n=8)	0.11 ± 0.03	0.29 ± 0.02	517 ± 16	476 ± 15
RECOVERY (n=8)	0.13 ± 0.03	0.25 ± 0.02	529 ± 19	490 ± 6
CONTROL (n=16)	0.36 ± 0.08		472 ± 47	

PCR	AMPLITUDE (mm)		LATENCY (ms)	
	AFFECTED EYE	UNAFFECTED EYE	AFFECTED EYE	UNAFFECTED EYE
ACUTE (n=8)	0.02 ± 0.01	0.17 ± 0.02	702 ± 37	553 ± 15
RECOVERY (n=8)	0.05 ± 0.02	0.14 ± 0.01	617 ± 27	565 ± 17
CONTROL (n=16)	0.20 ± 0.07		551 ± 41	

Table 7-2. Pupil constriction amplitudes and time delay of the response in a group of 8 patients with unilateral optic neuritis during the acute phase and after a short period of recovery (4 to 8 weeks). Statistically significant differences (p<0.01) were found in the affected eye both respect the unaffected eyes and the control group.

Even though it can be argued that the coloured stimuli elicited a smaller response in the control group and a comparison with the luminance response is not straightforward, the reduction in the pupil constriction amplitude of the affected eye as a percentage of the unaffected eye and the absence of PCR while a PLR was still substantial, gives strong evidence that there is a greater effect on the PCR in the ON patient group.

The unaffected eye did not show statistically significant differences in comparison with the responses in the normal group. This was expected a priori since the diagnosis was unilateral damage in all cases. Surprisingly, the unaffected eye response after recovery was smaller (although it failed significance at p=0.05) than during the acute phase. This could be attributed to the test being performed in different days. Indeed, is well within the variability expected in the pupil response from day to day. This variability is not large (only 0.04mm) and is not supposed to introduce relevant variance in the statistical comparison among different groups tested in different days. It could be also that the unaffected eye has also become slightly involved at the time of follow-up but in any case is very difficult to draw firm conclusions based on such small differences and a statistical sample of only 8 patients.

Pupillary deficit, visual acuity and visual fields

Fig. 7.2 summarises the results of the 8 patients for both the acute phase and the follow-up. The Snellen visual acuity of the affected eye is indicated for each patient together with the pupillary deficit, computed as the difference in constriction amplitude between the two eyes as a percentage of the response of the best eye. There is thus a different scaling factor (unaffected eye constriction) for each subject. Subjects with large pupil reactions will have generally larger constriction asymmetries (in mm) so is therefore more convenient to consider an adimensional quantity as an estimation of the pupillary deficit. This compensates for the large inter-subject variability found in the pupil constriction amplitudes, even in the normal population, and permits to compare results among different subjects.

During the acute phase, visual acuity was reduced to an ability to count fingers or discriminate hand movements and in the most severe cases, difficulties in the perception of light. Visual fields proved to be abnormal in all cases during the first examination and often impossible to measure due to the severity of the condition.

Patients were re-tested after a few weeks from the initial examination (bottom graph in Fig. 7.2) and only three of them (CB, YG and JT) showed a good recovery in the mean threshold deviation of the affected eye (below 3dB, Humphrey field analyzer). These patients also recovered their visual acuity to normal levels (6/6) and showed a significant recovery of pupillary function. It seems however that recovery in pupil and visual function might not always correlate well since large pupil deficits (50% or greater) were still found when visual acuity improved to fairly good levels eg. 6/7.5 or 6/9. A much clear lack of correlation was found in a separate study investigating the pupillary loss in ON for a longer follow-up period, when patients recovered visual acuity to normal or near-normal levels (Fig. 7.3).
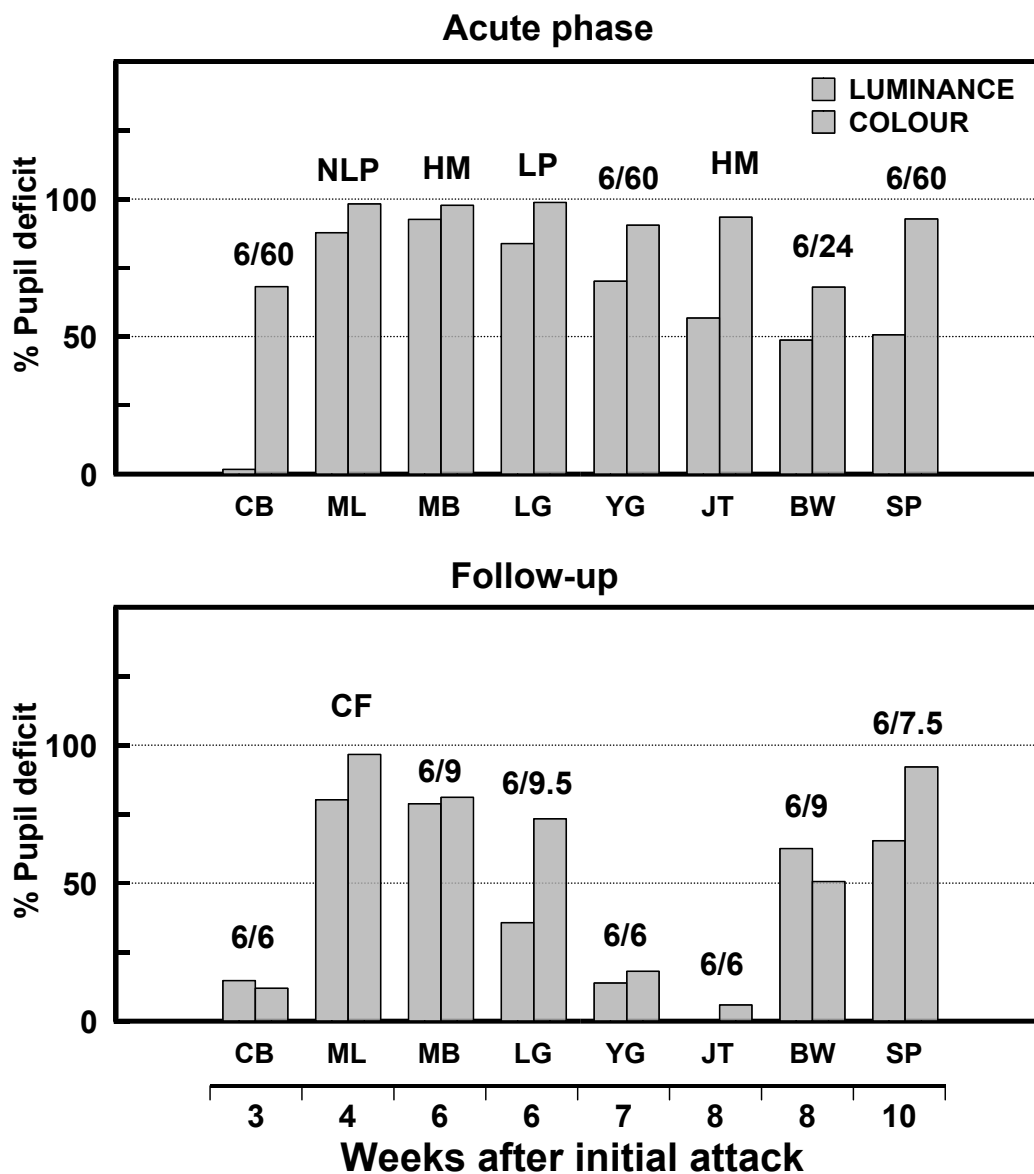
Fig. 7.2. Bars indicate pupillary deficits (as a percentage of the response of the best eye) for each of the eight patients with diagnosed unilateral optic neuritis, both at the onset (top graph) and after a short period of follow up when the recovery was not yet expected to be completed (bottom graph). Labels over bars indicate the Snellen visual acuity of the affected eye.

7.4 Data analysis and results: Group 2

A second group of patients with previous history of optic neuritis were examined following a longer period since the initial attack (mean 25 weeks, range of 6-52 weeks). The aim of this second study was to investigate the time evolution of the disease, the variability in the

recovery rate and how well the recovery of both achromatic and chromatic contrast sensitivity matched the recovery in the pupillary function.

The response of the affected eyes is compared to both the unaffected eye and a control group of 16 subjects in Table 7-3 below. Analysis of variance (ANOVA) showed statistically significant differences between the affected eye and both the unaffected eye and the control group. To test further for the significance of these differences, a paired t-test was used when comparing the affected versus the unaffected eyes and an independent t-test when considering differences with the normal group. Probability levels of significance are indicated for each group of eyes at the row-column intersection in Table 7-3 together with the mean and standard deviation of the response.

PLR	AMPLITUDES (mm)			LATENCIES (ms)		
	Affected eye			Affected eye		
Affected Eye	0.21 ± 0.08	Unaffected eye		537 ± 79	Unaffected eye	
Unaffected Eye	$p < 0.01$	0.31 ± 0.11	Normal group	ns	521 ± 72	Normal group
Normal Group	$p < 0.01$	$p = 0.04$	0.36 ± 0.08	$p < 0.01$	$p < 0.01$	472 ± 47

PCR	AMPLITUDES (mm)			LATENCIES (ms)		
	Affected eye			Affected eye		
Affected Eye	0.13 ± 0.07	Unaffected eye		631 ± 80	Unaffected eye	
Unaffected Eye	$p < 0.05$	0.18 ± 0.06	Normal group	ns	588 ± 75	Normal group
Normal Group	$p < 0.01$	ns	0.20 ± 0.07	$p < 0.01$	$p < 0.05$	551 ± 41

Table 7-3. Pupil responses to luminance (top table) and colour (bottom table) after a long period of partial recovery (mean 25 weeks) in optic neuritis. The mean and standard deviation are tabulated in each column for both eyes and the control group. The level of significance (t-statistics) of the difference, is given below each mean value. ns –not statistically significant difference between the means (p=0.05).

Affected eyes

The results show abnormal pupil responses in the affected eyes compared to the normal control group, with reduced amplitudes and increased latencies. The significant increase in the time delay of the response (about 75 ms for luminance modulation and 80ms for colour) compared to the normal group, together with the decrease in the amplitude of the constriction, confirms the fact that the pupillomotor system is severely affected in optic neuritis even after a long period of recovery when visual function has improved notably (see visual acuity values over bars in Fig. 7.3).

Unaffected eyes

Unexpectedly, response latencies in the unaffected fellow eyes showed an increased delay comparable to the values found in the affected eyes and both were significantly longer in comparison to the normal group. Although the damage was diagnosed as completely unilateral, this significant increased delay in the unaffected eyes latencies indicates that, in many cases, the fellow eye could have also been affected of ON to some extent. This is also consistent with the slight reduction found in the amplitudes of the unaffected eyes in comparison to the normal group (this reduction proved to be not significant at the p= 0.05 level).

Pupil deficit, visual acuity and visual fields

The recovery of visual function several weeks after the onset of the disease was not quite complete. Nevertheless, the majority of patients in this second group showed moderate to good visual acuity and a mild visual field loss with only 35% of cases showing a mean field deviation higher than 3 dB.

Interestingly neither the recovery of visual function or pupil sensitivity appeared to be related to the time elapsed since the onset of the disease, with some cases showing significant deficits even after 4 months, whilst others recovered in a matter of 4-6 weeks. This is illustrated in Fig. 7.3 where the percentage of pupillary deficit is plotted together with the values of the Snellen visual acuity for each subject. The pupillary deficit is evaluated as the pupil response differences between the affected and the unaffected eyes relative to the response of the good eye. When the constriction amplitude is the same in the two eyes, there is no pupil defect and the index is 0%.

To estimate the level of significance, whether a pupil defect is considered normal or not, both the inter-ocular variability in the normal population and the precision of the measurements have to be taken into account. For a 95% confidence interval (p= 0.05), a pupil deficit above 20% can be considered abnormal. This 20% value is also well above the fluctuation in pupil constriction expected when testing subjects on different days and can therefore be used as the criterion for the recovery of pupillary function to normal levels.

The large variability in the recovery of both visual acuity and pupil response, makes it difficult to establish a definite period of complete recovery which is commonly estimated to be 6 months approximately (Beck et al 1997). This large variability can be due to different recovery rates depending on the severity of the initial attack or cases where the disease has recurred after a transient recovery.

Even though many of these patients recovered their visual acuity to near-normal levels (8 patients with 6/7.5 or better), many of them still showed a significant pupillary deficit. It might be that supra-threshold pupil response recovery is not always associated with an improvement in luminance detection thresholds or recovery in the visual acuity. This suggests that visual acuity is not always a good predictor of pupillary deficit and that pupil measurements could be used as an independent estimator of both the extension and evolution of the disease. A similar example of poor correlation between pupil sensitivity and both visual acuity and visual field loss was found also in a case of compressive optic nerve meningioma (Barbur et al 2000).
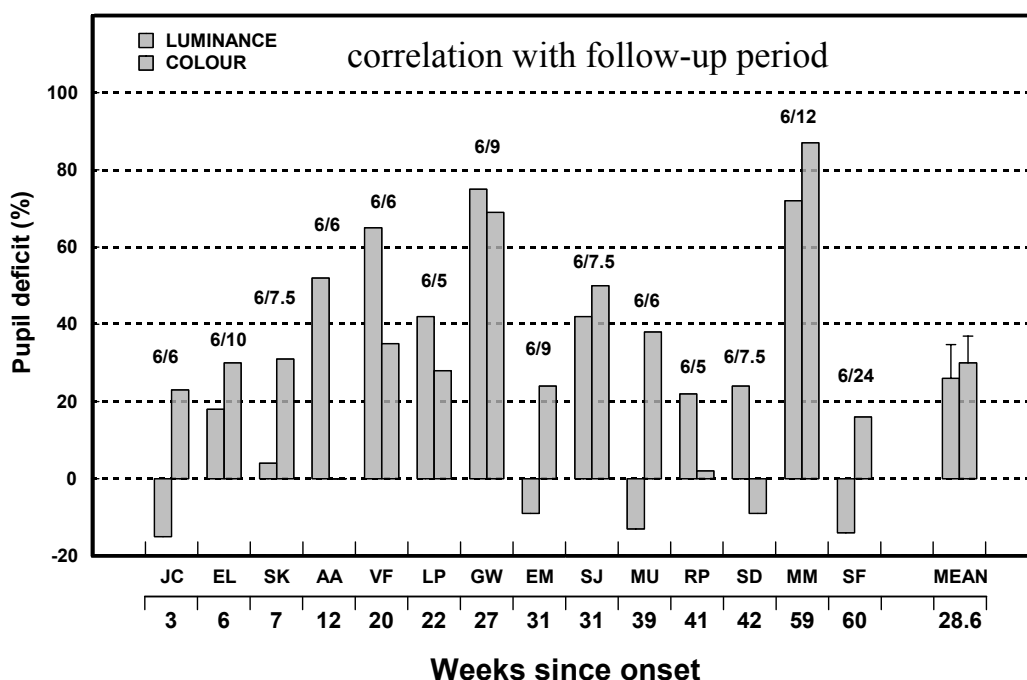
Fig. 7.3 Significant pupillary deficits remain after optic neuritis even for patients who improved their Snellen visual acuity to normal levels of 6/6 or better (labels over bars). A large variability was also found in recovery times suggesting that in some patients the disease might have recurred. The majority of patients showed abnormal PCR while the PLR was more variable.

Colour vision loss

In addition to the pupillometry studies and visual field testing, a colour vision test was performed in the long-term recovery group, to assess to what degree demyelinating lesions of the optic nerve affected chromatic sensitivity, in comparison to achromatic sensitivity (PLR, visual field and visual acuity).

Results for four different patients are given in Fig. 7.4. Seven weeks after the initial episode of optic neuritis, patient SK recovered visual acuity almost completely (6/7.5). She showed normal pupil response to light (4% deficit) but not to colour (31%), and presented significantly increased colour discrimination thresholds for all directions tested in the x-y CIE colour space. On the other hand, patient LP is an example of poor correlation between recovery of pupillary and visual functions; she showed normal colour vision, normal visual fields and acuity (6/5) but still presented an acute pupil deficit to both light and colour (PLR= 42% PCR= 28%). Finally, two patients with confirmed Multiple Sclerosis, MM and EL, show much increased chromatic detection thresholds.

It is well established that the mechanisms of Red-Green (RG) and Blue-Yellow (BY) colour signals have different retinal circuitry (for a recent review see Calkins 1999). This has led to speculations on possible hue-selective deficiencies in lesions of the optic nerve. The common belief is that in optic neuritis Red-Green defects are predominant over Blue-Yellow. However, we found that there is a general loss regardless of colour hue. This is illustrated in Fig. 7.4 where patients showed an increase in colour detection thresholds along any direction in the x-y CIE colour space. The high correlation found between RG and BY thresholds (Fig. 7.5) confirms that both mechanisms are affected to the same extent in optic neuritis. Similar results supporting the lack of colour-specific defects have been obtained in several other studies using standard clinical colour vision tests (Schneck & Haegerstrom-Portnoy 1997).
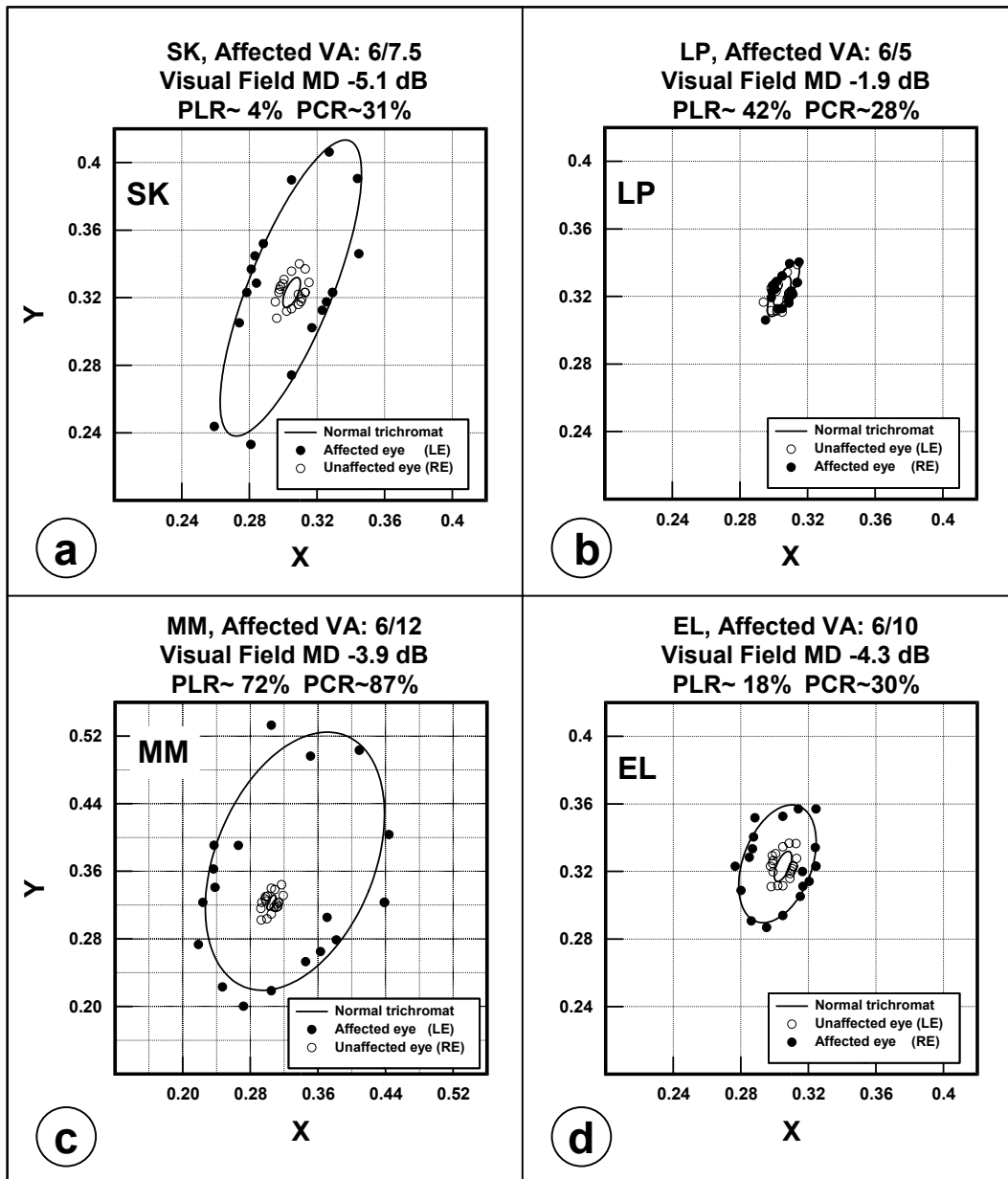
Fig. 7.4 Panels a&b: chromatic detection thresholds measured in optic neuritis (subjects SK and LP) show poor correlation with pupillary deficits (%). Patient LP exhibit near-normal achromatic and chromatic vision despite significant defects in both the pupil light reflex (PLR) and the pupil colour response (PCR). Panels c&d: patients MM and EL were diagnosed multiple sclerosis and show much increased thresholds. Visual acuity (VA) and the mean deviation (MD) in the Humprey's visual field is indicated for each patient. In all cases, the unaffected eye showed similar discrimination thresholds to that of a normal colour trichromat.
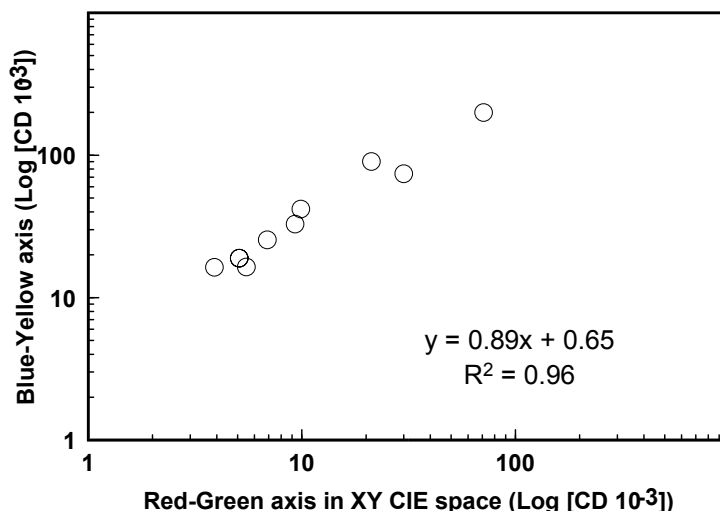
Fig. 7.5 Data points in Fig. 7.4 where fitted using a ellipse-specific algorithm (Fitzgibbon et al 1999) to give a measure of the chromatic threshold along the Blue-Yellow (BY) and Red-Green (RG) axis. The data shows a good correlation between the two axis and suggest that optic neuritis does not affects preferentially any particular colour. This is in agreement with the results of several other studies (Mullen & Plant 1986, Russell et al 1991, Schneck & Haegerstrom-Portnoy 1997).

Contrast sensitivity function (CSF)

Patient SK had recovered almost completely when she did the pupil and visual testing, 7 weeks after the initial attack, but still complained about poor vision in the affected eye. Six months later she volunteered for further testing. Visual acuity had now recovered to normal levels (6/6) and both the colour vision test and pupil responses were well within normal limits. However she showed a minor residual loss when we tested her contrast sensitivity (Fig. 7.6).

Contrast sensitivity can reveal residual visual loss undetected in visual acuity tests since it is a measure of performance near luminance contrast detection thresholds for a wide range of spatial frequencies, while standard letter charts test performance only at high contrast levels[1].

---

[1] Contrast is defined as the fraction of luminance increments respect to a background. For black letter charts contrast is usually greater than 90%.
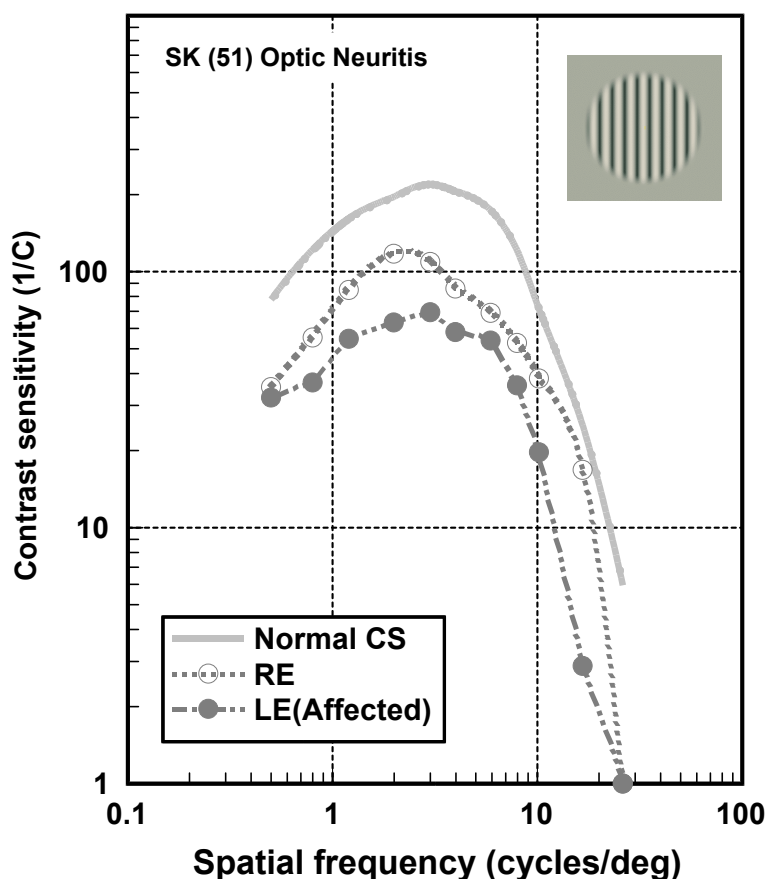
Fig. 7.6 Contrast sensitivity function (CSF) of patient SK. She still showed slightly worse than normal sensitivity even 6 months after the initial attack of optic neuritis. Visual acuity, pupil responses and colour vision were all within normal levels at this time.

7.5 Discussion

Visual and pupillary neural fibres

This is the first study to measure pupil responses in optic neuritis using stimuli that are isoluminant for both rods and cones (Young & Teller 1991). See also d-isoluminance in chapter 3). The doubly-isoluminance constraint, minimizes the luminance signals generated by coloured stimuli that are isoluminant in high-level luminance conditions (photopic) but generally fails to achieve isoluminance in low-level luminance conditions (scotopic).

The combined measurements of pupil responses, standard visual acuity and visual field tests provide evidence that testing of visual acuity alone is not enough to provide a complete description of the patient's visual performance. Particularly in cases of mild optic nerve lesion or after a period of recovery, patients showing normal visual acuity or visual fields often complain of poor vision and usually show significant deficits in the pupil response. This is not surprising, since visual acuity is commonly tested using high-contrast letter charts while everyday visual tasks involve a wide range of contrast levels.

The Pelli-Robson letter chart (Pelli et al 1988) includes letters of both high and low contrast and overcomes the limitation of traditional letter charts but the best estimation of low-contrast performance is given by the contrast sensitivity function (CSF). This function defines sensitivity as the inverse of the minimum contrast (respect to a background of uniform luminance) needed to detect gratings of different spatial frequencies (Levine 2000). The poor correlation between pupil deficits and visual acuity or visual field loss suggest that pupil measurements are an independent estimator of optic nerve damage and therefore can provide additional information to standard clinical examination procedures. For example,

patient LP (Fig. 7.4) shows recovered achromatic and chromatic vision but a significant defect in both the luminance and colour pupil response. Although damage early in the visual pathway, at the level of the optic nerve, will affect both the pupillary and the visual fibres, it is likely that the two functions do not share the same neural fibres, and this could explain the lack of correlation between pupillary function and higher visual functions (visual acuity, colour vision, and contrast sensitivity).

These findings, together with the large variability in visual performance usually found in optic nerve lesions, confirms the convenience of using a number of different tests to assess the evolution of the disease. This is important, particularly in ON patients, due to the high probability of recurring attacks and the risk of developing more serious neurological complications such as MS. It is also crucial to gather as much information when evaluating the degree of improvement during pharmacological trials studying the effectiveness of a particular drug.

Segregation of luminance and colour signals in the optic nerve

In common with other vertebrates, the human retina contains a large number of different ganglion cells that project to distinct areas in the brain. They have been classified mainly morphologically according to cell body size and the extension of their dendritic fields (Rodieck 1998, Perry et al 1984). The wide variety in cell morphology and the large number of projections to different areas in the brain make their functional classification difficult, but it is now widely accepted that chromatic signals are carried by a separate set of neural fibres from those carrying luminance signals (Shapley 1990). There is evidence that coloured isoluminant targets stimulates mainly a specific type of retinal ganglion cells in the optic nerve, the P neurones, that project to the Parvocellular laminae in the Lateral Geniculo-striate Nucleus (LGN) of the thalamus, while luminance (achromatic) signals are carried by cells (M neurones) projecting to the Magnocellular laminae of the LGN (Kandel et al 2000). The M-cells have a much larger body cell size and axon diameter than P-cells and there is also a trend for thin diameter fibres to have thinner myelin sheaths (Reese & Cowey 1988, Baker 2000).

Is important to emphasise that the traditional association of luminance and colour channels with the M and P pathways is a clear oversimplification (see also chapter 1). M cells do not lack total chromatic sensitivity. They are sensitive to modulation of the L+M cone signals. The isoluminant coloured stimuli used in the experiments reported here are modulated along two isoluminant axes in CIE space that also correspond to zero rod contrast signals. The stimuli are therefore photopically and scotopically isoluminant according to the CIE standard observer. One cannot however assure that such stimuli silent completely the contribution from the magnocellular pathway to the pupil colour response. Total silencing of the M pathway will require to cancel the contribution to the pupil response from L and M cones but this is impossible to achieve since we do not know how L and M cone signals are weighted to provided input to the pupil. In the same way, P cells do show some achromatic luminance sensitivity although their contrast gain is much smaller than that of M cells.

In addition, large intersubject variation among individual observers in L and M cone photoreceptor densities (Brainard et al 2000) cannot guarantee complete absence of residual luminance contrast signals in any coloured stimuli. The L:M photoreceptor ratio is also known to increase at large eccentricities within normal subjects and this is likely to affect the photopic luminance response of the eye. The size of the stimulus was therefore restricted to the central 8 deg of the visual field. Since the pupil response threshold to luminance contrast increments is significantly higher than the corresponding psychophysical detection threshold, any small, residual luminance contrast signal in the coloured stimulus is not likely to contribute significantly to the large pupil colour response measured in this study. Moreover, pupil constrictions to luminance contrast increments yield shorter pupil response latencies by comparison with equal amplitude responses driven by coloured stimuli (Barbur et al 1998). This was also observed in this study with significantly longer latencies elicited in response to coloured stimuli. It is therefore reasonable to assume that any small luminance contrast signals that may have been present in the coloured stimuli failed to contribute significantly to the measured pupil colour responses.

Direct axon counting in post-mortem examination of MS patients suggest that cells with smaller axons are more susceptible to damage caused by demyelination (Evangelou et al 2001). There is thus the possibility that chromatic sensitive cells (or the equivalent to P-cells mediating the pupil colour response) with small axon fibres are more susceptible to demyelination during ON than large diameter fibres. On the other hand, large axon diameter fibres mediating the pupil luminance response have a thicker myelin sheath, which could provide a greater resistance to demyelination (See Fig. 1.7 showing Magno and Parvo axons in chapter 1). In addition, thick axons are probably less susceptible to a complete blockade of the transmitting neural signals during inflammation or compression of the optic nerve. This hypothesis is also supported by others studies, including MRI, VEP, visual psychophysics and post-mortem examination, which suggest that patients suffering ON and MS show a greater deficiency in the parvocellular compared to the magnocellular pathway (Caruana et al 2000, Brusa et al 2001, Evangelou et al 2001). The hypothesis of selective damage to small fibres in optic neuritis was proposed earlier by other studies (Hess & Plant 1983, Mullen & Plant 1986).

We have shown that, during the acute phase of ON, the sensitivity of the pupil to an isoluminant colour modulation is more affected than the luminance response (Fig. 7.2). Most patients showed a greater loss in the pupil colour response when compared to the pupil light response. This could reflect a segregation between achromatic and chromatic signals and suggest the possibility of a selective damage to chromatic sensitive neurones driving the pupillomotor signals in the optic nerve.

The difference between the colour and luminance pupil responses seems to diminish after a longer period of recovery (Fig. 7.3), where partial remyelination of the axons might have helped to restore partially the chromatic sensitivity. Experiments in mice (Murray et al 2001) have shown that spontaneous remyelination can restore neurological function even after severe demyelinating lesions.

Directions for further research

Some of the experiments reported in this thesis were limited in the number of subjects and can only be considered as pilot studies since they typically involved extensive measurements, optimization of parameters, etc. with the consequent discomfort for patients and volunteers.

For instance, in order to reduce testing time, we avoid isoluminant calibration for each patient with optic neuritis in chapter 7. Our coloured 'isoluminant' stimulus is only an approximation to isoluminance. Moreover the amplitude of these residual luminance signals vary for each patient. However this approximation does not affect the main conclusions from this study given that the differences found between luminance and colour modulation were so broad but it could provide a more accurate picture in patients with less acute lesions. Another serious limitation was the small number of patients tested during the acute demyelinating phase of the disease and in the long-term follow-up studies but this is something that escaped the scope of the study which was to investigate the viability of new techniques derived from vision research to the clinical assessment of optic neuritis and not to obtain statistically robust results. I consider that the results obtained with pupillometry are very promising for other researchers who perhaps have more clinical experience and everyday access to patients to pursue the matter further. I believe that many of the experiments in this thesis (comparison achromatic and chromatic pupil responses, pupil and visual filed perimetry, etc.) can be easily applied to other diseases of the optic nerve such as glaucoma and other optic neuropathies.

Other limitations derived from lack of time to build the necessary technical equipment. For example to study in detail the sources of non-linearities to the pupil response is essential to break the feedback loop ('open-loop' conditions) of the pupil system, i.e. to use Maxwellian view so the pupil constriction does not reduced the light flux entering the eye and thus provide a constant input to the pupil. However extensive work has already been carried in this field (Usui & Stark 1982, Myers & Stark 1993, Bressloff et al 1996) and I consider that clinical studies should be given priority over other basic mathematical aspects.

References

Alexandridis E. 1985. *The Pupil*. Springer-Verlag.

Alpern M, Mason GL, Jardinico RE. 1961. Vergence and accommodation. Pupil size changes associated with changes in accommodative vergence. *American Journal Of Ophthalmology* 52:762-7

Alpern M, Campbell FW. 1962. The spectral sensitivity of the consensual light reflex. *J. Physiol.* 164:478-507

Amthor FR, Takahashi ES, Oyster CW. 1989. Morphologies of rabbit retinal ganglion cells with concentric receptive fields. *J. Comp. Neurol.* 280(1):72-96

Atchison D, Smith G. 2000. *Optics of the human eye*. Butterworth-Heinemann.

Atchison DA, Scott DH, Smith G. 2000. Pupil photometric efficiency and effective centre. *Ophthalmic Physiol Opt.* 20(6):501-3

Azzopardi P, Cowey A. 1998. Blindsight and visual awareness. *Consciousness and Cognition* 7(3):292-311

Azzopardi P, Cowey A. 2001. Motion discrimination in cortically blind patients. *Brain* 124:30-46

Bailey IL, Lovie JE. 1976. New design principles for visual acuity letter charts. *American Journal of Optometry and Physiological Optics.*(53):740-5

Baker G. 2000. Visual pathways. *http://www. optometry. co. uk.*

Bala ADS, Takahashi TT. 2000. Pupillary dilation response as an indicator of auditory discrimination in the barn owl. *J Comp Physiol* 186:425-34

Barbur JL, Thomson WD. 1987. Pupil response as an objective-measure of visual-acuity. *Ophthalmic And Physiological Optics* 7(4):425-9

Barbur JL, Harlow AJ, Sahraie A. 1992. Pupillary responses to stimulus structure, color and movement. *Ophthalmic And Physiological Optics* 12(2):137-41

Barbur JL, Watson JDG, Frackowiak RSJ, Zeki S. 1993. Conscious visual perception without V1. *Brain* 116:1293-302

Barbur JL, Harlow AJ, Plant GT. 1994a. Insights into the different exploits of color in the visual- cortex. *Proceedings Of The Royal Society Of London Series B-Biological Sciences* 258(1353):327-34

Barbur JL, Harlow AJ, Weiskrantz L. 1994b. Spatial and temporal response properties of residual vision in case of hemianopia. *Philosophical Transactions Of The Royal Society Of London Series B-Biological Sciences* 343(1304):157-66

Barbur JL, Hess RF, Pinney HD. 1994c. Pupillary function in human amblyopia. *Ophthalmic Physiol. Opt.*:139-49

References

Barbur JL. 1995. A study of pupil response components in human vision. In *Basic and clinical perspectives in vision research* , ed. Robbins JG, Djamgoz MBA, Taylor A,3-18 pp. New York: Plenum Press. 3-18 pp.

Barbur JL, Cole VA, Sahraie A, Simmons A, Weiskrantz L, Williams SCR. 1997. A study of pupil responses in a subject with damaged primary visual cortex. *IOVS* 38(4):343

Barbur JL, Wolf J, Lennie P. 1998. Visual processing levels revealed by response latencies to changes in different visual attributes. *Proceedings Of The Royal Society Of London Series B-Biological Sciences* 265(1412):2321-5

Barbur JL, Weiskrantz L, Harlow JA. 1999. The unseen color aftereffect of an unseen stimulus: Insight from blindsight into mechanisms of color afterimages. *Proceedings Of The National Academy Of Sciences Of The United States Of America* 96(20):11637-41

Barbur JL, Harlow AJ, Moro S, Levy IS. Perimetric study of relative afferent pupil defects. Lakshminarayanan, V. 35, 26-29. 2000. Washington DC, Optical Society of America. In Trends in Optics and Photonics Series - Vision Science and its Applications.

Barbur JL, Prescott NB. 2002. A comparative study of stimulus-specific pupil responses in the domestic fowl (Gallus gallus
domesticus) and the human. *Vision Research* 42(2):249-55

Barbur JL. 2002. Learning from the pupil - studies of basic mechanisms and clinical applications. In *The Visual Neurosciences*, ed. Chalupa LM, Werner JS, Cambridge, MA: MIT Press.

Barlow HB. 1979. Reconstructing the visual image in space and time. *Nature* 279(5710):189-90

Barlow HB, Hill RM, Levick WR. 1964. Retinal ganglion cells responding selectively to direction and speed of image motion in the rabbit. *J Physiol* 173:377-497

Beck RW. 1991. The clinical profile of optic neuritis - experience of the optic neuritis treatment trial. *Archives Of Ophthalmology* 109(12):1673-8

Beck RW, Trobe JD, Moke PS, Brodsky MC, Buckley EG, Chrousos GA, Goodwin JA, Guy JR, Katz B, Kaufman DI, Keltner JL, Kupersmith MJ, Miller NR, OrengoNania S, Savino PJ, Shults WT, Smith CH, Thompson HS, Wall M. 1997. Visual function 5 years after optic neuritis experience of the Optic Neuritis Treatment Trial. *Archives Of Ophthalmology* 115(12):1545-52

Beck RW. 1998. Optic Neuritis: Clinical considerations and the relationship to Multiple Sclerosis. In *Neuro-Ophthalmology*, ed. Rosen ES, 20: London: Mosby.

Belliveau JW. 1991. Functional mapping of the human visual cortex by magnetic resonance imaging. *Science* 254:716-9

Benevento LA, Rezak M, Santos A. 1977. An autoradiographic study of the projections of the pretectum in the rhesus monkey (Macaca mulatta): evidence for sensorimotor links to the thalamus and oculomotor nuclei. *Brain Res.* 127(2):197-218

Birch J, Barbur JL, Harlow AJ. 1992. New method based on random luminance masking for measuring isochromatic zones using high-resolution color displays. *Ophthalmic And Physiological Optics* 12(2):133-6

Brainard DH, Roorda A, Yamauchi Y, Calderone JB, Metha A, Neitz M, Neitz J, Williams DR, Jacobs GH. 2000. Functional consequences of the relative numbers of L and M cones. *J Opt. Soc. Am. A Opt. Image Sci. Vis.* 17(3):607-14

References

Brainard DH, Pelli DG. 2002. Display characterization. In *The Encylopedia of Imaging Science and Technology*, ed. Hornak J,172-188 pp. Wiley. 172-188 pp.

BremnerFD. 2001. Pupil abnormalities. http://www.optometry.co.uk.

Bressloff PC, Wood CV, Howarth PA. 1996. Nonlinear shunting model of the pupil light reflex. Proceedings Of The Royal Society Of London Series B-Biological Sciences 263(1373):953-60

Broca P. 1878. Anatomie compárea des circonvolutions cérébrales. Le grand lobe limbique et le scissure limbique dans le serie des mammitéres. *Rev Anthropol* 12:646-57

Brodmann K. 1909. *Vergleichende lokalisationslehre der grosshirnrinde in ihren Prinzipien dargestellt auf grund des Zellenbaues.* Leipzig: Barth.

Brodsky M et al. 1997. The 5-year risk of MS after optic neuritis - Experience of the optic neuritis treatment trial. *Neurology* 49(5):1404-13

Brusa A, Jones SJ, Plant GT. 2001. Long-term remyelination after optic neuritis: A 2-year visual evoked potential and psychophysical serial study. Brain 124(Pt 3):468-79

Burde RM, Williams F. 1989. Parasympathetic nuclei. *Brain res* 498(2):371-5

Burkhalter A, Felleman DJ, Newsome WT, Van Essen DC. 1986. Anatomical and physiological asymmetries related to visual areas V3 and VP in macaque extrastriate cortex. *Vision Res* 26(1):63-80

Cajal S. 1909. *Histologie du systeme nerveux de l'homme et des vertebres*. Norbet Maloine, Paris.

Calkins DJ. 1999. Synaptic organization of cone pathways in the primate retina. In *Color Vision. From genes to perception.*, ed. Gegenfurtner KR, Sharpe LS, 8:163-179 pp. Cambridge University Press. 163-179 pp.

Campbell FW, Gregory AH. 1960. Effect of pupil size on visual acuity. *Nature* 187:1121-3

Caruana PA, Davies MB, Weatherby SJ, Williams R, Haq N, Foster DH, Hawkins CP. 2000. Correlation of MRI lesions with visual psychophysical deficit in secondary progressive multiple sclerosis. *Brain* 123(Pt 7):1471-80

Cassady JM. 1996. Increased firing of neurons in the posterior hypothalamus which precede classically-conditioned pupillary dilations. *Behavioural Brain Research* 80:111-21

CIE. 1986. *Publication No 15.2, Colorimetry*. Commission Internationale deL'Éclairage, Vienna, Austria.

Clarke RJ, Ikeda H. 1985. Luminance and darkness detectors in the olivary and posterior pretectal nuclei and their relationship to the pupillary light reflex in the rat .1. Studies with steady luminance levels. *Experimental Brain Research* 57(2):224-32

Clarke RJ, Zhang H, Gamlin PD. 2003. Primate pupillary light reflex: receptive field characteristics of pretectal luminance neurons. *J Neurophysiol* 89(6):3168-78

Cleland BG, Dublin MW, Levick WR. 1971. Sustained and transient neurones in the cat's retina and lateral geniculate nucleus. *J Physiol* 217:473-96

Clynes M. 1962. The non-linear biological dynamics of unidirectional rate sensitivity illustrated by analog computer analysis, pupillary reflex to light and sound, and heart rate behavior. *Ann. N. Y. Acad. Sci.* 98:806-45

References

Cornblath WT. 1995. Optic neuritis and demyelination. *Curr. Opin. Ophthalmol.* 6(6):4-9

Cowey A, Stoerig P. 1991. The neurobiology of blindsight. *Trends in Neurosciences* 14(4):140-5

Cowey A, Stoerig P. 1997. Visual detection in monkeys with blindsight. *Neuropsychologia* 35(7):929-39

Cox TA, Drewes CP. 1984. Contraction anisocoria from half-field illumination. *American Journal Of Ophthalmology* 97(5):577-82

Crawford BH. 1936. The dependence of pupil size upon external light stimulus under static and variable conditions. *Proceedings Of The Royal Society Of London Series B-Biological Sciences* 121:376-95

Crick F, Koch C. 1995. Are we aware of neural activity in primary visual cortex? *Nature* 375(6527):121-3

Curcio CA, Allen KA, Sloan KR, Lerea CL, Hurley JB, Klock IB, Milam AH. 1991. Distribution and morphology of human cone photoreceptors stained with anti-blue opsin. *J Comp Neurol* 312(4):610-24

Dacey DM, Brace S. 1992. A coupled network for parasol but not midget ganglion cells in the primate retina. *Vis. Neurosci.* 9(3-4):279-90

Dacey DM, Lee BB. 1994. The 'blue-on' opponent pathway in primate retina originates from a distinct bistratified ganglion cell type. *Nature* 367(6465):731-5

Dacey DM, Packer OS. 2003. Colour coding in the primate retina: diverse cell types and cone-specific circuitry. *Curr. Opin. Neurobiol.* 13(4):421-7

Dale AM, Liu AK, Fischl BR, Buckner RL, Belliveau JW, Lewine JD, Halgren E. 2000. Dynamic statistical parametric mapping: combining fMRI and MEG for high-resolution imaging of cortical activity. *Neuron* 26(1):55-67

Davson H. 1980. *Physiology of the eye*. New York: Academic Press.

De Groot CJ, Bergers E, Kamphorst W, Ravid R, Polman CH, Barkhof F, van d, V. 2001. Post-mortem MRI-guided sampling of multiple sclerosis brain lesions: increased yield of active demyelinating and (p)reactive lesions. *Brain* 124(Pt 8):1635-45

De Groot SG, Gebhard JW. 1952. Pupil size as determined by adapting luminance. *J. Opt. Soc. Am.* 42:492-5

de Monasterio FM, Gouras P, Tolhurst DJ. 1976. Spatial summation, response pattern and conduction velocity of ganglion cells of the rhesus monkey retina. *Vision Res.* 16(6):674-8

de Monasterio FM. 1978a. Properties of concentrically organized X and Y ganglion cells of macaque retina. *J. Neurophysiol.* 41(6):1394-417

de Monasterio FM. 1978b. Properties of ganglion cells with atypical receptive-field organization in retina of macaques. *J. Neurophysiol.* 41(6):1435-49

De Valois RL, Abramov I, Jacobs GH. 1966. Analysis of response patterns of LGN cells. *J Opt Soc Am* 56(7):966-77

DeYoe EA, Van Essen DC. 1985. Segregation of efferent connections and receptive field properties in visual area V2 of the macaque. *Nature* 317(6032):58-61

References

Diller L, Packer OS, Verweij J, McMahon MJ, Williams DR, Dacey DM. 2004. L and M cone contributions to the midget and parasol ganglion cell receptive fields of macaque monkey retina. *J Neurosci.* 24(5):1079-88

Dowling JE. 1987. *The retina: an approachable part of the brain*. Harvard U P.

Dreher B. 1972. Hypercomplex cells in the cat's striate cortex. *Invest Ophthalmol.* 11(5):355-6

Dreher B, Fukada Y, Rodieck RW. 1976. Identification, classification and anatomical segregation of cells with X-like and Y-like properties in the lateral geniculate nucleus of old-world primates. *J Physiol* 258(2):433-52

Dreher B, Sefton AJ. 1979. Properties of neurons in cat's dorsal lateral geniculate nucleus: a comparison between medial interlaminar and laminated parts of the nucleus. *J Comp Neurol* 183(1):47-64

Druschky A, Heckmann JG, Claus D, Katalinic A, Druschky KF, Neundorfer B. 1999. Progression of optic neuritis to multiple sclerosis: an 8-year follow-up study. *Clinical Neurology And Neurosurgery* 101(3):189-92

Enroth-Cugell C, Robson JG. 1966. The contrast sensitivity of retinal ganglion cells of the cat. *Journal of Physiology* 187:517-52

Enroth-Cugell C, Robson JG, Schweitzer-Tong DE, Watson AB. 1983. Spatio-temporal interactions in cat retinal ganglion cells showing linear spatial summation. *J. Physiol. (Lond.)* 341:279-307:279-307

Erwin E, Baker FH, Busen WF, Malpeli JG. 1999. Relationship between laminar topology and retinotopy in the rhesus lateral geniculate nucleus: results from a functional atlas. *J Comp Neurol* 407:92-102

Evangelou N, Konz D, Esiri MM, Smith S, Palace J, Matthews PM. 2001. Size-selective neuronal changes in the anterior optic pathways suggest a differential susceptibility to injury in multiple sclerosis. *Brain* 124(Pt 9):1813-20

Fang JP, Donahue SP, Lin RH. 1999. Global visual field involvement in acute unilateral optic neuritis. *American Journal Of Ophthalmology* 128(5):554-65

Felleman DJ, Van Essen DC. 1987. Receptive field properties of neurons in area V3 of macaque monkey extrastriate cortex. *J Neurophysiol.* 57(4):889-920

Fitzgibbon A, Pilu M, Fisher B. 1999. Direct Least Squares Fitting of Ellipses. *IEEE Transactions on pattern analysis and machine intelligence* 21:476-80

Forrest FH, Snow HL. 1968. Progression of eye complications caused by phenothiazines. *Diseases of the nervous system* 29:26-8

Freedman D, Barbur JL, Lennie P. 1997. Pupil response latencies & reaction times to chromatic and achromatic stimuli. *IOVS* 38(4):4711

Gamlin PD, Reiner A. 1991. The Edinger-Westphal nucleus: sources of input influencing accommodation, pupilloconstriction, and choroidal blood flow. *J Comp Neurol* 306(3):425-38

Gamlin PD, Clarke RJ. 1995. The pupillary light reflex pathway of the primate. *J Am Optom Assoc* 66(7):415-8

References

Gamlin PDR, Zhang HY, Harlow A, Barbur JL. 1998. Pupil responses to stimulus color, structure and light flux increments in the rhesus monkey. *Vision Research* 38(21):3353-8

Gamlin PD, Smith VC, Dacey DM, Pokorny J, McDougal DH. 2004. Melanopsin-containing Retinal Ganglion Cells Drive the Pupillary Light Reflex in the Primate. *ARVO Meeting Abstracts* 45(5):2262

Gegenfurtner KR, Kiper DC, Fenstenmaker SB. 1996. Processing of color, form, and motion in macaque area V2. *Vis. Neurosci.* 13(161):172

Gegenfurtner KR, Kiper DC, Levitt JB. 1997. Functional properties of neurons in macaque area. *J Neurophysiol* 77:1906-23

Gegenfurtner KR, Sharpe LT (editors). 1999. *Color vision from genes to perception*. Cambridge University Press.

Goebel R, Muckli L, Zanella FE, Singer W, Stoerig P. 2001. Sustained extrastriate cortical activation without visual awareness revealed by fMRI studies of hemianopic patients. *Vision Research* 41:1459-74

Gray H. 1995. *Gray's Anatomy*. Churchill Livingstone.

Guillery RW. 1988. Retinal representations in prethalamic visual pathways. In *Physiological Aspects of Clinical Neuro-ophthalmology*, ed. Kennard C, Clifford Rose F, Chapman and Hall Medical.

Guy J, Qi XP, Wang H, Hauswirth WW. 1999. Adenoviral gene therapy with catalase suppresses experimental optic neuritis. *Archives Of Ophthalmology* 117(11):1533-9

Haley MJ. 1987. Interpreting test results with Statpac. *The field Analyzer Primer. San Leandro, CA. Allergan Humphrey.*:133

Hamann KU, Hellner KA, Muller-Jensen A, Zschocke S. 1979. Videopupillographic and VER investigations in patients with congenital and acquired lesions of the optic radiation. *Ophthalmologica* 178:348-56

Hartmann-von Monakov K, Akert K, Künzle H. 1979. Projections of precentral and premotor cortex to the red nucleus and other midbrain areas. *Experimental Brain Research* 34:91-105

Hasegawa S, Ishikawa S. 1989. [Age changes in pupillary light reflex. A demonstration by means of a pupillometer]. *Nippon Ganka Gakkai Zasshi JID - 7505716* 93(10):955-61

Heron JR. 1986. Diagnosis of optic neuritis. In *Optic neuritis*, ed. Hess RF, Plant GT, 4:51-72 pp. Cambridge University Press. 51-72 pp.

Hess EH. 1965. Attitude and pupil size. *Scientific American* 212(4):46-54

Hess RF, Plant GT. 1983. The effect of temporal frequency variation on threshold contrast sensitivity deficits in optic neuritis. *J. Neurol. Neurosurg. Psychiatry* 46(4):322-30

Hess RF, Plant GT. 1986. *Optic Neuritis*. Cambridge: Cambridge University Press.

Heywood CA, Cowey A. 1987. On the role of cortical visual area V4 in the discrimination of hue and pattern in macaque monkeys. *J Neurosci.* 7:2601-16

References

Holdefer RN, Norton TT. 1995. Laminar organization of receptive field properties in the dorsal lateral geniculate nucleus of the tree shrew (Tupaiaglis belangeri). *J. Comp. Neurol.* 358(3):401-13

Horton JC, Hedley-Whyte ET. 1984. Mapping of cytochrome oxidase patches and ocular dominance columns in human visual cortex. *Philosophical Transactions Of The Royal Society Of London Series B-Biological Sciences* 304:255-72

Hubel DH, Wiesel TN. 1959. Receptive fields of single neurones in the cat's striate cortex. *J Physiol* 148:574-91

Hubel DH, Wiesel TN. 1960. Receptive fields of optic nerve fibres in the spider monkey. *J Physiol* 154:572-80

Hubel DH, Wiesel TN. 1961. Intergrative action in the cat's lateral geniculate body. *J Physiol* 155:385-98

Hubel D, Wiesel TN. 1962. Receptive fields, binocular interaction and functional architecture in cat's visual cortex. *J Physiol* 160:106-54

Hubel D, Wiesel TN. 1965. Receptive fields and functional architecture in two non-striate visual areas (18 and 19) of the cat. *J Neurophysiol.* 28:229-89

Hubel DH, Wiesel TN. 1972. Laminar and columnar distribution of geniculo-cortical fibers in the macaque monkey. *J Comp Neurol* 146(4):421-50

Hubel DH, Wiesel TN. 1977. Ferrier lecture. Functional architecture of macaque monkey visual cortex. *Proc. R. Soc Lond B Biol. Sci.* 198(1130):1-59

Hubel DH, Wiesel TN, Stryker MP. 1977. Orientation columns in macaque monkey visual cortex demonstrated by the 2-deoxyglucose autoradiographic technique. *Nature* 269(5626):328-30

Hubel DH, Livingstone MS. 1987. Segregation of form, color, and stereopsis in primate area 18. *J Neurosci.* 7(11):3378-415

Hubel DH. 1988. *Eye, Brain and vision*. Scientific American Library; 22.

Hubel DH, Livingstone MS. 1990. Color and contrast sensitivity in the lateral geniculate body and primary visual cortex of the macaque monkey. *J Neurosci.* 10(7):2223-37

Ikeda H, Wright MJ. 1972. Receptive field organization of 'sustained' and 'transient' retinal ganglion cells which subserve different function roles. *J Physiol* 227(3):769-800

Jackson JH. 1915. On affections of speech from diseases of the brain. *Brain* 38:107-74

Jackson PC. 1986. Innervation of the iris by individual parasympathetic axons in the adult mouse. *J Physiol JID - 0266262* 378:485-95

Kaiser PK, Boynton RM. 1996. *Human Color Vision*. Washington, DC: Optical Society of America.

Kandel E, Schwartz JH, Jessell TM. 2000. *Principles of Neural Science and Behaviour*. Prentice Hall.

Kandel ER, Squire LR. 2000. Neuroscience: Breaking Down Scientific Barriers to the Study of Brain and Mind. *Science* 290(5494):1113-20

References

Kaplan E, Lee B, Shapley R. 1990. New views of primate retinal function. *Progress in Retinal Research* 9:273-336

Kardon RH, Kirkali PA, Thompson HS. 1991. Automated pupil perimetry. Pupil field mapping in patients and normal subjects. *Ophthalmology.* 98(4):485-95

Kardon RH. 1992. Pupil perimetry [editorial]. *Curr. Opin. Ophthalmol.* 3(5):565-70

Kardon RH, Haupert CL, Thompson HS. 1993. The relationship between static perimetry and the relative afferent pupillary defect. *American Journal Of Ophthalmology* 115(3):351-6

Kardon RH. 1995. Pupillary light reflex. *Curr. Opin. Ophthalmol.* 6:20-6

Kardon RH, Thompson HS. 1998. The Pupil. In *Neuro-ophthalmology*, ed. Rosen ES, Eustace P, 13:

Kass JH, Guillery RW, Allman JM. 1973. Discontinuities in the dorsal lateral geniculate nucleus corresponding to the optic disc: a comparative study. *J Comp Neurol* 147(2):163-79

Keltner JL, Johnson CA, Spurr JO, Beck RW. 1999. Comparison of central and peripheral visual field properties in the optic neuritis treatment trial. *American Journal Of Ophthalmology* 128(5):543-53

Kerr FW, Hollowell OW. 1964. Location of pupillomotor and accommodation fibres in the oculomotor nerve. *J. Neurol. Neurosurg. Psychiatry* 27:473-81

Kiper DC, Gegenfurtner KR, Movshon JA. 1997. Chromatic properties of neurons in macaque area V2. *Vis. Neurosci.* 14:1061-72

Kolb H. 1991. Anatomical pathways for color vision in the human retina. *Vis. Neurosci.* 7(1-2):61-74

Kolb H, Dekorver L. 1991. Midget ganglion cells of the parafovea of the human retina: a study by electron microscopy and serial section reconstructions. *J Comp Neurol* 303(4):617-36

Kolb H, Goede P, Roberts S, McDermortt R, Gouras P. 1997. Uniqueness of the S-cone pedicle in the human retina and consequences for color processing. *J Comp Neurol* 386(3):443-60

Kourouyan HD, Horton JC. 1997. Transneuronal retinal input to the primate Edinger-Westphal nucleus. *J Comp Neurol* 381(1):68-80

Kuffler SW. 1953. Discharge patterns and functional organisation of mammalian retina. *J Neurophysiol* 16:37-68

Kulikowski JJ, Tolhurst DJ. 1973. Psychophysical evidence for sustained and transient detectors in human vision. *J Physiol* 232(1):149-62

Kupfer C, Chumbely L, Downer JC. 1967. Quantitative of optic nerve, optic tract and lateral geniculate nucleus in man. *Journal of Anatomy* 101:393-401

Lee BB, Martin PR, Valberg A. 1989. Nonlinear summation of M- and L-cone inputs to phasic retinal ganglion cells of the macaque. *J Neurosci.* 9(4):1433-42

Lee BB. 1996. Receptive field structure in the primate retina. *Vision Res.* 36(5):631-44

<p style="text-align: center;">References</p>

Lennie P. 1980. Perceptual signs of parallel pathways. *Philos. Trans. R. Soc Lond B Biol. Sci.* 290(1038):23-37

Lennie P. 1998. Single units and visual cortical organization. *Perception* 27:889-935

Levatin P. 1959. Pupillary escape in disease of the retina or optic nerve. *Arch Ophthalmol* 62:768-79

Levine MW. 2000. *Fundamentals of Sensation and Perception*. Oxford University Press.

Livingstone MS, Hubel DH. 1982. Thalamic inputs to cytochrome oxidase-rich regions in monkey visual cortex. *Proc. Natl. Acad. Sci. U. S. A* 79(19):6098-101

Livingstone MS, Hubel DH. 1984. Anatomy and physiology of a color system in the primate visual cortex. *J Neurosci.* 4(1):309-56

Livingstone MS, Hubel DH. 1987. Psychophysical evidence for separate channels for the perception of form, color, movement, and depth. *J Neurosci.* 7(11):3416-68

Loewenfeld IE. 1969. The Argyll Robertson pupil 1869-1969: a critical survey of the literature. *Survey Of Ophthalmology* 14:199-299

Loewenfeld IE. 1977. Simple, central anisocoria: a common condition, seldomrecognized. *Am. Acad. Ophthal. Otolaryng.* 83:832-9

Loewenfeld IE. 1993. *The Pupil : Anatomy, Physiology, and Clinical Applications*. Iowa: Iowa State University Press.

Loewy AD, Saper CB. 1978. Edinger-Westphal nucleus: projections to the brain stem and spinal cord in the cat. *Brain res* 150(1):1-27

Logothetis NK, et al. 2001. Neurophysiological investigation of the basis of the FMRI signal. *Nature* 412:150-7

Loving RT, Kripke DF, Glazner LK. 1996. Circadian rhythms in the human pupil and eyelid. *Am J Physiol* 271(2 Pt 2):R320-R324

Lowenstein O, Loewenfeld IE. 1969. The Pupil. In *The eye*, ed. Davson H, 9:255-337 pp. New York: Academic Press. 255-337 pp.

Lu ZL, Lesmes LA, Sperling G. 1999. The mechanism of isoluminant chromatic motion perception. *Proc. Natl. Acad. Sci. U. S. A* 96:8289-94

Lucas RJ, Hattar S, Takao M, Berson DM, Foster RG, Yau KW. 2003. Diminished pupillary light reflex at high irradiances in melanopsin-knockout mice. *Science* 299(5604):245-7

Lund JS, Boothe RG. 1975. Interlaminar connections and pyramidal neuron organization in the visual cortex, area 17, of the macaque monkey. *Comp Neurol* 159:305-34

MacAdam DL. 1942. Visual sensitivities to colour differences in daylight. *Journal of the Optical Society of America* 32:247-74

Malpeli JG, Schiller PH. 1978. Lack of blue OFF-center cells in the visual system of the monkey. *Brain res* 141(2):385-9

Martin PR, Lee BB, White AJ, Solomon SG, Ruttiger L. 2001. Chromatic sensitivity of ganglion cells in the peripheral primate retina. *Nature* 410(6831):933-6

Martini FH. 1998. *Fundamentals of Anatomy and Physiology*.

Maunsell JHR, Newsome WT. 1987. Visual processing in monkey extra-striate cortex. *Annu. Rev. Neurosci.* 10:363-401

Merigan WH, Maunsell JHR. 1993. How parallel are the primate visual pathways? *Annu. Rev. Neurosci.* 16:369-402

Milton JG, Longtin A. 1990. Evaluation of pupil constriction and dilation from cycling measurements. *Vision Res.* 30(4):515-25

Mitome M, Low HP, van den Pol A, Nunnari JJ, Wolf MK, Billings-Gagliardi S, Schwartz WJ. 2001. Towards the reconstruction of central nervous system white matter using neural precursor cells. *Brain* 124(Pt 11):2147-61

Moon P, Spencer DE. 1944. On the Stiles-Crawford effect. *J Opt Soc Am* 34:319-29

Morland AB, Jones SR, Finlay AL, Deyzac E, Le S, Kemp S. 1999. Visual perception of motion, luminance and colour in a human hemianope. *Brain* 122:1183-98

Mullen KT, Plant GT. 1986. Colour and luminance vision in human optic neuritis. Brain 109 (Pt 1):1-13

Murray PD, McGavern DB, Sathornsumetee S, Rodriguez M. 2001. Spontaneous remyelination following extensive demyelination is associated with improved neurological function in a viral model of multiple sclerosis. *Brain* 124(Pt 7):1403-16

Myers GA, Gannon JA, Stark LW. 1993. Level dependent signal flow in the light pupil reflex. II. Phase velocity of responses to sinusoidal light stimuli. *Biol. Cybern.* 68(3):235-40

Niehaus L, Guldin B, Meyer B. 2001. Influence of transcranial magnetic stimulation on pupil size. *J Neurol Sci JID - 0375403* 182(2):123-8

Ogle JW. 1858. On the influence of the cervical portion of the sympathetic nerve and spinal cord upon the eye and its appendages, illustrated by clinical cases, with observations. *Medicochirurg. Trans.* 41:397-440

Ormerod IE, Miller DH, McDonald WI, du BE, Rudge P, Kendall BE, Moseley IF, Johnson G, Tofts PS, Halliday AM. 1987. The role of NMR imaging in the assessment of multiple sclerosis and isolated neurological lesions. A quantitative study. *Brain* 110(Pt 6):1579-616

Osterberg G. 1935. Topography of the layer of rods and cones in the human retina. *Acta Ophthal* 6:1-103

Oyster CW. 1999. *The Human Eye*. Sinauer Associates.

Palmer SE. 1999. *Vision science photons to phenomenology*. MIT Press.

Parkinson D. 1988. Further observations on the sympathetic pathways to the pupil. *Anat Rec* 220(1):108-9

Passatore M, Pettorossi VE, Casoni RP. 1977. Sympathetic preganglionic pupillodilator fibres in the light reflex. *Experientia* 33(2):218-9

Pearlman AI, Birch J, Meadows J. 1979. Cerebral colour blindness: an acquired defect in hue discrimination. *Annals of Neurology* 5:253-61

Pelli DG, Robson J, Wilkins A. 1988. The design of a new letter chart for measuring contrast sensitivity. *Clinical Vision Sciences*(2):187-99

Pelli DG. 1997. Pixel independence: Measuring spatial interactions on a CRT display. *Spatial Vision* 10(4):443-6

Perry VH, Cowey A. 1984. Retinal ganglion cells that project to the superior colliculus and pretectum in the macaque monkey. *Neuroscience* 12:1125-37

Perry VH, Oehler R, Cowey A. 1984. Retinal ganglion cells that project to the dorsal lateral geniculate nucleus in the macaque monkey. *Neuroscience* 12:1101-23

Polman CH, Thompson AJ, Murray TJ, McDonald WI. 2001. *Multiple Sclerosis: The guide to treatment and management.* New York: Demos Medical Publishing.

Polyak SL. 1957. *The verterbrate visual system.* University of Chicago Press.

Pong M, Fuchs AF. 2000. Characteristics of the Pupillary Light Reflex in the Macaque Monkey: Discharge Patterns of Pretectal Neurons. *J Neurophysiol* 84(2):964-74

Press WH, Flannery BP, Teukolsky SA, Vetterling WT. 1992. *Numerical recipes in C: the art of scientific computing.* Cambridge University Press.

Purpura K, Kaplan E, Shapley RM. 1988. Background light and the contrast gain of primate P and M retinal ganglion cells. *Proc. Natl. Acad. Sci. U. S. A* 85(12):4534-7

Reese BE. 1993. Clinical implications of the fibre order in the optic pathway of primates. *Neurological Research* 15:83-6

Reese BE, Cowey A. 1988. Segregation of functionally distinct axons in the monkey's optic tract. *Nature* 331:350-1

Reeves P. 1920. The response of the average pupil to various intensities of light. *J. Opt. Soc. Am.* 4:35-43

Reid RC, Shapley RM. 2002. Space and time maps of cone photoreceptor signals in macaque lateral geniculate nucleus. *J Neurosci.* 22(14):6158-75

Regan D. 1999. *Human perception of objects.* Sinauer Associates.

Rizzo JF, Lessell S. 1991. Optic neuritis and ischemic optic neuropathy. Overlapping clinical profiles. *Arch Ophthalmol JID - 7706534* 109(12):1668-72

Rockland KS, Pandya DN. 1979. Laminar origins and terminations of cortical connections of the occipital lobe in rhesus monkey. *Brain res* 170:3-20

Rodieck RW. 1998. *The First Steps in Seeing.* Sinauer Associates Inc.

Rodieck RW, Watanabe M. 1993. Survey of the morphology of macaque retinal ganglion cells that project to the pretectum, superior colliculus, and parvicellular laminae of the lateral geniculate nucleus. *J. Comp. Neurol.* 338(2):289-303

Rushton WAH. 1962. *Visual pigments in man.* Liverpool University Press.

Russell MH, Murray IJ, Metcalfe RA, Kulikowski JJ. 1991. The visual defect in multiple sclerosis and optic neuritis. A combined psychophysical and electrophysiological investigation. *Brain* 114(Pt 6):2419-35

References

Sahraie A, Weiskrantz L, Barbur JL, Simmons A, Williams SCR. 1997a. Motion processing with and without awareness: Pattern of increased brain activity detected using fMRI. *IOVS* 38(4):1056

Sahraie A, Weiskrantz L, Barbur JL, Simmons A, Williams SCR. 1997b. Pattern of neuronal activity associated with conscious and unconscious processing of visual signals. *Proceedings Of The National Academy Of Sciences Of The United States Of America* 94(17):9406-11

Schellart NA, Spekreijse H. 1973. Origin of the stochastic nature of ganglion cell activity in isolated goldfish retina. *Vision Res.* 13(2):337-45

Schiller PH, Malpeli JG. 1977. Properties and tectal projections of monkey retinal ganglion cells. *J Neurophysiol.* 40(2):428-45

Schiller P, Malpeli J. 1978. Functional specificity of lateral geniculate nucleus laminae of the rhesus monkey. J. Neurophysiol. 41:788-97

Schiller PH, Logothetis NK, Charles ER. 1990. Functions of the colour-opponent and broad-band channels of the visual system. *Nature* 343(6253):68-70

Schneck ME, Haegerstrom-Portnoy G. 1997. Color vision defect type and spatial vision in the optic neuritis treatment trial. *Invest. Ophthalmol. Vis. Sci.* 38(11):2278-89

Sellebjerg F, Nielsen HS, Frederiksen JJ, Olesen J. 1999. A randomized, controlled trial of oral high-dose methylprednisolone in acute optic neuritis. *Neurology* 52(7):1479-84

Semmlow J, Hansmann D, Stark L. 1975. Variation in pupillomotor responsiveness with mean pupil size. *Vision Res.* 15(1):85-90

Shapley R, Kaplan E, Soodak R. 1981. Spatial summation and contrast sensitivity of X and Y cells in the lateral geniculate nucleus of the macaque. *Nature* 292(5823):543-5

Shapley R. 1990. Visual sensitivity and parallel retino-cortical channels. *Annual review of Psychology* 41:635-58

Shipp S, Zeki S. 1985. Segregation of pathways leading from area V2 to areas V4 and V5 of macaque monkey visual cortex. *Nature* 315(6017):322-5

Shipp S, Zeki S. 1995. Segregation and convergence of specialised pathways in macaque monkey visual cortex. *J Anat.* 187 (Pt 3):547-62

Sillito AM, Zbrozyna AW. 1970. The activity characteristics of the preganglionic pupilloconstrictor neurones. *J Physiol* 211:767-79

Smith SA, Smith SE. 1980. Contraction anisocoria: Nasal versus temporal illumination. *British Journal Of Ophthalmology* 64(12):933-4

Smith SA. 1992. Pupil function: Tests and disorders. In *Autonomic failure: A texbook on clinical disorders of the autonomic nervous system*, ed. Bannister SR, Mathias CJ,421-441 pp. Oxford: OUP. 421-441 pp.

Stanley PA, Davies AK. 1995. The effect of field of view size on steady-state pupil diameter. *Ophthalmic And Physiological Optics* 15(6):601-603

Stark LW. 1984. The pupil as a paradigm for neurological control systems. *IEEE Trans. Biomed. Eng.* 31(12):919-24

References

Steele GE, Weller RE, Cusick CG. 1991. Cortical connections of the candal subdivision of the dorsolateral area (V4) in monkeys. *J Comp Neurology* 306:495-520

Stiles WH, Crawford BH. 1933. The luminous efficiency of rays entering the eye-pupil at different points. *Proc. Roy. Soc. London (B)* 112:428-50

Stockman A, Sharpe LT. 2000. The spectral sensitivities of the middle- and long-wavelength-sensitive cones derived from measurements in observers of known genotype. *Vision Res.* 40(13):1711-37

Stockman A, Sharpe LT, Merbs S, Nathans J. 2000. Spectral sensitivities of human cone visual pigments determined in vivo and in vitro. *Methods Enzymol.* 316:626-50

Stoerig P, Cowey A. 1989. Wavelength sensitivity in blindsight. *Nature* 342(6252):916-8

Stoerig P, Cowey A. 1992. Wavelength discrimination in blindsight. *Brain* 115:425-44

Stoerig P, Cowey A. 1997. Blindsight in man and monkey. *Brain* 120:535-59

Stone J, Hoffman KP. 1972. Very slow-conducting ganglion cells in the cat's retina; a major, new functional type? *Brain res* 43:610-6

Sur M, Sherman SM. 1982. Linear and nonlinear W-cells in C-laminae of the cat's lateral geniculate nucleus. *J. Neurophysiol.* 47(5):869-84

Suzuki H, Kato E. 1966. Binocular interaction of cat's lateral geniculate body. *J Neurophysiol* 29:909

Svaetichin G. 1953. The cone action potential. *Acta Physiol. Scand.* 29:565-99

Swartz NG, Beck RW, Savino PJ, Sergott RC, Bosley TM, Lam BL, Drucker M, Katz B. 1995. Pain in anterior ischemic optic neuropathy. *J. Neuroophthalmol.* 15(1):9-10

Thompson HS. 1992. The Pupil. In *Adler's physiology of the eye*, 12: London: Mosby.

Tolhurst DJ. 1975. Sustained and transient channels in human vision. *Vision Res* 15:1151-5

Trejo LJ, Cicerone CM. 1984. Cells in the pretectal olivary nucleus are in the pathway for the direct light reflex of the pupil in the rat. *Brain res* 300(1):49-62

Troelstra A. 1968. Detection of time-varying light signals as measured by the pupillary response. *J Opt. Soc. Am.* 58(5):685-90

Ts'o DY, Gilbert CD, Wiesel TN. 1986. Relationships between horizontal interactions and functional architecture in cat striate cortex as revealed by cross-correlation analysis. *J Neurosci.* 6(4):1160-70

Ts'o DY, Gilbert CD. 1988. The organization of chromatic and spatial interactions in the primate striate cortex. *J Neurosci.* 8(5):1712-27

Usui S, Stark L. 1982. A model for nonlinear stochastic behavior of the pupil. Biol. Cybern. 45(1):13-21

Vaina L, Cowey A. 2001. Regional cerebral correlates of global motion perception: Evidence from unilateral cerebral brain damage. *Brain* 124:310-21

Van Crevel H, Verhaart WJC. 1963. The rate of secondary degeneration in the central nervous system II. The optic nerve of the cat. *Journal of Anatomy* 97:451

References

Van Essen DC, Anderson CH, Felleman DJ. 1992. Information processing in the primate visual system: an integrated systems perspective. *Science* 255(5043):419-23

Van Orden KF, Limbert W, Makeig S, Jung TP. 2001. Eye activity correlates of workload during visuospatial memory task. *Human Factors* 43(1):111-21

Wald G. 1967. Blue blindness in normal fovea. *J Opt Soc Am* 57:1289-301

Wandell BA. 1995. *Foundations of vision*. Sinauer Associates.

Wassle H, Boycott BB. 1991. Functional architecture of the mammalian retina. *Physiol Rev* 71:447-80

Watanabe M, Rodieck RW. 1989. Parasol and midget ganglion cells of the primate retina. *J. Comp. Neurol.* 289(3):434-54

Weiskrantz L. 1986. *Blindsight: A Case Study and Its Implications*. Oxford University Press.

Weiskrantz L, Barbur JL, Sahraie A. 1995. Parameters affecting conscious versus unconscious visual- discrimination with damage to the visual-cortex (V1). *PNAS* 92(13):6122-6

Weiskrantz L. 1997. *Consciousness lost and found: a neuropsychological exploration*. Oxford: Oxford University Press.

Weiskrantz L, Cowey A, Le Mare C. 1998. Learning from the pupil: a spatial visual channel in the absence of V1 in monkey and human. *Brain* 121:1065-72

Weiskrantz L, Cowey A, Barbur JL. 1999. Differential pupillary constriction and awareness in the absence of striate cortex. *Brain* 122:1533-8

Wessinger CM, Fendrich R, Gazzaniga MS. 1997. Islands of residual vision in hemianopic patients. *Journal of Cognitive Neuroscience* 9(2):203-21

Wiesel TN, Hubel DH. 1966. Spatial and chromatic interactions in the lateral geniculate body of the rhesus monkey. *J Neurophysiol.* 29(6):1115-56

Wild HM, Butler D, Carden D, Kullikowski JJ. 1985. Primate cortical area V4 important for colour constancy but not wavelength discrimination. *Nature* 313:133-5

Wilhelm B, Wilhelm H, Ludtke H, Adler M, Streicher P. 1996a. [Pupillography for objective vigilance assessment. Methodological problems and possible solutions]. *Ophthalmologe* 93(4):446-50

Wilhelm B, Wilhelm H, Streicher P, Ludtke H, Adler M. 1996b. [Pupillography as an objective attention test]. *Wien. Med. Wochenschr.* 146(13-14):387-9

Wilhelm B, Wilhelm H, Lüdtke H, Streicher P, Adler M. 1998. Pupillographic assessment of sleepiness in sleep-deprived healthy subjects. *Sleep* 21:258-65

Wilhelm B, Giedke H, Ludtke H, Bittner E, Hofmann A, Wilhelm H. 2001. Daytime variations in central nervous system activation measured by a pupillographic sleepiness test. *J Sleep Res.* 10(1):1-7

Wilhelm BJ, Wilhelm H, Moro S, Barbur JL. 2002. Pupil response components: studies in patients with Parinaud's syndrome. *Brain* 125(Pt 10):2296-307

Wolf JE, Finlay A, Bissessur K, Harlow JA, Barbur JL. 1999. Pupil latencies to sinusoidally modulated stimulus attributes. *IOVS* 40(4):242B202

<div style="text-align: center;">References</div>

Wolff E. 1997. *Wolff's Anatomy of the Eye and Orbit*. London: Chapman and Hall.

Wong-Riley M. 1979. Changes in the visual system of monocularly sutured or enucleated cats demonstrable with cytochrome oxidase histochemistry. *Brain res* 171:11-28

Wyszecki G, Stiles WS. 1982. *Color Science - Concepts and Methods, Quantitative Data and Formulae.* John Wiley & Sons.

Yoss RE, Moyer NJ, Hollenhorst RW. 1970. Pupil size and spontaneous pupillary waves associated with alertness, drowsiness and sleep. *Neurology* 20:545-54

Young MJ, Lund RD. 1998. The retinal ganglion cells that drive the pupilloconstrictor response in rats. *Brain res* 787(2):191-202

Young RS, Teller DY. 1991. Determination of lights that are isoluminant for both scotopic and photopic vision. *J. Opt. Soc. Am. [A.]* 8(12):2048-52

Young RS, Han BC, Wu PY. 1993. Transient and sustained components of the pupillary responses evoked by luminance and color. *Vision Res.* 33(4):437-46

Zeki S. 1993. *A Vision of the Brain*. Oxford: Blackwell Scientific.

Zeki S. 2001. Localization and globalization in conscious vision. *Annu. Rev Neurosci.* 24:57-86

Zeki S, Ffytche DH. 1998. The Riddoch syndrome: insights into the neurobiology of conscious vision. *Brain* 121:25-45

Zeki S, Marini L. 1998. Three cortical stages of colour processing in the human brain. *Brain* 121 (Pt 9):1669-85

Zeki SM. 1973. Colour coding in rhesus monkey prestriate cortex. *Brain res* 53(2):422-7

Zeki SM. 1978a. Functional specialisation in the visual cortex of the rhesus monkey. *Nature* 274(5670):423-8

Zeki SM. 1978b. The third visual complex of rhesus monkey prestriate cortex. *J Physiol* 277:245-72

Zeki SM. 1978c. Uniformity and diversity of structure and function in rhesus monkey prestriate visual cortex. *J Physiol* 277:273-90

Zihl J, Von Cramon D, Mai N. 1983. Selective disturbances of movement vision after bilateral brain damage. *Brain* 106:313-40.